INVESTIGATION OF CHROMATIC FUNCTION IN THE NORMAL AND ABNORMAL EYE

IAN DAVID MOSS

Doctor of Philosophy

THE UNIVERSITY OF ASTON IN BIRMINGHAM

February 1995

The University of Aston in Birmingham

Investigation of chromatic function in the normal and abnormal eye

Ian David Moss

Doctor of Philosophy

1995

This study examined the use of non-standard parameters to investigate the visual field, with particular reference to the detection of glaucomatous visual field loss.

Evaluation of the new perimetric strategy for threshold estimation - FASTPAC, demonstrated a reduction in the examination time of normals compared to the standard strategy. Despite an increased within-test variability the FASTPAC strategy produced a similar mean sensitivity to the standard strategy, reducing the effects of patient fatigue.

The new technique of Blue-Yellow perimetry was compared to White-White perimetry for the detection of glaucomatous field loss in OHT and POAG. Using a database of normal subjects, confidence limits for normality were constructed to account for the increased between-subject variability with increase in age and eccentricity and for the greater variability of the Blue-Yellow field compared to the White-White field. Effects of individual ocular media absorption had little effect on Blue-Yellow field variability. Total and pattern probability analysis revealed five of 27 OHTs to exhibit Blue-Yellow focal abnormalities; two of these patients subsequently developed White-White loss. Twelve of the 24 POAGs revealed wider and / or deeper Blue-Yellow loss compared with the White-White field. Blue-Yellow perimetry showed good sensitivity and specificity characteristics, however, lack of perimetric experience and the presence of cataract influenced the Blue-Yellow visual field and may confound the interpretation of Blue-Yellow visual field loss. Visual field indices demonstrated a moderate relationship to the structural parameters of the optic nerve head using scanning laser tomography. No abnormalities in Blue-Yellow or Red-Green colour CS was apparent for the OHT patients.

A greater vulnerability of the SWS pathway in glaucoma was demonstrated using Blue-Yellow perimetry however predicting which patients may benefit from B-Y perimetric examination is difficult. Furthermore, cataract and the extent of the field loss may limit the extent to which the integrity of the SWS channels can be selectively examined.

Blue-Yellow perimetry, Short-Wavelength-Sensitive pathway, forward light scatter, learning effects, glaucoma.

ACKNOWLEDGEMENTS

I thank my supervisor, Dr JM Wild, for his guidance, encouragement and help, and the Royal National Institute for the Blind for their financial support of this research.

I also thank the following individuals: Dr D Whitaker for his expert help in the development of the colour contrast sensitivity testing paradigm and his guidance in matters relating to the effects of light scatter on visual function, Mr E O'Neill for providing access to the ocular hypertensive and glaucoma patients; Mr M Hussey and Mr D Shaw for statistical advice; Mr J McCloughlin and the staff of the Glaucoma Department, Birmingham and Midland Eye Hospital for their help in the recruitment of the ocular hypertensive and glaucoma patients; and to all the subjects and patients who volunteered to participate in the clinical studies. Finally, to my family and my fiancé, Karen, for their support whilst writing this thesis.

LIST OF CONTENTS

LIST OF FIGURES

LIST OF TABLES

Chapter 2

Chapter 3

Chapter 4

Chapter 8

LIST OF PLATES

Chapter 4

CHAPTER 1: REVIEW OF AUTOMATED PERIMETRY

1.1 Introduction

The visual field can be described as that portion of space in which objects are simultaneously visible to the steadily fixating eye. It has been likened to "an island of vision surrounded by a sea of blindness" (Traquair 1927) such that large and / or bright stimuli can be seen towards the periphery of the visual field, whilst small and/or dim stimuli may only be detected if they are near to the visual axis. The area in space corresponding to the visual field is a representation of the entire visual system and its' integrity as a whole. Disturbances in function are represented by characteristic defects within the visual field.

The technique of perimetry involves the measurement of the differential light threshold which is defined as the minimum stimulus luminance (ΔL) necessary to evoke a response against a background (L) of a constant luminance. The differential light threshold is represented in units of sensitivity ($L/\Delta L$). The visual field can be examined by two distinct methods: kinetic and static perimetry (Figure 1.1).

Kinetic perimetry involves the movement of a stimulus of constant luminance towards the hill of vision until the stimulus is detected by the centrally fixating patient. The stimulus is usually moved from non-seeing to seeing. The area within which a given stimulus is perceived is known as the stimulus isopter. The size of the isopter depends upon the size, luminance and colour of the stimulus. Traditionally, Goldmann perimetry has employed the kinetic technique. Kinetic perimetry suffers from a number of disadvantages. The size of the recorded isopter is influenced particularly by the reaction time of the patient. Furthermore, the speed and direction of the stimulus movement dictates the reliability of the measured visual field, particularly when the visual field sensitivity is reduced (Aulhorn 1969; Fankhouser 1969; Greve 1973; Stewart and Shields 1991).

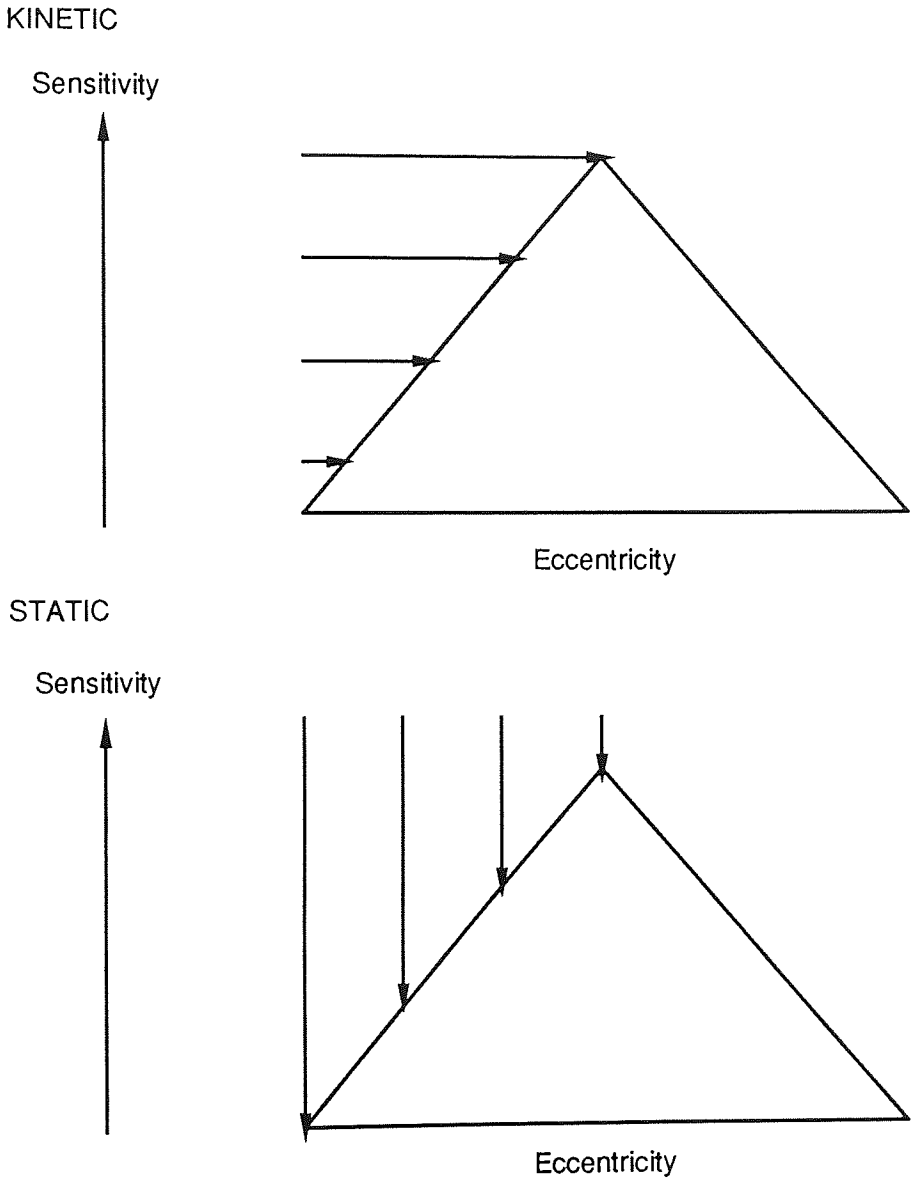

Figure 1.1 Comparison of kinetic (top) and static (bottom) perimetry. Kinetic perimetry involves the movement of a fixed luminance stimulus towards the hill of vision until the stimulus is perceived; static perimetry involves the presentation of a stimulus at a fixed location and the luminance is increased until the stimulus is perceived.

With static perimetry, the stimulus intensity and / or size is discreetly changed until the stimulus is perceived. Although static perimetry is considered to be more time consuming, it is not influenced by the reaction time of the patient (Greve 1975; Trope and Britton 1987). The technique is more precise than kinetic perimetry (Harms 1952; Drance et al 1967; Aulhorn and Harms 1972; Armaly 1971; Trope and Britton 1987) and is better at detecting the isolated scotomata which occur in early glaucoma (Greve and Verduin 1976).

The majority of early glaucomatous defects occur within 30° eccentricity (Gramer et al 1982b; Hart and Becker 1982; Armaly 1971) and are most suited to evaluation by automated static perimetry. However, several reports have suggested a combination of kinetic and static techniques for the investigation of glaucoma (Armaly 1969, 1971, 1972; Greve 1973; Rock et al 1987). Indeed, the use of automated kinetic perimetry for the examination of the peripheral field has shown that approximately 5% of glaucoma patients manifest an abnormal peripheral field but a normal central field to automated static perimetry (Stewart et al 1988; Ballon et al 1992; Miller et al 1989).

An automated perimeter is a perimeter in which "the decision process of the examination strategy is exclusively controlled by computer" (Greve 1983). Automated perimetry facilitates standardization of the stimulus parameters, reproducible examination procedures and extensive data storage and appropriate statistical analysis (Fankhouser et al 1972). It is at least as accurate as conventional manual perimetry with the added advantage of a greater time-saving for the operator. Commercially available automated perimeters differ in terms of the mode of stimulus presentation, the magnitude of the bowl luminance and in the examination strategy (Heijl 1977a; Greve 1983). The stimuli are presented in a pseudo-random order across the field; this procedure improves patient fixation (Heijl and Krakau 1977; Krakau 1978; Aulhorn et al 1979; Keltner and Johnson 1981) and minimises the influence of expectancy of the stimuli (Keltner and Johnson 1981). Randomizing the order and position of perimetric stimuli also results in an enlargement of the size and / or depth of visual field defects compared to that recorded when stimuli are exposed to the patient in a regular sequence (Heijl and Krakau 1977).

The stimulus size, duration and luminance in association with the adaptation level of the perimeter bowl determine the dynamic range of the perimeter. The dynamic range can be defined as the measurement range over which the visual system can be tested with a given set of instrument parameters. It is the range from the maximum stimulus luminance of the perimeter to the threshold luminance of the normal eye (Fankhouser 1979). The response of the visual system to perimetric stimuli is usually defined in terms of sensitivity. The unit of sensitivity is the decibel (dB) where 0dB represents the maximum stimulus luminance of the perimeter. The magnitude of the dynamic range should be as large as possible to permit the maximum range over which sensitivity can be measured. A large dynamic range is obtained by maximising the stimulus luminance and by minimising the background luminance. Extraneous limiting factors restrict the dynamic range of the perimeter, particularly the neural responses within the visual system and the straylight interference within the eye. The maximum stimulus luminance is limited by straylight scattered beyond the geometric boundaries of the stimulus image. The straylight results in an increase in the apparent size of the perimetric stimulus which may reduce the apparent size and depth of a scotoma (Wilson 1967; Weale and Wheeler 1977; Fankhouser and Haeberlin 1980; Dengler-Harles et al 1990; Funkhouser et al 1992b).

1.2. Stimulus Parameters

1.2.1 Stimulus Presentation

Stimuli can be generated through a projection system, by light emitting diodes or by fibre-optic light guides. A projection system permits the presentation of stimuli at any location within the visual field. Variations in the stimulus luminance are achieved by the use of neutral density filters interposed within the stimulus path. The stimulus colour can be altered by the addition of appropriate filters. The use of a single light source facilitates ease of control over the stimulus luminance output. The stimulus size is produced by a set of fixed apertures and the position of the stimulus within the visual field is altered by means of a movable mirror. The main disadvantages of the system are the cost and the vulnerable mechanical construction (Heijl 1984). In addition, the incandescent light source is subject to changes in output over time due to ageing of the bulb.

The accuracy of the position of the mirror, and therefore the accuracy of the stimulus position must also be constantly checked (Heijl 1985a). The sound of the stepper motors which control the position of the mirror may also condition the patient as to when to respond to a possible stimulus (Taylor et al 1984).

The use of LED stimuli limits the number of stimulus locations within the visual field. The available number may be increased, however, by altering the patient's fixation point. The size of the LED stimulus cannot be varied and a high frequency pulse current is used to adjust the luminance of the stimulus. The directional properties of the LED emission demands accurate mounting within the perimeter bowl and the individual diodes require calibration. LEDs have the advantage of being silent in operation, mechanically robust and relatively cheap (Taylor et al 1984). Some perimeters utilise LEDs mounted in apertures within the bowl surface giving rise to the effect of black-holes on the surface. Black-holes on the perimeter bowl are thought to produce changes in local retinal adaptation (Mills 1985; Heijl 1985; Flanagan et al 1988). However, localised adaptational effects are only thought to have marginal clinical significance (Britt and Mills 1987). In other instruments, the LED stimuli are mounted behind a translucent film to avoid the 'black hole' effects.

Fibre optics can be used to guide light from a centrally located tungsten light source to fixed stimulus locations. Compared to the other techniques of stimulus projection, this is a relatively expensive method of stimulus generation but offers a consistent luminance level and a facility to alter the stimulus colour (Mills 1984). It is difficult to retain a constant spectral response from a tungsten light source since there is a shift towards longer wavelengths at low intensities. The stimulus luminance has therefore to be altered by the use of neutral density filters in the presence of a constant voltage supply. This procedure cannot easily be achieved and fibre-optic instruments are more suited for supra-threshold examination than for threshold evaluation (Phelps 1985).

1.2.2. Stimulus duration

The duration of the stimulus is relatively less important compared to the consideration of the background and stimulus luminances in controlling the dynamic range of the instrument. The stimulus duration of the perimeter is governed by the law of temporal summation - Bloch's Law:

$$\Delta L \,.\, T = \text{constant}$$

where ΔL is the differential threshold and T is the duration of the stimulus.

The law only applies to stimuli with a duration of less than the critical time. The critical time at which sensitivity is independent of stimulus duration varies with eccentricity, stimulus size and adaptation level (Barlow 1958) and is in the region of 60-100ms. The latency of saccadic eye movement varies between 50-250ms (Robinson 1964). Longer stimulus durations will therefore encourage saccadic eye movements away from fixation occur on presentation of the stimulus. A further argument against the use of long stimulus durations is the potential for temporal summation to increase in diseased eyes (Wilson 1970). In most perimeters the stimulus duration is defaulted at durations between 100ms and 200ms.

1.2.3. Stimulus size

The dynamic range of the perimeter can be extended by increasing the stimulus diameter (Fankhouser 1979). The increase in dynamic range occurs due to the increase in spatial summation. In the central retina, spatial summation can be described by Ricco's Law and Piper's Law:

$$\Delta L^{k} \,.\, A = \text{constant}$$

where ΔL is the differential threshold, A is the stimulus size and k is the coefficient of summation.

When k=1, Ricco's Law is operative and when k=0.5 Piper's Law becomes valid. Goldmann was aware that the coefficient, k, varied with retinal position but concluded that a value of k=0.8 was a good approximation out to 30° (Goldmann 1945a, b). The coefficient of summation also increases with increase in eccentricity and with decrease in adaptation level and in stimulus duration (Fankhouser and Schmidt 1960; Gougnard 1961).

Automated static perimetry utilizes larger stimuli compared to kinetic perimetry since they enhance the dynamic range and are more resistant to optical degradation (Fankhouser 1979; Heijl 1985a; Atchison 1987; Radius 1978; Greve 1979; van den Berg 1987; Wood et al 1987b). The default stimulus in automated perimetry is a Goldmann size III (0.431°) which reduces the influence of optical defocus and media opacities (see Chapter 4), but saturates the sensitivity in the central retina (Wild et al 1986; Wood et al 1987b). Larger stimuli (sizes III and V) demonstrate a smaller within- and between-test fluctuation (Gilpin et al 1990; Wall et al 1993) and a higher mean sensitivity (MS) compared to smaller stimuli in normal eyes (Sloan 1961; Choplin et al 1990; Wall et al 1993). This latter finding can be explained on the basis of an increase in spatial summation with larger stimuli due to an increase in receptive field coverage (Johnson et al 1978). A greater capacity for spatial summation has been reported in glaucoma patients compared to normals (Fellman et al 1989).

The use of a larger stimulus size has been advocated in cases of advanced field loss recorded with smaller stimulus sizes (Fellman et al 1989; Wilensky et al 1986; Zalta 1991). Indeed, more recently Zulauf and Caprioli (1993) have recommended the use of a size V stimulus if more than 10% of the stimulus locations have absolute loss to a stimulus size III or if the MS falls below 15dB. Conversely, the use of a Goldmann size I has been advocated in the early detection of glaucoma (Zalta and Burchfield 1990; Uyama et al 1993), since larger stimuli saturate the central 10° and are insensitive for the early detection of abnormality in this region (Wild et al 1986; Wood et al 1986). However, Gunderson et al (1993) were unable to detect additional glaucomatous field loss utilizing a size I stimulus compared to size III and V stimuli. The use of small stimuli has also been advocated in the examination of neuro-ophthalmological patients (Matsumoto et al 1991). Small

stimuli in conjunction with high density stimulus grids are considered to be more appropriate for the detection of small scotomata. Straylight effects within the eye increase the apparent size of the stimulus and a stimulus presented within a small scotoma may in fact be seen by the patient due to the spread of the stimulus onto normal regions of the retina (Bek and Lund-Anderson 1989). However, Dengler-Harles et al (1993) found little differences in the global indices for stimulus sizes I and III in cases of diffuse glaucomatous field loss.

1.2.4. Stimulus location density

The probability of detecting localised areas of reduced sensitivity by static perimetry depends not only on the number of stimulus locations examined but also on the spatial configuration of the locations (Greve 1975; Bebié et al 1976b; Fankhouser and Bebié 1979; Johnson and Keltner 1981). The spatial arrangement may be varied according to which disease the test program is designed to detect (Johnson and Keltner 1981). Greve (1975) calculated that 452 stimulus locations would be required to detect focal loss 3° in diameter within 30° of fixation with 95% confidence. Conversely, Johnson and Keltner (1981) demonstrated that the detection of focal loss was optimal using 140-150 stimulus locations in the testing configuration.

Three possible options exist for the density of stimulus locations: systematic sampling, higher density sampling in areas of the visual field at risk or a combination of both systematic and higher density sampling (Gutteridge 1984).

Systematic sampling utilizes a constant separation of the stimulus locations across the field. The default interstimulus separation is 6° and the stimuli are displaced by 3° either side of the horizontal and vertical midlines. The choice of this grid is based upon the findings of Fankhauser and Bebié (1979), who found that the probability of detecting focal loss of 8.4° diameter using a 6° interstimulus square grid was 100%, whilst a 6° diameter area of focal loss was detected on 79% of occasions. However, the probability of detecting focal loss less than 2° in diameter, was low and independent of the type of stimulus grid utilized (Fankhauser and Bebié, 1979). Furthermore, an increase in the density of stimulus locations increases the total examination time (Fankhauser and

Bebié 1979). Nevertheless, King et al (1986b) demonstrated that a grid resolution as fine as 6° was not adequate for the identification of scotomata in the central field of the size and depth of the physiological blind spot and Wild et al (1986) considered that straylight within the eye was the reason for the inability of a 6° grid to detect scotomata of similar to the size of the blind spot.

However, Weber and Dobek (1986) advocated the utilization of a 3° interstimulus square grid within 10° eccentricity, a 4.2° grid between 10° and 20° eccentricity and a 6° grid between 20° and 30° eccentricity for the optimal detection of glaucomatous visual field defects. The Octopus G1 program incorporates an increasing resolution with decrease in eccentricity, such that a 2.8° resolution is achieved within the macular area (Flammer et al 1987). The G1 program has been demonstrated to improve both the detection and the assessment of visual field defects when compared to a 6° interstimulus square grid of the Humphrey Field Analyser (Gloor and Gloor 1986; Dannheim 1987). A 6° interstimulus square grid is also considered to be suitable for the detection of visual field loss due to chiasmal and suprageniculate lesions.

Stimulus density can also be increased by the combination of two or more separate programs. In addition, specific regions of the field can be examined in more detail by the use of customised programming which permit independent control over the selection of the stimulus locations. Alternatively, a program (SAPRO) has been described which continually modifies the spatial resolution within an examination on the basis of the patient response. A coarse grid is employed in areas of normal sensitivity, whilst an increasingly finer grid is employed in areas of apparent visual field loss (Fankhauser et al 1981; Häeberlin et al 1983; Funkhouser and Fankhauser 1985). Asman et al (1988), however, found that such spatially adaptive techniques did not improve sensitivity or specificity when employed in conjunction with a threshold-related, supra-threshold program.

Recent reports have investigated the possibility of reducing the number of stimulus locations in order to reduce the examination time whilst retaining sensitivity and specificity. Weber and Diestelhorst (1992) demonstrated that programs with a reduced number of stimulus locations can

be very accurate in the follow-up of glaucomatous visual field loss. Indeed, theoretical calculations show that trend analysis can be improved if the reduction in examination time is combined with a greater frequency of examination (Weber and Diestelhorst 1992). Furthermore, Zeyen et al (1993) have suggested that by utilizing the stage concept in which the examination is divided into subsets of stimulus locations the option is provided to curtail the test when sufficient information has been gathered. In addition, reducing the number of stimulus locations has been shown to increase the MS and reduce the SF due to a reduction in the magnitude of the fatiguing effect (Fujimoto and Adachi-Usami 1992a, b). Conversely, Heijl (1993) argued that the density of stimulus locations is not a limiting factor in the early detection of glaucomatous defects since early defects exhibit an increased variability over a wide area of the visual field. Therefore, simply repeating the examination on a further occasion would be as effective as performing two fields with inter-locking stimulus locations to increase the resolution of the stimulus configuration.

1.2.5. Adaptation Level

An adaptation level of 10.0cdm^{-2} (31.5 asb) is the standard used in commercially available automated perimeters. Fankhouser (1979) calculated that reducing the background from 10cdm^{-2} to 1.3cdm^{-2} (4 asb) would increase the dynamic range at 50° eccentricity by 12 dB, whereas, due to a reduction in spatial summation, the gain in the central visual field would be only 3-4 dB. Furthermore, the use of a size III (0.431°) stimulus compared with a size I (0.108°) amounted to a gain of 19dB in dynamic range at 50° eccentricity. Alternatively, the use of a 10.0cdm^{-2} (31.5 asb) background luminance requires less pre-adaptation and is less prone to changes in ambient room illumination (Heijl 1985a). Furthermore, a background luminance level below 10.0cdm^{-2} offers no diagnostic advantage (Heijl 1985a).

The relationship between the change in background luminance, L, and the consequent change in the threshold stimulus luminance, ΔL, is equivocal. In the photopic range (greater than 31.8cdm^{-2} ie greater than 100 asb) the Weber-Fechner Law ($\Delta L/L$=constant) is considered to be operative. In the low photopic and mesopic ranges, however, the Rose-de-Vries Law ($\Delta L/L^{0.5}$) applies. Several reports suggest that the Rose-de-Vries Law is applicable to perimetry

(Fankhouser and Bebié 1979; Flanagan et al 1991b) whilst other studies consider the Weber-Fechner law to be more appropriate (Greve 1973; Aulhorn and Harms 1972; Klewin and Radius 1986).

A number of studies have proposed that visual field investigation repeated at different levels of adaptation may be of use in the differential diagnosis of ocular disease (Jayle and Aubert 1958; Greve 1979; Nara 1979). Greve et al (1977) demonstrated that examination under mesopic and photopic conditions could discriminate between maculopathies and central neuropathies. Dark- and light-adapted perimetry has been used to classify types of retinitis pigmentosa (Mamor et al 1983; Jacobsen et al 1986). Perimetry performed under dark-adapted conditions has also been suggested to be of use in the detection of early glaucoma (Drum et al 1986; Quigley et al 1991; Glovinsky et al 1992). These latter studies were only able to demonstrate a diffuse loss in scotopic sensitivity. Indeed, the inability of dark-adapted perimetry to detect focal glaucomatous loss has been demonstrated by Felius et al (1993).

Use of higher adaptation levels have also been suggested to enhance the detection of visual defects. Wilson (1968) demonstrated at an adaptation level of 214.5cdm^{-2} (674 asb), abnormalities of both temporal and spatial summation in lesions of the post-geniculate pathways and abnormalities of spatial summation, only, in pre-geniculate ganglions. Shiga (1968) reported a greater depression of isopters relative to those for the normal eye in the early stages of glaucoma and third neuron disease at a background of 70.0cdm^{-2} (220 asb) compared to 222.8cdm^{-2} (700 asb). Paige (1985) enhanced the detection of early visual field loss at an adaptation of 100.3cdm^{-2} (315 asb) compared with 10.0cdm^{-2} (31.5 asb) in a mixed sample of glaucoma suspects, glaucoma patients and neurological patients using a modified Humphrey Field Analyser. Conversely, Asman and Heijl (1988) demonstrated no difference in the apparent depth of glaucomatous focal loss recorded at 1.0cdm^{-2} (3 asb) and 100.3cdm^{-2} (315 asb).

1.3. Examination Strategy

All automated perimeters employ a form of static examination strategy. The type of strategy depends upon whether the instrument is designed for screening, accurate measurement and follow-up of established field loss or a combination of both.

1.3.1. Suprathreshold (supraliminal) strategies

One level strategy

Stimuli can be presented across the visual field at single luminance regardless of eccentricity. Due to the decline in sensitivity of the hill of vision with increase in eccentricity, the apparent brightness of the stimulus increases towards fixation. Thus small relative defects at the fovea may be missed. The sensitivity of this type of test is increased if a lower luminance stimulus is presented. This single-level approach therefore has limited uses (Gramer et al 1981, 1982a) but a large number of locations can be examined in a minimum amount of time (Bebié et al 1976a; Fankhouser 1979).

Gradient-adapted luminance strategy

An alternative single-level approach involves presentation of stimuli at a constant luminance above threshold at each location across the field ie stimuli are presented at increasing brightness to allow for the decline in sensitivity of the hill of vision with eccentricity (Greve 1980). This type of examination is termed gradient adapted. The brightness of the stimuli towards the periphery of the field can be increased by increasing the stimulus bulb brightness, by increasing the size of the stimulus or by reducing the magnitude of neutral density filters across the visual field. Although both the single intensity and gradient-adapted methods are one-level strategies, the gradient adapted strategy has a greater ability to detect focal defects (Keltner 1979).

Threshold-related gradient-adapted

The gradient-adapted approach relies on knowledge of the pre-defined hill of vision for a normal observer (Fankhouser et al 1977; Li et al 1979; Schmied 1980). However, an inter-individual

variation in normal sensitivity of approximately 2dB is present in individuals of the same age (Verriest and Israel 1965; Greve and Wijnans 1972). Heijl (1984) suggested that such variation may approach 10dB depending on the reliability of the patient, the pupil size and the quality of the media. To account for the inter-individual variations, a threshold-related approach may be employed whereby the threshold of a number of central locations is measured prior to supraliminal screening. The supraliminal intensities at each location are then based upon the measured central thresholds, and the decline in sensitivity with eccentricity. The magnitude of the stimulus luminance is 4-6dBs brighter than the expected threshold. Threshold-related tests have a greater sensitivity and specificity than a simple one-level test. A further refinement of the test procedure measures the depth of any defect identified by the supraliminal stimulus. This type of test is usually termed 'quantification of defects' (Heijl 1977a, Heijl 1985b). Although gradient-adapted threshold related tests offer the optimum format for suprathreshold examination, they may fail to detect early shallow glaucomatous defects particularly if the level of the initial threshold has been incorrectly estimated (Stewart et al 1989).

1.3.2. Threshold

Threshold estimations in perimetry attempt to record the precise contour of the hill of vision. In manual static perimetry, threshold is determined using a modification of the psychophysical technique known as the 'method of limits' (Guilford 1954). The technique consists of a series of stimuli whose luminance is increased from an infraliminal level until the stimulus is perceived ie becomes supraliminal. Threshold is usually estimated in automated static perimetry using another modified psychophysical technique, the 'up-and-down' staircase or bracketing procedure developed by Stiles and Crawford (1934). This technique is more precise but requires computerisation for it to be of use in clinical perimetry (Fankhouser et al 1972; Koch et al 1972). The average number of stimuli required for the 'up and down' method is greater than the less reliable 'method of limits' (Bebié et al 1976a). The precise methodology for determining threshold depends upon the type of perimeter. The response to a single stimulus presentation contributes to the standard psychophysical frequency-of-seeing curve regardless of the threshold technique. The frequency-of-seeing curve describes the relationship between the probability of seeing a

stimulus at a given location and the property of the stimulus. The stimulus luminance at which the frequency of perception is 50% is defined as threshold for the given location and the curve is a characteristic S-shaped function (Cornsweet 1970) (Figure 1.2). The threshold value is surrounded by a transition zone, where the frequency of detection of a stimulus ranges from 0% to 100%. A threshold coefficient (ΔT) can be defined as the difference in the stimulus luminance which produces a positive response on 50% of occasions compared to that on 84% of occasions (Bebié et al 1976a, b). The curve may be a cumulative Gaussian function arising from physiological variability or a Poisson curve arising from variations in the number of photons stimulating a given receptive field (Weber and Rau 1992). Strategies for the determination of threshold will be discussed more fully in Chapter 3.

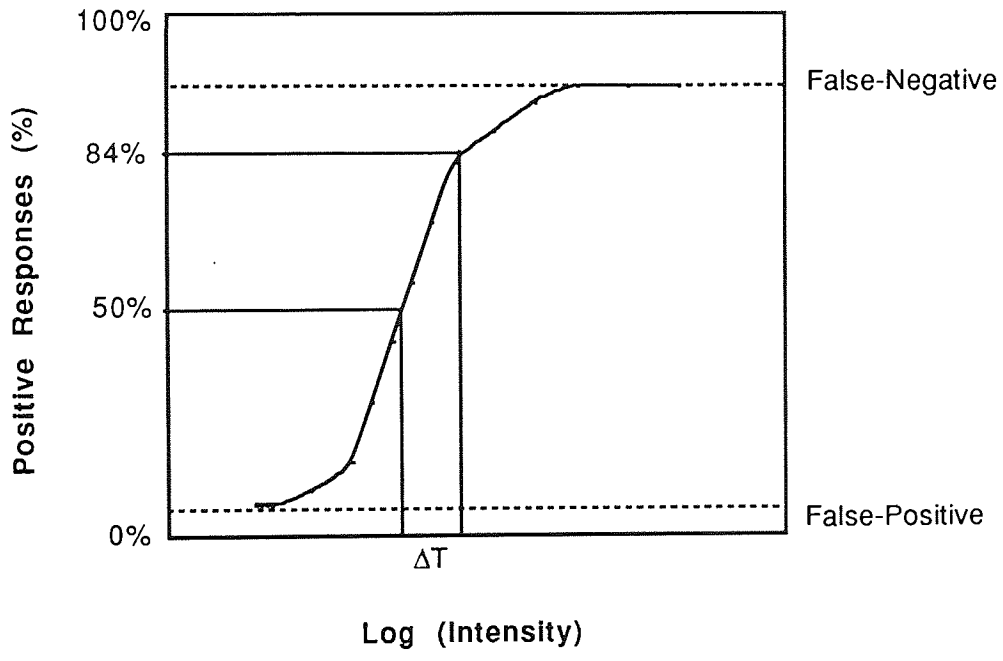

Figure 1.2. The standard frequency-of-seeing curve or psychometric function. Threshold is defined as the intensity at which a stimulus is seen 50% of the stimulus presentations. The difference in the stimulus luminance (ΔT) from which a stimulus is seen 50% to 84% is termed the threshold coefficient.

1.4. Threshold Fluctuation

Due to the nature of the threshold estimation, the threshold estimate at a given location varies both within a single visual field examination and between examinations.

Short-Term Fluctuation (SF)

The fluctuation at a given location which arises during a single automated visual field examination is termed the local short-term fluctuation (SF) (Bebié et al 1976b; Flammer et al 1984a, b). The estimation of local SF is based upon the standard deviation of two threshold estimates at a given stimulus location. The SF for the entire field (the global SF) can be calculated from a double determination of threshold at each of the stimulus locations or can be estimated from the double determination of threshold at a limited number of locations. The calculation of SF varies upon the type of perimeter. The formula for calculation of the SF for the Humphrey Field Analyser is:

$$\text{Global SF} = \sqrt{\left\{1/10 \sum_{i=1}^{10} S^2_{2i}\right\} \left\{1/10 \sum_{i=1}^{10} (X_{i1} - X_{i2})^2 / 2S^2_{2i}\right\}}$$

where X_{i1} is the threshold from the first estimate at location i, X_{i2} is the second threshold estimate, the weighting function or the normal intra-test variance at stimulus location i is denoted by S^2_{2i}.

The statistical weighting procedure gives greater emphasis to stimulus locations positioned more centrally where the fluctuation in threshold is less (Brenton and Phelps 1986). The weighting function serves to minimise the value of SF in normals (Heijl et al 1987c). The SF calculation for the Octopus perimeter does not utilize a weighting function (Bebié et al 1976b; Flammer et al 1985; Flammer 1986).

The calculation of SF, with the Humphrey Field Analyser is based on the double determination of threshold at ten pre-determined stimulus locations within 21° eccentricity. The standard threshold strategy also repeats a threshold measurement if the initial estimate differs from an expected age-matched value or adjacent stimulus location by more than 4dB. Flanagan et al (1993a)

demonstrated that the magnitude of the SF increased with an increase in the number of stimulus locations requiring a repeated threshold estimate. Furthermore, they found that calculation of global SF based upon the 10 standard stimulus locations underestimated the SF in patients with glaucoma. Indeed, Bebié et al (1976b) had previously shown that the estimation of SF with two threshold estimates at ten stimulus locations, only provided an estimate of SF within 44% of the true value at a 95% confidence level. Additionally, Casson et al (1990) demonstrated that a more reliable approach to the estimation of SF could be obtained by increasing the number of threshold determinations at a fewer number of stimulus locations. Nevertheless, it is important to obtain a representative measure of the fluctuation of the entire visual field. Indeed, Flanagan et al (1993a) suggested that a more realistic measure of SF might be obtained if all locations were to receive a double determination of threshold. The value of the SF achieved by this approach is likely to be within 19% of the true value of SF at a 95% confidence level (Schulzer et al 1990). The magnitude of the SF has been shown to be greater with the Octopus perimeter than with the Humphrey Field Analyser by approximately 0.3dB (Brenton and Argus 1987). However, Fankhouser et al (1988) considered the differences in the SF to be an 'artifact' of the Humphrey Field Analyser arising from the design of the threshold strategy. The estimation of threshold by the algorithm of the Humphrey Field Analyser is based upon the last 'seen' stimulus, whereas the Octopus perimeters use the average of the last 'seen' and 'not seen' stimulus to estimate threshold.

An alternative approach to the estimation of SF has been proposed by Schulzer et al (1990). They applied a polynomial function to describe the distribution of sensitivity across the field. The difference between the measured threshold and that described by the polynomial indicated the mathematical SF. The mathematical SF correlated well with the SF calculated using the Root Mean Square approach applied to the repeated estimates of threshold (Mills et al 1990). The value for the mathematical SF was within 25% of the SF derived by the Root Mean Square approach at a 95% confidence level.

The SF increases as the mean sensitivity decreases (Holmin and Krakau 1976; Flammer et al 1984b). It is larger in glaucoma patients than in normal subjects and is larger around the borders of

scotomata (Flammer et al 1984a). This latter finding may be due to fixation instability (Henson et al 1991; Eizenman et al 1993; Vingrys and Demirel 1993). However, Safran et al (1992) reported an increase in SF from 1.63dB to 2.65dB when the brightness of the perimeter fixation target was increased from 12.5cdm^{-2} to 435.0cdm^{-2}. They suggested that local adaptation effects may adversely effect the steadiness of fixation thereby resulting in an increased within-test variance.

An increased SF may also be an early sign of developing glaucoma in ocular hypertensive (OHT) patients (Werner and Drance 1977; Flammer et al 1984a; Gloor et al 1984; Rabineau et al 1985; Sturmer et al 1985). This has been explained on the basis of 'adaptive mechanisms' which compensate for areas of nerve fibre drop out. Such mechanisms serve to maintain normal sensitivity but at the expense of an increase in the local SF (Flammer et al 1984b). The magnitude of the local SF increases with increasing depth of scotoma, until the scotoma becomes absolute after which the SF decreases (Flammer et al 1984c).

Some authors have reported that the SF is independent of eccentricity out to 30° eccentricity for both manual (Werner et al 1982) and automated perimetry (Flammer et al 1984b; Flammer and Zulauf 1985). Most studies, however, report an increase with increase in eccentricity (Aulhorn and Harms 1967; Greve and Wijnans 1972; Werner and Drance 1977; Donovan et al 1978; Brenton and Phelps 1986; Heijl et al 1987a, c; Langerhorst 1988; Rutihouser et al 1989). Pupil size has a small effect on SF in glaucoma patients: a decrease in pupil size produces an increase in the SF (Flammer et al 1984b). The magnitude of the SF is greater for smaller stimulus sizes (Gilpin et al 1990), but is independent of the background intensity (Crosswell et al 1991) and stimulus duration (Pennebaker et al 1992). Some studies have reported an increase in the SF with increase in age (Haas et al 1986; Autzen and Work 1990; Chauhan et al 1990b) and the SF is also higher in patients with general health problems (Langerhorst et al 1989a). The magnitude of the SF in both manual and automated perimetry is dependent on the degree of perimetric experience and the level of patient fatigue (Heijl 1977b; Heijl et al 1989a; Wood et al 1987a; Werner et al 1988, 1990; Wild et al 1989c; Autzen and Work 1990; Gloor et al 1991; Marchini et al 1991;

Searle et al 1991a, b; Hudson et al 1994). Learning and fatigue effects will be reviewed fully in Chapter 5.

Long-Term Fluctuation (LF)

The LF is defined as the variation in threshold over time that cannot be accounted for by the SF, learning effects and age. The LF can be divided into two components (Bebié et al 1976b; Flammer et al 1984c). The uniform variation across the field between examinations is termed the homogeneous component (Ho), whilst the localised variation is termed the heterogeneous component (He). The two components are derived by the statistical technique of analysis of variance,using the root mean square of the variance estimates. The components can be calculated from a double determination of threshold at any number of stimulus locations (Flammer et al 1983, 1984a, c). The normal value for each of the two components is approximately 0.5dB and 0.2dB for the Ho and He components respectively and 1.2 and 0.5dB in glaucoma (Flammer et al 1984c). Furthermore, the magnitude of the LF in glaucoma suspects lies between those of normal and abnormal. The Ho component of the LF can be considered as the fluctuation of MS or MD over time, whilst the He is the localised fluctuation between adjacent points, within the visual field, after consideration of the overall fluctuation (Zulauf and Caprioli 1991). Other studies have considered the long-term fluctuation as a total component (Rutihauser et al 1989; Katz and Sommer; Heijl et al 1987b, 1989b; Werner et al 1989; Boeglin et al 1991).

The magnitude of the LF increases with an increase in defect depth (Boeglin et al 1991; Flammer et al 1984c; Heijl 1977b; Heijl et al 1989b, 1991; Piltz and Starita 1990; Zulauf et al 1991; Werner et al 1991). Indeed, Zulauf et al (1991) demonstrated an increase in variance of $0.5dB^2$ for each dB decrease in sensitivity. The LF also increases with an increase in eccentricity in the normal eye (Heijl et al 1987; Rutishauser and Flammer 1988) and in glaucoma (Boeglin et al 1991; Zulauf et al 1991). Whether LF increases with age is unclear (Katz and Sommer 1987; Heijl et al 1987b); however LF is correlated with SF (Flammer et al 1984b; Hutchings et al 1993) and increases in patients with poor general health (Langerhorst et al 1989a).

1.5. Assessment of reliability

Automated perimeters assess the reliability of the patient within a given visual field examination by calculating the number of false-positives and false-negative responses and the number of fixation losses. A false-negative trial involves the presentation of a stimulus at a luminance considerably brighter than the threshold defined earlier in the examination at the same location. The absence of a response by the patient indicates a lack of attention. A false-positive trial involves the sound attributed to the presentation of the stimulus but without the stimulus. A response to the absence of a stimulus indicates a lack of co-operation during the test. Fixation can be monitored by the use of a video monitor and by the presentation of a stimulus of maximum luminance positioned on the centre of the blind spot. This latter technique is termed the Heijl-Krakau method (Heijl and Krakau 1975a, b). A positive response to the blind-spot stimulus from the patient indicates a fixation loss. The efficiency of the technique has recently been called into question (Fankhouser 1993) in cases of pericaecal field loss involving the blind spot since eye movements may not be detected. In addition, straylight within the eye may result in the stimulus being detected beyond the borders of the blind spot (Fankhouser and Haeberlin 1989).

A field is usually designated as unreliable if the number of fixation losses are greater than 20% or if the number of false-positives or false negatives are greater than 33%. The number of false-negative responses are more prevalent in glaucomatous eyes and increase as the field loss becomes more advanced (Heijl et al 1987a; Katz and Sommer 1988; Reynolds et al 1990). Reynolds et al (1990) also found a positive correlation between the number of fixation losses and the number of false-positives. A false-positive response may occur at the same time as a blind spot presentation occurs. The perimeter software is unable to differentiate between the two type of responses and the response is recorded as a fixation loss rather than as a false-positive error (Fankhouser 1993). Indeed, approximately 40% of glaucomatous eyes and 27% of normals can be considered unreliable based upon the criteria of greater than 20% fixation losses and greater than 33% false-positives or false-negative responses (Enger and Sommer 1987; Katz and Sommer 1988). However, an increased number of false-positive responses may occur in individuals who lack perimetric experience (Bickler-Bluth et al 1989; Sanabria et al 1991), or result

from the fatiguing effect due to prolonged examination time (Heijl and Drance 1983). Furthermore, Bennett et al (1991) demonstrated that the reliability of the field was not correlated with the test-retest reproducibility in young normal subjects. Katz et al (1991) reported that 36% of normals, 51% of ocular hypertensive patients and 68% of glaucoma patients had at least one unreliable field over a 3-4 year period which may result from excessive fixation (Johnson and Nelson-Quigg 1993). They recommended that increasing the fixation loss criterion of the perimeter to 33% would be more appropriate to achieve 5% confidence limits. Age, pupil diameter and visual acuity do not influence the number of false responses (Katz and Sommer 1988; Bickler-Bluth et al 1989).

An alternative approach to the control of fixation is the use of eye-movement based perimetry. This type of perimetry is based upon the patient's saccadic eye movement which occurs on the presentation of the stimulus (Trope et al 1989). Periodic eye movements avoid prolonged central fixation which has been shown to increase the magnitude of the central threshold, the level of stress and boredom (Singer et al 1977). Eye-movement perimetry has been shown to be 100% sensitive in detecting glaucomatous field defects but has low specificity due to the inability of the technique to detect small eye movements and it remains unclear whether a patient changes fixation as a response to a stimulus or merely by chance alone. Although an accurate eye tracker has been developed (Eizenman et al 1984), eye-movement perimetry as an alternative to conventional fixation perimetry currently remains a research application.

The upper limits of the normal values for the catch trials dictate the utility of false-positives, false-negatives errors and fixation losses in the early detection of glaucoma. A balance exists between a field in which an increasing number of false-positives, false-negatives errors and fixation losses is caused by a disease process and one in which a field is considered to be unreliable. A considerable amount of time is spent checking the reliability of the patient during a perimetric examination. Increase in the examination time increases the fatiguing effect that occurs in perimetry (Heijl 1977b; Heijl and Drance 1983; Holmin and Krakau 1979; Johnson et al 1988a; Searle et al 1991a, b; Marra and Flammer 1991; Wild et al 1989c,1991b; Hudson et al 1994). As a

consequence, other parameters have been suggested for the assessment of patient reliability which do not increase the examination time. Olsson et al (1989) utilized a mathematical approach based upon the staircase procedure to estimate threshold and the normal frequency-of-seeing curve to estimate the frequency with which false-positive and false-negative responses occur. Consequently, there was an improvement in the accuracy with which false-positives and false-negatives could be estimated and a reduction in the examination time (Olsson et al 1994a). Lee et al (1991) suggested calculating the number of inconsistent responses introduced by the patient during the bracketing procedure used to estimate threshold. Whilst Zulauf et al (1992) also suggested calculating the number of stimulus presentations within a given perimetric examination to indicate the reliability of the patient. This latter approach has been adopted by Wu et al (1994) for assessing reliability in glaucoma patients. Currently, these alternatives to estimate the reliability of patient responses during a perimetric examination have not become accepted into current perimetric threshold strategies.

1.6 Representation of Sensitivity

Perimetric sensitivity can be represented by a variety of methods, depending on the type of perimetry performed. The computer capacity of automated perimeters allows many mathematical and statistical manipulations to be applied to the data.

1.6.1 Numerical Representation

The representation of the results from supra-threshold examination are usually displayed by a given symbol defining the presence of normality or abnormality. In threshold automated perimetry, sensitivity is specified in terms of decibels (dB) which is a logarithmic representation of the stimulus luminance referenced to the maximum luminance of the stimulus.

$$\text{Sensitivity (dB)} = k + 10 \log \left(L/\Delta L\right)$$

In the case of the Humphrey Field Analyser, when $L=10cdm^{-2}$ (31.5 asb) and the maximum stimulus luminance = $3183cdm^{-2}$ (10000 asb),

$$\text{Sensitivity (dB)} = 25 + 10 \log \left(L/\Delta L\right)$$

The display of numerical values is considered to be the most accurate form of representation, however, the display of such values from a large number of stimulus locations is difficult to interpret (Greve 1982).

1.6.2 Graphical Representation

Grey Scale

The grey scale notation is used to display the sensitivities recorded across the field (Heijl et al 1977a; Fankhouser 1979). A series of greys is assigned to the range of sensitivities for the given perimeter whereby increasingly darker shades of grey represent increasingly lower sensitivity values. The display incorporates a continuous grey scale rather than the presentation of discrete symbols at the given location. The interpolated grey scale is derived from the measured sensitivities at the four adjacent locations. Different forms of interpolation have been compared. Weber and Geiger (1989) concluded that linear interpolation in specific horizontal and vertical meridia was preferable to other forms of interpolation since it resulted in a smoother outline to the borders of a scotoma. Graphical displays do not adequately represent diffuse visual field loss (Flammer 1986). Furthermore, differences in the dynamic range between perimeters dictates that the shade of grey assigned to a given sensitivity value differs as a function of the type of perimeter.

3-D Representation

Sensitivity can also be represented three-dimensionally (Haas et al 1986; Jaffe et al 1986) allowing the topography of the field to be visualised. Three-dimensional plots do not enhance the diagnostic capability and are more appropriate for presentation purposes. Caution must be exercised when comparing three-dimensional plots, since the scales allocated to the stimulus locations and to the sensitivity together with the orientation of the plot must all be identical (Hart and Hartz 1982; Wild et al 1987).

Bebié Curve

The Bebié curve displays the defect depth at all the given test locations in the format of a cumulative curve (Bebié 1985, 1990; Bebié et al 1989). The defect depth is defined as the difference between the recorded sensitivity at a given location and that of the age-matched normal sensitivity. The Bebié curve ranks the stimulus locations according to the depth of defect. The stimulus locations with the smallest defect depth are displayed towards the left side of the cumulative curve and the stimulus locations with the largest defect depth are displayed towards the right hand side of the curve. The characteristics of the shape and slope of the curve indicate the type and extent of the field loss. Pure diffuse damage is characterised by a curve displaying an overall reduction in sensitivity with the slope of the curve parallel to that for the curve of a normal field. Localised defects are characterised by a steepening of the curve with respect to the normal curve. A mixture of both diffuse and focal loss results in a combination of the two types of curve, allowing a differentiation of field loss resulting from local and diffuse damage (Kaufmann and Flammer 1989). The Bebié curve suffers from the disadvantage of a lack of information regarding the spatial characteristics of the field loss (Asman and Heijl 1989).

1.7. Statistical Representation

1.7.1. Visual Field Indices

The graphical representations of visual field data permit a rapid view of the visual field. However, such displays do not differentiate true general or localised loss from deviations due to patient variability (Flammer 1986). The visual field indices have been devised to highlight various characteristics of the measured field at the expense of less important aspects of the data. They are calculated from the sensitivity at each stimulus location. The indices were first developed for the Octopus system (Flammer et al 1985; Flammer 1986) and later for the Humphrey Field Analyser by Heijl et al (1987c). The Humphrey indices incorporate a weighting function to account for the intra- and inter-subject variation in sensitivity across the visual field. The weighting function is based on the deviations in sensitivity in the mid-periphery of the field encountered in the normal observer. Such deviations are considered to have a greater probability of occurring due to random

fluctuation than do the deviations in the central field. A recent study demonstrated that the Humphrey field indices were able to correctly identify 80% of patients with glaucoma (Wood and Bruce 1993). This is consistent with the findings for the equivalent indices of the Octopus perimeters (Flammer et al 1985).

Mean Sensitivity (MS)

The mean sensitivity (MS) is the arithmetic mean of the differential light sensitivity at all stimulus locations examined within the visual field. The magnitude of MS is not influenced greatly by localised fluctuations in sensitivity or by localised scotomata but is sensitive to generalised reductions in sensitivity. The MS can be defined as:

$$MS = {}^{1}/_{n} \sum_{i=1}^{n} X_i$$

where $X_i = {}^{1}/_{m} . \sum X_{ik} . X_{ik}$, the average of the local thresholds at location i, X_i is the local threshold at location i, which is replicated on m occasions, n is the number of stimulus locations.

Mean Deviation (MD)

The mean deviation (MD) is based upon the arithmetic mean of the difference between the measured sensitivity and the age-corrected normal value at each of the tested stimulus locations. A worsening of the field is represented as a negative value. The MD is affected by a diffuse depression of the hill of vision and can be defined as:

$$MD = \left\{ {}^{1}/_{n} \sum_{i=1}^{n} (X_i - N_i) / S^2_{1i} \right\} / \left\{ {}^{1}/_{n} \sum_{i=1}^{n} 1 / S^2_{1i} \right\}$$

where X_i is the measured threshold, N_i is the age-corrected normal threshold at stimulus location i and S^2_{1i} is the variance of the normal thresholds at location i. The number of test locations (excluding the blind spot) is denoted by n.

The mean defect is the equivalent term for the Octopus perimeters. The mean defect does not incorporate a weighting function. A positive mean defect represents a worsening of the hill of vision.

Pattern Standard Deviation (PSD)

PSD represents the local non-uniformity of the hill of vision (Heijl et al 1987c) and is similar to the loss variance (LV) on the Octopus perimeter (Flammer 1986). The magnitude of the PSD is influenced by the presence of localised defects and by the magnitude of the short-term fluctuation. The magnitude of the PSD increases as the depth of the non-uniform loss increases. PSD can be defined as:

$$PSD = \sqrt{\left\{1/n \sum_{i=1}^{n} S^2_{1i}\right\} \left\{1/n-1 \sum_{i=1}^{n} (X_i - N_i - MD)^2 / S^2_{1i}\right\}}$$

where X_i is the measured threshold, N_i is the age-corrected normal threshold at location i, S^2_{1i} is the variance of the normal thresholds at location i, MD is the mean deviation, and n is the number of test locations (excluding the blind spot).

Corrected Pattern Standard Deviation (CPSD)

The CPSD allows a differentiation of localised (or non-uniform) reductions in sensitivity due to disease from that resulting from localised fluctuations in sensitivity (Flammer et al 1985). The CPSD is similar to the corrected loss variance (CLV) for the Octopus perimeters and can be defined as:

$$CPSD^2 = PSD^2 - k(SF)^2$$

where k is a correction factor (1.28 for Program 30-2 and 1.14 for Program 24-2) to account for the narrower spatial distribution of the ten stimulus locations utilised for calculation of the SF compared with the distribution of the locations involved in the PSD calculation.

Heijl et al (1987c) suggested that the weighting function would minimize the effects of variability on the magnitude of the SF and the PSD in normal eyes.The LV does not incorporate a weighting function and is given as the variance (dB^2) instead of the standard deviation (dB). Flanagan et al (1993a) compared the visual field indices calculated with and without the weighting function. They found that the weighting function slightly increased the magnitude of the SF, the PSD and the CPSD but made little difference to the MD. Similarly, Fankhouser and Funkhouser (1991) demonstrated that in early glaucoma patients, the indices mean defect and mean deviation could be interchanged.

As the index for uniform loss (MD) worsens, the index for non-uniform loss (CPSD, CLV) tends to zero. Indeed, Pearson et al (1990) were able to demonstrate a good correlation between mean defect and corrected loss variance (R^2=0.85) for early to moderate visual field loss (mean defect of <18dB). However, the CLV declined in cases where the mean defect was greater than 18dB. Different stages of the glaucomatous disease process may therefore result in different relationships between the CLV and the MD (Gollamundi et al 1988; Pearson et al 1990). The use of global indices have been shown to lack sensitivity for detecting small changes over time (Chauhan et al 1990a). Similar visual field indices have been proposed for the automated kinetic perimetry (Capris et al 1989).

Third Central Moment (M3) and Skewness (Q)

The third central moment (M3) was introduced for the Octopus perimeters and considers the distribution of the deviation of measured values from the expected values and can be scaled with respect to the LV to calculate the degree of skewness (Q) (Brechner and Whalen 1984). Both the M3 and the Q are theoretically more sensitive than the MD, LV and CLV for detecting small localised defects within the visual field. The cubed function within the calculation emphasises a defect. The M3 can be defined as:

$$M3 = {}^{1}/_{n} \sum_{i=1}^{n} (N_i - MD - X_i)^3$$

where n is the number of stimulus locations, N_i is the age-corrected normal threshold at location i, MD is the mean defect and X_i is the measured threshold.

The skewness (Q) can be defined as:

$$Q = {}^{M3}/_{\sqrt{(LV)^3}}$$

The Q statistic becomes less sensitive as the extent of the field loss increases or if the sensitivity of the field is uniformly depressed. However, Pearson et al (1989) reported that the Q statistic was of little use in the detection of glaucoma. They suggested that the Q statistic would be insensitive to early glaucoma which manifests as an increased SF, a cluster of depressed stimulus locations or a general reduction in sensitivity.

Spatial Correlation (SC)

The clustering of abnormal stimulus locations is particularly important in the detection of glaucomatous visual field loss. The spatial correlation (SC) index was developed by Bebié (1985). SC is defined as the average value obtained when the mean defect at each stimulus location is multiplied by the loss at each of its adjacent locations:

$$SC = {}^{1}/_{p} \sum_{(ij)} (Z_i - MD - X_i)(Z_j - MD - X_j)$$

where p is the number of pairs involved in the summation and the terms i and j indicates a summation over pairs of adjacent test locations. If defects are small and random then the correlation decreases but if the defects are clustered the correlation increases.

Defect Volume (DV)

The defect volume is defined as the difference between the volume of the normal field and that of the measured field. The DV utilises the three dimensional characteristics of the visual field (van den Berg et al 1985; Langerhorst 1985; Langerhorst et al 1987a) and can be defined as:

$$DV = \sqrt{n'^2 \cdot \partial^2} / (2n - 2) + n' \cdot \partial^2$$

where n and n' represent the normal and depressed test locations and ∂ and ∂' are the respective standard errors.

Congruence Index

The spatial configuration of the visual field loss permits the localization of the site of the damage along the visual pathway. In neurological cases, the congruence between the right and left visual fields becomes important. The closer a post-chiasmal lesion is to the visual cortex, the greater the degree of congruence of the field loss (Harrington 1971). Weber (1993) devised an objective index termed the congruence index to assess the similarity between the right and left visual fields. It was based upon the differences in variance at each test location between each field. The local sensitivity L of any location i of the right visual field is expected to be:

$$L_{ri} = GM_r \pm \sqrt{GV_r}$$

where GM is the global mean and GV is the global variance of all the local differences between the measured sensitivity and the age-related sensitivity at a location i. For the left side of the field:

$$L_{li} = GM_l \pm \sqrt{GV_l}$$

The local difference of these two locations on each hemifield is expected to be:

$$L_{ri} - L_{li} = GM_r - GM_l \pm \sqrt{(GV_r + GV_l)}$$

The global variance of local lateral differences is expected to be:

$$GV(\Delta L_i)\ \text{expected} = GV_r + GV_l$$

When the expected value is compared to the true variance of lateral differences the congruence index CI can be defined:

$$CI = GV(\Delta L_i)\ \text{expected} / (\Delta L_i)\ \text{true}$$

To decide whether there is homonymous or heteronymous congruence, a combined index, can be given:

$$CCI = \log (CI_{homonymous} / CI_{heteronymous})$$

Homonymous CI compares similar locations and heteronymous CI makes a comparison after transposition of one of the fields about the vertical plane. The magnitude of the CCI is greater than 1.0 in homonymous congruence and less than 1.0 in heteronymous congruence.

Diffuse Loss Index

Early glaucomatous loss may manifest as either a diffuse reduction in sensitivity or a focal reduction in sensitivity or a combination of both (Airaksinen et al 1984, 1985b; Anctil and Anderson 1984; Caprioli et al 1987a; Glowazki and Flammer 1987; Drance 1991). However, the presence of diffuse loss in glaucoma has been called into question by some studies (Heijl 1989a; c; Heijl and Asman 1994; Langerhorst et al 1989b). Aspects of diffuse and focal field loss in glaucoma will be discussed in more detail in Chapters 5 and 6.

The simplest analytical technique of separating diffuse and focal field loss is by the cumulative defect or Bebié curve (Bebié 1985, 1989; Bebié et al 1990; Kaufmann and Flammer 1989). The standard perimetric index MD is also unsuitable for quantification of the diffuse component since it also is contaminated by any areas of localised loss within the field. Langerhorst et al (1988, 1989b) devised an alternative index to estimate the diffuse component of visual field depression - the general reduction in sensitivity (GRS) index. The GRS index suffers from the disadvantage that it is difficult to treat statistically, furthermore where a hypersensitivity is recorded at a number of stimulus locations the index may underestimate the degree of visual field depression (Funkhouser et al 1992a). A further refinement termed the diffuse loss (DL) index has been devised by Funkhouser (1992a) which ignores the sensitivity at locations exhibiting high degrees of fluctuation or when it is outside certain predefined limits.

1.8. Statistical Interpretation of the visual field

Interpretation of the results of automated static threshold perimetry necessitates a precise knowledge of the normal hill of vision and the factors which influence its variability. Furthermore, the exclusion of extraneous factors is equally important in the determination of visual field progression. Knowledge of these factors is particularly important for the separation of cases of early visual field loss from those exhibiting physiological variability. Deviations of the measured threshold from the age-corrected normal threshold (Bebié 1985, Heijl et al 1987b) require further clinical interpretation. In the normal eye, the deviation of threshold at any given stimulus location from that of the corresponding age-matched normal value was initially assumed to exhibit a Gaussian distribution (Bebié 1985; LeBlanc 1985; Fankhouser and Bebié 1979; Bebié et al 1976b). Furthermore, the between-subject variability at each stimulus location in the normal eye was also assumed to be independent of eccentricity. As a consequence, deviations of 5dB or more were considered to be abnormal (Fankhouser et al 1979; Wilensky and Joondeph 1984; Anderson 1992). However, the within-test between-subject variability in sensitivity increases with eccentricity (Brenton and Phelps 1986; Katz and Sommer 1986; Heijl et al 1987b,1988). Furthermore, the distribution of measured sensitivity in a normal population at each stimulus location is now considered to be non-Gaussian exhibiting negative skewness and positive kurtosis at most stimulus locations (Heijl et al 1987b, 1988).

Heijl et al (1987c) introduced two empirical probability maps: the total deviation probability map and the pattern deviation probability map. These account for the normal variation in sensitivity and delineate the statistical significance with which a measured sensitivity at any given stimulus location departs from the expected normal value. A deviation in sensitivity which is statistically significant from the normal age-matched sensitivity is highlighted by use of an appropriate symbol. Probability maps were originally introduced by Schwartz and Nagin (1985); however their model assumed constant between-subject variability across the field and normal distributions of sensitivities.

Total deviation probability map

The total probability map indicates the frequency with which the measured sensitivity at each individual location deviates from that found in the normal age-matched population.

Pattern deviation probability map

The pattern probability analysis indicates the frequency with which the measured sensitivity at each individual stimulus location deviates from that found in the normal age-matched population having adjusted for any overall differences in the height of the measured hill of vision. The overall height of the hill of vision is defined as the seventh highest ranked deviation in sensitivity compared to the age-matched normal population. The probability plots separate the general reduction in sensitivity, arising from such factors as media opacities, pupillary miosis and defocus from the localised reduction in sensitivity.

Glaucoma Hemifield Test (GHT)

Glaucomatous visual field loss is not usually symmetrical about the horizontal meridian (Hart and Becker 1984; Mikelberg and Drance 1984). Statistical techniques have been introduced which compare the sensitivity between the two hemifields (Duggan et al 1985; Sommer et al 1987; Asman and Heijl 1992a, b). The Glaucoma Hemifield Test (GHT) was developed by Asman and Heijl (1992a). This test utilises the probability maps (Heijl et al 1987c) to compare the sensitivities between the two hemifields. The field is divided into 10 anatomical sectors based upon the retinal nerve fibre bundle pattern. Each tested location is given a probability score based upon the pattern deviation probability map (Heijl et al 1987c), where a high score represents a greater depth of defect. For each of the 10 sectors the sum of the probability scores is determined. The difference between the scores of the mirror-image sectors in the two hemifields is then calculated and compared to that in the normal population. Recently, a colour coded probability map has also been introduced to assist the differentiation between localised and diffuse visual field loss (Asman 1994).

Cluster Analysis

Cluster analysis has been used to evaluate visual field damage in glaucoma. The technique investigates the spatial relationship between two or more stimulus locations (Chauhan et al 1989b, c) and is based upon the premis that clusters of locations exhibiting reduced sensitivity are more common in a glaucomatous visual field rather than in the normal field (Heijl et al 1989d; Chauhan et al 1989b, c).

The selection of appropriate clusters of stimulus locations has been defined in terms of the nerve fibre bundle pattern (Sommer et al 1987; Werner et al 1989; Chauhan et al 1989b, c; Heijl and Asman 1989; Asman and Heijl 1991, 1992a, c, 1993), from an empiric perimetric retinal map (Weber 1991) or from patterns of actual glaucomatous field loss (Mandava et al 1992, 1993). A more objective approach has been used by Suzuki et al (1993) using the VARCLUS procedure, which in addition to being compatible with nerve fibre layer anatomy was mathematically optimal, accounting for the relationship between adjacent stimulus locations, in the choice of the sectors. An expert system for cluster analysis has been developed by Fankhouser et al (1993).

The indices calculated from localised areas of the field may be more sensitive at detecting early localised loss than those calculated from the global indices (Chauhan et al 1989b, c; Asman and Heijl 1993). In addition, averaging the sensitivity within a selected region may reduce the effects of long-term fluctuation within specific regions of the field and facilitate the detection of changes in the visual field (Werner et al 1989; Chauhan et al 1990a; Asman et al 1992; Mandava et al 1993).

Computer Interpretation

The interpretation of visual field data is demanding and time-consuming, and requires a considerable degree of experience. When the field cannot be easily interpreted, incorrect or inappropriate clinical decisions can be made (LeBlanc 1985).

An expert system, OCTOSMART interprets visual field results within a set criteria (Bebié 1990). Although assisting the clinician in the decision making process, the system is limited by extraneous factors such as previous perimetric experience of the patient or change in pupil size. Furthermore, the interpretation of the field is only as good as the predefined criteria (Kaufmann et al 1990; Hirsbrunner et al 1990).

Several studies have applied neural networks to visual field interpretation (Goldbaum et al 1990, 1994; Shields and Trick 1990; Kelman et al 1991; Nagata et al 1991; Martin-Boglind and Wanger 1991; Keating et al 1992; Mutlukan and Keating 1994; Henson et al 1994). In comparison to expert systems, neural networks have the ability to learn from previous experience. The network can be likened to the nervous system such that input units correspond to dendrites and output units to axons. Mutlukan and Keating (1994), applied a PC-based neural network to a series of 135 simulated fields and 100 neurological and 200 glaucomatous fields. A classification accuracy of 91-97% and 65-100% respectively was achieved with the simulated and actual fields. Henson et al (1994) have also demonstrated the capability of such systems to monitor the progression of glaucomatous visual field loss.

Change Analysis

Visual field examination is important in the monitoring of the progression of disorders such as glaucoma. When changes in the field are extensive little demand is placed on the clinician in the interpretation of loss. However, subtle changes in the field in the presence of a variable patient response can make the interpretation of changes attributable to the disease process more difficult.

The numeric sensitivity values, the cumulative defect curve of Bebié, the grey scale and probability plots display the entire field. The serial analysis of fields over a period of time displayed in this manner becomes more difficult. Between-test threshold variability is high in glaucomatous visual fields. This makes it difficult to differentiate between the fluctuation in sensitivity due to

chance and that due to true change (Heijl et al 1989b; Holmin and Krakau 1979; Flammer et al 1984; Werner et al 1989).

Progression of glaucomatous visual field loss can also be evaluated by the slope derived from the univariate linear regression of a given index against time (Holmin and Krakau 1982a, b; Wu et al 1987; Wild et al 1989a; Heijl et al 1991; O'Brien et al 1990; Hitchings et al 1994). The field loss may progress in a number of ways, namely an enlargement and deepening of existing scotoma and / or the appearance of new defects (Mikelberg et al 1984). The index can express the field as a whole (Holmin and Krakau 1980; Holmin et al 1982), a particular region of the field or for each individual stimulus location (O'Brien and Schwartz 1990; O'Brien et al 1991; O'Brien and Schwartz 1993; Hitchings et al 1991; Hoskins et al 1989; Noureddin et al 1991).

The difference between the actual distribution of sensitivities across the field at a given visit and the predicted distribution of sensitivities derived from a suitable mathematical model may provide information on whether the field has deteriorated in a predictable manner or whether an episodic change has occurred (Wild et al 1989a, 1991a, 1993). These authors proposed two models: a topographical model and a longitudinal model. The topographical model used a second order polynomial to describe the sensitivity at any stimulus location and defined the shape of the hill of vision. The longitudinal model used a linear function based upon the sensitivity at a given stimulus location determined at one or more previous examinations. The approach differed from other linear regression analysis in that it did not use time as a continuous parameter and only two previous field examinations were required to estimate sensitivity. In glaucoma patients, the central field could be modelled to within 3dB of the actual recorded sensitivity. Application of the visual field model can be applied to situations where confirmation of glaucomatous visual field progression is required. Like all forms of linear regression analysis it suffers from the disadvantage that it does not account for the lack of independence of the individual locations (Chauhan et al 1989c).

Various graphical packages have been developed to delineate the progression of visual field loss. STATPAC, the analytical package for the Humphrey Field Analyser (Heijl et al 1987c) (subsequently updated to STATPAC 2) offers various printout options to identify the progression of visual field loss. The Overview printout condenses the grey scale, decibel plots, the total and pattern probability plots into four columns. A more critical evaluation of the pointwise numeric change can be obtained using the Compare program. A follow-up field is compared to a baseline field; a negatively displayed value represents a deterioration of sensitivity. The identification of progression of visual field loss for both types of printout, relies upon the judgement of the clinician (Anderson 1992). The Glaucoma Change Analysis printout identifies the frequency with which the pointwise degree of change could have occurred in a stable glaucomatous field. Consideration is given to the field location, the initial threshold at the given location and the initial MD in the interpretation of change (Heijl et al 1991). The Glaucoma Change Analysis printout also provides a plot of the MD over time. An analytical summary of changes in the global field indices (SF, MD, PSD, CPSD) from the first to the nth field for each examination is provided in the Change Analysis printout (Heijl et al 1991). The corresponding MD slope in dB / year and the significance of the slope is displayed. Additionally, box plots for each field display in percentile format the full range of recorded deviations from the normal reference field (Heijl et al 1987c). The Change Analysis printout provides a more objective evaluation of evaluating visual field loss (Shin et al 1991). Tuulonen and Airaksinen (1991a) demonstrated that the level of agreement between the Statpac 2 Glaucoma Change Probability printout and the standard clinical evaluation of progression varied between clinicians with the correlation upto an R^2 of 0.87.

The statistical package for the Octopus perimeter is program DELTA, which allows evaluation of normality or progression (Gloor et al 1980; Bebié and Fankhouser 1981). A statistical t-test on visual field data selected from two of examinations is carried out to determine whether change has occurred in MS (Fankhouser and Jenni 1981). Program DELTA is thought to be too sensitive and insufficiently specific in differentiating between random fluctuations and real change in sensitivity (Gramer et al 1993); furthermore, the distributions of sensitivity values under comparison are frequently non-Gaussian and have different standard deviations (Hills and Johnson 1988).

A graphical analysis of topographical trends (GATT) (Weber and Kriegelstein 1989) is based upon the interpolated greyscale maps of two comparison fields and is incorporated in the software package PERIDATA for the Humphrey and Octopus perimeters (Brusini et al 1991). GATT produces a number of characteristic patterns depending upon the stability of the sensitivity at each field location. A series of alternate black and white stripes are used to indicate change in the visual field. Vertical orientation of the stripes signifies that a given location in the current field has improved whilst a horizontal orientation indicates a deterioration. The program also displays results in chronological order in both a numeric display and a graphical display (ie grey scale or Bebié curve).

Multi-dimensional vector field analysis has been used for observing serial visual field changes at each stimulus location (Cyrlin et al 1991). The proportionate change in sensitivity from a baseline value can be displayed for up to sixteen fields. Trend analysis of the proportion change is used to indicate the significance of the changes over time. The 'Progressor' program, a colour coded display, has been used to delineate visual field progression (Noureddin et al 1991; Poinoosawmy et al 1993; Fitzke and McNaught 1994). A bar chart is displayed at each stimulus location. The length of each bar indicates the depth of any defect and the colour coding indicates the statistical significance of the slope of the linear regression of sensitivity against examination time. Significant regression slopes that are negative (ie deteriorating) are displayed in red ($p<0.05$) or bright red ($p<0.01$). Nonsignificant regression slopes are indicated in yellow whilst outliers are indicated in blue.

A graphic bar or stack histogram was described by Weber and Papoulis (1993) in which the stimulus locations are ordered from lowest sensitivity at the bottom of the bar to highest sensitivity at the top. The grey scale assigned to each sensitivity is then used to construct the grey scale bar.

1.9. Factors affecting the visual field

1.9.1. Age

The results from all psychophysical tests are age dependent, whereby sensitivity declines with age (Ross et al 1985a). Contraction of the peripheral isopters with age has been demonstrated using manual kinetic perimetry (Feree et al 1929; Goldmann 1945a; Drance 1985a). Haas et al (1986) recorded using static automated perimetry a linear decline in static sensitivity with age, declining on average by 0.58dB per decade. The reduction in sensitivity was greater for the superior field and in the periphery (greater than 30°), compared to that in the inferior and central areas. A decline in sensitivity with age was also noted by Jaffe et al (1986), Heijl et al (1988) and Johnson et al (1989b). The reduction in sensitivity in the peripheral field between 30°-60° eccentricity with age is upto 0.4dB per decade, compared to 0.6dB in the central field (Brenton and Phelps 1986). Brenton and Argus (1986) suggest the greater decline in sensitivity in the peripheral field with age (Haas et al 1986; Brenton and Phelps) may be explained by the effect of trial lens rim artifacts on the peripheral field. Interestingly, Zalta (1989) suggested that trial lens rim artifact may influence the superior visual field on 3.3% of occasions and the overall field on 6.2% occasions.

Most studies concerning the effect of age on perimetric sensitivity have reported a linear decrease in sensitivity with an increase in age. Johnson and Choy (1987) however demonstrated a greater loss of sensitivity for eyes over the age of 50. The age-related reduction in sensitivity is not accounted for solely on the basis of pre-retinal factors such as a decrease in the transmission of the ocular media (Pokorny et al 1987; Norren and Vos 1974, Savage et al 1993) or a reduction in the pupil size (Weale 1992). Indeed, a reduction in the efficiency of the neural system or random cell loss have been suggested to account for the age-related decline in visual field sensitivity (Johnson et al 1989b; Weale 1992).

1.9.2. Refractive Error

Several reports have considered the effect of defocus on visual function (Feree 1931; Marmor and Gawande 1988). Using manual perimetry, Sloan (1960) and Fankhouser and Enoch (1962) demonstrated that defocus increased threshold particularly for small stimulus sizes. Sloan (1960) and Atchison (1987) demonstrated that the effect was greatest in the central field recorded with manual perimetry. Weinreb and Perlman (1986) reported similar results using automated Octopus perimetry; where they found a 2 dioptre blur resulted in a reduction of sensitivity of approximately 2.5dB at eccentricities greater than 6°. However, Henson and Morris (1993) concluded that uncorrected refractive error was unlikely to affect the sensitivity of the threshold-related suprathreshold strategy in the detection of localised glaucomatous visual field loss, due to its general effect on the field.

Other studies have considered the effect of peripheral refractive error on the visual field. Wild et al (1988) found that correction of the peripheral refractive error had little influence on the MS and SF. However, it has also been suggested that differences in peripheral refractive error within an eye may result in localised reductions in sensitivity termed refraction scotomata (Greve and Verduin 1972; Aulhorn and Harms 1972; Greve 1973).

Interest is growing in new perimetric procedures which employ either flickering (Lachenmayr et al 1989, 1991a, b, c; 1992a, b, 1994; Lachenmayr and Drance 1992a, b; Lachenmayr and Gleissner 1992; Tyler 1981) or coloured stimuli (Sample and Weinreb 1989, 1990, 1992; Sample et al 1988a, 1993a, b, c, d, 1994; Johnson et al 1988b, c, 1989a, b; 1993a, b, d; Adams et al 1991; Hart et al 1990; Flanagan et al 1991a; deJong et al 1991, 1993; Heron et al 1988; Weinreb and Sample 1991; Hudson and Wild 1993; Casson et al 1993b; Lewis et al 1993). Lachenmayr and Gleissner (1992) compared the effect of refractive defocus on both conventional perimetry and flicker perimetry in a sample of normal subjects. Defocus of one dioptre reduced the MS by approximately 3dB, but had no noticeable effect on flicker perimetry. Indeed, Tyler (1991) found no reduction in sensitivity to flicker stimuli for a defocus of 10 dioptres. Johnson et al (1993d) using the technique of Blue-Yellow (B-Y) colour perimetry demonstrated that a defocus of 8

dioptres produced only a 1-2 dB reduction in B-Y sensitivity compared to an attenuation of 8 dB for conventional W-W perimetry.

1.9.3. Pupil Size

The transmission of light through the pupil is less effective at the periphery due to a decrease in the effective pupil area, the rate of which decreases more slowly than the cosine of the angle of eccentricity (Spring and Stiles 1948; Jay 1962). Although the summation of the peripheral retina is better than that centrally, a small correction for the reduction in pupil area is required in terms of perimetric sensitivity: 0.07 dB at 40°, 2.8dB at 70° and 7.6dB at 96° eccentricity (Greve 1973). Differences in pupil size are thought to have little effect on the kinetic visual field determined using a manual approach (Drance et al 1967; Williams 1983).

Pharmacological agents have a profound effect on the size of the pupil. The drug, pilocarpine, is a parasympathomimetic agent and although it reduces intraocular pressure it has the side-effect of producing pupillary miosis and accommodative spasm. Pharmacologically induced miosis, in normals, causes isopter constriction with the Goldmann perimeter (Engel 1942; Day and Scheie 1953; Forbes 1966). The reduction in pupillary area can be correlated with the reduction in isopter area (McCluskey et al 1986). In patients with retinitis pigmentosa, mydriasis produces no significant change in visual field area with Goldmann perimetry (Lam et al 1992). In automated perimetry, age-related declines in perimetric sensitivity are not thought to occur as a result of age-related reductions in pupil size (Johnson et al 1989b). In the examination of normal eyes and glaucoma patients a deterioration in the MD of approximately 1.0dB results from pupillary miosis (Lindenmuth et al 1989; Webster et al 1993). Other studies have demonstrated an equivalent improvement in sensitivity following dilation of the pupil (Forbes 1966; Wood et al 1988; Reboleda et al 1992) although these changes in sensitivity are considered to be clinically insignificant (Lindenmuth et al 1990). Webster et al (1993) discussed reasons for the effects of pupil size on the visual field sensitivity. As the pupil constricts the retinal illumination falls; the influence of change in pupil size on the visual field must be considered with respect to the Weber-Fechner Law:

$$\Delta I / I = \text{constant}$$

where the perceived change in the stimulus luminance the change in luminance required would vary in proportion to the luminance of the background. For cone function, the Weber-Fechner Law is thought to be constant over a range of 3 log units (Hart 1987). A reduction in pupil size reduces both the background and the stimulus intensity, sensitivity remains constant. At low levels of retinal illumination, the Weber-Fechner Law is believed to increase, such that a greater stimulus intensity is required to reach threshold (Klewin and Radius 1986). Furthermore, when the pupil diameter is less than 2.4 mm, the effects of diffraction become significant (Campbell and Gubisch 1966) which reduces the quality of the retinal image. Conversely, a reduction in the pupil size may reduce the effect of optical aberrations, increasing the depth of focus. The optimum pupil size to balance the positive and negative effects of pupillary miosis is thought to be 2.4mm (Tate and Lynn 1977).

1.9.4 Experience and fatigue

Perimetric experience results in an increase in sensitivity and a more reliable response from the patient. This is confounded by the fatiguing effect which results in a decrease in sensitivity, the magnitude of which increases with the duration of the examination and opposes any learning effect. Learning and fatigue effects will be fully discussed in Chapter 5.

1.9.5. Quality of the optical media

Perimetric sensitivity is reduced in the normal and abnormal eye as a result of light scatter, absorption and image distortion arising from imperfections in the quality of the optical media. The effects of the ocular media on the hill of vision will be discussed in Chapter 4.

1.9.6. Inter-Ocular Effects

The extent to which the visual fields of both eyes of a given individual are symmetrical is an important consideration in perimetry. Frequently, between eye comparisons of data are made in

cases of unilateral or asymmetric disease. Indeed, Brenton et al (1986) found that pointwise asymmetry between the two visual fields of normal subjects ranged from 0.0dB to 9.0dB with the greatest difference occurring in the superior hemifield. A pointwise asymmetry greater than 6.0dB was found to occur in less than 1% of stimulus locations, whilst an asymmetry in the global MS exceeding 1.4dB was found to occur on less than 1% of normal subjects. Indeed, Feuer and Anderson (1989) considered that the difference in MS between the two eyes (0.65dB) in a normal individual was less than the measurement error incurred when testing the same eye twice (0.7dB). They considered that abnormality was indicated by a 2.0dB between-eye difference in MS at a single examination, or by a 1.5dB between-eye difference in MS confirmed at a second examination, or by a 1.0dB between-eye difference in MS exhibited over four examinations (Feuer and Anderson, 1989). Similarly a difference in the MS of approximately 1.5dB between the two eyes in ocular hypertensive patients has been shown to predict the future onset of glaucoma (Tholen et al 1992; Lewis et al 1993).

Interestingly, Hudson et al (1994) also demonstrated a greater fatiguing effect in the second eye to be examined with the Octopus 1-2-3 perimeter in a sample of ocular hypertensives. There was a deterioration in the MD of 2.14dB in the first eye and a reduction of 2.33dB in the second eye to be examined. Similarly, there was a deterioration of the LV of 5.32dB^2 and 6.02dB^2 in the first and second eyes respectively. This between-eye fatiguing effect has also been demonstrated by Searle et al (1991a, b). Both studies suggest that the confidence limits for normality should account for the observed fatiguing effect in the second eye examined.

1.9.7. Extraneous factors

Zulauf et al (1986) demonstrated that a blood alcohol concentration of 0.08% had little influence on the sensitivity of the central field. However at a higher blood alcohol concentration of 100mg / l, a decrease in the peripheral sensitivity has been reported (Reidel et al 1985). Both studies demonstrated an increase in the magnitude of the SF and a reduction in the overall reliability of the field. In contrast, Wild et al (1990) reported a statistically significant deterioration in the global indices: MD, PSD and CPSD at a blood alcohol level of 50-70mg / l. An impaired response to the

standard reliability trials was also noted in keeping with other studies. Klein et al (1993), as part of the Beaver Dam Eye study, were not able to demonstrate an increased prevalence of open-angle glaucoma in those who heavily smoked or consumed alcohol. Excessive consumption of alcohol however has been associated with centro-caecal visual field defects (Harrington 1971).

The effect of the benzodiazepine drug, diazepam, on the visual field has been reported, with differing results (Haas and Flammer 1985; Elder 1992). Sensitivity decreased slightly and the number of catch trials and the learning effect remained unaffected when the effect of a single 10mg dose of the drug was compared to a placebo (Haas and Flammer 1985). However, Elder (1992) reported a constriction of the visual field in a single patient prescribed 100mg / day for anxiety. Interestingly, the visual field loss improved upon cessation of the treatment. Wild et al (1989b) compared single doses of the antihistamines: triprolidine (10mg), loratadine (10mg and 20mg) and terfenadine (60mg and 120mg) to a placebo on the visual field. Although the SF was significantly higher than the placebo for loratadine, no statistically significant differences compared to the placebo were found for any of the other indices or reliability parameters. Similarly, Mann et al (1989) found no correlation between the visual field indices and dose of either the drugs: Chloroquine (approximately 250mg / day) and Hydroxychloroquine (approximately 400mg / day) when patients were examined retrospectively. In addition, Guttridge et al (1992) demonstrated no repeatable alterations in the visual field as a consequence of the menstrual cycle in 11 perimetrically experienced females.

CHAPTER 2: RATIONALE FOR THE RESEARCH

2.1. Aims of the Research

The research was seen as a natural continuation of the work on automated perimetry previously undertaken within the Department of Vision Sciences, Aston University, Birmingham. The aim of the research was to extend the understanding of Blue-Yellow (B-Y) perimetry. The more detailed aims were to:

a) quantify the influences of forward light scatter and the learning effects on the B-Y visual field.

b) corroborate,with particular emphasis on rigid statistical analysis, the findings of the preliminary reports which indicated that B-Y visual field loss in POAG occurred prior to that recorded using conventional W-W perimetry with particular emphasis on rigid statistical analysis.

c) compare and contrast the findings in ocular hypertension of B-Y perimetry with those of foveal B-Y isoluminance contrast sensitivity.

2.2 Rationale

2.2.1. Evaluation of the FASTPAC strategy

The time required to complete a perimetric threshold examination with the standard 4-2dB strategy is in the order of 10-15 minutes. Previous studies, largely undertaken in the Department, have identified a progressive decline in sensitivity as the duration of the examination increases which has been termed the fatiguing effect (Heijl 1977b, 1983; Johnson et al 1988a; Searle et al 1991a, b; Wild et al 1989c, 1991b; Hudson et al 1994). The need for shorter examination times without loss of accuracy is essential in automated perimetry. Immediately prior to the start of the research, the Department was given the opportunity to participate in the collection of normative data for the commercial release of the FASTPAC strategy by Humphrey Instruments Inc. The strategy involved a stimulus luminance step size of 3dB. Furthermore, the staircase procedure crossed threshold on only one occasion at each pre-determined stimulus location. The aim of the

study was to compare the visual field recorded with the FASTPAC strategy to that recorded with the standard 4-2dB strategy to provide an insight as to whether the FASTPAC strategy might suitable for the subsequent investigation of the B-Y visual field. The sample comprised 98 normal eyes spanning a wide age range.

2.2.2. Evaluation of Blue-Yellow perimetry

The processing of visual information which originates within the retinal photoreceptors proceeds via two major parallel systems which project to different cellular layers within the lateral geniculate body. These two separate systems have markedly different anatomical, physiological and functional properties (DeValois et al 1966; Wiesel and Hubel 1966; Gouras 1968; deMonasterio and Gouras 1975; Lennie 1980; Kaplan and Shapley 1986; Zeki and Shipp 1988; De Yeo and van Essen 1988; Livingstone and Hubel 1988; Bassi and Lehmkuhle 1990).

One system is based upon the P Alpha ganglion cells which constitute about 10% of the total ganglion cell count (Perry and Cowey 1981) and which possess large dendritic fields (10-30μm diameter) and which have large ganglion cell axons (Leventhal et al 1981; Perry and Cowey 1981). Neurophysiologically the P Alpha cells have large receptive fields, a high conduction velocity (21m / s) (Gouras 1968; Schiller and Malpeli 1977), and are responsive to high temporal but low spatial resolution (Derrington and Lennie 1984). Alpha cells correspond to the 'phasic' Y or Magnocellular (M) cells (Shapley and Perry 1986). The other system is mediated by the P Beta ganglion cells which are more numerous than the alpha cells and constitute about 90% of the total number of ganglion cells (Perry et al 1984). The P Beta cells have smaller dendritic fields (10μm diameter) (Perry and Cowey 1981), thinner ganglion cell axons and predominate in the foveal region (Leventhal et al 1981; Perry and Cowey 1981). Neurophysiological studies demonstrate that the P Beta cells possess small receptive fields, a low conduction velocity (13m / s) (Gouras 1968; Schiller and Malpeli 1977) and are responsive to high spatial but low temporal resolution (Cleland et al 1973; deMonasterio 1978; Derrington and Lennie 1984). Beta cells and their neurones are also colour-opponent (Gouras 1968; Schiller and Malpeli 1977; Kaplan and

Shapley 1986; De Yeo and van Essen 1988; Zeki and Shipp 1988). The beta cells have also been termed the 'tonic' X or Parvocellular cells (P) (Shapley and Perry 1986).

The recognition of two main functional pathways originating within the retina has lead to the development of psychophysical tests which proport to selectively investigation either parvocellular (P) or magnocellular (M) function. The P pathways can be preferentially investigated by the use of coloured stimuli and by high spatial frequency luminance contrast sensitivity. The M pathways are particularly sensitive to scotopic levels of illumination, lower spatial frequencies and the perception of flicker at high temporal frequencies. The functional differentiation of these two systems is summarised in Table 2.1.

Property	Geniculate subdivision	
	Parvocellular	Magnocellular
Colour	Yes (colour-opponent)	No (broadband)
Contrast Sensitivity	Low (threshold >10%)	High (threshold (<2%)
Spatial resolution	High	Lower (by 2-3 fold at a given eccentricity)
Temporal resolution	Slow (sustained responses, low conduction velocity)	Fast (transient responses, high conduction velocity)

Table 2.1. Physiological properties of the magno- and parvocellular geniculate divisions

Furthermore, within the parvocellular system chromatic information is mediated by the three kinds of photoreceptors at the receptor level (Wald 1964) and two colour-opponent neural channels in the inner layers of the retina (Hurvich and Jameson 1957). Input from the red and green cone photoreceptors is directed to the red-green (R-G) opponent channel and a blue-yellow (B-Y) channel receives input from the blue, or Short-Wavelength-Sensitive (SWS), cone photoreceptors and from both the Medium-Wavelength-Sensitive (MWS) and Long-Wavelength-Sensitive (LWS) cone photoreceptors (DeValois et al 1966). The P ganglion cells and axons receiving input from

the SWS cones are larger and have faster conduction velocities than the corresponding MWS and LWS ganglion cells (deMonasterio 1979). Luminance information is mediated by the achromatic M-system which receive input from the rod photoreceptors in addition to the MWS and LWS cone photoreceptors. The contribution of the SWS cones to the luminance M-channel remains controversial (Gouras 1969; Ingling and Martinez 1980; Eisner 1980; Stockman et al 1991; DeValois and DeValois 1993). The mechanisms of colour vision processing in the retina can be generalised in Figure 2.1.

The rationale for the recent clinical interest in B-Y perimetry is based firstly upon the sub-divisions of ganglion cell function and anatomy within the visual system and secondly upon the damage that occurs to the ganglion cells in primary open angle glaucoma. Histological studies have demonstrated that 40-50% of the ganglion cell nerve fibres can be lost prior to the development of a confirmed W-W visual field defect in POAG (Quigley et al 1982, 1989). Techniques which evaluate the structural parameters of the optic nerve and reflect the number of ganglion cell axons have been developed to allow the early detection of glaucomatous damage. Indeed, assessment of the retinal nerve fibre layer and of the topography of the optic disc has demonstrated the presence of localised or diffuse defects or a combination prior to any recorded W-W visual field loss (Sommer et al 1977; Pederson and Anderson 1980; Caprioli et al 1987b; Funk et al 1988; Quigley et al 1989; Sommer et al 1991; Tuulonen and Airaksinen 1991b; Airaksinen et al 1983, 1992; Tuulonen et al 1993; Montgomery 1993; Zeyen and Caprioli 1993). A preferential loss of larger diameter axonal fibres has been demonstrated by electron microscopy in animal and human studies of glaucoma (Quigley 1987a, Quigley et al 1988; Glovinsky et al 1991). The larger ganglion cell fibres are selectively damaged in early glaucoma because they are more vulnerable to damage and are positioned in the weakest areas of the nerve head (Quigley 1987a; Radius 1987; Miller and Quigley 1988).

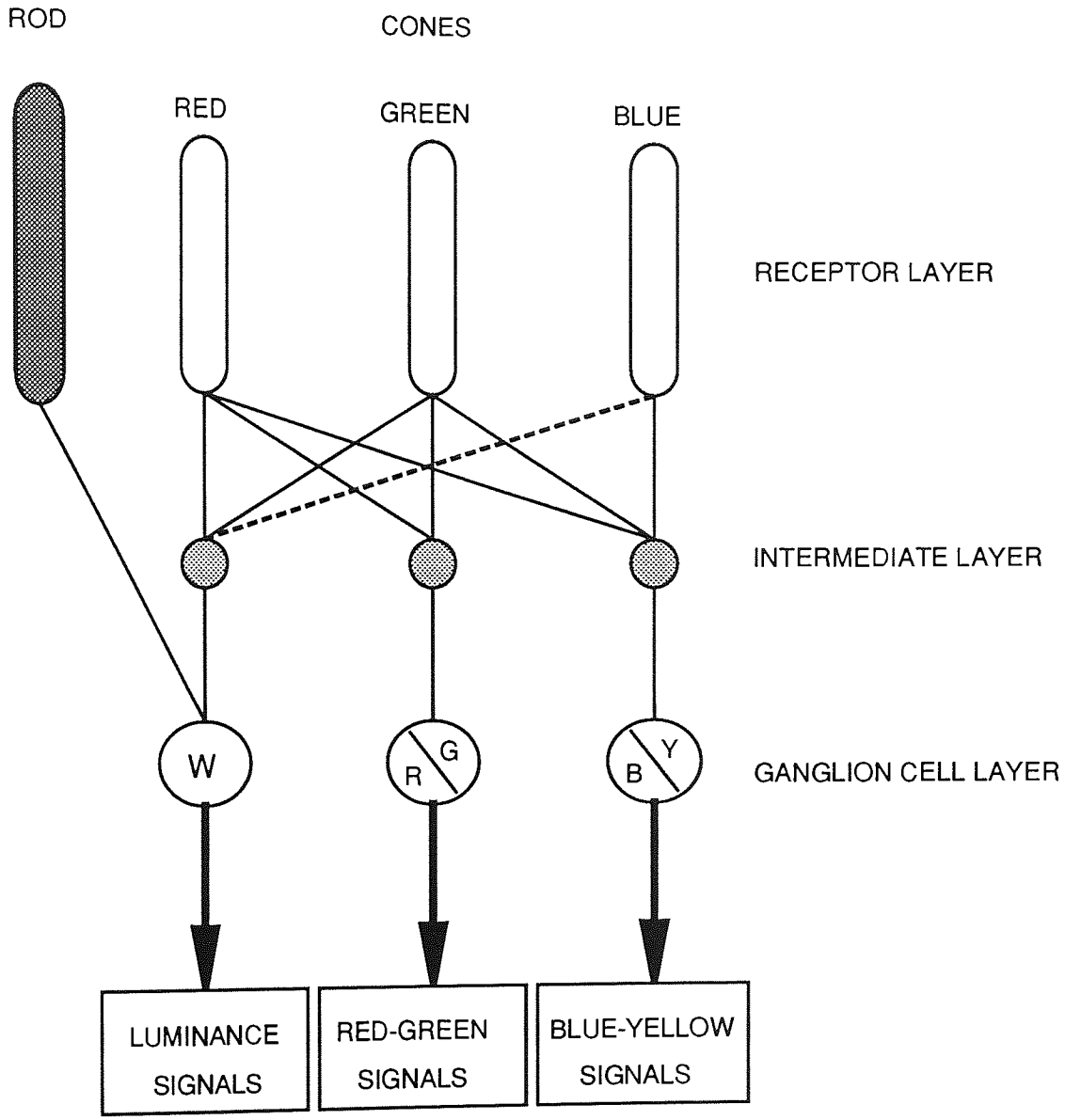

Figure 2.1. Schematic model of chromatic and luminance processing within the early stages of visual processing. The model is based upon a trichromatic input and and a colour-opponent output. Solid lines linking each component of the model represents possible neural inter-connections. The input from the blue or SWS cones into the luminance system channel remains controversial (represented by the hatched line).

The technique of B-Y perimetry selectively investigates the response from the blue or short wavelength sensitive (SWS) pathways. The technique involves the presentation of a blue stimulus on a high luminance yellow background. The yellow background suppresses both the green or medium wavelength sensitive (MWS) and the red or long wavelength sensitive (LWS) pathways. It has been suggested that B-Y perimetry detects glaucomatous visual field loss at an earlier stage of the disease process than conventional W-W perimetry (Johnson et al 1988c, 1993a, b, d; deJong et al 1991, 1993; Flanagan et al 1991a; Adams et al 1991; Sample and Weinreb 1989, 1990, 1992; Sample et al 1986b, 1988a, 1993b, c, d, 1994; Weinreb and Sample 1991; Casson et al 1993b; Lewis et al 1993). Previous research within the Department (Hudson et al 1993; Wild and Hudson 1995) has been concerned with the development of B-Y perimetry for the detection of diabetic maculopathy.

The influence of forward light scatter on the B-Y visual field was unknown. Earlier research in the Department had demonstrated that forward light scatter resulted in a general reduction in sensitivity across the W-W visual field and impaired the interpretation of glaucomatous visual field loss (Wood et al 1987b, 1989; Dengler-Harles et al 1990). The aim of the first study investigating SWS function was to determine the effect of forward light scatter on the B-Y visual field. A control visual field using Yellow-Yellow perimetry was also measured for comparative purposes. Forward light scatter was induced using a scatter solution contained in a specially constructed optical cell placed before the eyes of 15 normal subjects. Perimetry was undertaken using the modified HFA 640 with and without the scatter cell placed before the subjects eye. The method to induce varying amounts of light scatter was identical to that used in previous perimetry studies (Wood et al 1987b, 1989; Dengler-Harles et al 1990). The data were corrected for ocular media absorption using a technique previously adopted for automated perimetry based on the determination of scotopic sensitivity (Sample et al 1988b, 1989; Johnson et al 1988b, 1989a). A second study investigated the effect of forward light scatter on the B-Y visual field in 20 age-related cataract patients. The visual field sensitivities were compared to a sample of 40 age-matched normal eyes with no significant cataract defined using the LOCS II classification system (Chylack et al 1989).

The influence of the learning effect in B-Y perimetry was unknown. The learning and fatiguing effects in W-W perimetry have been extensively investigated in the Department (Wood et al 1987a; Wild et al 1989c, 1991b; Searle et al 1991a, b; Hudson et al 1994). Learning effects are characterised by an increase in sensitivity over time, which occurs both within- and between-examinations. Such effects are opposed by fatigue effects which also occur within- and between-examinations and increase as the examination time increases. It was envisaged that situations might arise where patients could have had prior experience of W-W perimetry but were then subsequently required to undertake a B-Y perimetric examination. Alternatively, B-Y perimetry might be performed as the initial perimetric examination. The influence of prior experience of conventional W-W perimetry on the B-Y field was therefore an important question to be answered. In addition the extent of the B-Y learning effect in those patients naive to any form of perimetric technique was also unknown. A sample of 61 normal subjects performed B-Y perimetry on three consecutive days and after one week. Subjects were stratified into 4 categories according to their age and previous experience of conventional W-W perimetry. Both eyes were examined at each visit. The effects of age, prior perimetric experience and the eye examined were considered in terms of the change in the MS and the SF over the 10 days of examination.

At the onset of the study there was a pressing need to corroborate the reports of Johnson et al (1988c) and Sample et al (1986b, 1988a) which suggested that B-Y perimetry could indicate visual field loss in glaucoma prior to that recorded by W-W perimetry. These early reports considered visual field loss purely in terms of the deviation from age-matched normal controls and failed to take into account any correction for the differences in the shape of the hill of vision (ie the Pattern Deviation). In particular it was therefore considered essential to submit any data to stringent statistical analysis. A study was undertaken to compare B-Y perimetry with that of conventional W-W perimetry in the detection of glaucomatous visual field loss. Fifty-one patients (27 OHT and 24 POAG) underwent W-W and B-Y perimetry using the modified Humphrey Field Analyser. The recorded visual field for each patient was compared to an age-matched normal field constructed from a normal database comprised of 50 eyes (Age Range 60-82 years; 25 eyes in each decade). All normal subjects and patients were experienced in B-Y and W-W perimetry

and had no significant cataract. All normal subjects and patients were individually measured for lenticular absorption using the previously described technique of Sample et al (1988b, 1989). The distribution of between-subject sensitivities across the visual field in the normal control group were analysed and confidence limits for abnormality calculated. Probability maps (Heijl and Asman 1989) were constructed for both the B-Y and W-W visual field data. Most patients were investigated on at least 2 occasions over a period of approximately 18 months.

2.2.3. Evaluation of colour contrast sensitivity

The clinical technique of isoluminance colour contrast sensitivity has been applied in the detection of early glaucomatous damage (Gunduz et al 1988; Falcao-Reis et al 1991; Yu et al 1991). The sample of normal subjects and OHT patients for the B-Y visual fields study underwent a testing paradigm which measured isoluminance R-G CS and B-Y CS using the Venus Neuroscientific Visual Stimulator. This equipment allows independent control over the proportion of red, green and blue output from the phosphors such that only variations in colour contrast and not luminance contrast were required for detection. Hues were modulated along the protan, deutan and tritan colour confusion lines for trichromatic vision within the CIE 1931 diagram of colour space. Sine wave gratings of low spatial frequency (1 cycle per degree) were presented and a forced-choice technique employed to determine the threshold for each grating pattern. The isoluminant point was determined using the minimum motion technique of Mullen (1985) for each individual to compensate for lenticular absorption and macular pigmentation. The data from the OHT patients was compared to the normal database.

2.2.4. Topographical assessment of the optic nerve head

Towards the end of the research, the Department acquired a Heidelberg Retinal Tomograph (HRT) (Heidelberg Engineering GmbH, Heidelberg, Germany), a confocal laser scanning ophthalmoscope for in-vivo three dimensional imaging of the posterior segment of the eye. The system provides topographical images of the optic nerve head. The acquisition of this instrument permitted a pilot study which was not originally part of the study protocol into the relationship between the topographical characteristics of the optic nerve head and the W-W and B-Y visual

field in OHT and POAG. The sample comprised the 51 patients for the B-Y visual field study together with 20 of the 50 age-matched normal subjects.

2.3. Logistics

The research was carried out within the Department of Vision Sciences, Aston University, Birmingham and the study had approval from the Aston University Human Science Ethical Committee. Normal control subjects were recruited from old-age pensioner associations and from students and staff of the University. All subjects conformed to rigid inclusion criteria. The natures of the procedures and the number of required visits were fully explained to all those subjects and patients taking part in the research. Subjects and patients were asked to sign a consent form and were free to withdraw from the study at any time. Where necessary travelling expenses were paid to and from the University.

The cataract patients were recruited from the University Optometry teaching clinic or from optometric practice. Patients were required to attend the Department on four separate occasions. Initial contact was made by letter explaining the nature of the procedures involved. Patients were requested to return a reply statement indicating whether they were prepared to volunteer for the study. Appointments were then made by telephone and confirmed later by letter.

Recruitment for the investigation of learning effects in B-Y perimetry proved to be most difficult since patients were asked to attend the University on three consecutive days.

The OHT and POAG patients were recruited from the Glaucoma Department, Birmingham and Midland Eye Hospital (BMEH). Patients were preselected according to their age, diagnosis, presenting IOP, method of glaucoma therapy, extent of existing W-W visual field loss and positive family history with advice from consultant ophthalmologist Mr Eamon O'Neill. Full access to the medical records was given by the Hospital and the technical support staff at the Hospital were extremely helpful in providing any further information required. Initial contact with the patients was made by letter which explained the nature of the procedures involved. Patients were requested to

return a reply statement indicating whether they were prepared to volunteer for the study. Appointments were then made by telephone and confirmed later by letter. Patients initially attended the Department on 4 separate occasions and were followed-up at approximately 3-12 month intervals. Unfortunately, a number of patients were lost to follow-up either due to changes in their personal circumstances or to health reasons. Any patients demonstrating repeatable initial or progressing field loss of which the Hospital were unaware were referred directly back to the Glaucoma Department for further clinical investigation.

In the evaluation of the FASTPAC algorithm, additional data was independently collected at the University of Waterloo, Canada and was analysed with the data from Birmingham. It was felt that the ensuing larger sample size increased the power of the subsequent statistical analysis whilst at the same time permitting the assessment of any between-site differences in the sensitivities of the two samples.

CHAPTER 3: STRATEGIES FOR THE ESTIMATION OF PERIMETRIC THRESHOLDS

3.1 Introduction

The fundamental basis of perimetric strategies was discussed in Chapter 1. Strategies can be divided into two types: suprathreshold (or supraliminal) evaluation and threshold estimation. The latter approach is thought to be more capable of detecting early shallow visual field loss than a suprathreshold procedure (Heijl 1985b). Threshold estimation measures the contour of the hill of vision within the limits of accuracy of the measurement procedure.

3.2 Psychophysical aspects

Techniques for threshold determination at a given location within the visual field have generally employed one of two procedures: the 'method of limits' or the repetitive 'up and down' method. The 'method of limits' consists of an ascending series of stimuli, whose luminance increases until the stimulus is perceived (Guilford 1954). The initial value of the series is approximately 2-4dB below the normal age-matched value (Bebié et al 1976a). The technique suffers from the disadvantage that the threshold estimate is biased by the magnitude of the step size and the choice of the initial stimulus level (Levitt 1971). The repetitive 'up and down' staircase method (Cornsweet 1962; Feeney et al 1966; Rose et al 1970; Levitt 1971) is considered to be optimal (Spahr 1975). With this method, the initial luminance level is selected from the mean threshold for the given age group. If the initial stimulus is not perceived the luminance of the next stimulus is increased by an appropriate amount; if the initial stimulus is perceived the luminance of the next stimulus is decreased. The procedure continues until threshold is crossed and threshold is defined as the luminance level which is seen on 50% of occasions. In the case of the staircase method, the procedure is governed by four conditions: the starting point of the staircase, the size of the staircase steps, the end point of the staircase series and any modifications of the staircase. The precision of a threshold determination can be increased by permitting several reversals across threshold. A schematic representation of such a staircase procedure is illustrated in Figure 3.1. The average number of stimuli required for the repetitive 'up and down' method is greater

than the 'method of limits'; however, the latter is less reliable and is dependent on whether the first stimulus is presented at an infra or supraliminal level (Bebié et al 1976a).

The duration of a perimetric examination is a function of the desired accuracy (Spahr and Fankhouser 1974). Spahr (1975), applying the principles of mathematical information theory, developed an optimal strategy for perimetry based upon the optimum information gain per unit response. The number of stimuli required to reach an end point is approximately 4 or 5. Increased precision requires more stimulus presentations and increased testing time (Bebié et al 1976a; Heijl 1977a). Indeed, Heijl (1977a) using both a computer simulation and investigations of normals and glaucoma patients evaluated different testing logics. Using the simulation, reproducibility was highest when threshold was estimated in four seed locations within the field using a three-reversal staircase procedure, followed by a shortened staircase for other locations. In patients, the highest reproducibility was obtained using a three-reversal staircase across all locations.

Perimetric sensitivity has been shown to decrease with increasing examination duration in normals (Searle et al 1991a, b; Hudson et al 1994), ocular hypertensives and glaucoma patients (Heijl and Drance 1983; Johnson et al 1988a; Langerhorst et al 1987b; Hudson et al 1994) and optic neuropathies (Wilderberger and Robert 1988). The reduction in sensitivity has been attributed to patient fatigue which increases with eccentricity (Heijl and Drance 1983) and is greater for the second eye examined (Searle et al 1991a, b; Hudson et al 1994). A more comprehensive discussion on the effect of fatigue in automated perimetry is given in Chapter 5. The development of a strategy which permits a reduction in the examination time, ie the efficiency, without loss of the quality of the clinical information, ie accuracy, is therefore essential.

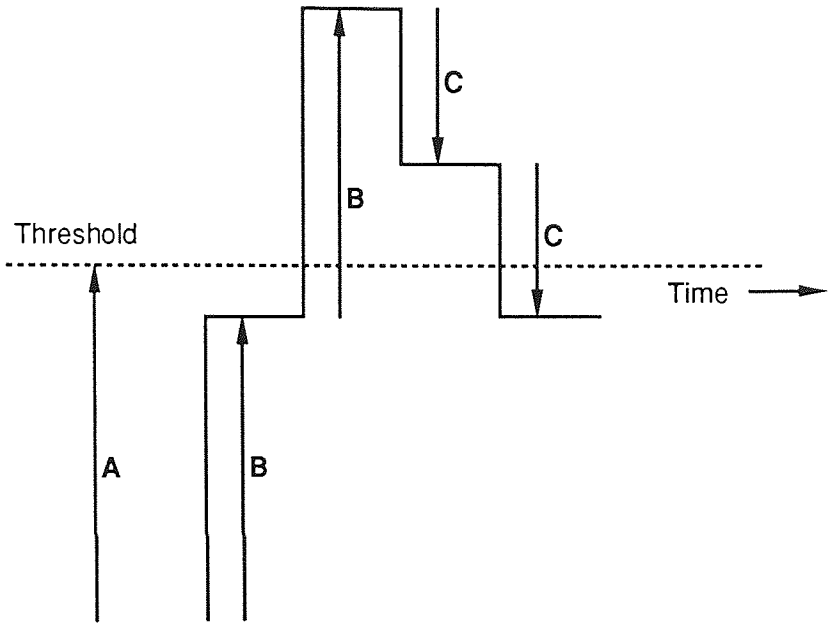

Figure 3.1. Schematic representation of an 'up and down' psychophysical staircase. A stimulus of brightness (B) is presented at a certain level (A) below threshold. If the stimulus is 'not seen' it is increased in brightness with a step size of interval B, until it is 'seen' as threshold is crossed. Subsequent stimuli are then presented with decreasing intensity in reduced step sizes of C. The time taken to estimate threshold is a function of the magnitude of the starting intensity in the staircase with respect to the actual threshold A, the staircase step sizes (B and C) and the required number of reversals of the staircase across the threshold. Alternatively, the staircase may begin at a suprathreshold level and the stimulus intensity is decreased until threshold is crossed.

An alternative strategy to estimate threshold with a modified procedure termed MOBS (modified binary search) demonstrated an increase in accuracy of 10% but at the expense of a 5-7% increase in the number of stimulus presentations (Johnson and Shapiro 1989). A more heuristic procedure was developed and subsequently assessed using a computer simulation program-KRAKEN. RIOTS (real-time interactive optimized test sequence) involved comparisons of the estimated threshold in real time at a given stimulus location with neighbouring stimulus locations in addition to a set of established rules in the software design to estimate threshold (Johnson and Shapiro 1991). Furthermore, the stimulus locations were not considered to be independent events and comparisons were made between the measured and predicted responses after 12 seed points had been accurately measured with the MOBS procedure. RIOTS was considered to be slightly more accurate but 2-3 times more efficient than the standard staircase strategy.

The current design and evaluation of 'up and down' staircase procedures in clinical perimetry assumes that the shape of the frequency-of-seeing curve remains constant, regardless of threshold level (Fankhouser et al 1972; Spahr 1975; Bebié et al 1976a; Heijl 1977a; Johnson and Shapiro 1989, 1991; Johnson et al 1992). As described in Chapter 1, the frequency-of-seeing curve describes the relationship between the probability of seeing a stimulus and a property of the stimulus. The threshold coefficient of the frequency-of-seeing curve is highly dependent on the threshold level (Weber 1992; Chauhan et al 1993; Olsson et al 1993). When sensitivity is high, the curve is steep and the threshold coefficient ranges between 1 and 2dB; when sensitivity is low in glaucoma cases the curve is flat and the threshold coefficient reaches values of upto 12.6dB (Weber and Rau 1992; Chauhan et al 1993). This would suggest that an optimum staircasing strategy would utilise, within a given examination, larger step sizes for areas of lower sensitivity and would serve to improve both the accuracy and efficiency. Indeed, the use of this type of strategy, termed the dynamic strategy, has been developed by Weber (1990) whereby the luminance steps alter dynamically to the average threshold coefficient of the current threshold level. The increase in efficiency with the dynamic strategy is partly at the expense of a loss in accuracy for areas with deep loss (Weber 1991). Indeed, a time saving of 34-57% has been achieved compared to the standard 4-2dB strategy (Weber 1989; Vivell et al 1991; Klimaschka

and Weber 1994; Zulauf et al 1994). It is further argued whether accurate determination of the depth of defects is necessary, particularly when the defects are the source of high within-test fluctuation (Flammer et al 1984).

The dynamic strategy is based upon the alteration of the strategy depending on the threshold level and the slope of the frequency-of-seeing curve. Interestingly, Chauhan et al (1993) have identified situations whereby, although the threshold remains identical in different regions of the visual field, the slope of the frequency-of-seeing curve may be different. The dynamic strategy relies upon the dependency of the slope of the frequency-of-seeing curve on threshold; the implications of the findings of Chauhan et al (1993) on the dynamic strategy remain unknown.

A statistical approach to estimate threshold which also uses information from the frequency-of-seeing curve has been employed by Olsson et al (1989). The technique uses maximum likelihood analysis and was originally applied to estimate the number of false- positive and negative responses in a perimetric examination. Maximum likelihood analysis involves calculation of the probability of occurrence of a given set of observations compared to a pre-defined mathematical model based upon the standard frequency-of-seeing curve (Olsson et al 1989). The technique utilizes all available information concerning patient responses during the staircase procedure and contrasts with the use in conventional strategies of the specific values at which reversal occurs. The technique to estimate threshold has been termed Bayesian Posterior Mean Threshold estimation (BPM) (Olsson et al 1991, 1994b). Furthermore, the inclusion of frequency-of-seeing curve characteristics into the statistical model from both normal and abnormal fields for different eccentricities and defect depths increases the accuracy of threshold estimation by about 15% and reduces the number of stimulus presentations required by 30% in a normal eye and by 22% in a glaucomatous eye. Furthermore, the mathematical model allows specified levels of accuracy to be selected depending on the type of perimetric test required. Nevertheless, the staircase strategy, itself, remains unaltered. This type of strategy remains in development and has not yet been released commercially.

3.3. Current strategy for the Humphrey Field Analyser

A full threshold examination of the central field with the Humphrey Field Analyser program 30-2 involves approximately 500-600 stimulus presentations and takes approximately 15 minutes per eye. The strategy uses a 4-2dB step size double crossing of the threshold. Threshold is initially determined at each of four primary seed points situated at 9°, 9° eccentricity in each quadrant (Haley 1987). If the patient responds, the stimulus is decreased in intensity in 4dB steps until the patient no longer responds. The stimulus is then increased in 2dB steps until threshold is crossed again (Figure 3.2). The final crossing may occur in either an ascending or descending direction and threshold is taken as the last seen presentation. The threshold determination at the adjacent locations starts at 2dB brighter than that predicted from the thresholds of the seed points. When the measured threshold departs by 4dB or more from the expected value for a given location, the threshold is re-measured. This latter value is represented as a bracketed term on the standard HFA printout and is in addition to the ten pre-determined locations at which threshold is estimated twice for the calculation of the short-term fluctuation (SF) (see Chapter 1).

3.4 A new strategy for threshold estimation - FASTPAC

In 1991, Humphrey Instruments Inc (San Leandro, CA, USA) introduced a new strategy "FASTPAC" for estimating the differential light threshold. In this strategy, the four primary seed points are measured in a similar manner to the standard 4-2dB strategy. However half of the subsequent seeded points start at 1dB brighter and one half at 2dB dimmer than the predicted threshold; the threshold is estimated from only a single crossing and the step size is maintained at a constant 3dB. A schematic representation of the standard 4-2dB strategy and the alternative FASTPAC strategy is illustrated in Figure 3.2. Threshold is taken as the last seen stimulus luminance and stimulus locations differing from the expected value by ±4dB or more are re-thresholded.

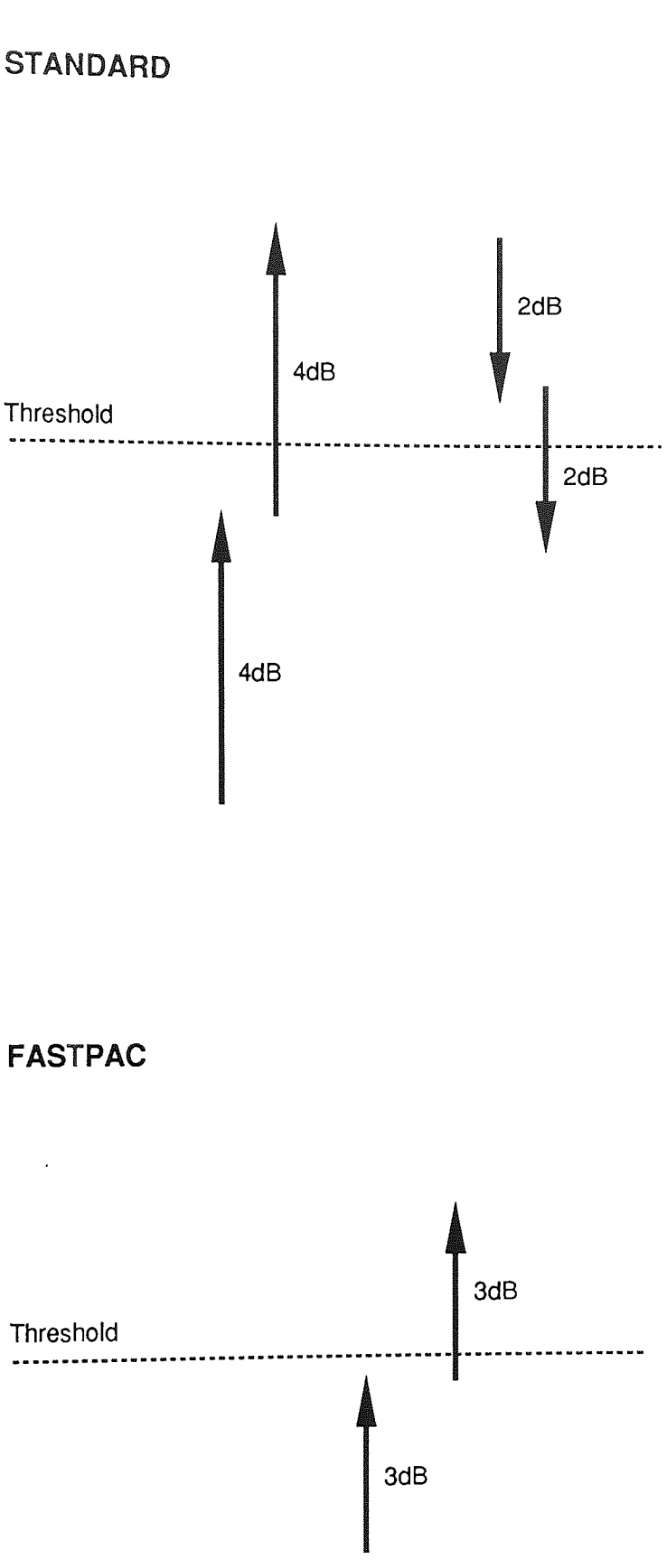

Figure 3.2. Schematic representation of the standard 4-2dB strategy currently employed in the Humphrey Field Analyser, compared to the FASTPAC strategy which utilizes a 3dB staircase step size and a single crossing of threshold.

3.5. Evaluation of the FASTPAC strategy in a normal population

At the time of the study in 1991, the performance of the FASTPAC strategy compared to the standard strategy was unknown. The aim of the study was to compare the FASTPAC strategy with the standard 4-2 double staircase strategy with a view to using FASTPAC in the subsequent studies on B-Y perimetry.

3.5.1. Materials and Methods

Sample

The sample consisted of 98 clinically normal volunteers (42 males and 56 females) with a mean age of 49.6 (SD 16.9) years and a range between 23 and 83 years. The data was collected at two centres Birmingham, UK and Waterloo, Canada. The Birmingham sample had a mean age of 48.1 years (SD 18.2) and a range from 23 to 83 years. The Waterloo sample had a mean age of 51.3 years (SD 15.6) and a range from 25 to 78 years. Prior to visual field examination each volunteer underwent a full ophthalmological examination. Exclusion criteria comprised visual acuity worse than 6/7.5 for those under 50 years of age and worse than 6/9 for those over 50 years of age; ametropia of greater than ±5 dioptres sphere and 2.5 dioptres cylinder; intraocular pressure greater than 22mmHg; history of amblyopia; suspicious or abnormal optic nerve head appearance; reproducible visual field loss of known cause; history of eye disease, trauma or surgery; the presence of ocular findings that could adversely affect the visual field; medical history of diabetes mellitus; neurological or psychiatric illness; and use of central nervous system depressants.

Perimetry

Subjects underwent perimetry on two separate visits. One randomly assigned eye of each subject was examined at each visit with the standard and FASTPAC strategies using Program 30-2 (stimulus size III) of the HFA 640 (Humphrey Instruments Inc, San Leandro, CA, USA). The order of examination for the two strategies was randomly assigned at the first visit to ensure an approximately equal number of subjects for each examination sequence and was reversed for the second visit. The results from the first visit were discarded in order to minimise the influence of

the between- and within-examination learning effects (Heijl et al 1989a; Rabineau et al 1985; Searle et al 1991a, b; Werner et al 1988, 1990; Wild et al 1989c, 1991b). Learning effects are discussed in Chapter 5. Fixation losses were less than 20%, and false-negative and false-positive responses less than 33% for each subject in all examinations.

3.5.2. Analysis

Group mean mean sensitivity (MS), unweighted short-term fluctuation (SF) calculated from the ten standard stimulus locations, number of stimulus presentations and total examination time were calculated for each strategy. Indices were calculated from the formulae of Heijl et al (1987c). Mean sensitivity was used rather than mean deviation due to the absence of normal data for FASTPAC. The data was analysed using a repeated measures analysis of covariance (ANCOVA) for a two-period crossover trial. Mean sensitivity, SF, number of stimulus presentations and total examination time were each separately considered as within-subject factors and examination centre, examination sequence and age as between-subject factors. Normalising transforms of the Box-Cox family (Box and Cox 1964) were applied to the distributions of the data where necessary. For each variable (MS, SF, number of stimulus presentations and examination time) a value λ is calculated for which the equation: $z^{(\lambda)} = (y^{\lambda} - 1) / [gm]\,\lambda\text{-}1$ normalised the distribution of the respective data and stabilised the variance, such as to be constant over groups. The term gm is the geometric mean of the observations; $z^{(\lambda)}$ represents the transformation index; a linear function of y^{λ}. The transform value, λ, minimises the residual sum of squares. In order to overcome the negatively skewed distribution of MS (Searle et al 1991b), a linear transform was initially performed.

A pointwise analysis of the difference in sensitivity between the two strategies was performed by calculating the mean and standard deviation of the differences at each of the 76 stimulus locations as a function of test sequence and age. The benefit / cost ratio was calculated whereby:

benefit = reproducibility = 1 / variance

cost = time = number of stimulus presentations

benefit / cost = 1 / (variance X no. of presentations).

A further indication of the intra-test variance was gained by calculating the number of double determinations of threshold for each strategy. In addition, the coefficient of determination, R^2, between the measured pointwise distribution of sensitivity and that modelled by a second order polynomial in terms of the respective stimulus coordinates (Wild et al 1993) was calculated for the Birmingham sample. The polynomial function describes the shape of the hill of vision.

3.5.3. Results

The group mean MS, SF, number of stimulus presentations and total examination time for the sample as a whole is illustrated in Table 3.1 and is further illustrated in Table 3.2 as a function of examination centre, examination sequence and age. For the Birmingham group 24 subjects underwent the standard test first (Mean age 50.5 years (SD 19.6)) and 21 subjects the FASTPAC strategy first (Mean age 45.2 years (SD 17.7)). Similarly for the Waterloo group 23 subjects underwent the standard test first (Mean age 53.4 years (SD 14.5)) and 30 subjects the FASTPAC strategy first (Mean age 49.2 years (SD 15.7)).

Variable	Strategy	
	Standard	FASTPAC
MS (dB)	27.24 (2.84)	27.38 (2.65)
SF (dB)	1.36 (0.52)	1.78 (0.65)
Stimulus Presentations	463.80 (51.10)	267.40 (27.30)
Time (mins)	13.99 (1.77)	7.91 (1.09)

Table 3.1. Group mean MS, SF, number of stimulus presentations and examination duration between the standard strategy and the FASTPAC strategy.

Birmingham	Examination Sequence			
Variable	Standard	FASTPAC	Standard	FASTPAC
MS (db)	28.18 (2.16)	27.92 (2.66)	28.14 (2.03)	27.68 (2.74)
SF (db)	1.27 (0.36)	1.97 (0.88)	1.66 (2.16)	1.27 (0.46)
Presentations	465.17 (62.82)	265.04 (27.60)	264.38 (21.61)	461.14 (42.71)
Time (mins)	14.01 (1.65)	7.87 (1.08)	7.85 (0.91)	13.96 (1.76)

Waterloo	Examination Sequence			
Variable	Standard	FASTPAC	Standard	FASTPAC
MS (db)	26.70 (2.77)	26.52 (3.17)	27.06 (2.45)	26.58 (3.28)
SF (db)	1.41 (0.36)	1.74 (0.59)	1.74 (0.56)	1.45 (0.53)
Presentations	457.96 (46.79)	273.48 (36.66)	266.76 (22.37)	469.10 (51.32)
Time (mins)	13.85 (1.54)	8.12 (1.39)	7.82 (0.98)	14.10 (1.95)

Table 3.2. Group mean MS, SF, number of stimulus presentations and examination duration for the standard and FASTPAC strategies as a function of examination sequence and examination centre.

The global mean MS was 27.38dB (SD 2.65) for FASTPAC and 27.24dB (SD 2.84) for the standard strategy. The MS was corrected for skewness using a linear transform of 33-y where y was the measured MS and the ANCOVA was performed following a Box-Cox logarithm transform of $\lambda = 0.112$ (Table 3.3). Mean sensitivity was greater for the Birmingham study ($p=0.017$). It decreased with increase in age ($p<0.001$) and this reduction was greater for the Waterloo study ($p=0.014$). No overall difference in MS was found between the two strategies ($p=0.287$) although in the Waterloo study MS recorded with FASTPAC tended to be lower with increase in age ($p=0.049$). Mean sensitivity tended to be lower for the second test irrespective of the test sequence; however this effect did not reach statistical significance ($p=0.075$) although the difference was more marked with increase in age ($p=0.048$).

The global mean SF was 1.78dB (SD 0.65) for FASTPAC and 1.36dB (SD 0.52) for the standard strategy. The ANCOVA was performed following a Box-Cox logarithm transform of $\lambda = 0.013$ (Table 3.4). Short-term fluctuation was significantly higher for FASTPAC ($p<0.001$).

The global mean number of stimulus presentations was 267.40 (SD 27.30) for FASTPAC and 463.80 (SD 51.10) for the standard strategy. The ANCOVA was performed following a Box-Cox logarithm transform of $\lambda = -0.196$ (Table 3.5). The number of stimulus presentations was significantly less for FASTPAC compared to the standard strategy ($p<0.001$). The number of stimulus presentations increased with increase in age for both strategies ($p<0.011$) (Figure 3.3). The increase in stimulus presentations as a function of age described by linear regression was 3.39 per decade for FASTPAC compared to 7.66 for the standard strategy.

The global mean total examination time was 7.91 minutes (SD 1.1) for FASTPAC and 13.99 minutes (SD 1.8) for the standard strategy. The ANCOVA was performed following a Box-Cox transform of $\lambda = 0.053$ (Table 3.6). The total examination time was significantly less for FASTPAC compared to the standard strategy ($p<0.001$) and the time increased with increase in age for both strategies ($p=0.001$) (Figure 3.4). The increase in time as a function of age described by

univariate linear regression was 10.5 seconds per decade for FASTPAC compared to 19.5 seconds for the standard strategy.

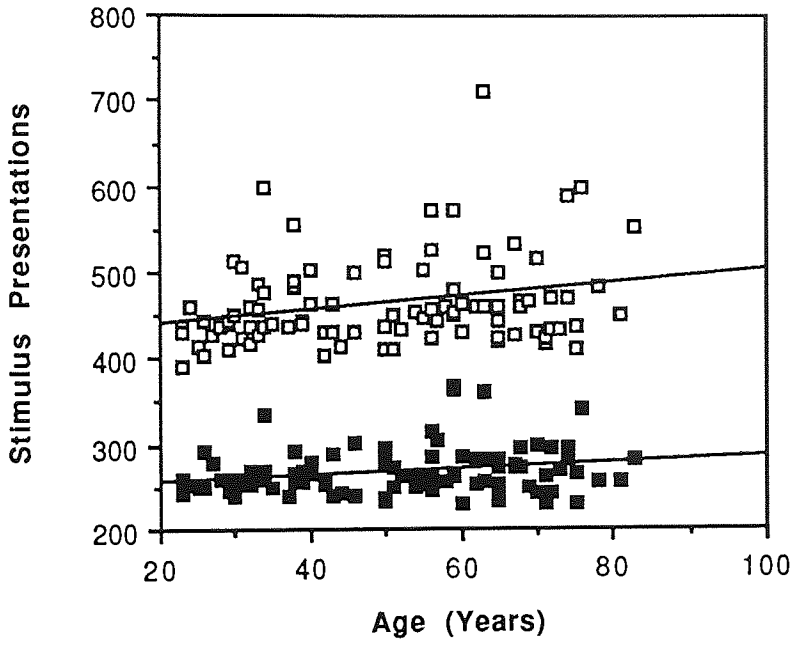

Figure 3.3. Number of stimulus presentations as a function of age for the 98 subjects in the study. Open symbols represent the stimulus presentations recorded with the standard 4-2 strategy; closed symbols, that recorded with the FASTPAC strategy.

Source	Degrees of Freedom	Sums of Squares	Mean Square	F value	P value
Age	1	298.935	298.935	48.22	p<0.001
Examination centre	1	36.274	36.274	5.85	p=0.018
Age x Examination centre	1	38.529	38.259	6.21	p=0.015
Strategy x Test order	1	1.433	1.433	0.23	p=0.632
Age x Strategy x Test order	1	1.433	1.433	0.23	p=0.632
Strategy x Test order x Examination centre	1	1.417	1.417	0.23	p=0.634
Age x Strategy x Test order x Exam centre	1	5.785	5.785	0.93	p=0.337
Error	92	570.379	6.200		

Table 3.3. Repeated measures analysis of covariance for Mean Sensitivity (MS).

Source	Degrees of Freedom	Sums of Squares	Mean Square	F value	P value
Strategy	1	0.540	0.540	1.14	p=0.288
Test order	1	1.527	1.527	3.23	p=0.076
Age x Strategy	1	0.318	0.318	0.67	p=0.414
Age x Test order	1	1.902	1.902	4.03	p=0.048
Strategy x Examination centre	1	0.030	0.030	0.06	p=0.801
Test order x Examination centre	1	0.059	0.059	0.12	p=0.726
Agex Strategy x Examination centre	1	1.878	1.878	3.98	p=0.049
Age x Test order x Examination centre	1	0.259	0.259	0.55	p=0.461
Error	88	41.531	0.472		

Table 3.3 (cont). Repeated measures analysis of covariance for Mean Sensitivity (MS).

Source	Degrees of Freedom	Sums of Squares	Mean Square	F value	P value
Age	1	0.78	0.78	2.25	p=0.137
Examination centre	1	0.04	0.04	0.12	p=0.735
Age x Examination centre	1	0.10	0.10	0.29	p=0.590
Strategy x Test order	1	0.04	0.04	0.10	p=0.748
Age x Strategy x Test order	1	0.08	0.08	0.24	p=0.628
Strategy x Test order x Examination centre	1	0.29	0.29	0.84	p=0.362
Age x Strategy x Test order x Exam Centre	1	0.00	0.00	0.01	p=0.917
Error	92	31.92	0.35		

Table 3.4. Repeated measures analysis of covariance for Short-term Fluctuation (SF).

Source	Degrees of Freedom	Sums of Squares	Mean Square	F value	P value
Strategy	1	7.704	7.704	46.38	p<0.001
Test order	1	0.263	0.263	1.59	p=0.211
Age x Strategy	1	0.277	0.277	1.67	p=0.200
Age x Test order	1	0.076	0.076	0.46	p=0.501
Strategy x Examination centre	1	0.293	0.293	1.76	p=0.188
Test order x Examination centre	1	0.051	0.051	0.31	p=0.582
Age x Strategy x Examination centre	1	0.039	0.039	0.23	p=0.631
Age x Test order x Examination centre	1	0.367	0.367	2.21	p=0.141
Error	88	14.617	0.166		

Table 3.4. (cont). Repeated measures analysis of covariance for Short-term Fluctuation (SF).

Source	Degrees of Freedom	Sums of Squares	Mean Square	F value	P value
Age	1	12823.905	12823.905	6.77	p=0.011
Examination centre	1	155.798	155.798	0.08	p=0.018
Age x Examination centre	1	4420.371	4420.371	2.33	p=0.775
Strategy x Test order	1	1.148	1.148	0.00	p=0.980
Age x Strategy x Test order	1	60.625	60.625	0.03	p=0.130
Strategy x Test order x Examination centre	1	8.188	8.188	0.00	p=0.858
Age x Strategy x Test order x Exam Centre	1	4190.093	4190.093	2.21	p=0.948
Error	92	174204.861	1893.53		

Table 3.5. Repeated measures analysis of covariance for the number of stimulus presentations.

Source	Degrees of Freedom	Sums of Squares	Mean Square	F value	P value
Strategy	1	1819988.211	1819988.21	4881.83	p<0.001
Test order	1	577.973	577.97	1.55	p=0.216
Age x Strategy	1	392.339	392.34	1.05	p=0.308
Age x Test order	1	10.137	10.14	0.03	p=0.869
Strategy x Examination centre	1	498.543	498.54	1.34	p=0.251
Test order x Examination centre	1	848.265	848.27	2.28	p=0.135
Age x Strategy x Examination centre	1	88.843	88.84	0.24	p=0.627
Age x Test order x Examination centre	1	99.289	99.29	0.27	p=0.607
Error	88	32807.140	372.80		

Table 3.5. (cont). Repeated measures analysis of covariance for the number of stimulus presentations.

Source	Degrees of Freedom	Sums of Squares	Mean Square	F value	P value
Age	1	99460.83	99460.83	10.96	p=0.001
Examination centre	1	178.80	178.80	0.02	p=0.889
Age x Examination centre	1	21074.26	21074.26	2.32	p=0.131
Strategy x Test order	1	454.63	454.63	0.05	p=0.823
Age x Strategy x Test order	1	1648.63	1648.63	0.18	p=0.671
Strategy x Test order x Examination centre	1	541.23	541.23	0.06	p=0.808
Age x Strategy x Test order x Exam centre	1	12292.49	12292.49	1.35	p=0.248
Error	92	834925.42	9075.28		

Table 3.6. Repeated measures analysis of covariance for examination time.

Source	Degrees of Freedom	Sums of Squares	Mean Square	F value	P value
Strategy	1	6270643.86	6270643.86	3408.22	p<0.001
Test order	1	2050.50	2050.50	1.11	p=0.294
Age x Strategy	1	296.60	296.60	0.16	p=0.689
Age x Test order	1	1.54	1.54	0.00	p=0.977
Strategy x Examination centre	1	697.20	697.20	0.38	p=0.540
Test order x Examination centre	1	3103.37	3103.37	1.69	p=0.197
Age x Strategy x Examination centre	1	54.31	54.31	0.03	p=0.864
Age x Test order x Examination centre	1	1090.46	1090.46	0.59	p=0.443
Error	88	161907.75	1839.86		

Table 3.6. (cont). Repeated measures analysis of covariance for examination time.

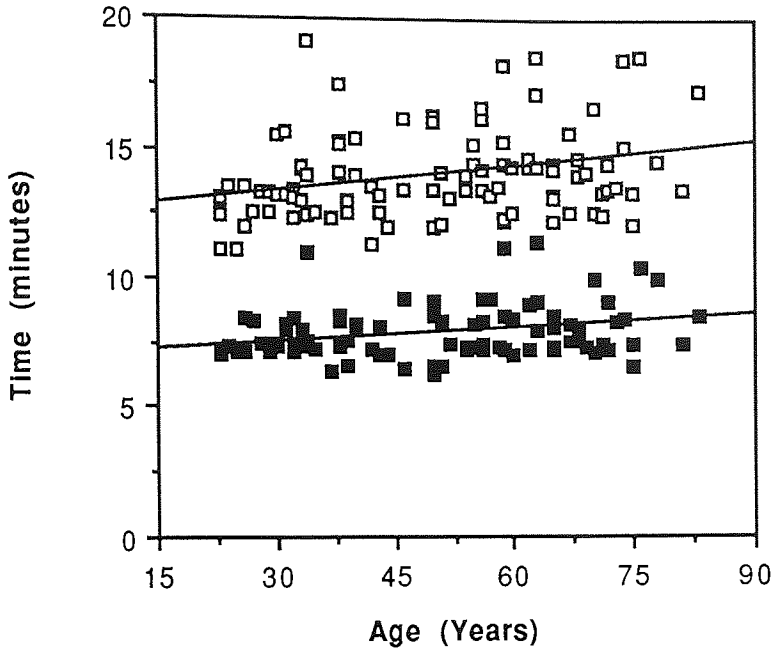

Figure 3.4. Examination time (minutes) as a function of age for the 98 subjects in the study. Open symbols represent the examination time recorded with the standard 4-2dB strategy; closed symbols, that recorded with the FASTPAC strategy.

The global mean and standard deviation of the difference in sensitivity between the two strategies at each stimulus location as a function of age is illustrated in Figure 3.5a and b. The pointwise distribution of the means showed no particular trend whilst that of the standard deviations increased with increase in eccentricity although the differences did not reach statistical significance. The decrease in mean sensitivity as a function of age described by univariate linear regression was 0.81dB per decade for FASTPAC compared to 0.90dB for the standard strategy (Figure 3.6).

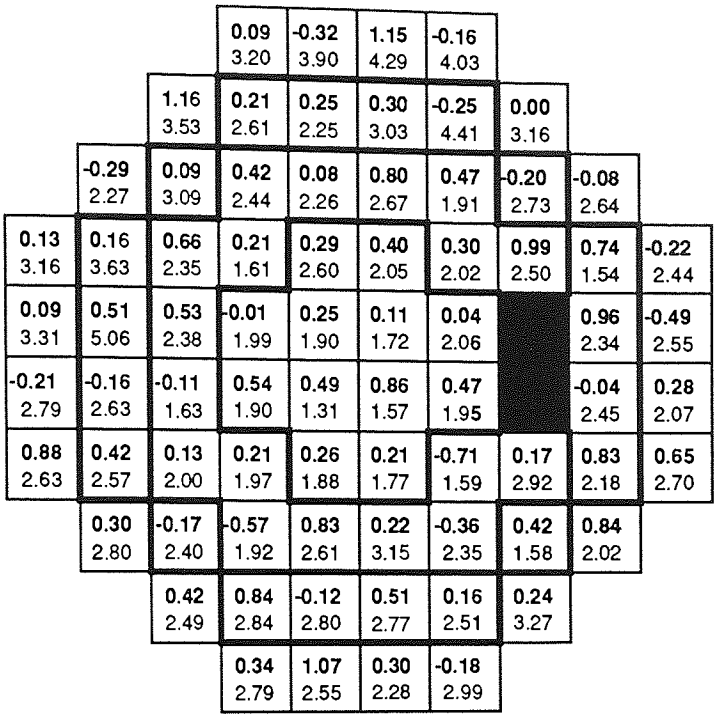

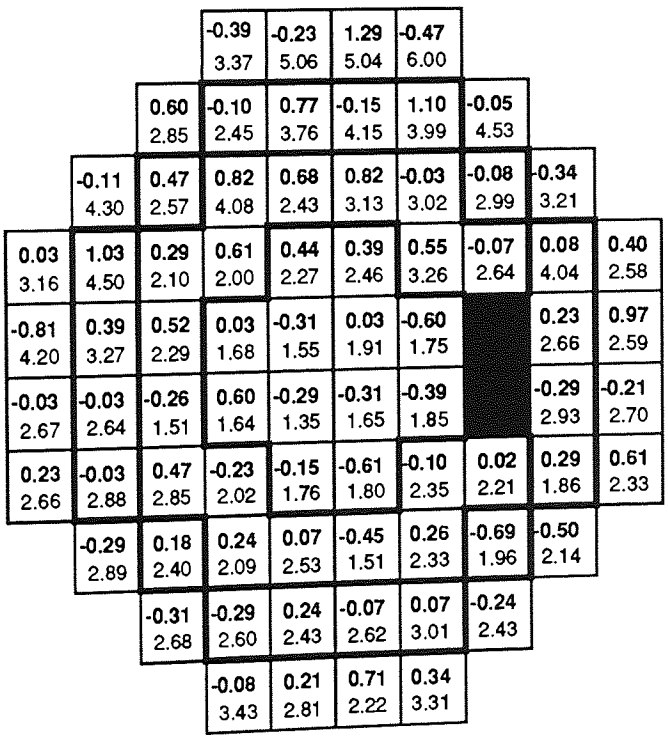

Figure 3.5a. Mean (bold) and one standard deviation of the differences in sensitivity between the FASTPAC and standard strategies at each stimulus location for the 20-40 year (upper) and 40-60 year (lower) age groups. A negative value indicates the FASTPAC strategy exhibited a lower sensitivity than the standard 4-2dB strategy.

			1.27 5.77	**1.12** 5.72	**2.75** 6.36	**1.85** 6.70		
		0.65 5.10	**-0.37** 4.94	**0.48** 6.44	**1.08** 4.59	**1.22** 4.22	**0.47** 4.84	
	1.13 4.68	**1.35** 5.73	**0.98** 4.13	**0.92** 5.18	**0.60** 3.51	**2.33** 3.00	**-0.48** 3.37	**0.32** 3.43
1.57 4.32	**0.45** 4.31	**0.67** 2.87	**0.48** 2.91	**0.92** 3.83	**0.78** 3.22	**-0.48** 3.76	**0.72** 3.42	**0.45** 3.27	**0.57** 2.62
1.34 3.98	**2.03** 3.80	**0.68** 3.06	**-0.17** 2.02	**0.22** 2.71	**-0.18** 1.56	**-0.43** 2.60		**1.05** 3.61	**0.30** 3.23
-0.50 3.15	**0.68** 3.50	**0.17** 2.23	**0.22** 3.12	**-0.22** 1.17	**-0.27** 1.53	**0.30** 2.69		**0.20** 3.21	**0.00** 2.82
0.63 4.58	**0.52** 5.42	**-0.15** 3.30	**0.02** 1.93	**0.00** 3.25	**0.82** 2.33	**-0.15** 2.04	**0.18** 3.97	**0.70** 2.74	**-0.95** 5.03
	0.59 3.45	**0.08** 2.76	**0.22** 2.19	**0.12** 2.23	**0.30** 3.53	**0.25** 3.34	**0.48** 3.39	**0.58** 2.95	
		1.38 4.56	**0.30** 3.37	**0.53** 2.66	**0.18** 2.77	**0.22** 2.40	**-0.40** 2.08		
			0.55 2.86	**-0.57** 2.24	**0.93** 3.04	**-0.12** 3.41			

Figure 3.5b. Mean (bold) and one standard deviation of the differences in sensitivity between the FASTPAC and standard strategies at each stimulus location for the 60+ years age group. A negative value indicates the FASTPAC strategy exhibited a lower sensitivity than the standard 4-2dB strategy.

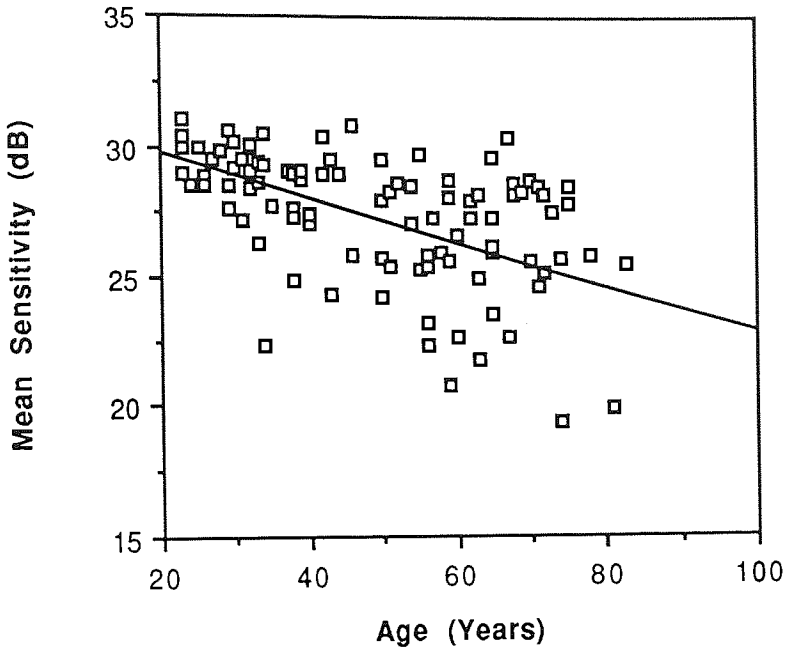

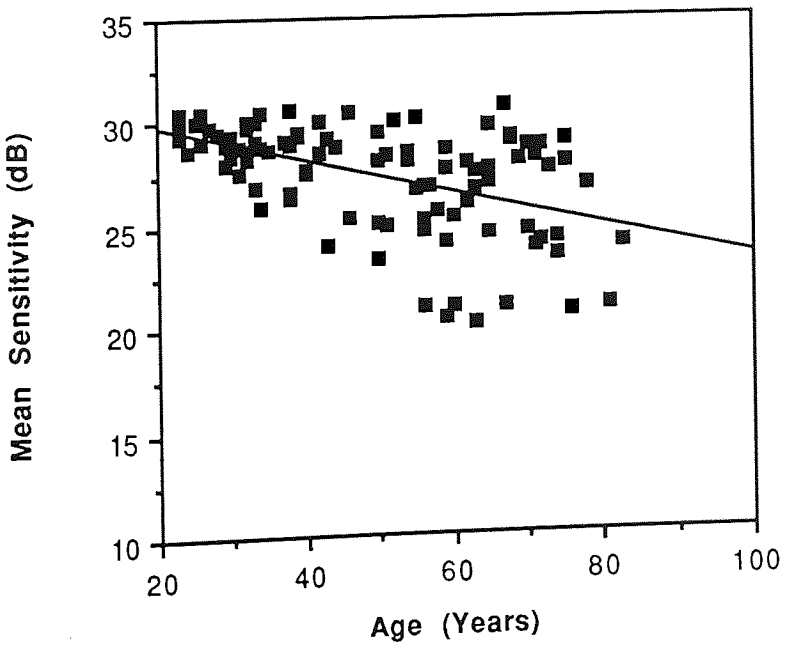

Figure 3.6. Univariate linear regression analysis of mean sensitivity against age for the standard (upper graph) and FASTPAC (lower graph) strategies.

The mean number of double determinations of threshold was greater with the FASTPAC strategy (6.6, SD 4.7) compared with the Standard strategy (4.6, SD 5.3) (paired t-test; $p<0.001$) (Figure 3.7).

The cost / benefit relationship was 0.00117 for the standard strategy and 0.00118 for the FASTPAC strategy thus indicating no real improvement in information gain.

The goodness of fit between the measured and modelled pointwise distribution of sensitivity was 67.3% (SD 1.0) and 66.9% (SD 4.0) for the FASTPAC and standard strategies respectively.

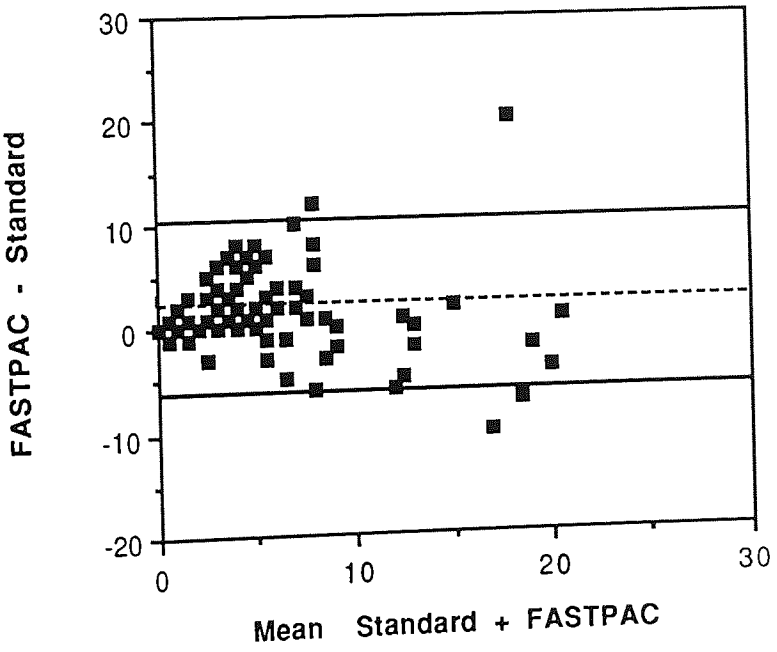

Figure 3.7. The difference between the number of double determinations of threshold with the standard 4-2dB strategy and that with the FASTPAC strategy against the mean of the number of double determinations for both strategies. The broken line represents the mean of the differences between the two strategies; solid lines represent mean ±2 SDs.

3.5.4 Discussion

The results indicate that FASTPAC produces a similar mean sensitivity to the standard strategy in a considerably shorter examination time (43% faster). The reason for the minor differences in mean sensitivity for both strategies between the two centres is unclear but may be associated with the subtle differences in the distributions of prior perimetric experience and age between the two samples. The reduction in time between the two strategies is at the expense of an increased short-term fluctuation with FASTPAC relative to that recorded by the standard strategy. FASTPAC therefore offers a dramatic improvement in efficiency (defined as the overall time to perform the test) at the expense of a small loss in accuracy (defined as the level of agreement between the recorded results and the actual visual field sensitivity). The reduction in examination time and the increase in the short-term fluctuation together with the increased number of double determinations of threshold could be expected because of the relative simplicity of the larger step size and the single crossing of threshold by the FASTPAC strategy. The coefficient of determination, R^2, between the measured and modelled pointwise distributions of sensitivity, however, was similar for both strategies using the topographical model of Wild et al (1993).

The step size for the standard and FASTPAC strategies at the point of reversal is 2 and 3dB respectively. If the short-term fluctuation is calculated for an equal number of single-step errors then the resulting decibel difference between the Standard and FASTPAC strategies is in the ratio of 2:3. Therefore, if 1.36 dB is taken as being representative of a typical value for short-term fluctuation for the standard strategy then the FASTPAC strategy should give a fluctuation of 2.04dB. This increase in the short-term fluctuation, however, was less than the calculated difference between the two strategies of 0.7dB. It could also be argued that there would be more two step errors when using the standard strategy which would lower the expected difference.

The present study does not address the effects of the increased intra-test variance on the reproducibility of serial results or on the assessment of visual field abnormality. Heijl (1977a) investigated two similar strategies and concluded that it would be justifiable to use a quicker and simpler strategy with greater inherent variability for the detection of field loss in suspect

populations but that the greater reproducibility of the longer and more complex strategy was desirable for serial field analysis. Interestingly, the larger initial step size of the standard strategy compared to FASTPAC ensures that, as the severity of any field loss increases, the standard strategy requires fewer stimulus presentations to estimate the threshold at the given stimulus location.

The FASTPAC strategy has subsequently been evaluated in patients with glaucomatous visual field loss. Indeed, Flanagan et al (1993b) found that the saving of time between the two strategies in glaucoma becomes less pronounced as the severity of the field defect increased. Furthermore, the difference in the intra-test variance between the two strategies also increased as the severity of the defect increased. This was attributed to the larger step size of the FASTPAC strategy and to the nature in which the strategy seeds locations within absolute field loss. The FASTPAC strategy seeds neighbouring absolute points by presenting a dimmer target than the predicted threshold whereas the standard strategy presents the maximum stimulus luminance. Indeed, a negative relationship between the standard deviation of threshold estimates and the number of bracketing steps has also been reported for high pass resolution perimetry (House and Chauhan 1991).

The FASTPAC strategy has subsequently been found to also underestimate the extent and severity of glaucomatous visual field loss (Flanagan et al 1993b; O' Donnell et al 1994; O'Brien et al 1994). The underestimation of field loss with FASTPAC has also been demonstrated by computer simulation; the underestimation is dependent on the initial starting value with respect to the actual threshold (Glass et al 1993). The repeatability of FASTPAC in a sample of glaucoma patients with respect to the 95% confidence limits for change has been found to be similar to that of the standard strategy (Hatch et al 1994).

In the current study, the results of FASTPAC were compared to the current clinical standard 4-2 strategy. It could be argued that the latter strategy may not be optimum in terms of efficiency and accuracy both in the normal and in the abnormal eye. However Johnson et al (1992) evaluated

staircase procedures using a computer simulation program - KRAKEN and found a balance between accuracy and efficiency such that the present 4-2 double staircase strategy was close to the optimum for a staircase procedure.

The results of the current study suggest that FASTPAC should be considered as an alternative to the standard strategy in the examination of those patients undergoing visual field examination for the first time and in those with suspected normal fields (for example those with ocular hypertension) and should always be considered as an alternative to the present threshold-related screening strategies.

In conclusion, the FASTPAC strategy offered significant advantages over the standard strategy for the normal population in terms of the examination time with no measurable differences in the global and pointwise mean sensitivities. There was a slight increase in the intra-test variability, but this increase was of smaller magnitude than expected due to the apparent reduction in the fatigue effect.

4.1 Light Transmission through the ocular media

The ocular media comprises the cornea, aqueous and vitreous humours, and the crystalline lens. A large proportion of the light incident at the eye is never utilised in the stimulation of the retinal photoreceptors. The light is lost within the eye principally due to two processes: absorption and light scatter. Absorption reduces the brightness of a retinal image, whilst scatter reduces the translucence or the quality of the retinal image.

The crystalline lens is predominantly responsible for the reduction in light transmission throughout the visible spectrum (Said and Weale 1959; Boettner and Wolter 1962; Norren and Vos 1974; Werner 1982; Mellerio 1971, 1987; Pokorny et al 1987; Weale 1988; Weale 1992). The reduction in transmission primarily occurs at wavelengths below 450nm (Boettner and Wolter 1962; Ruddock 1972; Norren and Vos 1974; Werner 1982, 1983; Weale 1954, 1959, 1988, 1992; Mellerio 1971, 1987; Pokorny et al 1987; Johnson et al 1988b,1989b, 1993c; Sample et al 1988b, 1989, 1991a; Beems and Best 1990; Hudson and Wild 1993; Savage et al 1993).

The absorption by the ocular media as a whole (ie crystalline lens, cornea, aqueous and vitreous humours) (Boettner and Wolter 1962; Tan 1971; Coren and Girgus 1972; Werner 1982; Pokorny et al 1987; Sample et al 1988b, 1991a; Johnson et al 1988b; Haegestrom-Portnoy et al 1989; Savage et al 1993) and by the crystalline lens considered in isolation (Said and Weale 1959; Mellerio 1971; Weale 1988, 1992; Zeimer and Noth 1984) increases with increase in age (Said and Weale 1959; Mellerio 1971; Coren and Girgus 1972; Werner 1982; Pokorny et al 1987; Weale 1988; Sample et al 1988b, 1991a; Johnson et al 1988b, 1993c; Hudson and Wild 1993). Indeed, Weale (1963) originally attributed the age-related decline in visual field sensitivity to the increased absorption of the crystalline lens and to a reduction in pupil size. However, retinal factors such as the decreases in photopigment absorption (Norren and Meel 1985; Kilbride et al 1986; Weale 1992), photoreceptor density (Marshall 1987) ganglion cell density (Dolman et al 1980; Balazsi et al 1984) and the number of cells in the visual cortex (Devaney and Johnson 1980) are now thought to be of more significance in age-related sensitivity loss. Moreover, clinical

studies using automated perimetry (Johnson et al 1988b) and electrophysiology (Celesia 1977; Weleber 1981) have further concluded that the age-related sensitivity loss is due to neural rather than to pre-retinal influences such as the change in the optical density of the crystalline lens.

A variety of methods have been employed to measure the absorption characteristics of both the total ocular media and that of the crystalline lens considered in isolation. In-vitro methods using enucleated eyes have established a direct measurement of the crystalline lens optical density in the human eye (Boettner and Wolter 1962; Weale 1954, 1988; Mellerio 1971, 1987). An in-vivo method to estimate lens optical density, based on the comparison of the spectral sensitivity of phakic, pseudophakic and aphakic eyes has been used by other workers (Wright 1951; Weale 1954; Werner and Hardenberg 1983). An additional in-vivo method for the measurement of lens optical density utilised by Said and Weale (1959) involved a comparison between the intensities of light reflected from the anterior (Purkinje Image III) and posterior (Purkinje Image IV) crystalline lens surfaces. Densitometric measures of photographic plates were obtained from the reflected Purkinje images for a series of wavelengths. The photographic process, however, was rather time consuming. The use of Purkinje images has been subsequently applied to a more recent and less time consuming video-based system - the Lens Absorption Monitor (LAM) (Johnson et al 1993c; Nelson-Quigg et al 1994). In this procedure, the optical density spectrum of the crystalline lens with respect to wavelength was determined by comparing the intensity of the 4th Purkinje image at eight different wavelengths. Similar optical density values were obtained to those of Said and Weale (1959) and the device also exhibited good test-retest reliability (Johnson et al 1993c).

Using a subjective approach, Tan (1971) compared the scotopic sensitivity of the eye at series of wavelengths to the rhodopsin pigment spectrum in a group of normal and aphakic observers. Differences in the sensitivity spectra between the two groups of observers were attributed to the optical density of the crystalline lens. Norren and Vos (1974) also adopted a subjective procedure. They developed a lens density spectrum for a 'standard observer' based upon the CIE data of the scotopic sensitivity function and the rhodopsin pigment spectrum. Differences in scotopic spectral sensitivity from the rhodopsin spectrum were attributed to the crystalline lens

optical density. Their measured lens density spectrum compared well with a previous model suggested by Wyszecki and Stiles (1967) using data derived by objective techniques. Furthermore, Norren and Vos (1974) described a clinical technique for the determination of an individual absorption curve. The technique of Norren and Vos (1974) has been applied to an increment threshold procedure using either the Tübinger perimeter (Johnson et al 1988b, c, 1989a, 1993a, b, d; Adams et al 1991; Lewis et al 1993) or the Humphrey Field Analyser (Sample et al 1986b, 1988a, b, 1989a, 1993a, b; Sample and Weinreb 1989, 1990, 1992; Weinreb and Sample 1991; Hudson and Wild 1993). Alternative techniques for the measurement of crystalline lens OD include a matching procedure (Pokorny et al 1987; Coren and Girgus 1972; Savage et al 1993) and also the recording of scotopic visual evoked potentials (Werner 1982). The perimetric technique will be described in more detail in Section 4.10.1.

4.2 Influence of age on ocular media transmission

The increase in absorption increases with age as a result of an increase in the optical density of the crystalline lens. The increase in optical density with age may be linear (Said and Weale 1959; Mellerio 1971; Werner 1982; Weale 1988; Savage et al 1993) or the increase may non-linear (Coren and Girgus 1972; Pokorny et al 1987; Sample et al 1988b; Johnson et al 1988b, 1993c; Hudson and Wild 1993). Sample et al (1988b) found that the lens optical density demonstrated a greater increase in absorption beyond 70 years of age. However, this finding may have resulted from the inclusion of cataract patients within the sample (Savage et al 1993). Pokorny et al (1987) proposed a similar biphasic function, a slope from 20-60 years, and an increased slope from aged 60 years onwards. Two functions of lens optical density were described:

20-60 years

$$TL = TL_1 [1 + 0.02 (A-32)] + TL_2$$

>60 years

$$TL = TL_1 [1.56 + 0.0667 (A-60)] + TL_2$$

where TL is the lens optical density and is a combination of two components, TL_1 and TL_2; TL_1 is influenced by age, TL_2 remains stable after 20 years of age; and A is the observers age.

The increase in lens optical density with age may result from an increase in pigment within the lens. Increases in pigment may result from an increase in pigment concentration or from the lens becoming progressively thicker and depositing greater amounts of pigment, or from a combination of both processes. Weale (1971) found little change in the photometric density per unit pathlength of the lens with increase in age. He considered the increases in lens optical density with age to be due to an increase in the total lens thickness.

Studies have also considered the change in the lens optical density with age over a series of different wavelengths. This approach enables the spectral lens density function to be derived as a function of age. Pokorny et al (1987) were unable to model the change in lens optical density with age across all wavelengths simply by scaling the spectral density function of the young crystalline lens. They suggested that a component of lens optical density was affected by the age of the observer (TL_1), in addition to a residual component (TL_2) which was unaffected by the observers age. This hypothesis is consistent with the suggestion of Tan (1971), who proposed that the spectral lens optical density function was influenced by two factors. One factor resulted in an increase in the optical density in the ultra-violet region of the spectrum in the first decades of life and was attributed to an increase in cellular material within the lens - ie a growth factor. The other factor influenced the optical density by increasing with an increase in age and resulted from an accumulation of yellow pigment - ie an ageing factor. The yellow pigment demonstrated a peak absorption in the visible spectrum. However, other studies have been able to describe the spectral lens density function at any age by applying a scaling function to a predefined spectral density curve. The scaling function increased with an increase in age (Norren and Vos 1974; Werner 1982; Savage et al 1993; Johnson et al 1993c). Savage et al (1993) suggested that a gradual accumulation of a single pigment resulting in the yellowing of the lens or, alternatively, an increase in a combination of pigments in fixed proportion would produce the change in the shape of the lens density spectrum with age. Furthermore, using a laboratory-based approach, Kurzel and Wolbarsht (1973) demonstrated that the emission spectra of the proportion of pigments within the crystalline lens did not vary significantly with age. Cases of brunescent cataract did, however,

demonstrate an alteration in the proportion of pigment within the crystalline lens. The change in the shape of the spectral density function with age suggested by Pokorny et al (1987) may therefore result from inclusion of cataract patients within their study.

Considerable between-subject variation is present in media density within a given age group (Coren and Girgus 1972; Werner 1982; Sample et al 1988b; Johnson et al 1993c; Hudson and Wild 1993; Savage et al 1993). This variation can increase with increase in age and can extend upto one log unit in magnitude (Boettner and Wolter 1962; Johnson et al 1988b).

4.3 Influence of pupil size on ocular media transmission

Differences have been documented in the magnitude of total ocular media absorption and lens optical density between the Purkinje image technique of Said and Weale (1959) and those obtained by psychophysical measures (Werner 1982; Weale 1992; Johnson et al 1993c). These differences have been attributed partly due to the between-subject differences in lens optical density (Weale 1992; Johnson et al 1993c). However, the findings of Mellerio (1971, 1987) suggest that transmission losses in the crystalline lens are due to absorption in the lenticular nucleus and that the amount of absorption is dependent on the pathlength through the nucleus. Weale (1992) also proposed that the between-subject differences in ocular media absorption could be attributed to differences in pupil size. He suggested that eyes with small pupils would demonstrate a relatively greater ocular media absorption than those eyes with larger pupils in that light would pass through relatively thicker regions of the crystalline lens in eyes with smaller pupils resulting in a greater degree of absorption. Interestingly, Nelson-Quigg et al (1994) found pupil size to influence the ocular media absorption measured with the Lens Absorption Monitor (LAM) in samples of diabetic patients and normal subjects. Pupil size is considered to be of little clinical significance (Sample et al 1988b; Savage et al 1993) in the measurement of ocular media absorption using the scotopic threshold technique with the Humphrey Field Analyser. Indeed, Sample et al (1988b) calculated that a 0.06 log unit increase in ocular media absorption would occur for a reduction in pupil diameter from 7mm to 2mm.

4.4 Lenticular absorption and Blue-Yellow perimetry

Recent psychophysical procedures evaluating the short-wavelength sensitive pathways (SWS) of the central and peripheral retina have been developed for the early detection of glaucoma (Sample et al 1986b,1988a, 1993a, b; Sample and Weinreb 1989, 1990, 1992, Weinreb ands Sample 1991; Johnson et al 1988c, 1989a, 1993a,b,d; deJong et al 1991, 1993; Flanagan et al 1991a; Casson et al 1993; Lewis et al 1993). In view of the wavelength dependent transmission characteristics resulting from ocular media absorption and in particular that resulting from the crystalline lens density, it is essential to separate reductions in B-Y sensitivity due to neural processes from that due to the ocular media. The scotopic threshold technique utilizing the standard observer data of Norren and Vos (1974) has become the accepted technique for the measurement of ocular media absorption in the study of Blue-Yellow perimetry. The procedure has been utilised for the assessment of ocular media absorption in normal subjects, OHTs and glaucoma patients (Sample et al 1986b, 1988a, 1993a, b; Sample and Weinreb 1989, 1990, 1992; Sample and Weinreb 1991; Johnson et al 1988b, c, 1989a, 1993a, b, d; Hudson and Wild 1993; Lewis et al 1993). Furthermore, the magnitude and variation of ocular media absorption currently necessitates the individual measurement of ocular media absorption (Sample et al 1988b; Savage et al 1993; Hudson and Wild 1993). Indeed, Johnson et al (1988b) have suggested a protective role for optical lens density, whereby those subjects with increased ocular media absorption demonstrated higher B-Y mean sensitivities. The current perimetric technique for the measurement of ocular media absorption suffers from the disadvantage of requiring more clinic time (Sample et al 1993c).

4.5 Macular pigmentation

The macular pigmentation has the highest absorbance within the retina. It is localised in the inner and outer plexiform layers of the retina (Snodderly et al 1984) and is a mixture of two carotenoids: lutein and zeaxanthin (Bone et al 1985). The pigment is most dense in the centre of the fovea and declines with eccentricity, such that at 400μm from the foveal centre similar amounts of pigment are present in the other layers of the retina as in the receptor axon layer. At eccentricities greater than 7°, the absorption of light by the macular pigment is minimal. The composition of the pigment

also changes with eccentricity such that the lutein: zeaxanthin ratio increases with eccentricity in proportion to the rod:cone ratio in the retina. The correlation can be explained by the different uptake mechanisms of lutein and zeaxanthin by the rods and cones respectively (Bone et al 1988).

The macular pigment acts as an optical filter to counteract the chromatic aberration of the optical components of the eye and the light scattering by the ocular media. Indeed, Reading and Weale (1974) calculated the filter characteristics necessary to reduce the blur circle, resulting from chromatic aberration within the eye, to a nominal level. The necessary absorption spectrum was similar to that of the macular pigment. The yellow macular pigment may also provide a protective function through absorption of short wavelength light, which has been shown to be more harmful than longer wavelengths (Ham et al 1976). The pigment may also have a metabolic role in destroying free radicals formed on exposure to light (Kirschfeld 1982). Using a Tübinger perimeter, Haegestrom-Portnoy (1988) recorded a greater loss of blue (SWS) sensitivity at non-foveal locations compared to the fovea. The greater SWS sensitivity in areas of increased macular pigmentation supported the hypothesis that the pigment protects the foveal area from light damage.

Non-invasive techniques for the estimation of macular pigment absorption include fundus reflectometry (Norren and Tiemeijer 1986; Kilbride et al 1989), determination of the change in colour match at the fovea and parafovea (Ruddock 1963; Moreland and Bhatt 1984), comparison of the difference in the spectral sensitivity at the fovea and parafovea (Pease and Adams 1983; Pease et al 1987; Werner et al 1987; Hammond and Fuld 1992; Hudson and Wild 1993) and measurement of the brightness match between a polarised stimulus and an unpolarised surround (Bone and Sparrock 1971). The pigment absorption spectrum does not vary with age (Pease et al 1987; Werner et al 1987; Bone and Sparrock 1971; Ruddock 1965; Bone et al 1988) but exhibits a large variation (upto 1.0 log unit) between individuals (Pease and Adams 1983; Pease et al 1987; Bone et al 1992; Hudson and Wild 1993). Indeed, little variation in the quantity and

formation of macular pigment has been found with age using the laboratory technique of high performance liquid chromatography (Bone et al 1988).

A perimetric approach was utilized by Hudson and Wild (1993); Wild and Hudson (1995) to measure macular pigmentation with special reference to Blue-Yellow perimetry. The technique adapted the method of Pease et al (1983, 1987) to the Humphrey Field Analyser, whereby green cone sensitivity at 460nm and 570nm was measured at a foveal and a parafoveal location. Stimuli were presented on a red adapting background to adapt the red cones whilst the rods and blue cones were excluded by measuring flicker sensitivity at 25Hz. The technique assumed green cone sensitivity to be independent of eccentricity and the absorption of the pigment to be negligible at wavelengths greater than 560nm (Bone et al 1985). Macular pigment was calculated relative to 460nm:

$$OD_{mac} = (\log S_{p460} - \log S_{f460}) + (\log S_{f570} - \log S_{p570})$$

where OD_{mac} is the optical density of the macular pigmentation at 460nm, S is the sensitivity recorded at foveal (f) and parafoveal (p) locations for both 460nm and 570nm stimuli.

Estimates of the macular pigment optical density at 460nm have ranged from 0.32 log units to 0.87 log units (Pease and Adams 1983; Bone et al 1992; Hammond and Fuld 1992; Hudson and Wild 1993; Wild and Hudson 1995). It is therefore necessary to correct for the reduction in SWS sensitivity as a result of the macular pigmentation within the central 10° field if B-Y perimetry is to be valid in the assessment of central visual function.

4.6 Intraocular Light scatter

Intraocular light scatter occurs when light reaching the retina is deviated away from the original direction of travel. Early theories assumed uniform scattering in the ocular media (Stiles 1929; Fry 1954). However, light scatter is principally derived from the cornea, crystalline lens and fundus

(Vos 1984). The cornea contributes approximately 30%, the retina 20%, with the remainder attributable to the crystalline lens (Vos 1984).

4.7. Classification of light scatter

Scattering of light within the eye can be broadly divided into two types: backward and forward light scatter (Figure 4.1).

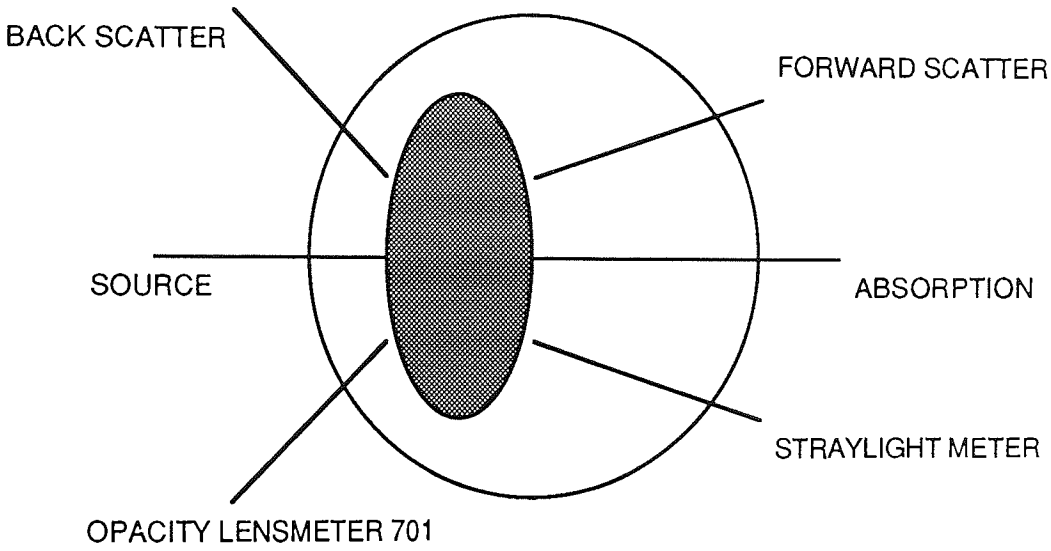

Figure 4.1 The relationship between backward and forward light scatter within the human eye.

Light scattered at angles of more than 90° to the incident light is termed backward light scatter, whilst light scattered at angles of less than 90° to the incident source is termed forward light scatter. Forward light scatter results in a veiling luminance superimposed upon the retinal image, with a corresponding reduction in image contrast (Miller and Benedek 1973; Phelps-Brown 1993). The severity of the reduction in contrast depends on the illuminance ratio between the background and the image. Disability glare is assumed to be a result of forward light scatter (Miller and Benedek 1973; Paulsson and Sjostrand 1980; Abrahamsson and Sjostrand 1986; van den Berg 1991; Phelps-Brown 1993) and is a common problem in patients with cataract, pseudophakia or corneal dystrophy and in contact lens wear (van den Berg 1986, deWaard et al 1992; Elliott et al 1991b).

4.7.1. Backward light Scatter

Various objective or subjective methods have been utilised to quantify the components of backward light scatter. Wolf and Gardiner (1965) measured backscatter using a slit lamp photometer and found a correlation with disability glare. Later, Siegelman et al (1974) quantified backscatter arising from cataract using the technique of microdensitometry based upon negatives produced by slit lamp photography. More recently, the Schiempflug slit-lamp camera has been used to document lens opacities quantitatively (Olbert et al 1985; Brown et al 1987; Baraldi et al 1987; Chen et al 1985; Datiles et al 1987; Edwards et al 1988, 1990; West et al 1988; Vivino et al 1993; Magno et al 1994) whereby a section of the lens is photographed and subjected to densitometric analysis. Indeed, Scheimpflug photographs have demonstrated that diabetic lens transparency is due to the duration of the diabetes rather than to the age of the patient (Olbert et al 1985). The Schiempflug system has also been utilised to quantify the effect of lens opacity on the visual field (Guthauser et al 1987).

A quantitative approach, the Opacity Lens Meter (OLM) 701, was devised by Flammer and Bebié (1987). The OLM was originally developed to measure the influence of cataract on the visual field in patients with both glaucoma and cataract. The instrument measures light back scattered from the crystalline lens. A 700nm wavelength beam of light 1.5mm in diameter is used to create scatter within the crystalline lens. The scattered light is detected and the degree of scatter converted to a digital scale, where a cataract would measure 25 or more depending on the severity of the cataract. The OLM measurement correlates well with age in patients with clear media (DeNatale et al 1988; Wegener and Hockwin 1988; Costagliola et al 1989; Elliott and Hurst 1989; Tuft et al 1990; Bonomi et al 1990; Dengler-Harles 1991; Sample et al 1991a). The high correlation can be explained by the fact that, in a normal eye, the majority of light scatter is thought to arise from the nuclear region (Zeimer and Noth 1984; Sparrow et al 1986). Indeed, Elliott and Hurst (1989) were only able to demonstrate a good relationship between VA and the OLM in normal eyes and in nuclear cataract. Similar findings have also been reported by Bonomi et al (1990). The relationship between VA and backward scatter in normal eyes and nuclear cataracts has also been documented for the Schiempflug camera (Brown et al 1987; Chen et al

1985; Datiles et al 1987). The poor relationship for other types of cataract is thought to be due to their irregular nature of scattering (Elliott and Hurst 1989) or their location (Bonomi et al 1990). Sample et al (1991a) also reported a good relationship between the psychophysical assessment of ocular media absorption at short wavelengths and the degree of back scatter recorded with the OLM. Caution must be exercised in eyes with a pupil diameter of less than 4mm, where absorption of scattered light by the iris may limit the measurement of back scatter with this method (Clarke et al 1990).

4.7.2. Forward light scatter

The distribution of a point source of light projected onto the retina can be represented by a bell-shaped function when light scatter occurs - the point spread function (PSF). The PSF can be divided into two parts: a central part upto 10 minutes of arc in width and a peripheral part beyond 1° eccentricity, which is termed straylight. The terms straylight and forward light scatter are synonymous. The degree of straylight has been quantified using a psychophysical technique, known as the equivalent veil technique. The technique involves the determination of an increment threshold at a given location away from the retinal image in the presence of a glare source at a given angular distance. The equivalent luminance level is then measured for a homogeneous patch of light that results in the same increment threshold (Vos 1984). The ratio of the luminances of the homogeneous (L_{eq}) and the image (E) fields determines the scatter estimate. Therefore, if a glare source produces an illumination (E) at the observer's eye at a given angle, then, according to the PSF, the straylight or light scatter factor (LSF) can be quantified by the equivalent luminance (L_{eq}) divided by the illuminance from a point glare source at the pupil plane (E) (Vos 1984). For example:

$$Leq / E = \text{constant}$$

The equation Leq/E does not remain constant for all angles of glare. Straylight also demonstrates angular dependency at glare angles greater than approximately 1°. Theoretical studies of intraocular light scattering have found the decline of L_{eq}/E with glare angle to occur at $1/\phi 2$

(Stiles 1930; Fry 1954) where ø represents the glare angle. Other angular functions extending over a variety of glare angles have been reported by other workers and are reviewed by Vos (1984). The Stiles-Holladay approximation has been used in many studies (Stiles 1929; Holladay 1926; Stiles and Crawford 1934; Vos 1984; van den Berg 1986; IJspeert et al 1990) and is defined as:

$$Leq / E = 10 / ø2.$$

The determination of veiling luminance (Leq) at a variety of different levels of glare intensity (E) has been measured by the presentation of a test object for a brief period of time (approximately 0.04 seconds) (Vos 1984). Other studies have determined the L_{eq} by measuring the contrast threshold of a series of sinusoidal gratings (Paulsson and Sjostrand 1980; Abrahamsson and Sjostrand 1986; Wood et al 1987b, 1989; Elliott et al 1989; Dengler-Harles et al 1990). Both types of experimental approach involve the difference between two threshold measurements, one performed in the presence of a glare source and the other without the glare source. The approach utilising contrast sensitivity measurements defines the LSF in terms of a contrast threshold with (M2) and without (M1) the glare source:

$$LSF = (L/E) \times [(M2 / M1) - 1]$$

The formula assumes that variations in the factors, L and E, do not alter the magnitude of the LSF since alterations in the contrast thresholds, M1 and M2, would alter to compensate for any alterations in L and E. The validity of this approach has recently been called into question (van den Berg and IJspeert 1992; deWaard et al 1992; Yager et al 1992). Yager et al (1992) calculated the LSF at two different values of L/E; the LSF did not remain constant using the equation defined above. A non-linear relationship between the straylight measured with the van den Berg Straylight meter and the LSF measured with and without a glare source using the Vistech MCT8000 has also been demonstrated by deWaard et al (1992). van den Berg and IJspeert (1992) considered that contrast threshold measurements may vary, particularly in the presence of a glare source,

due to adaptational and subjective criterion changes. Whitaker et al (1994) measured contrast thresholds at each of three glare illuminance levels for each of three stimulus luminances with and without a glare source. They found agreement with the Paulsson and Sjostrand equation and stressed the need for the high adaptation levels, where contrast thresholds are independent of luminance.

A more direct approach to measure forward light scatter, the direct compensation method, has been devised by van den Berg (van den Berg 1986; van den Berg 1990; IJspeert et al 1990; van den Berg et al 1990). The technique does not involve the measurement of a threshold but directly measures in-vitro forward light scatter at different glare angles. The observer positions the eye against a rubber cup at the end of a viewing tube and views a circular target of 1° radius, surrounded by a circular ring with an outer radius of 2° and a fixed luminance of $30cdm^{-2}$ (Figure 4.2). Concentric to the target are three rings of yellow LEDs (570nm, colour temperature 2900-3150K) subtending angles of 3.5°, 10° and 28° respectively from the patients eye. Yellow light is used to minimise the amount of light transmitted through the ocular wall (van den Berg 1992). The LED sources flicker at 8Hz and are illuminated individually. When the patient views the target, flicker is perceived, due to forward light scatter within the eye. The luminance modulation of the central target, flickering in counterphase with the glare source, is increased until no flicker is perceived. The measurement is repeated several times at each glare angle. The straylight parameter can be calculated from the equation:

$$s(\phi) = \phi^2 \times L / E$$

where L is the compensating luminance modulation of the central target, ø is the scattering angle and E is the illuminance of the straylight source at the pupil plane. The technique has demonstrated an increase in light scatter with age (van den Berg 1986; Elliott et al 1991a) and in the presence of cataract (deWaard et al 1992), corneal dystrophy, hypopigmentation (IJspeert et al 1990; van den Berg 1990; Elliott et al 1991a) and in contact lens wear (Elliott et al 1991b).

The relationship between the degree of backward light scatter and disability glare in normal healthy eyes has been studied previously (Wolf 1960; Allen and Vos 1967; Wolf and Gardiner 1965 Elliott and Hurst 1989). Wolf (1960) demonstrated a linear relationship between the two factors but this has not generally been substantiated in later studies (Allen and Vos 1967; Elliott and Hurst 1989; Dengler-Harles 1991). The degree of forward light scatter assessed by the direct compensation technique shows a poor correlation with backward scatter using the OLM for cortical and for PSC cataracts and a moderate correlation for nuclear cataract (deWaard et al 1992). Mitchell and Hurst (1993) found no correlation between forward light scatter, measured by the direct compensation technique, and backward light scatter measured with the Schiempflug camera. Similarly, various studies have demonstrated little relationship between VA and forward light scatter assessed by contrast sensitivity (Hess and Garner 1977; Hess and Woo 1978; Elliott et al 1991a) or by the direct compensation technique (Elliott et al 1991a).

4.8. Effects of media opacity on the White-White visual field

The effect of media opacities on the conventional W-W visual field has been studied using various types of cataract simulations. Heur et al (1988) simulated light scatter using ground-glass diffusers placed in front of the normal eye. They found a reduction in sensitivity recorded with both the Octopus and Humphrey perimeters which was independent of eccentricity and increased as the strength of the diffuser increased. Their findings were explained on the basis of a reduction in the stimulus luminance as a result of light scatter. Bundenz et al (1993) applied a similar procedure to a sample of glaucoma patients. The visual field was found to be diffusely depressed. Consequently, it was suggested that scotomata demonstrating a greater degree of progression compared to areas of the visual field considered to be normal were more likely to be indicative of glaucomatous progression rather than to an increase in light scatter (Bundenz et al 1993). Other simulations of cataract have included petroleum jelly spread over optical lenses (Zuckerman 1973), neutral density filters (Eichenberger et al 1987) and orthoptic occluders (Niesel et al 1978;

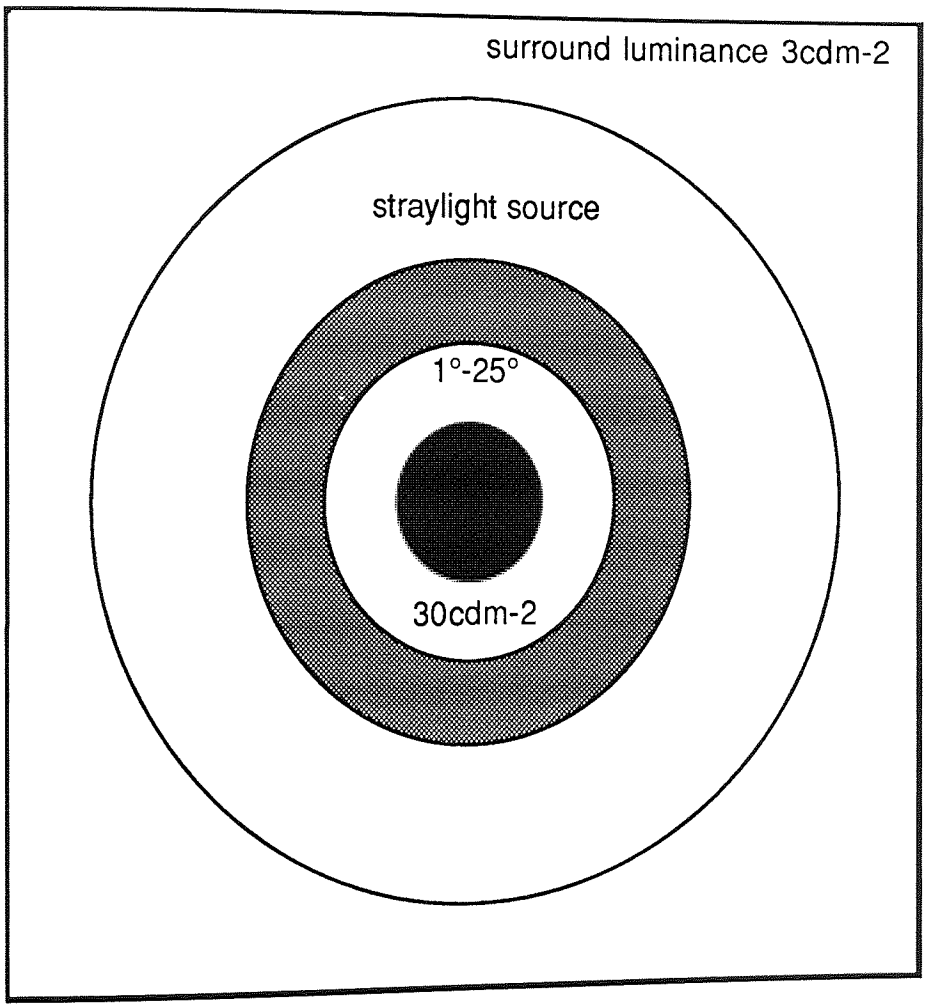

Figure 4.2. The spatial configuration of the viewing stimulus of the Straylight meter. Fixation is maintained on the dark central patch. A counterphase flickering light is adjusted within the patch to compensate for straylight induced by the peripheral glare source. The 30cdm^{-2} intermediate ring suppresses the perception of flicker in the area adjacent to the fixation patch. The grey area represents part of the instrument housing.

Niesel and Wiher 1982; Urner-Bloch 1987). These latter studies have also demonstrated a predominantly general reduction in sensitivity across the visual field. Increases in the degree of focal loss have also been recorded in some studies (Eichenberger et al 1987; Urner-Bloch 1987). Wood et al (1987b) utilised various concentrations of polystyrene microspheres suspended in solutions of distiled water and contained in optical cells placed before the normal eye. A specific bead diameter of 500nm was selected, as it is thought that the diameter of protein aggregates is between 300nm and 500nm in human (Bettelheim and Siew 1982) and calf (Delaye et al 1982) cataractous lenses. Wood et al (1987b) found a reduction in sensitivity which increased with increase in light scatter. The attenuation was greater centrally for the LED stimuli of the Dicon Autoperimeter compared to that with the projected stimuli of the Octopus Automated Perimeter 201 whilst the converse applied in the periphery. It was suggested that the larger (Goldmann size III, 0.43°) stimuli of the Octopus perimeter may saturate the central area rendering it relatively insensitive to light scatter compared to the smaller stimuli of the Dicon (0.28°). This finding was in agreement with that of Greve (1979) who noted that cataract flattened the hill of vision by depressing central sensitivity. The model of Wood et al (1987b) was compared to a sample of uniocular cataract patients (Wood et al 1989). Non-nuclear cataracts showed agreement with the model, however, nuclear cataracts showed a reduction in sensitivity that was greater centrally for both types of perimetric stimuli. The model was subsequently applied to a sample of glaucoma patients by Dengler-Harles et al (1990). They found a linear increase in MD and a curvilinear decrease in LV, with increase in light scatter, indicating a decrease in the depth and / or area of focal loss. Two possible explanations were suggested: firstly adjacent areas of greater sensitivity may be responsible for the detection of a stimulus as a result of light scatter and secondly a localised reduction of focal loss may occur in that light scatter has a more adverse effect in areas of high sensitivity compared to areas of reduced sensitivity.

Studies of the automated visual field following cataract extraction and intraocular lens implantation have shown that MS increases both in normal (Urner-Bloch 1987; Guthauser et al 1988; Lam et al 1991) and in glaucomatous eyes (Hendrickson et al 1987; Urner-Bloch 1987) following IOL implantation. The relationship between backward light scatter and visual field

sensitivity has also been investigated. deNatale and Flammer (1989) studied the relationship between the OLM reading and the visual field index MS, pre- and post-operatively In a sample of 113 cataract patients. A good relationship was demonstrated between the pre-operative OLM reading and the post-operative MS for both nuclear and cortical cataract types (r=0.88), but not for posterior sub-capsular cataract type (r=0.28). The effects of straylight on visual performance in pseudophakic eyes has also been studied . Witmer et al (1989) demonstrated a greater degree of straylight in pseudophakic eyes without capsular opacification compared to normal phakic eyes. The greater straylight was considered to be due to the combination of the posterior capsule and the implant lens. Hard et al (1993) demonstrated similar findings, namely increased straylight in pseudophakic eyes compared to normal eyes; contrast sensitivity measured with and without a glare source revealed an increase in the magnitude of glare induced visual loss in the pseudophakic group. The effects of straylight on the visual field of a pseudophakic eye compared to a normal eye is unknown.

A new psychophysical procedure, flicker perimetry, has been reported to be of use in the early detection of glaucoma (Breton et al 1991; Lachenmayr et al 1989, 1991a, b, c, 1992a; Lachenmayr and Drance 1992a, b). Image degradation induced by simulated media opacities has a more adverse effect on conventional W-W perimetry compared to flicker sensitivity (Lachenmayr and Gleissner 1992). This differential effect can be used to explain the difference in the rates of decline with age of conventional W-W and flicker sensitivity (Casson et al 1993a; Lachenmayr et al 1992b, 1994).

4.9. Aim of the study

The incidence of glaucoma and cataract increase with increase in age and the two conditions frequently coexist. The influence of forward light scatter on the B-Y visual field is unknown. The aim of the first part of the study was to investigate the effect of induced forward light scatter on the B-Y perimetric profile in normal subjects and to compare this to the conventional W-W profile using a previously accepted model of induced scatter (Wood et al 1987b; Dengler-Harles et al

1990). The aim of the second part of the study was to determine the effect of age-related cataract and cataract type on the B-Y perimetric profile.

4.10. The effect of induced forward light scatter on the normal Blue-Yellow perimetric profile

4.10.1. Materials and methods

Sample

The sample comprised 15 emmetropic Caucasian volunteers (ten males and five females) randomly recruited from the Department of Vision Sciences, Aston University. The mean age of the sample was 24.13 years (SD 3.56). All subjects conformed to rigid inclusion criteria namely a corrected visual acuity of better than 6/6, intraocular pressure of less than 22mmHg, no history of ocular disease or trauma, no history of amblyopia, no neurological history or history of systemic disease, no systemic medication known to influence visual field sensitivity and normal colour vision by the Farnsworth-Munsell 100-Hue test. Informed consent was obtained from each subject.

Perimetry

Perimetry was performed on the right eye of each subject using a modified Humphrey Field Analyser 640 (Plate 4.1). The modifications comprised the addition of a high-intensity external illumination system consisting of two ELE/ELT 80W/30V tungsten halogen bulbs (GE Thorn, Ohio, USA) mounted either side of the perimeter housing behind infra-red filters, diffusing filters and a Schott OG530 yellow long pass filter (Schott Glaswerke, Mainz, Germany). The diffusing filter was positioned flush with the surface of the perimeter bowl to ensure uniform illumination over the perimeter bowl surface (±2% within 30° of fixation). The background luminance was 330cdm^{-2}. The lamp life was extended by deliberately under running the voltage at 28.5V using a stabilised Farnell power unit (Farnell Instruments Ltd, Wetherby, Yorkshire, UK). Cooling fans were used to dissipate heat from the bulbs. To increase the dynamic range of the perimeter, a concave mirror (28mm radius, 40mm diameter) was placed 28.8mm behind the stimulus bulb to increase the maximum stimulus luminance to 16000 apostilbs thereby producing a gain of 2dB in

dynamic range (Hudson et al 1993). The stimulus filter was contained in a filter holder attached to the projector arm. The blue OCLI dichroic filter (OCLI, Santa Rosa, CA, USA) achieved approximately 1.4 log units of SWS isolation and a dynamic range of 2.94 log units. This compares with the dynamic range of 3.00 log units employed by Sample and Weinreb (1990, 1992) and 2.74 log units by Johnson et al (1988b). The stimulus and background spectral transmission characteristics are compatible with those of Johnson et al (1988b, c, 1989a, 1993a, b, d); Flanagan et al (1991a); Adams et al (1991); Lewis et al (1993) and Casson et al (1993b) (Figure 4.3). The background adaptation level of 330cdm^{-2} results in a greater adaptation of the MWS and LWS pathway (Yeh et al 1989) compared to the 89cdm^{-2} background employed by Sample and Weinreb (1990, 1992). Furthermore, saturation of rod function is assured at a background intensity of greater than 300cdm^{-2} (Aguilar and Stiles 1954). The modifications became operative after the instrument had performed the standard calibration routine and after the standard 31.5asb background had been extinguished using 5.3 software commands. The background and filters were calibrated using an LMT L1003 photometer (LMT Lichtmesstechnik GmbH, Berlin, Germany).

The decibel printout at each stimulus location on the HFA is referenced to 10000asb. The HFA calibration system remains unaware of the increase in the maximum stimulus intensity from the mirror modification and of the reduction in stimulus luminance arising from the introduction of the given broadband filters. The recorded sensitivity was recalculated to account for the attenuation in stimulus luminance as a result of the stimulus filter. All sensitivity values recorded in decibels underwent the following mathematical procedure:

$$dB = k + 10 \log L/\Delta L$$

where dB is the sensitivity measured in decibels, k is a constant dependent upon the state of retinal adaptation, L is the background luminance and ΔL is the threshold.

When the perimeter is in the normal mode, ie when dB=0, the maximum stimulus luminance of the perimeter is 10000asb. By substitution:

$$0 = k + 10 \log L/10000$$

$$0 = k + 10 \log L - 10 \log 10000$$

$$k = 40 - 10 \log L$$

Thus for any dB value:

$$dB = 40 - 10 \log \Delta L$$

When the perimeter is in the colour mode, dB_f is the dB printout for a given filter with a stimulus luminance of ΔL_f, then

$$\log \Delta L_f = (40 - dB_f)/10$$

However, the HFA does not account for the attenuation of the maximum stimulus luminance, ΔL_{att}, resulting from the use of a stimulus filter. When $dB_f = 0$, then $\Delta L_f = \Delta L_{f\ max}$ and the attenuation can be calculated as:

$$\Delta L_{att} = 4.0 - \Delta L_{f\ max}$$

where 4.0 is the maximum ΔL in log units of the HFA in its normal mode and $\Delta L_{f\ max}$ is the maximum stimulus luminance of the particular filter. The true threshold ΔL_t can then be expressed as:

$$\Delta L_t = \Delta L_f - \Delta L_{att}$$

The maximum stimulus luminance of the blue OCLI filter was 275.4cdm^{-2} (865asb) and that of the yellow OG530 filter 4029.3cdm^{-2} (12658asb). All data was normalised relative to the maximum stimulus luminance of the yellow stimulus filter.

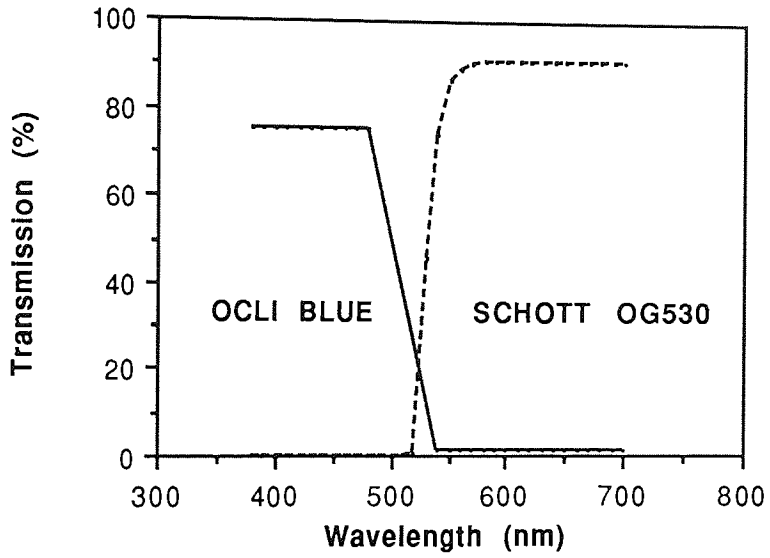

Figure 4.3. Spectral transmission characteristics of the blue OCLI stimulus filter and the yellow OG530 background filter employed for Blue-Yellow perimetry.

Perimetry was performed for each of four stimulus configurations: conventional W-W (background luminance 10cdm^{-2}) using stimulus sizes III (0.43°) and V (1.72°), Yellow-Yellow (Y-Y) (background luminance 330cdm^{-2}, stimulus size V) and Blue-Yellow (background luminance 330cdm^{-2}, stimulus size V). The stimulus duration for each of the four combinations was 200ms. The W-W (size III) was chosen since it is the clinical standard currently employed on the HFA. A size V stimulus was used for B-Y perimetry to further enhance the dynamic range of the perimeter and is compatible with the increase the isolation of the SWS response reported for a 2° diameter stimulus (King-Smith and Carden 1974). Furthermore, a size V stimulus is compatible with that of other B-Y perimetric studies (Heron et al 1988; Johnson et al 1988b, c, 1989a, 1993a, b, d; Adams et al 1991; Sample and Weinreb 1990, 1992; de Jong et al 1991, 1993; Casson et al 1993b; Lewis et al 1993). The Y-Y (size V) stimulus combination was chosen as a control for the

chromatic B-Y stimulus combination and was achieved with a Schott OG530 long pass filter (Schott Glaswerke, Mainz, Germany). The W-W (size V) was used to control for the effect of background luminance, maintaining the same size as the chromatic stimuli.

Forward light scatter

Intraocular light scatter was induced using 0.00%, 0.08% and 0.16% concentrations of 500nm diameter monodispersed polystyrene microspheres suspended in saline (Polysciences Ltd, Warrington, USA). The solutions were contained in cells constructed from 75mm diameter plano CR39 lens blanks mounted either side of a perspex ring 15mm in thickness. The scatter cells were mounted on the head rest of the perimeter and positioned as close to the eye as possible to minimize the influence of vertex distance and rim artifacts (Plate 4.2). The cell remained perpendicular to the eye at all times but could be adjusted in the x and y planes with respect to the eye.

The degree of straylight in the cell-free situation and for each scatter cell was measured for each subject using the direct compensation technique of van den Berg (1986, 1987, 1990, 1992) (Plate 4.3). This method of scatter assessment was chosen because it measures light scatter at different angles, needs little prior patient experience and since a threshold is not measured the outcome is not influenced by retinal disturbances. When straylight was measured in association with the scatter cells, the eye-cup was removed from the instrument and the cell placed between the eye and the instrument. As a consequence, the vertex distance remained constant between the eye and the glare sources and the measurement of straylight remained valid (van den Berg, personal communication). All measurements were made in complete darkness. As a result of forward light scatter, flicker is perceived in the central target. The luminance modulation (L) is adjusted until cancellation of the flicker occurs. The technique was discussed in more detail in Section 4.7.2. The measurement was repeated 6 times at each of the three angles of scatter (3.5°, 10° and 28°) for all four cell configurations.

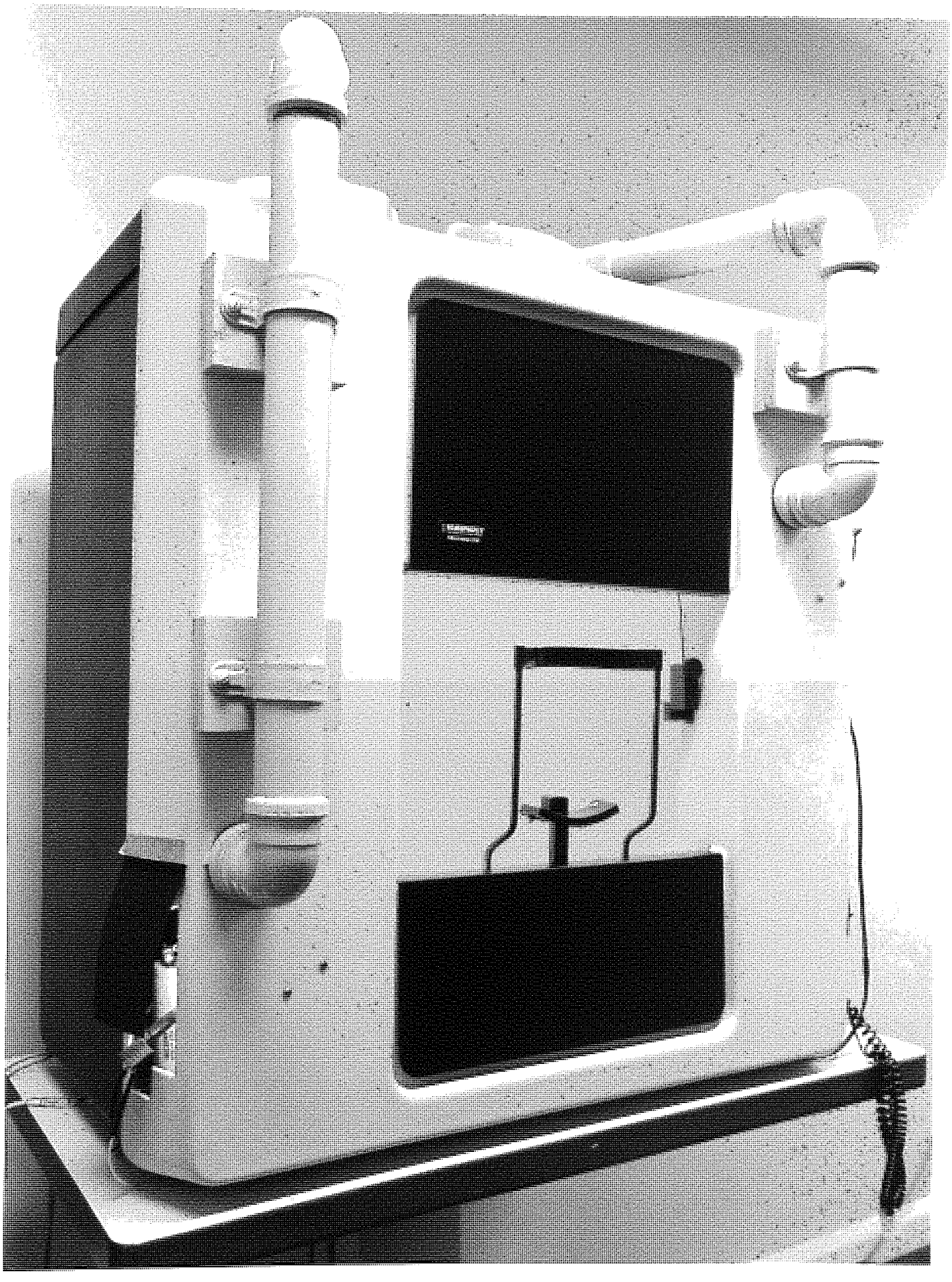

Plate 4.1. The modified Humphrey Field Analyser 640 adapted for high luminance colour perimetry. Tubing mounted on the outside serves as a cooling system whereby air is drawn over bulbs and air expelled via ducting.

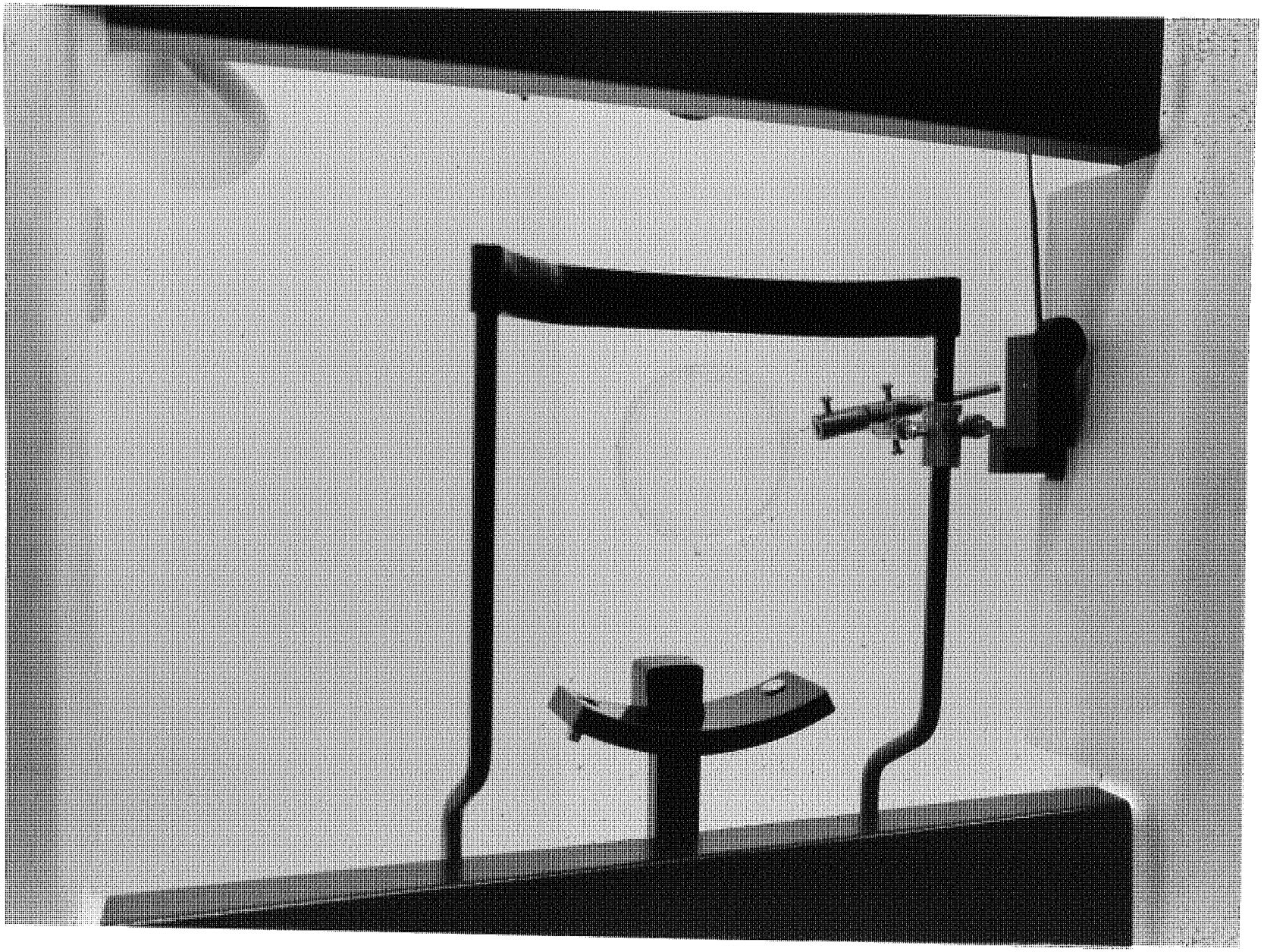

Plate 4.2. An optical cell containing the scatter suspension mounted on the head rest of the perimeter. The cell is positioned before the right eye of the subject. Adjustment of the cell position is made using the mounting bracket attached to the head rest.

Plate 4.3. The straylight meter of van den Berg measures the degree of forward light scatter by the direct compensation technique. The measurement is taken in complete darkness, the non-tested eye is occluded.

The measurement was repeated 6 times at each of the three angles of scatter (3.5°, 10° and 28°) for all four cell configurations. Straylight was quantified by the equation:

$$\text{Straylight parameter} = \text{ø}^2 \times (L/E)$$

where ø is the diameter of the glare ring, E is the illuminance of the glare source at the eye and L is the luminance required to compensate for straylight. The mean straylight parameter was calculated for each subject at each of the three glare angles.

Ocular media absorption

The degree of wavelength dependent lenticular absorption for each subject was determined with the HFA by measuring two scotopic thresholds of equal sensitivity to rhodopsin pigment ie. 410nm and 560nm using the technique of Norren and Vos (1974). The measured differences in scotopic sensitivity between the two wavelengths are attributed to wavelength dependent absorption. The technique however assumes the rhodopsin action spectrum is invariant (Alpern 1987), the absorption of light per unit path length remains constant during life whilst the lens thickness increases (Mellerio 1971) and that any difference in sensitivity to 410nm and 560nm stimuli is predominantly due to absorption by the crystalline lens (Weale 1988).

The HFA background illumination was extinguished and the ambient room conditions made as dark as possible ($<0.01 cdm^{-2}$). Fixation was assessed using an infra-red light source (20W/12V tungsten halogen bulb mounted behind a Schott RG830 black light filter) mounted within the perimeter and observed via the perimeter monitor. Subjects were dark adapted for at least 30 minutes prior to measurement of lenticular absorption. Shorter dark adaptation times in older individuals may not result in complete rod adaptation (Sample and Weinreb 1992). Stimuli (size V, stimulus duration 100ms) of 410nm (HW 11nm) and 560nm (HW 9mm) were presented at 15.6° eccentricity in each quadrant along the 45° / 225° meridians to avoid the effects of macular pigmentation. Such stimulus parameters are considered to maximize the responses from rod mechanisms (King-Smith and Carden 1974). Threshold measurements were repeated three times

for each filter and were taken in the cell-free condition and with the 0.08% and 0.16% scatter cells. The data was scaled relative to the crystalline lens of the 'standard observer' after Norren and Vos (1974) and to the characteristics of the OCLI filter:

$$OD_{lens} = OD_{stand} \times (Y/_{0.90})$$

where OD_{lens} is the individual lens optical density at a particular wavelength, OD_{stand} is the mean "standard observer" optical density at a particular wavelength, Y is the measured difference in log relative sensitivity between the 410nm and 560nm stimuli and 0.90 is the mean "standard observer" density difference between the 410nm and 560nm stimuli. The B-Y sensitivity for each subject was corrected for individual ocular media absorption by adding the calculated ocular media absorption value to the sensitivity at each stimulus location.

4.10.2. Analysis

The sensitivities for the B-Y, Y-Y and W-W stimulus combinations at each stimulus location were calculated in log units. Perimetric attenuation, defined as the difference in perimetric sensitivity measured with and without the induced scatter was calculated for the 0.00%, 0.08% and 0.16% scatter combinations. The representation of B-Y sensitivity in decibels is not identical to that used for conventional W-W perimetry. The difference in measurement scales arises from the difference in the maximum stimulus luminance of the blue stimulus compared to that of the standard white stimulus. The measurement scales for B-Y and W-W perimetry, however, are both logarithmic in nature. Therefore, a difference between any two recorded B-Y sensitivities (ie sensitivity with and without a scatter cell) is based upon the same measurement scale as the difference between any two recorded W-W sensitivities. This mathematical approach will also be used in later sections (Sections 4.11.2, 5.4.3 and 6.2.3) to compare abnormal sensitivity to the age-matched normal value.

4.10.3. Results

Group mean pupil size measured on the video monitor of the HFA and corrected for the magnification of the monitor was 5.42mm (SE 0.22) and 3.54mm (SE 0.16) for the white and yellow adapting backgrounds respectively. The effect of the cell configuration ie no cell, 0.00%, 0.08% and 0.16% had no effect on pupil size.

Group mean lenticular absorption was 0.40 log units (SD 0.01) for the cell free situation, and 0.40 log units (SD 0.02), 0.40 log units (SD 0.04) and 0.43 log units (0.04) in combination with the 0.00%, 0.08% and 0.16% scatter combinations respectively. A repeated measures ANCOVA with scatter combination as a within-subjects factor and age as a covariate revealed that the magnitude of absorption was similar across all scatter combinations (p=0.09) (Table 4.1). The ANCOVA is an analysis of variance technique which corrects for the differing ages within the sample.

Source	dF	Sums of Squares	Mean Square	F value	P value
Age	1	0.000	0.000	0.239	0.640
Error	7	0.006	0.001		
Scatter Cell	2	0.003	0.002	3.133	0.093
Age x Scatter cell	2	0.000	0.000	0.267	0.769
Error	14	0.008	0.001		

Table 4.1. Repeated measures ANCOVA for ocular media absorption in the cell free situation and in conjunction with the 0.08% and 0.16% scatter combinations.

The reduction in group mean global mean sensitivity (where a negative value represents a reduction in sensitivity) as a function of scatter configuration is illustrated in Table 4.2.

The group mean reduction in sensitivity for each cell configuration and stimulus combination as a function of eccentricity is shown in Figure 4.4. Repeated measures ANCOVA with stimulus combination, eccentricity and scatter configuration as within-subjects factors and age as a

covariate showed that perimetric attenuation increased as a function of scatter cell concentration ($p=0.055$) irrespective of colour ($p=0.257$) and age ($p=0.052$). The reduction in sensitivity increased with increase in eccentricity ($p=0.023$) particularly for the B-Y stimulus combination ($p=0.029$) and with increase in scatter ($p=0.012$) irrespective of age ($p=0.010$) (Table 4.3).

	Scatter Configuration		
Stimulus / Background combination	0.00%	0.08%	0.16%
B-Y size V	-0.11 (0.18)	-0.56 (0.19)	-0.81 (0.27)
Y-Y size V	-0.12 (0.12)	-0.33 (0.15)	-0.43 (0.15)
W-W size III	-0.04 (0.14)	-0.32 (0.16)	-0.45 (0.13)
W-W size V	-0.09 (0.08)	-0.32 (0.15)	-0.45 (0.14)

Table 4.2. Group mean reduction in global mean sensitivity for each of the four stimulus combinations. Values are expressed in log units. One log unit is equivalent to 10dB. One standard deviation is given in parenthesis.

Group mean straylight parameters for each angle of scatter and each cell configuration are displayed in Figure 4.5. A repeated measures ANCOVA with glare angle (ie small, medium and wide) and scatter configuration as within-subjects factors and age as a covariate showed that the straylight parameter increased as a function of the scatter concentration ($p<0.001$), was greater for larger glare angles ($p<0.001$), particularly for the higher scatter concentrations ($p=0.001$), but was independent of age ($p=0.455$) (Table 4.4). The reduction in perimetric sensitivity plotted against the average straylight parameter for the 0.00%, 0.08% and 0.16% scatter concentrations combined is displayed in Figure 4.6 a and b. A reasonable correlation ($r=0.77$) was found between the reduction in B-Y sensitivity and the average straylight parameter.

Source	dF	Sums of Squares	Mean Square	F value	P value
Age	1	0.038	0.038	0.096	p=0.763
Error	12	4.721	0.393		
Scatter combination	2	1.094	0.547	3.388	p=0.548
Age x Scatter combination	2	1.116	0.558	3.456	p=0.052
Error	24	3.876	0.161		
Stimulus combination	3	0.942	0.314	1.438	p=0.257
Age x Stimulus combination	3	0.623	0.208	0.951	p=0.398
Error	36	7.858	0.218		
Eccentricity	5	0.776	0.155	3.429	p=0.023
Eccentricity x Age	5	0.641	0.128	2.831	p=0.047
Error	60	2.716	0.045		
Stimulus comb x Scatter comb	6	1.036	0.173	2.522	p=0.029
Stimulus comb x Scatter comb x Age	6	0.839	0.140	2.043	p=0.138
Error	72	4.928	0.068		
Scatter combination x Eccentricity	10	0.432	0.043	2.400	p=0.012
Scatter comb x Eccentricity x Age	10	0.446	0.045	2.478	p=0.059
Error	120	2.162	0.018		
Stimulus combination x Eccentricity	15	0.523	0.035	0.971	p=0.451
Stimulus comb x Eccentricity x Age	15	0.541	0.036	1.005	p=0.429
Error	180	6.460	0.036		
Scatter comb x Colour comb x Ecc	30	0.936	0.031	2.609	p=0.027
Scatter x Colour x Ecc x Age	30	0.979	0.033	2.731	p=0.022
Error	360	4.303	0.012		

Table 4.3 Repeated measures analysis of covariance for the perimetric attenuation.

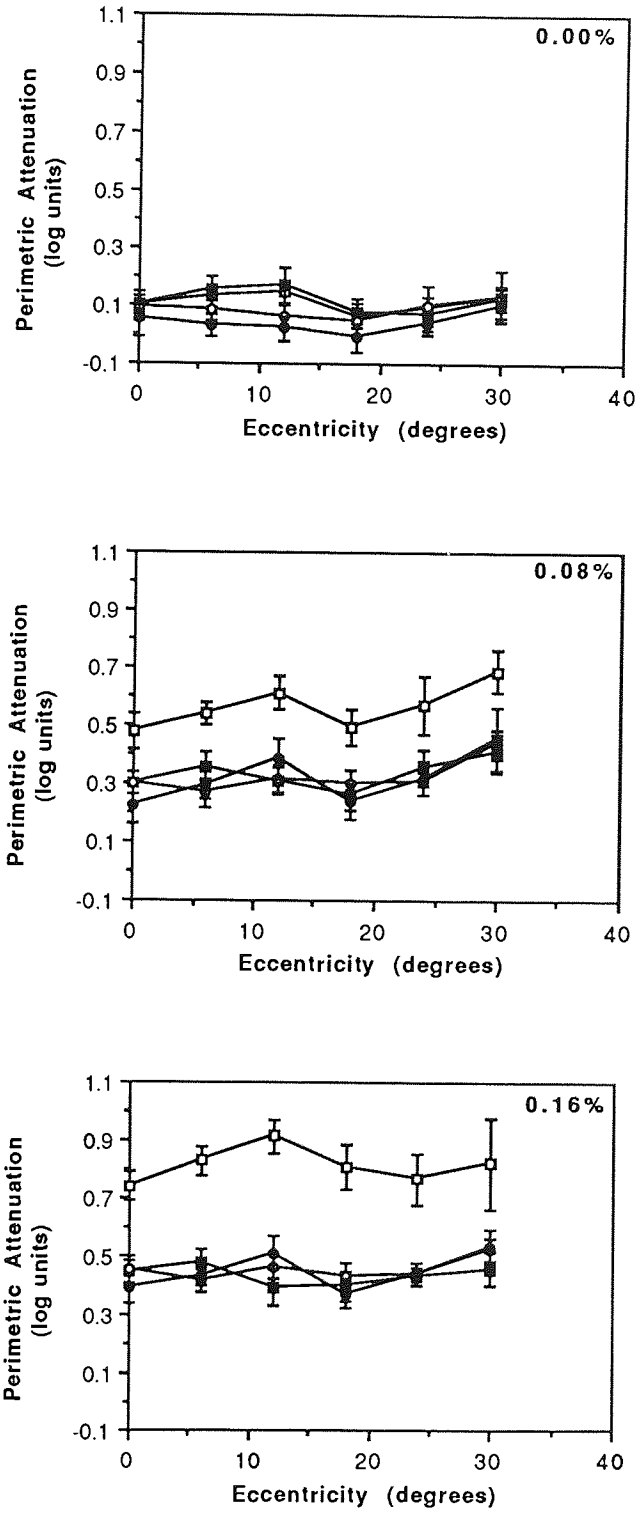

Figure 4.4. Group mean reduction in sensitivity for each cell configuration as a function of eccentricity. Open squares represent B-Y, closed squares Y-Y, open circles W-W size III and closed circles W-W size V stimulus combinations. Error bars represent one standard deviation of the mean.

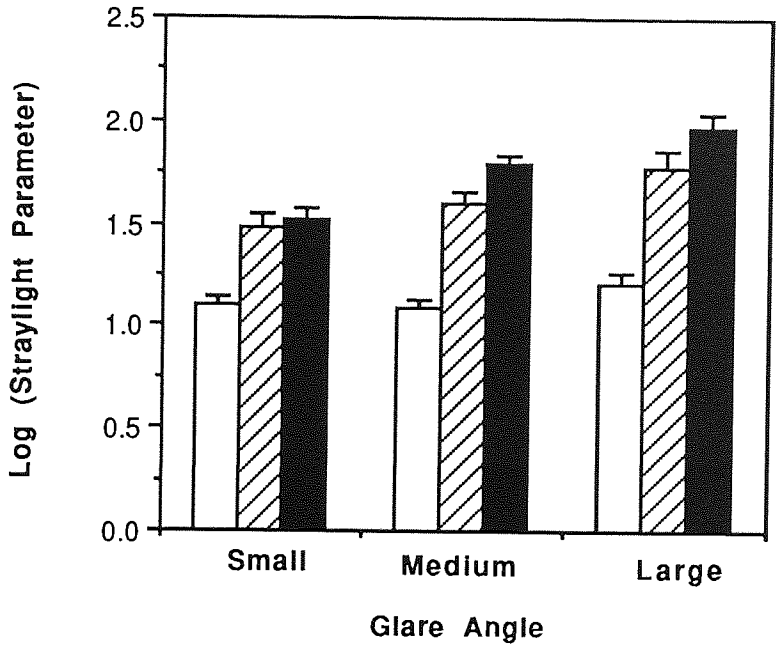

Figure 4.5. Group mean straylight parameter at small, medium and large glare angles against scatter concentration. Open columns represent the 0.00%, hatched columns the 0.08% and filled columns the 0.16% scatter concentrations. Error bars represent one standard deviation of the mean.

Source	dF	Sums of Squares	Mean Square	F value	P value
Age	1	0.071	0.071	0.597	p=0.455
Error	12	1.424	0.119		
Scatter cell	2	8.409	4.204	67.741	p<0.001
Age x Scatter cell	2	0.129	0.064	1.038	p=0.370
Error	14	1.490	0.062		
Glare angle	2	1.581	0.791	26.001	p<0.001
Age x Glare angle	2	0.070	0.035	1.159	p=0.331
Error	24	0.730	0.030		
Scatter cell x Age	4	0.455	0.114	5.446	p=0.001
Scatter cell x Glare angle	4	0.027	0.007	0.328	p=0.858
Error	48	1.003	0.021		

Table 4.4. Repeated measures analysis of covariance for the log straylight parameter.

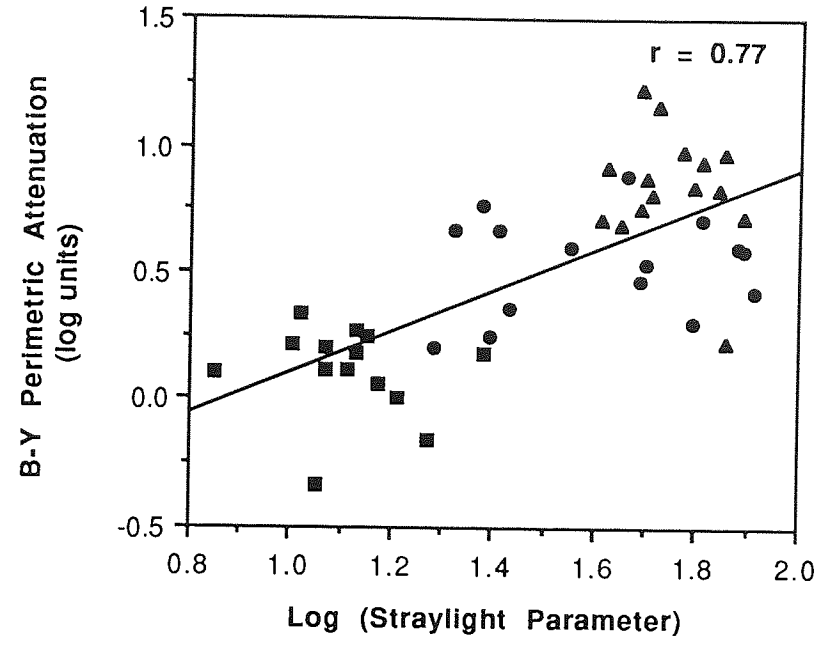

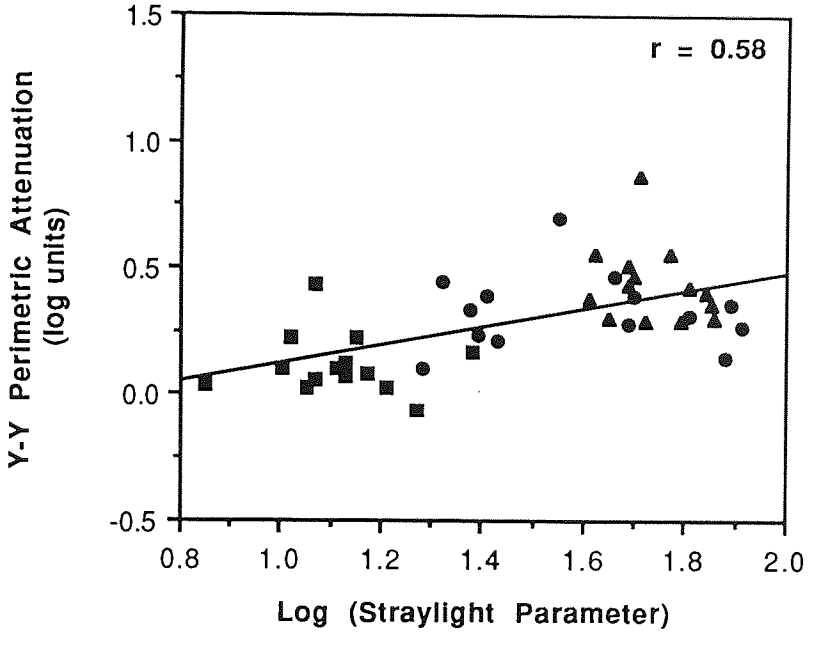

Figure 4.6a. Reduction in B-Y (top) and Y-Y (bottom) sensitivity against the average straylight parameter as a function of scatter concentration. Squares represent the 0.00%, Circles the 0.08% and triangles the 0.16% scatter concentrations.

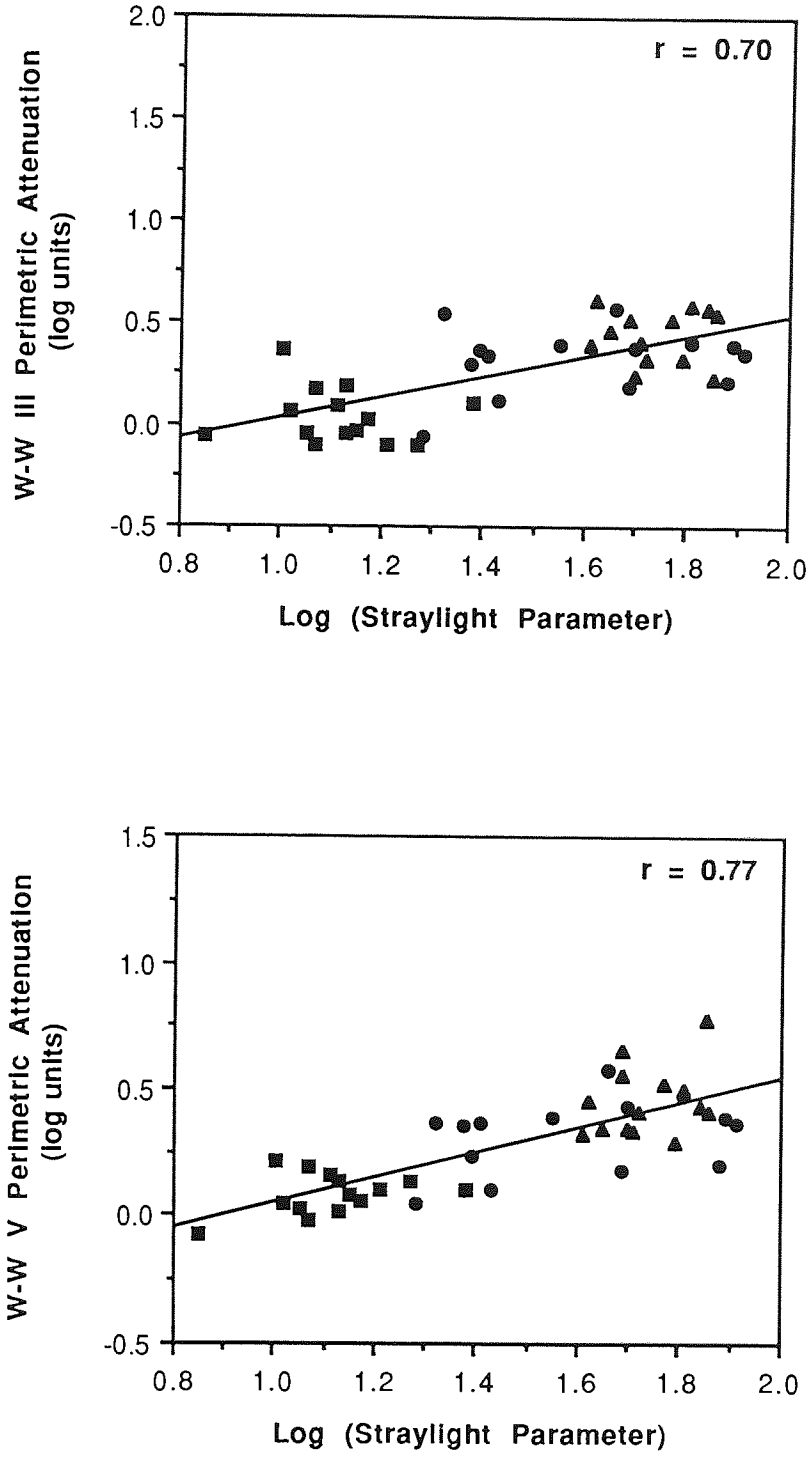

Figure 4.6b. Reduction in W-W size III (top) and size V (bottom) sensitivity plotted against the average straylight parameter as a function of scatter concentration. Squares represent the 0.00%, Circles the 0.08% triangles the 0.16% scatter concentrations.

4.10.4. Discussion

The finding that forward light scatter reduces perimetric sensitivity for the W-W stimulus combination is in agreement with other studies (Eichenberger et al 1987; Funkhouser 1991; Heur et al 1988; Wood et al 1987b, 1989). The reduction of the Y-Y sensitivity is consistent with that for the W-W stimulus combination. Furthermore, both reductions in sensitivity increased as the degree of forward light scatter increased. The general reduction in sensitivity resulting from forward light scatter will therefore serve to under-estimate the degree of focal loss in cases where glaucoma and cataract co-exist (Dengler-Harles et al 1990; Bundenz et al 1993; Fankhouser and Haeberlin 1980). The attenuation of both the W-W and Y-Y sensitivity is due to light scatter merging the stimulus and background together; consequently the stimulus loses its sharp-edged profile. This can be likened to the effect of cataract on the contrast sensitivity function at high spatial frequencies (Hess and Woo 1987).

The results also demonstrate a greater and predominantly diffuse loss of B-Y sensitivity. The greater attenuation of the B-Y than of the Y-Y response can be explained on the basis of the chromatic content of the stimulus since the stimulus size and background luminance characteristics are the same. The B-Y stimulus, in addition to the loss of luminance contrast, also exhibits a change in chromaticity towards that of the yellow background because of the difference in colour between the stimulus and background. The results also suggest an increased variability in the group mean B-Y response, particularly for larger amounts of scatter, compared to the W-W and Y-Y luminance responses. This increased variability may reduce the clinical efficacy of the B-Y technique in detecting early visual field loss.

The influence of differences in pupil size between the different stimulus combinations has little or no effect on the results. The background luminance was identical between the B-Y and the Y-Y stimulus combinations. Similarly, the differences in pupil size which occurred between the W-W and the Y-Y stimuli are unlikely to produce any differences in attenuation due to the operation of Weber's Law at these background luminances.

The relationship between stimulus wavelength and scatter is equivocal. Early studies assumed that Rayleigh scattering occurred within the eye (Stiles 1929; Fry 1954). This involves the preferential scattering of short wavelength light such that light is scattered in proportion to the reciprocal of the wavelength raised to the power of four. Boettner and Wolter (1962) showed greater scatter at short wavelengths in a sample of enucleated eyes, but less than that predicted by Rayleigh scattering. More recent studies have failed to demonstrate significant wavelength dependent scattering within both normal and cataractous eyes (Wooten and Geri 1987; Whitaker et al 1993) although a small amount of wavelength dependent scatter occurs due to eye-wall transmittance and fundal reflections (IJspeert et al 1990; van den Berg et al 1991). Interestingly, straylight is higher in blue-eyed than in dark eyed Caucasians, particularly for larger angles. Furthermore, increased scatter occurs at longer wavelengths, particularly in blue-eyed Caucasians. The degree of wavelength scatter may be pupil size dependent, since the pupil diameter governs the effective area of the iris (van den Berg et al 1991).

A laboratory experiment was performed to determine the degree of wavelength dependent scatter ocurring within the scatter cells. The spectral distribution of scattered light emanating from the back of the scatter cell, when illuminated from the front, was assessed by a computer-controlled spectrophotometric technique. The 0.00%, 0.08% and 0.16% scatter cells were mounted within an optical system between a light source and an image plane consisting of a magnesium carbonate block. The surface of the cell was focused onto the image plane. The spectral distributions of the scattered light emanating from the cells were measured at 5nm intervals from 380nm to 610nm using the spectrophotometer which was focused on the magnesium carbonate block (Bentham Instruments, Reading, UK). The proportion of scattered light emanating from the cell at these wavelengths was compared to the curve describing the characteristic of Rayleigh scatter (Figure 4.7). The curve of the experimental data demonstrates a relationship with wavelength that is proportional to the 0.98th power. However, it is evident from the graph that there is a greater proportion of scattered light for the 0.16% concentration. Nevertheless, it is apparent that the perimetric attenuation of the blue stimulus is largely independent of wavelength dependent scatter.

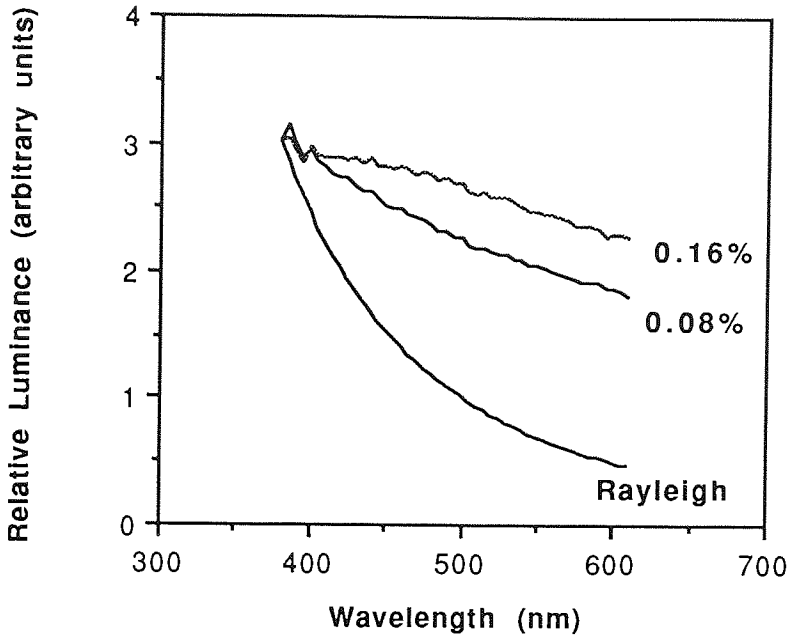

Figure 4.7. The relationship of wavelength dependent scatter between the 0.08% and 0.16% scatter solutions and pure Rayleigh scatter in which scatter is proportional to the wavelength raised to the fourth power.

The study demonstrates that forward light scatter attenuates the perimetric sensitivity profile diffusely across the field for all three stimulus combinations. The general reduction in sensitivity is more pronounced for the B-Y stimulus combination. Clinically, diffuse glaucomatous visual field loss is likely to be contaminated by the effects of forward light scatter. The study therefore highlights the need to separate diffuse loss arising from neural damage from that due to forward light scatter. The degree of perimetric attenuation arising from optical factors could be predicted from a knowledge of the straylight function (Figure 4.6). Until the two components of diffuse loss can be separated, careful interpretation of B-Y visual field data will be required in cases where the presence of early glaucomatous field loss co-exists with the diffuse attenuation resulting from forward light scatter.

4.11 The influence of age-related cataract on Blue-Yellow perimetry

4.11.1 Materials and Methods

Sample

The sample consisted of a cataract group and a normal age-matched control group. The cataract group comprised 20 age-related cataract subjects (Mean age 74.3 years; SD 5.7 Range 60-82 years) conforming to rigid inclusion criteria: refractive error in the examined eye of less than ±5D sphere and ±3D cylinder for the 33cm viewing distance of the perimeter bowl, intraocular pressure of less than 22mmHg, normal optic nerve head appearance, no family history of glaucoma or diabetes, no history of ocular disease or trauma, no neurological history, no systemic medication known to influence the visual field and no known congenital colour vision anomaly. Visual acuities ranged from 6/6 to 6/36.

The normal age-matched control group comprised 40 subjects (Mean age 69.6 years, SD 6.5, Range 60-81 years). Twenty subjects were aged between 60-69 years (mean 64.2 years SD 3.5) and 20 between 70-81 years (mean 75.3 years SD 3.3). The subjects confirmed to identical inclusion criteria as the cataract group with the exception that the corrected VA was 6/9 or better in each eye and there was no significant media opacity classified by LOCS II (see Section: Cataract Classification). Informed consent was obtained from each subject after the nature of the procedure had been fully explained.

Cataract Classification

The type and severity of each cataract was classified using the Lens Opacities Classification System II (LOCS II) (Chylack et al 1988, 1989, 1991) whereby the cataract is compared at the slit lamp to a standard reference photographic colour plate. A grade is assigned according to the morphology and severity of the cataract. Seven patients had anterior cortical cataract, 7 had nuclear cataract and 6 had posterior subcapsular cataract. The LOCS II system has been shown to be valid and repeatable (Maraini et al 1989, 1991; Khu et al 1989; Leske et al 1988; Wolfe et al 1991; Magno et al 1993, 1994; Lasa et al 1992; Chylack et al 1993a). Interestingly, since the

study was undertaken, a LOCS III system has been developed (Chylack et al 1993b, c) and validated (Karbassi et al 1993) which permits a decimalised system of cataract grading (Chylack et al 1993b). This new approach is believed to be more sensitive than LOCS II (Bullimore and Bailey 1993).

Perimetry

Data was collected over two visits within a maximum period of two weeks. Perimetry was undertaken with the modified Humphrey Field Analyser 640 previously described in Section 4.10.1. At the first visit, the designated eye of each subject was examined with program 24-2 for each of three stimulus combinations (Table 4.5). In the normal group, the designated eye was selected at random whilst in the cataract group the designated eye was determined by cataract type and severity.

Stimulus / Background combination	Stimulus size	Background Luminance (cdm^{-2})
B-Y	V	330
Y-Y	V	330
W-W	III	10

Table 4.5. The stimulus and background combinations for each of the three perimetric stimulus combinations.

The blue and yellow filter characteristics were identical to those in the previous study investigating induced forward light scatter and to those utilised by Johnson et al (1988b, c, 1989a, 1993a, b, d). The size III W-W stimulus was selected since it is the clinical standard currently employed on the HFA. The Y-Y stimulus was used as the MWS / LWS control for the B-Y stimulus combination.

The order of tests was randomised between subjects to minimize order effects. Appropriate refractive correction was used for the viewing distance of the perimeter bowl. Fixation losses were <20%, and false-negative and false-positive responses less than 33% for all subjects. However

the efficiency of the Heijl-Krakau blind spot measuring technique to detect fixation loss is reduced in B-Y perimetry (see Section 4.10.1.) and is also questionable in conventional W-W perimetry (Fankhouser 1993). Fixation was therefore constantly monitored with the video monitor. Mean and standard deviation pupil sizes measured on the HFA monitor and corrected for the magnification of the monitor for the B-Y, Y-Y and W-W stimulus combinations are displayed in Table 4.6.

Stimulus / Background combination	Normal group	Cataract Group
B-Y	3.2 (0.5)	3.3 (0.3)
Y-Y	3.2 (0.5)	3.3 (0.3)
W-W	4.1 (0.5)	4.2 (0.6)

Table 4.6. Group mean pupil size for the three stimulus combinations for the normal and cataract subjects. Values are expressed in mm. One standard deviation is given in parenthesis.

A repeated measures ANCOVA with group as a between-subjects factor, stimulus combination as a within subjects factor and age as a covariate revealed that pupil size for the W-W stimulus combination was significantly larger than for either the B-Y or Y-Y combinations ($p<0.001$); the difference in pupil size between the cataract and normal groups did not reach statistical significance (Table 4.7).

Subjects not experienced in perimetry received training in both B-Y and W-W perimetry on at least two sessions prior to the start of the study minimising potential learning effects. The impact of the learning effect on automated perimetry is discussed more fully in Chapter 5.

Source	dF	Sums of Squares	Mean Square	F value	P value
Age	1	1.080	1.080	2.886	p=0.095
Group	1	0.056	0.056	0.149	p=0.701
Age x Group	1	1.116	1.116	2.983	p=0.090
Error	53	19.835	19.835		
Stimulus combination	2	29.774	29.774	115.225	p<0.001
Stimulus combination x Age	2	0.075	0.075	0.289	p=0.750
Stimulus combination x Group	2	0.078	0.078	0.304	p=0.739
Stimulus combination x Age x Group	2	0.041	0.041	0.159	p=0.853
Error	106	13.695	13.695		

Table 4.7. Repeated measures analysis of covariance for pupil size.

Ocular media absorption and forward light scatter

At the second visit, measurements were undertaken of ocular media absorption and of forward light scatter on all the subjects in each group. Both techniques have been described in Section 4.10.1.

4.11.2. Analysis

The B-Y data for each subject was individually corrected for ocular media absorption by adding the ocular media absorption value to the B-Y sensitivity at each stimulus location. The two stimulus locations immediately above and below the blind spot were omitted from the analysis. The mean sensitivity at each of the 52 stimulus locations for the Program 24-2 was calculated for each of the two normal age groups for the B-Y, Y-Y and W-W stimulus combinations. The average straylight parameter across the three glare angles was calculated for each normal subject and then expressed as the group mean average straylight parameter for the 20 subjects in each age group. The unweighted visual field indices, mean deviation (MD) and corrected pattern standard deviation (CPSD) were calculated for each cataract subject using the formulae of Heijl et al (1987c). These formulae have been defined in Chapter 1. The difference between the average straylight parameter of each cataract patient and that of the group mean age-matched normal average straylight parameter was calculated. This procedure compensates for the increase in straylight with age and measures the isolated cataract straylight parameter (ICSP) (deWaard et al 1992).

4.11.3 Results

Normal Subjects

The group mean Mean Sensitivity (MS) and short-term fluctuation (SF) for each of the B-Y, Y-Y and W-W stimulus combinations for each age normal group are displayed in Table 4.8. The Group mean ocular media absorption, with respect to the blue OCLI filter, and the group mean straylight parameter for the two normal age groups are displayed in Table 4.9.

The variation in ocular media absorption (with respect to the OCLI blue filter) and straylight parameters as a function of age is illustrated in Figure 4.8. Both measures increased linearly with increase in age over the age range employed in the study (ocular media absorption: $r=0.67$, $p<0.001$; straylight parameter: $r=0.69$, $p<0.001$); although considerable inter-subject variation was present. No obvious trend was apparent between the ocular media absorption and straylight parameter.

Stimulus / Background combination	60-69 yrs age group		70-81 yrs age group	
	MS	SF	MS	SF
B-Y	2.03 (0.25)	0.15 (0.04)	2.02 (0.24)	0.14 (0.03)
Y-Y	1.07 (0.11)	0.12 (0.04)	1.02 (0.11)	0.12 (0.04)
W-W	2.80 (0.19)	0.12 (0.03)	2.77 (0.18)	0.14 (0.06)

Table 4.8. Group mean mean sensitivity (MS) and group mean short-term fluctuation (SF) for each of the three stimulus combinations for each of the two age groups of normal subjects. Values are expressed in log units. One log unit is equivalent to 10dB. One standard deviation is given in parenthesis.

Variable	Age group	
	60-69 years	70-81 years
Ocular media absorption	0.97 (0.11)	1.09 (0.11)
Log (Straylight Parameter)	1.01 (0.25)	1.20 (0.35)

Table 4.9. Group mean ocular media absorption and group mean log straylight parameter for each of the two age groups of normal subjects. Values are expressed in log units. One standard deviation is given in parenthesis.

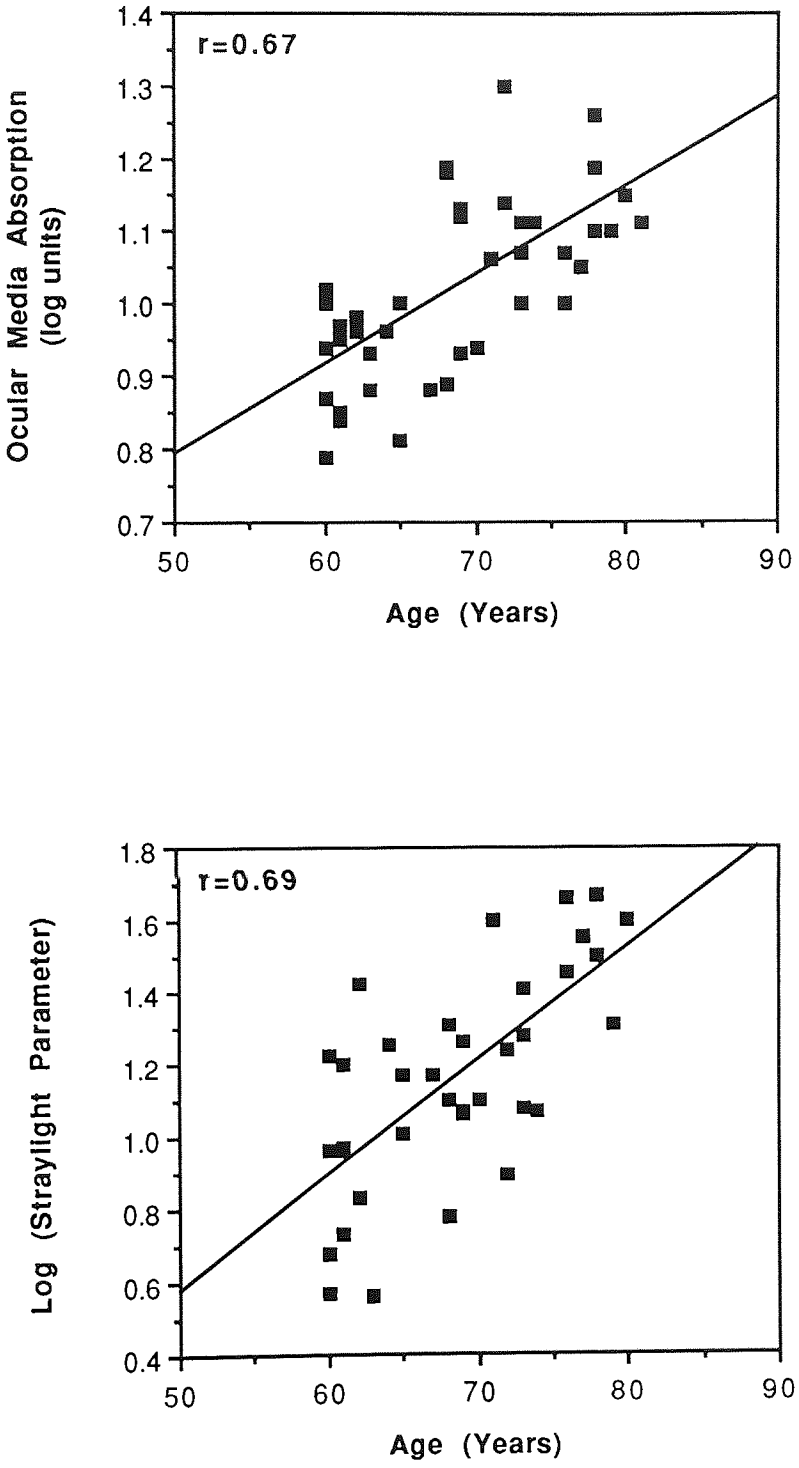

Figure 4.8. Ocular media absorption, relative to the blue OCLI filter, (top) and straylight parameter as a function of age (bottom). Note the vertical axis scales are different. Slopes represent the least squares linear regression lines.

Cataract Subjects

The group mean unweighted indices MD, SF and CPSD for each stimulus combination for the cataract group are illustrated in Table 4.10.

Stimulus / Background combination	MD	SF	CPSD
B-Y	-0.48 (0.30)	0.18 (0.06)	0.20 (0.09)
Y-Y	-0.29 (0.22)	0.13 (0.09)	0.14 (0.01)
W-W	-0.50 (0.31)	0.15 (0.06)	0.24 (0.15)

Table 4.10. Group mean unweighted mean deviation (MD), short-term fluctuation (SF) and corrected pattern standard deviation (CPSD) for each of the three stimulus combinations for the cataract group. Values are expressed in log units. One log unit is equivalent to 10dB. One standard deviation is given in parenthesis.

The relationship between the MD for a given stimulus combination and that of the two remaining stimulus combinations is shown in Figure 4.9. The diagonal line through the graph represents a slope of unity ie equality of the MDs. The B-Y MDs were more negative (ie of lower sensitivity) than for those of the Y-Y stimulus combination (Figure 4.9 (top)) indicating that cataract has a more profound effect on the SWS profile than on the control MWS/LWS profile. This difference between the two profiles increased with increasing cataract severity. The MDs for the standard W-W stimulus combination (size III) were more negative (ie of lower sensitivity) than those of the Y-Y size V stimulus combination (Figure 4.9 (middle)), indicating that cataract has a more adverse effect on the smaller stimulus than on the higher background luminance. Again the difference between the two profiles increased with increasing cataract severity. The corresponding graph for the W-W and B-Y MDs (Figure 4.9 (bottom)) showed no consistent trend.

The B-Y CPSD plotted against the Y-Y CPSD is shown in Figure 4.10 (top). The B-Y CPSD was greater than that of the Y-Y CPSD although the magnitude of both CPSDs was small. The W-W CPSD was greater than that of the Y-Y particularly for anterior cortical cataracts and as cataract severity increased (Figure 4.10 (middle)). The corresponding graph for the B-Y and W-W CPSDs

tended towards a slightly greater reduction in the W-W CPSD for the more severe cataracts (Figure 4.10 (bottom)).

The "isolated cataract straylight parameter" (ICSP) as a function of the MD for each of the three perimetric stimulus combinations is shown in Figure 4.11. The regression slope was constrained to pass through the origin since in the normal eye both the MD and the ICSP would theoretically be expected to be zero. However, even when the regression line was unconstrained, it passed very close to the origin for each of the stimulus combinations. Of the three MDs, the B-Y MD was most affected by forward light scatter (r=0.84) (Figure 4.11 (top)). The ICSP showed only a moderate correlation for the W-W (r=0.69) and Y-Y (r=0.70) stimulus combinations. The CPSD correlated poorly with the ICSP for the B-Y (r=0.08) and W-W (r=0.12) stimulus combinations and moderately with the Y-Y stimulus combination (r=0.60) (Figure 4.12). The SF correlated poorly with the ICSP for all three stimulus combinations: of the three SFs, the B-Y SF was most affected by forward light scatter (r=0.22) (Figure 4.13).

The MDs for each of the three stimulus combinations as a function of individual cataract type and severity are shown in Figure 4.14. Anterior cortical cataracts caused a greater reduction in sensitivity for the W-W stimuli (Figure 4.14 (top)) whilst posterior subcapsular cataracts caused a greater reduction in sensitivity for the B-Y combination (Figure 4.14 (bottom)). The degree of attenuation increased with increase in the LOCS II classification of cataract severity for all three types of cataract. The corresponding CPSDs also show an increase with increasing catataract severity (Figure 4.15).

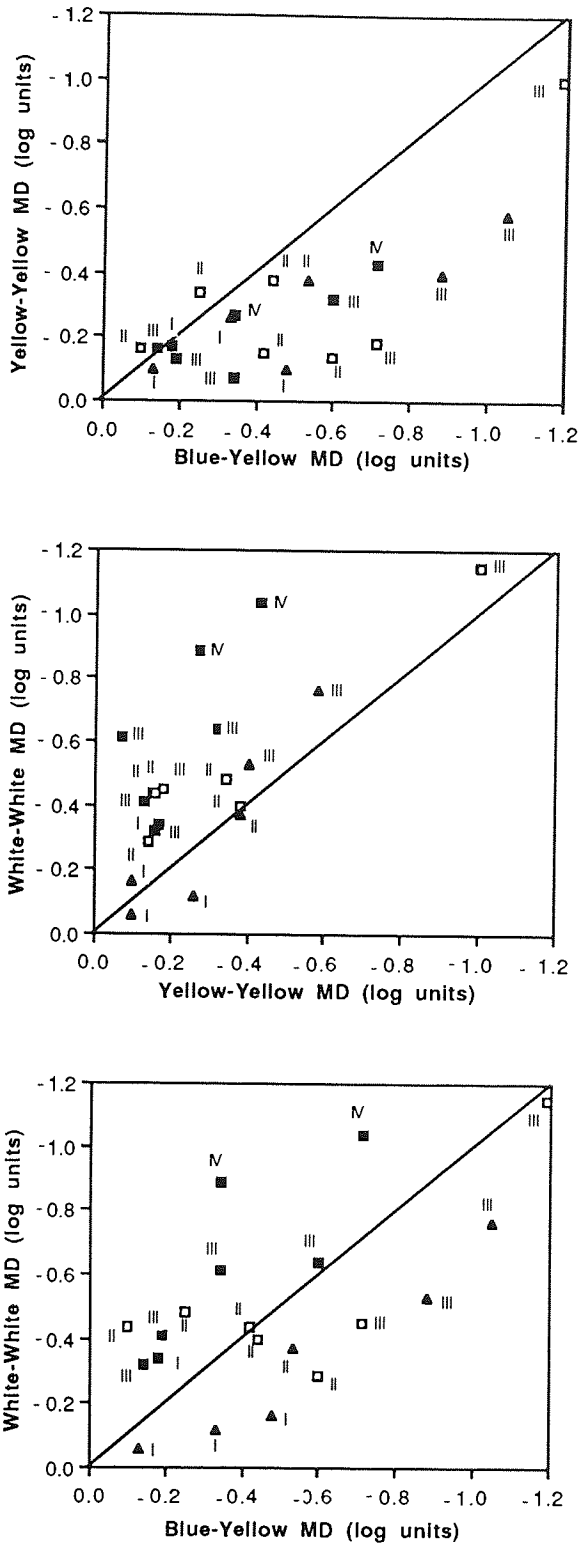

Figure 4.9. (Top) Y-Y MD plotted against the corresponding B-Y MD as a function of cataract type and severity. (Middle) W-W MD plotted against the corresponding Y-Y MD as a function of cataract type and severity. (Bottom) W-W MD plotted against the corresponding B-Y MD as a function of cataract type and severity. Cataract type and severity is classified by LOCS II whereby increase in severity is denoted by an increase in the Roman numeral. Filled squares represent cases of anterior cortical cataract, filled triangles posterior subcapsular cataract and open squares nuclear cataract. A negative MD represents a reduction in sensitivity. A slope of unity representing equality between the two given MDs is illustrated for reference. One log unit is equivalent to 10dB.

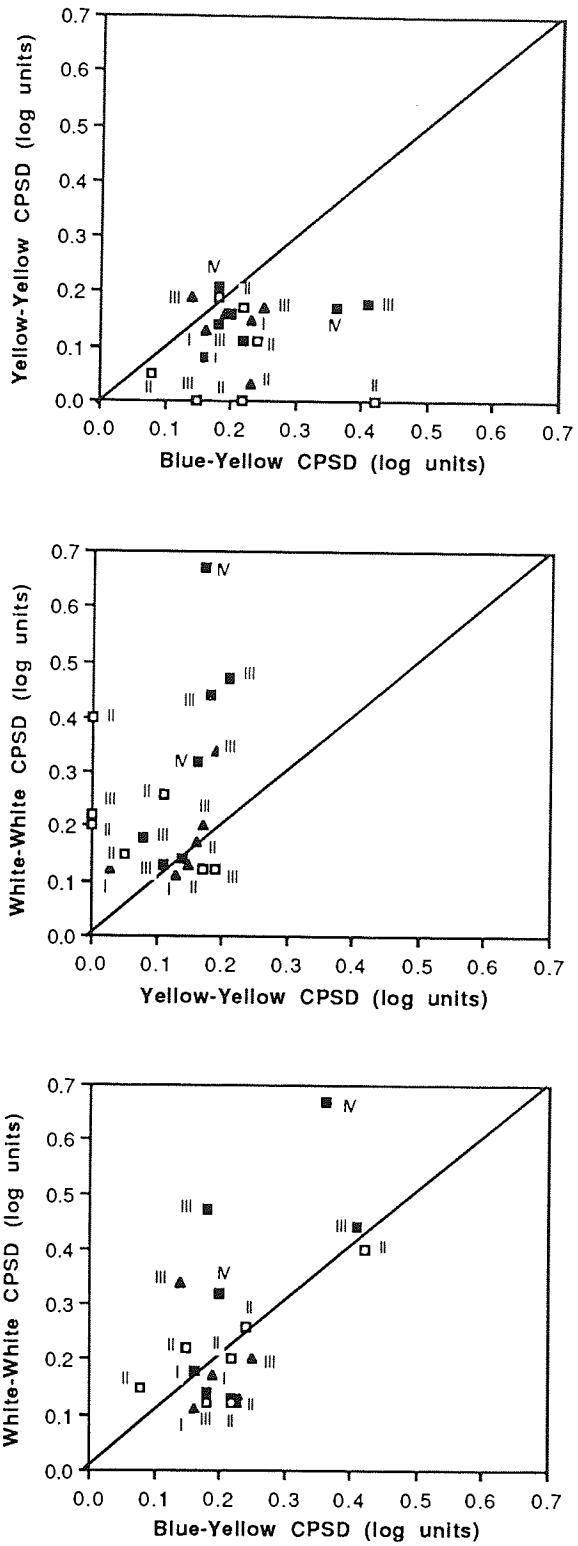

Figure 4.10. (Top) Y-Y CPSD plotted against the corresponding B-Y CPSD as a function of cataract type and severity. (Middle) W-W CPSD plotted against the corresponding Y-Y CPSD as a function of cataract type and severity. (Bottom) W-W CPSD plotted against the corresponding B-Y CPSD as a function of cataract type and severity. The cataract type and severity classification is that contained in the legend of Figure 4.9. A slope of unity representing equality between the two given CPSDs is illustrated for reference. One log unit is equivalent to 10dB. Note the scaling on the abscissa is different to that in Figure 4.9.

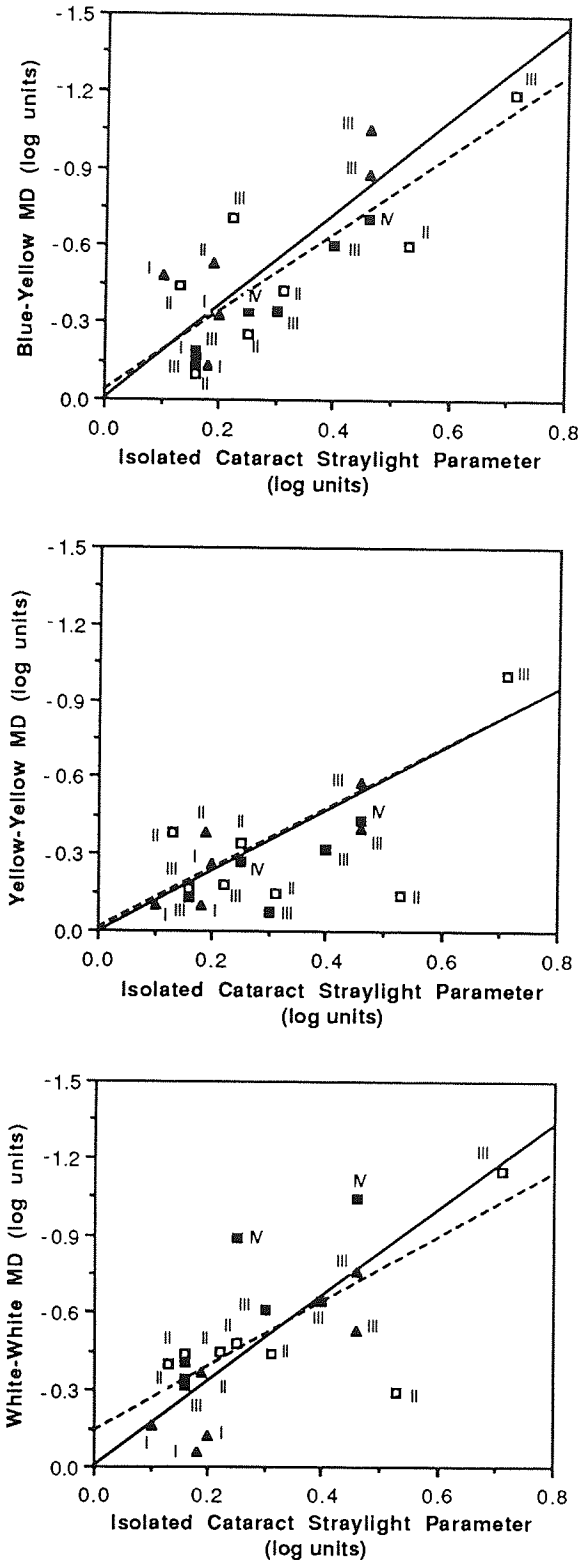

Figure 4.11. (Top) B-Y MD against the isolated cataract straylight parameter averaged for the three glare angles. The two slopes represent the linear regression line determined by least squares; the broken line indicates the best fit of the data and the continuous line that constrained to pass through the origin at x=0, y=0. (Middle) The corresponding function for the Y-Y stimulus combination and (Bottom) for the W-W stimulus combination.

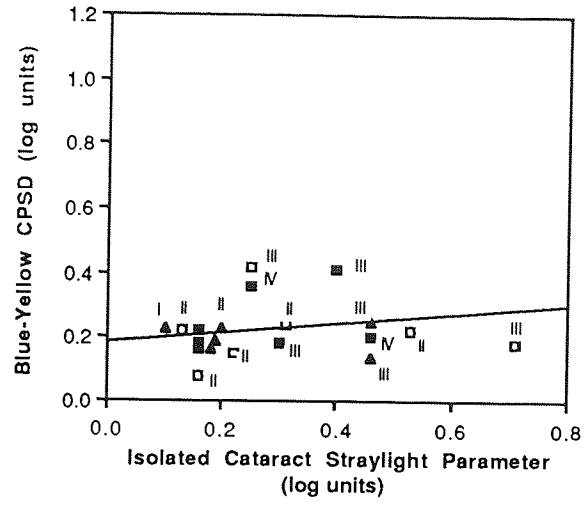

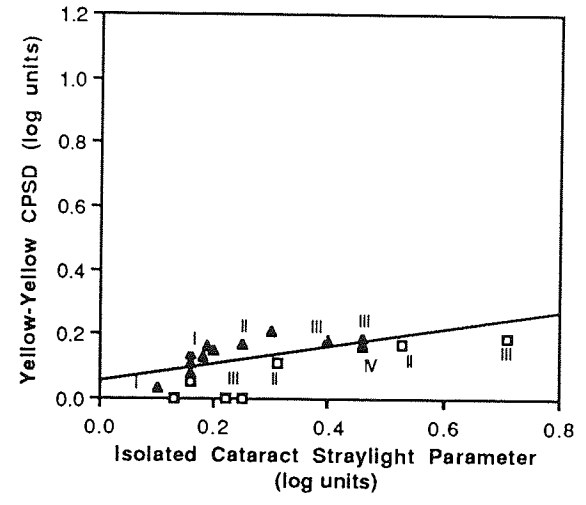

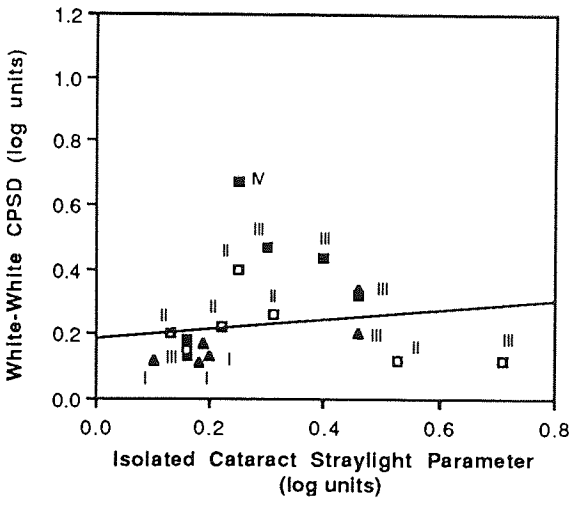

Figure 4.12. (Top) B-Y CPSD against the isolated cataract straylight parameter averaged for the three glare angles. The slope represents the linear regression line determined by least squares. (Middle) The corresponding function for the Y-Y stimulus combination and (Bottom) for the W-W stimulus combination.

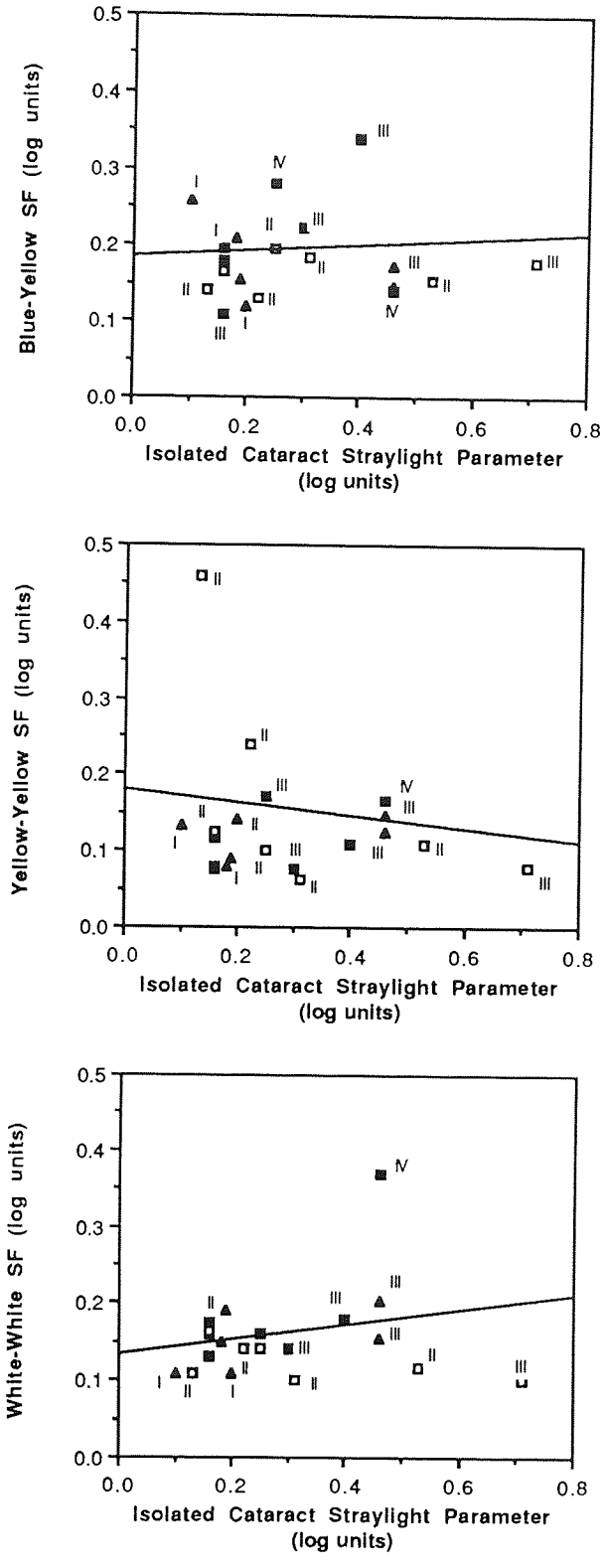

Figure 4.13. (Top) B-Y SF against the isolated cataract straylight parameter averaged for the three glare angles. The slope represents the linear regression line determined by least squares. (Middle) The corresponding function for the Y-Y stimulus combination and (Bottom) for the W-W stimulus combination.

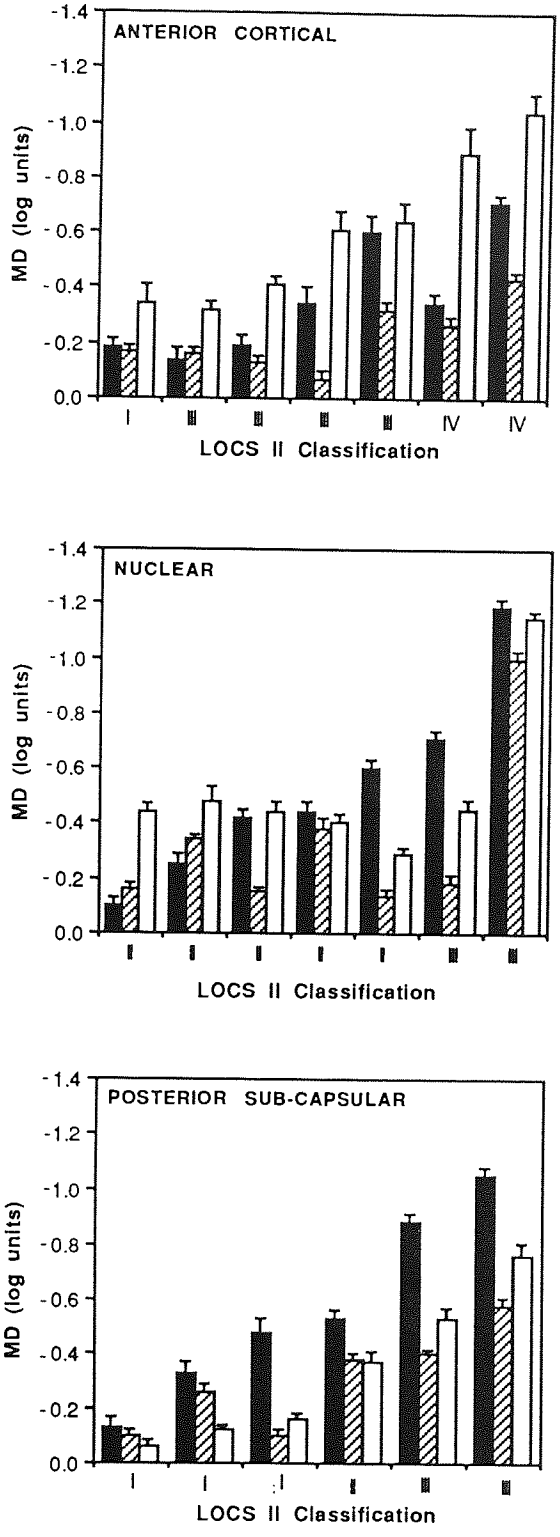

Figure 4.14. Bar charts illustrating the relationship between MD and the type and severity of cataract (LOCS II) for each subject as a function of the three perimetric stimulus combinations (Top) anterior cortical cataract, (Middle) nuclear cataract, (Bottom) posterior capsular cataract. The filled bar represents the B-Y MD, the hatched bar the Y-Y MD and the open bar the W-W MD. Error bars represent ± one standard deviation of the mean.

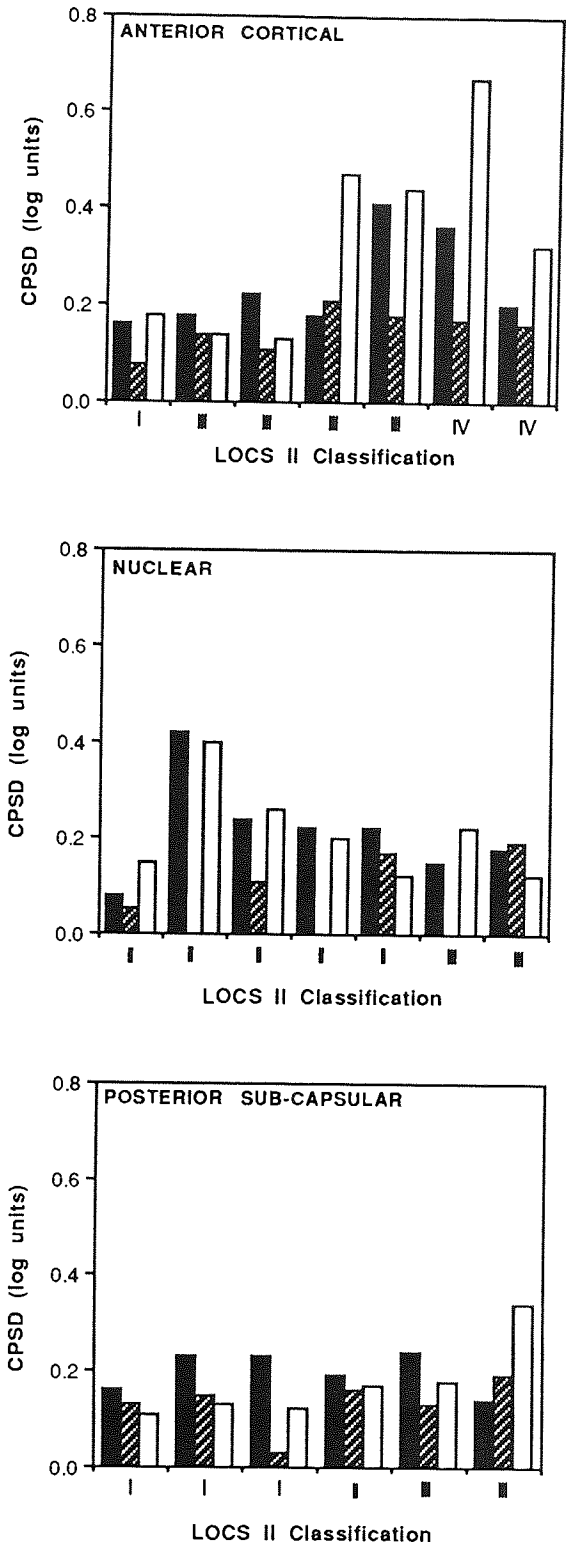

Figure 4.15. Bar charts illustrating the relationship between CPSD and the type and severity of cataract (LOCS II) for each subject as a function of the three perimetric stimulus combinations (Top) anterior cortical cataract, (Middle) nuclear cataract, (Bottom) posterior capsular cataract. The filled bar represents the B-Y CPSD, the hatched bar the Y-Y CPSD and the open bar the W-W CPSD.

4.11.4. Discussion

The study demonstrates that cataract has a profound effect on the visual field primarily resulting in a predominantly general reduction in sensitivity across the field. The findings of the study are in agreement with other studies (Dengler-Harles et al 1990; Lam et al 1991; Bundenz et al 1993).

The findings are also in accord with those of the previous study which investigated the effect of induced forward light scatter on the perimetric profile. The attenuation of the W-W and Y-Y response can again be attributed to the reduction in luminance contrast between the stimulus and background. Forward light scatter merges the stimulus borders to the background with the consequent loss of stimulus contrast (Hess and Woo 1977). The greater attenuation of the B-Y stimulus combination compared to the Y-Y stimulus combination (Figure 4.10, top) can again be explained on the basis of the chromatic content of the stimulus. The B-Y stimulus, in addition to the loss of luminance contrast, also exhibits a change in chromaticity towards that of the yellow background. Effectively the stimulus becomes less blue and more yellow. An alternative explanation for the greater attenuation of the B-Y response might be that of a preferential scattering of short wavelength stimuli. However, studies of the normal, elderly and cataractous eye suggest that light scatter is independent of wavelength (Wooten and Geri 1987; Whitaker et al 1993).

The greater attenuation of the W-W response in comparison to that of the Y-Y response (shown by the distribution of data points above the slope of unity in Figure 4.9 (middle)) involves consideration of both stimulus size and background luminance, along with the associated reduction in pupil size for the Y-Y stimulus combination. The effect of light scatter is known to be more pronounced for smaller perimetric stimuli (Wood et al 1987b, 1989; van den Berg 1987). This provides a convenient explanation for the greater attenuation of the W-W sensitivity. The selective attenuation of the smaller stimulus is analogous to the effect of cataract upon contrast sensitivity for sinusoidal gratings where stimuli of medium and high spatial frequencies are preferentially affected (Hess and Woo 1978; Paulsson and Sjostrand 1980; Elliott et al 1989). Alternatively, the greater attenuation of W-W sensitivity could be due to the fact that the sensitivity

of the white stimulus was not corrected for ocular media absorption, despite the fact that white contains a measure of blue light. However, the similar age-related decline in Y-Y sensitivity, which is generally independent of wavelength dependent ocular media absorption, compared to that for W-W stimuli, suggests that W-W stimuli are unaffected by short wavelength ocular media absorption (Johnson et al 1989a). Thus, given the well documented evidence for greater attenuation of small stimuli by light scatter, this factor is considered to dominate the findings of the study.

Evidence of selective absorption at shorter wavelengths is present in the results of both the normal and cataract groups (Figure 4.16). The increasing difference in the threshold for the 410nm stimulus compared to the 560nm stimulus can be attributed to the preferential increase in ocular media absorption for short-wavelengths with increase in age. In addition, the cataract subjects also showed a greater reduction in sensitivity compared to normal subjects for the 410nm stimulus and to some extent the 560nm stimulus. This is consistent with the reduced light transmission at all wavelengths in cataract (Boettner and Wolter 1962; Sadun and Libondi 1990). However, the greater attenuation of the B-Y stimulus combination cannot be explained on the basis of preferential absorption of short wavelength light by the crystalline lens since the B-Y data for each subject was individually corrected for ocular media absorption.

The degree of perimetric attenuation resulting from forward light scatter may be predicted from a knowledge of the straylight parameter. The suitability of such a method, however, remains unknown.

It is clear that the effect of cataract type on MD is dependent upon the stimulus configuration used. The B-Y MD is greater for posterior subcapsular cataract whereas anterior cortical cataract has a preferential effect on the W-W MD. This phenomenon can be explained on the basis of pupil size. At high bowl luminances, as employed for colour perimetry, the pupil will constrict around any centrally located opacity such as a posterior subcapsular cataract, with severe consequences for visual performance. Alternatively, at lower background luminances, the larger

pupil size will cause peripheral anterior cortical opacities to produce their maximal effect. The impact on the visual field of cataract progression will also be governed by the interaction of cataract type and pupil size.

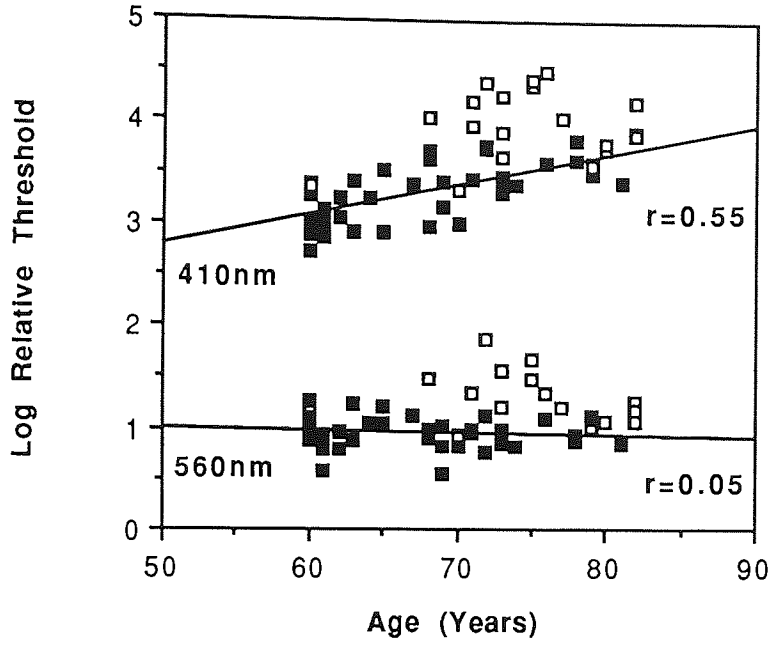

Figure 4.16. Relative thresholds to narrowband 410nm and 560nm stimuli as a function of age. Closed squares represent normal subjects and open symbols cataract subjects. The two slopes represent the least squares regression lines. For reasons of clarity the cataract data have not been classified for type and severity.

Previous studies with the Octopus automated perimeter have shown that the attenuation of the perimetric profile due to forward light scatter increased with increase in eccentricity both in the normal and in the cataractous eye, ie the visual field preferentially steepened in the periphery (Wood et al 1987b, 1989). Other studies have failed to demonstrate any alteration of the visual field with respect to eccentricity in the presence of simulations of media opacity using the Humphrey Field Analyser in normals (Heur et al 1988) and glaucoma patients (Bundenz et al 1993; Dengler-Harles et al 1990). Furthermore, the effect of cataract on the visual field before and after cataract extraction results in a generalized reduction in sensitivity in both normal (Greve 1980; Lam et al 1991) and glaucomatous eyes (Guthauser and Flammer 1988; Costagliola et al

1990; Heider et al 1991). A repeated measures ANCOVA using the Greenhouse-Geiser correction for the assumption of compound asymmetry, with age as a covariate and stimulus combination and eccentricity as within-subjects factors, showed for this study, overall, the perimetric attenuation due to forward light scatter was independent of eccentricity (p=0.527) (Table 4.11). The increase in the W-W CPSD compared to the Y-Y CPSD and to some extent to the B-Y CPSD therefore suggests that the increase in CPSD with the smaller stimulus merely reflects a random increase in the overall variability of the threshold estimate across the field rather than a specific shape change in the hill of vision.

The adverse effect on the MDs for the three stimulus combinations increased as a function of the LOCS II severity classification and as a function of the isolated cataract straylight parameter. This is in agreement with the results of Guthauser and Flammer (1988) who demonstrated that visual field changes were correlated with the degree of media opacity quantified photographically using the Schiempflug technique. The pupil size for the straylight measurements would have been larger than the pupil size for the perimetry. Since, as has been shown, the effect of cataract on the outcome of the visual field is pupil size dependent, the discrepancy in the pupil sizes between the two measurements is likely to have reduced the correlation between the straylight function and the visual field indices. If the pupil size had been artificially maintained at the same level for both measurement procedures, the apparent agreement would have been still higher. The correlation between the LOCS II classification and the isolated cataract straylight parameter was only moderate (r=0.49). The LOCS system is a measure of back scatter. Indeed, previous studies have shown only limited agreement between measures of back scatter and those of forward scatter (deWaard et al 1992; Elliott and Hurst 1989; Dengler-Harles et al 1991). Furthermore, Rouhiainen et al (1993) compared two measures of backscatter: the OLM 701 and LOCS II. Agreement between the two systems was only found in nuclear cataract. The SF has been previously shown to be higher in B-Y perimetry than in conventional W-W perimetry by approximately 10-30% (Nelson-Quigg et al 1991; Johnson et al 1993d). Sample et al (1993a) demonstrated a greater B-Y SF compared to that for W-W perimetry, however this difference was

Source	dF	Sums of Squares	Mean Square	F value	P value
Age	1	1.472	1.472	1.313	p=0.267
Error	18	20.177	1.121		
Stimulus combination	2	3.957	1.978	9.880	p<0.001
Age x Stimulus combination	2	0.197	0.099	0.493	p=0.562
Error	36	7.208	0.200		
Eccentricity	4	0.162	0.040	0.770	p=0.527
Age x Eccentricity	4	0.345	0.086	1.642	p=0.185
Error	72	3.784	0.053		
Stimulus combination x eccentricity	8	1.366	0.171	3.377	p=0.021
Age x Stimulus comb x eccentricity	8	0.321	0.040	0.793	p=0.513
Error	114	7.278	0.051		

Table 4.11. Repeated measures analysis of covariance for the perimetric attenuation.

not considered to be clinically significant. Indeed, for the present study, a repeated measures ANCOVA with age as a covariate, group as a between-subjects factor and stimulus combination as a within-subjects factor showed that the B-Y SF was higher than that for the Y-Y or W-W stimulus combinations in both the cataract and normal groups ($p=0.003$). The SF for all three stimulus combinations was higher in the cataract group ($p=0.02$) and this difference increased with increase in age ($p=0.03$) (Table 4.12).

Glaucomatous visual field loss is suggested to have two major components: diffuse and focal. The extent to which diffuse loss (ie a general reduction in sensitivity) is a component of early glaucomatous damage is equivocal using conventional W-W automated perimetry (Flammer et al 1985; Caprioli et al 1987a; Drance et al 1987b; Glowazki and Flammer 1987; Langerhorst 1988; Feuer and Anderson 1989; Heijl 1989; Funkhouser 1991; Drance 1991; Funkhouser et al 1992b; Asman and Heijl 1994). The separation of diffuse from focal visual field loss is important for evaluating the type and extent of glaucomatous visual field damage and for evaluating progression of the disease. A diffuse type of glaucomatous loss has also been reported using B-Y perimetry (Johnson et al 1988b, c, 1989a, 1993a, b, d; Sample et al 1986b, 1988a, 1993b, c, d, 1994; Sample and Weinreb 1989, 1990, 1992; Weinreb and Sample 1991; Flanagan et al 1991a; Heron et al 1988; deJong et al 1991; Lewis et al 1993; Casson et al 1993b).

Statistical methods have been derived to separate diffuse and focal W-W visual field loss (Heijl et al 1987c, 1989c; Bebié et al 1989; Funkhouser 1991; Funkhouser et al 1992a, b). It has also been suggested that there is a lack of precision of the statistical procedures for identifying W-W diffuse loss (Funkhouser 1991; Funkhouser et al 1992b). However, the effects of forward light scatter on the magnitude of any focal loss remains a complex issue; since stimuli within areas of focal loss may be detected by adjacent retinal areas as a result of light scatter. This leads to an under-estimation of the depth of actual focal loss (Fankhouser and Haeberlin 1980). Similar approaches to separate different patterns of visual field loss could be applied to B-Y perimetry. However, the difficulty inherent in W-W perimetry, namely, that of separating any diffuse loss from the focal loss would remain (Fankhouser et al 1992a, b). Alternatively, the diffuse component

arising from optical effects could be ignored since the reduction in perimetric sensitivity due to light scatter and to short wavelength lenticular absorption is similar at all stimulus locations across the field. The sensitivity at a given location could then be analysed on an intra-individual basis eg. by comparison with the sensitivity at the mirror image location in the opposite hemifield (Sommer et al 1987; Asman and Heijl 1992a, b; Sample et al 1993c). Such an approach would accept that the depth and / or severity of any focal loss would be reduced by the general reduction in sensitivity caused by the cataract; however it would be in the knowledge that focal loss in B-Y perimetry, whatever the true depth, precedes that in W-W perimetry (Johnson et al 1988c, 1989a, 1993a, b, d; Sample et al 1986b, 1988a, 1993b, c, d; 1994 Sample and Weinreb 1989, 1990, 1992; Weinreb and Sample 1991; Flanagan et al 1991a; Heron et al 1988; deJong et al 1991, 1993; Lewis et al 1993; Casson et al 1993b).

The greater reduction for the B-Y stimulus compared to that for the Y-Y stimulus is consistent with the effect of induced forward light scatter on the B-Y visual field. Indeed, the results for the two studies bear a striking similarity (Figure 4.17).

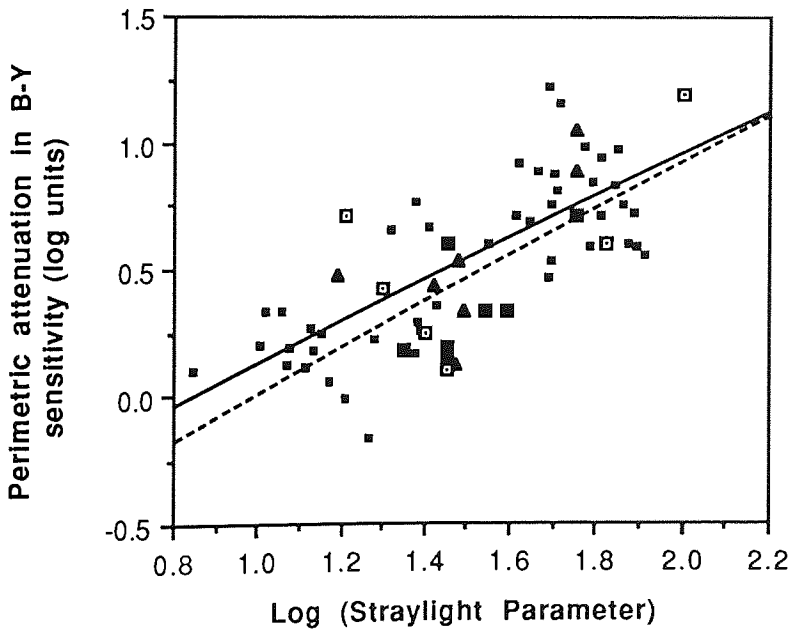

Figure 4.17. B-Y perimetric attenuation as a function of the straylight parameter resulting from induced light scatter (small closed squares) and as a function of cataract. Closed triangles represent posterior subcapsular cataract, large closed squares anterior cortical and open squares nuclear cataract type. The slopes represent the least squares linear regression lines for the induced scatter (complete line) and cataract (dashed line) groups.

Source	dF	Sums of Squares	Mean Square	F value	P value
Age	1	0.001	0.001	0.224	p=0.638
Subject Group	1	0.000	0.000	0.114	p=0.737
Age x Subject Group	1	0.001	0.001	0.309	p=0.581
Error	56	0.157	0.003		
SF	2	0.041	0.020	7.751	p=0.003
Age x SF	2	0.009	0.005	1.794	p=0.172
SF x Subject Group	2	0.026	0.013	4.861	p=0.020
Age x SF x Subject Group	2	0.023	0.012	4.436	p=0.030
Error	112	0.294	0.003		

Table 4.12. Repeated measures analysis of covariance for the short-term fluctuation (SF).

In conclusion, forward light scatter falsifies the visual field resulting in a general reduction in the overall height of the hill of vision. It is essential to separate visual field loss as a result of optical or pre-retinal factors from that due to neural factors. The preferential effect on the B-Y stimulus combination may limit the clinical potential of B-Y perimetry in the early detection and follow-up of glaucomatous damage particularly where glaucoma co-exists with cataract. Furthermore, progression of cataract will limit the ability of B-Y perimetry to monitor glaucomatous visual field progression.

CHAPTER 5: LEARNING EFFECTS IN AUTOMATED PERIMETRY

5.1 Learning effects in White-White perimetry

Although automated perimetry has reduced the influence of the perimetrist on the outcome of the examination, considerable patient-related variables associated with the nature of the response still remain. Such elements serve to contribute to the variation in threshold at a given stimulus location which occurs both within a test (the Short-term Fluctuation) and also between tests (the Long-term Fluctuation). The magnitude and variability of the threshold response is influenced by physiological factors such as age, refractive error, pupil size, media opacities and drugs. These factors have been discussed fully in Chapter 1. It is also known that the degree of prior perimetric experience and the length of a perimetric examination also influences the magnitude and variability of the threshold response.

5.1.1 Learning effects in manual perimetry

The learning effect in perimetry can be defined as a continued improvement in the threshold response as the patient becomes increasingly familiar with the test. The phenomenon has been known for some time and is not specific to automated perimetry. Aulhorn and Harms (1967, 1972) performed repeated manual static perimetry on a sample of normal subjects using the Tübinger perimeter. Twenty consecutive threshold determinations were performed on each subject in one day. Sensitivity improved by upto one log unit with practice; the improvement was independent of eccentricity and generally occurred over the first ten sessions. The sensitivity attained at the end of the last session was maintained when the test was repeated upto seven days later. Using the Goldmann perimeter, Greve (1973) was also able to demonstrate an improvement in perimetric performance associated with a reduction in the variability of the threshold response. The improvement in performance between successive examinations was similar across the entire field but was considered to be clinically insignificant as the relative depth of any focal visual field loss would remain constant.

The learning effect can be explained in part by a steepening of the slope of the frequency-of-seeing curve. The range of luminances over which the chance of detection of the stimulus occurs has been found to be approximately 0.50 log units for untrained normal subjects and 0.30 log units for trained normal subjects (Tate and Lynn 1977). The learning effect has been attributed to a change in the criterion for stimulus detection: as familiarity with the test procedure was gained the patient would respond to stimuli that were previously ignored. The learning process could also be accelerated if feedback or encouragement was given to the patient (Tate and Lynn 1977).

5.1.2. Learning effects in automated perimetry

Learning effects in automated perimetry have been investigated by the repeated examination of selected stimulus locations. Such studies have generally compared the standard perimetric indices; MS, MD, SF, CPSD and the reliability parameters over a period of time to assess the evidence of any learning effect.

A within-eye between-examination learning effect in the normal eye was reported by Wood et al 1987a; Heijl et al 1989a; Autzen and Work 1990; Guttridge et al 1991; Searle et al 1991a, b). Wood et al (1987a) quantified the learning effect in normal eyes using Program 21 of the Octopus automated perimeter. Eight out of ten subjects demonstrated a mean increase in sensitivity of approximately 10dB over five separate examinations undertaken on five consecutive days. Nine of the subjects exhibited a mean decrease of 3dB in the short-term fluctuation. Three specific patterns of learning were reported: some subjects demonstrated an immediate increase in sensitivity at the initial examinations followed by little further improvement; others demonstrated a more gradual improvement over the five days and some showed little improvement at all. The learning effect was greater at eccentricities greater than 30° and in the superior field. The learning effect was subsequently retained when the test was repeated on days 15, 16 and 44. These findings were in accord with the later study of Heijl et al (1989a) who also demonstrated an improvement in perimetric performance of 210 normal subjects examined with program 30-2 of the Humphrey Field Analyser over a five test period. Mean sensitivity increased on average by 1.3dB and the SF declined on average by 0.27dB. The improvement was greater in the periphery

but was independent of the age of the subject. However, considerable variation in the learning effect between individuals was also noted. Heijl et al (1989a) concluded that a single visual field examination was inadequate to provide accurate baseline information. An improvement in the peripheral field of upto 5dB was reported by Guttridge et al (1991) for 12 normal subjects undergoing Program 30/60-2 of the Humphrey Field Analyser on five separate occasions. They also found considerable between-subject variability in the pattern of learning.

A within-examination learning effect was demonstrated by Searle et al (1991a, b). Both eyes of a sample of 38 normal subjects underwent a custom program of the Humphrey Field Analyser consisting of 30 stimulus locations between 9° and 24° eccentricity. The test was repeated three times for each eye at each of two separate examinations. They found an improvement in sensitivity for the first eye examined of approximately 1.5dB both within a given examination and also between-examinations. The magnitude of the improvement for the second eye examined was less than 1dB. Similar trends were apparent for the SF. Autzen and Work (1990) examined each eye of 33 naive normal subjects on two separate occasions with Program 32 of the Octopus 2000R automated perimeter. A learning effect was demonstrated for both MS and SF. Mean sensitivity improved by 0.95dB and short-term fluctuation declined by 0.30dB for both eyes between the two visits. Furthermore, the learning effect increased with increase in age for MS. Their analysis was contaminated, however, by the pooling of data from both eyes.

The extent of the learning effect in OHTs and glaucoma patients consists of an improvement in sensitivity and / or a reduction in the SF which generally occurs between the first two examinations (Gloor et al 1980a, b; Niles and Trope 1988; Kulze et al 1990; Marchini et al 1991; Wild et al 1989c, 1991b; Werner et al 1988, 1990; Heijl and Bengtsson 1994). Werner et al (1990) found little change in MS measured with Program 32 of the Octopus automated perimeter 201 out to 20° eccentricity when the first four fields of 20 OHTs were examined prospectively over 12 months; however, there was a small improvement beyond 20° eccentricity. The SF declined from 1.7dB to 1.3dB. Differing patterns of learning were also present between patients; five out of 29 patients showed a marked improvement in MD, however the majority showed little improvement

after the first examination. It was recommended that two baseline fields were required to exclude the learning effect since the majority of learning occurred between the first and second examinations. An alternative testing protocol was used by Wild et al (1989c) in a study of 20 OHTs. Both eyes were examined using a custom program of the Humphrey Field Analyser on three consecutive days and after an interval of 12 days. An increase in MS (approximately 4.0dB) and decreases in the MD, SF (approximately 0.9dB), number of stimulus presentations and false negatives were observed over the first two examinations. The improvements were greater in the first eye examined. Follow-up of these patients 5 to 15 months later demonstrated little evidence of any further improvement of sensitivity (Wild et al 1991b). Gloor et al (1980b) employed Program 31 of the Octopus 201 automated perimeter to study the long-term fluctuation of 120 eyes of 66 patients with either ocular hypertension or glaucoma. The learning effect occurred between the first and second examinations and was characterized by a reduction in the depth of focal loss and an increase in sensitivity of up to 2dB at stimulus locations deemed to be normal. A similar increase in sensitivity, however, was not found between the second and third examinations. Gloor et al (1980b) stated that there was a need to differentiate between true change in the visual field and learning effects.

The magnitude of any learning effect is dependent on the depth of the initial field loss: a greater learning effect is present for lower sensitivities (Wild et al 1989c; Heijl and Bengtsson 1994). This finding was also mirrored by Heijl et al (1989a) who demonstrated a greater improvement in the initial fields of normal eyes with the lowest baseline sensitivity.

The influence of prior experience of manual perimetry on the magnitude of the learning effect recorded in automated perimetry is equivocal (Werner et al 1988, 1990; Katz and Sommer 1987; Kulze et al 1990; Marra and Flammer 1991). In a retrospective study, Werner et al (1988) examined 20 glaucomatous eyes on four separate occasions using program 32 of the Octopus 201 automated perimeter. The four examinations were carried out over a period of 20 months and all patients were experienced in Goldmann manual perimetry. No change was found in the global indices MS and MD, or in the number of abnormal points (a location at which the sensitivity was

5dB or more below the age-matched normal value) over the four visits. However, a significant decrease in the short-term fluctuation was reported between the first and second visits. It was concluded that the learning effect was insignificant in glaucoma patients who had had previous experience of manual perimetry and that a single baseline examination would be sufficient in this population. Katz and Sommer (1987) were also unable to demonstrate a learning effect in automated perimetry and this was attributed to the subjects having first performed manual perimetry. Conversely, in a similar type of study based upon the results of one eye from each of 45 clinically stable glaucoma patients examined with program 30-2 of the Humphrey Field Analyser at each of two visits, Kulze et al (1990) found that the group mean MD decreased by 1.7dB (ie improved) between the two visits. There was also an increase in the number of fixation losses. Previous experience of manual or automated suprathreshold static perimetry has no significant effect on learning. Marra and Flammer (1991) were unable to demonstrate any difference in perimetric performance between experienced and naive groups comprising a total of 70 normal subjects, 16 glaucoma patients and 14 cataract patients. Sensitivity remained stable for the three selected stimulus locations situated between 3° and 28° eccentricity when repeated on 12 occasions using the Octopus automated perimeter. Furthermore, no difference was found between trained and untrained subjects or between normal and diseased eyes. Unfortunately, the overall test time was only 5-8 minutes in duration.

Kulze et al (1990) considered that the prediction of which patient required a second baseline field examination in order to minimize learning effects was difficult. Interestingly, Asman et al (1993) have suggested a learner's index (LI) to highlight those patients who may require more experience before reliable interpretation of the visual field can be made. Comparisons of the deviation in sensitivity from the age-corrected normal sensitivity across the field between naive subjects and those subjects experienced in perimetry permitted a linear discriminant function to be calculated (LI) based upon the measured deviations in sensitivity. A given field was assigned an LI value which expressed the deviation from a normal experienced patient ($LI \approx 0$) towards a naive patient ($LI \approx 1$).

5.2 Fatigue effects in White-White perimetry

The magnitude of any learning effect is counterbalanced by the presence of a fatigue effect. Fatigue effects have also been reported in both manual and automated perimetry whereby sensitivity decreases during a perimetric examination.

5.2.1. Fatigue effects in manual perimetry

Enoch and co-workers (Sunga and Enoch 1970; Enoch et al 1979) described a "short-term saturation" or fatigue effect in patients with optic nerve and cortical lesions. A modified Goldmann perimeter was employed to present static stimuli at selected locations in the visual field. Sensitivity declined in a progressive manner and depended on the length of the examination. The reduction in sensitivity occurred in all areas of the visual field and was less pronounced at decreased background luminances. Haider and Dixon (1961) demonstrated a decrease in performance between the second and tenth minute of continuous contrast threshold recording. Ronchi and Salvi (1973) found an increase in absolute threshold in scotopic conditions after 40-60 minutes of the test. The deterioration in sensitivity over time was less pronounced with increase in eccentricity beyond 30° and in monocular areas of the binocular visual field. Greve (1973) suggested that fatigue could be minimized by allowing the patient rest periods during the examination. However, little quantitative work has been published relating to manual perimetry.

5.2.2. Fatigue effects in automated perimetry

Fatigue effects have also been investigated using the repeated thresholding of selected stimulus locations. The fatigue effect is of greater magnitude in automated perimetry compared to manual perimetry and may partly explain the apparently greater visual field loss recorded with automated perimetry (Heijl and Krakau 1975b; Fankhouser 1976; Heijl 1977b; Heijl and Drance 1983). Such effects have been assessed within a single examination of a given eye (Heijl 1977b; Heijl and Drance 1983; Hudson et al 1994; Johnson et al 1988a; Marchini et al 1991; Searle et al 1991a, b), between-examinations of a given eye (Wild et al 1989c; Searle et al 1991a, b) or between-eyes at a single examination (Hudson et al 1994).

Heijl (1977b) examined the effect of repeated threshold measurements on a sample of 12 normal subjects and 19 glaucoma patients. Using the Competer perimeter, threshold was assessed over a continuous period of 30 minutes at 6 stimulus locations located at 5°, 10° and 15° eccentricity. Sensitivity was generally stable for the first 4 to 10 minutes but decreased over the remainder of the test. The deterioration in mean threshold was less than 1.5dB for the normal group but was higher for the glaucomatous group reaching up to 10dB at some stimulus locations. Both the SF and the number of fixation losses increased over the duration of the test for the glaucomatous group.

A greater reduction in sensitivity in areas of visual field loss compared to that at locations exhibiting normal sensitivity has been reported (Holmin and Krakau 1979; Heijl and Drance 1983). Holmin and Krakau (1979) utilized the Competer automated perimeter to study the effect of fatigue on 5 normal and 13 glaucomatous eyes. Threshold was assessed on 12 occasions over a 30 minute test session at each of 6 stimulus locations. Normal regions of the field exhibited a stable sensitivity; however the areas of field loss exhibited a decline in sensitivity.

The fatigue effect is independent of bowl luminance. Heijl and Drance (1983) continuously assessed six stimulus locations between 5° and 20° eccentricity with the Competer automated perimeter over a period of 30 minutes in a sample of 23 OHT and glaucoma patients. Background luminances of 0.1, 1.0 or 10.0cdm^{-2} were randomly employed for each individual. Manual static perimetry was also undertaken using the Tübinger perimeter at background luminances of 10cdm^{-2} and 20cdm^{-2}. The glaucoma patients demonstrated a significant rise in threshold during prolonged continuous testing which was more pronounced in areas of focal loss. The fatigue effect was found to be independent of background luminance and was of a greater magnitude for automated perimetry.

The fatigue effect has been suggested to be an indicator of early glaucomatous damage and to be of potential as a provocative test (Heijl 1977b; Heijl and Drance 1983). However, this suggestion has not been substantiated by other reports. Indeed, Langerhorst et al (1987b)

assessed the fatigue effect in 44 normal subjects, 26 OHTs and 36 glaucoma patients using the Scoperimeter. The deterioration in group mean MS over time was greatest for the glaucoma group, however considerable overlap occurred between the three diagnostic groups. The use of fatigue as a provocative test for disease was therefore regarded as unreliable. Furthermore, the fatigue effect was found to be more pronounced with increase in age for all four groups. The proximity of visual field loss was found not to have any influence on the magnitude of the fatigue effect.

An increase in the magnitude of the fatiguing effect with eccentricity has been demonstrated in glaucoma and OHT (Johnson et al 1988a; Suzumara et al 1988; Searle et al 1991a, b; Wild et al 1989c, 1991b; Hudson et al 1994). Johnson et al (1988a) used the Digilab 750 automated perimeter to continuously measure sensitivity at 5°, 10°, 15° and 20° eccentricity. The sample comprised 16 normal subjects and 16 glaucoma patients with varying degrees of visual field loss. Both groups exhibited a reduction in sensitivity as a function of test duration. The magnitude of the fatigue effect was greater for the patient group, however, and increased with increase in stimulus eccentricity. Fatigue effects have also been observed in optic neuropathy patients, whereby demyelinated axons fatigue rapidly. Wildberger and Robert (1988) demonstrated a reduction in sensitivity of upto 77% in optic neuropathy patients compared to 32% in normal eyes, when Octopus perimetry was performed. The decline increased with increase in eccentricity. The lack of correlation between fatigue in the central field and that for the entire visual field also suggests an eccentricity dependency of the fatigue effect (Langerhorst et al 1987b).

Studies have also identified between-eye differences in the fatigue effect both in normals (Searle et al 1991a, b; Hudson et al 1994) and OHT and glaucoma patients (Wild et al 1989c, 1991b; Hudson et al 1994). In normals, Searle et al (1991a, b) measured a decline of sensitivity over each of the 3 phases for each eye at each visit - a within-eye fatigue effect. The decline in sensitivity was greater over the 3 phases for the second eye examined at both examination sessions. Indeed, sensitivity decreased on average by 1.1dB for the first eye at the first visit and by 2.0dB for the second eye. The reduction in sensitivity over the three phases of each eye was

greater at the first visit. The reduction was also greater in the periphery particularly in the superior field. Similar trends for the increase in SF, number of stimulus presentations and duration of phase were present in both eyes, being greater for the second eye although less pronounced at the second visit. The fatiguing effects were also apparent when the stimulus duration was reduced from 200ms to 100ms. In view of the greater fatigue effect in the second eye examined, it was suggested that confidence limits for abnormality should be different between the two eyes and should reflect the order in which the eyes are examined. Between-eye fatiguing effects have also been identified in ocular hypertensive patients (Wild et al 1989c; Hudson et al 1994) and glaucoma patients (Wild et al 1989c, 1991b). Wild et al (1989c) examined 20 OHT and glaucoma patients with the Humphrey Field Analyser on three consecutive days and then after an interval of 12 days. None of the patients had previously performed automated perimetry. A custom program was used consisting of 60 points arranged in a 12° square stimulus grid between 9° and 24° eccentricities. Both eyes were examined at each visit, the right eye followed by the left eye. There was an apparent learning effect in the right eyes, demonstrated by an improvement in group mean MS of 2.8dB between the first and second examinations. However there was little improvement in the left eye performance. This was explained either as a result of a between-eye learning effect at visit one, resulting in an increased baseline sensitivity such that at the subsequent visit there was little potential for improvement, or, alternatively, in terms of the fatigue effect opposing any learning effect. The longer-term effects of fatiguing were considered in a sample of 16 ocular hypertensive and glaucoma patients who were monitored over a 5 to 15 month period by Wild et al (1989c). Patients underwent a training period of 4 prior visits. The long-term follow-up comprised a perimetric examination on 2 successive days with the Humphrey Field Analyser. Both eyes were examined at each visit, the right eye before the left. Although there was little residual learning effect at the long-term follow-up, the MS was still lower and the SF still higher in the second eye examined, indicating the continued presence of a between-eye fatiguing effect.

Hudson et al (1994) compared both the within- and between-eye fatigue effect of normal and ocular hypertensive subjects using program G1X of the Octopus 1-2-3 perimeter. Twenty patients

with OHT and 20 age-matched normal subjects performed perimetry separately on both eyes at a single session. Program G1X is divided into two phases and each phase comprises four stages. Phase 1 thresholds all 59 locations out to an eccentricity of 28°. Phase 2 repeats the threshold measurement at all the stimulus locations. The initial stimulus intensities for the staircase strategy in Phase 2 are selected from the results of Phase 1. MD was larger (ie worse) for the second eye examined and declined over stage by approximately 2.5dB, the decline was greater beyond 17°. LV was also greater in the second eye and declined over stage by 6.0dB^2. There was little difference between the normal and OHT groups in the decline of sensitivity within- and between-eyes. This study again challenged the concept of identical confidence limits for abnormality for the two eyes. Retrospective studies considering interocular differences in sensitivity have been discussed in Chapter 1.

Other studies have been unable to identify a fatigue effect (Rabineau et al 1985; Marra and Flammer 1991). Rabineau et al (1985) was unable to demonstrate any decline in sensitivity when 8 normal subjects performed four successive field examinations over a 1 hour period using the Octopus perimeter. Marra and Flammer (1991) were also unable to demonstrate a time-related trend within a single perimetric session. Using the Octopus program J1, threshold was measured 12 times at each of 3 test locations on 70 normal eyes, 16 glaucomatous eyes and 14 eyes with cataract. No fatiguing effect was observed in any of the three diagnostic groups. It is questionable whether three locations are representative of a perimetric examination.

The within-eye fatiguing effect can be reduced by rest periods both during the examination of a given eye and between the examination of the two eyes. Johnson et al (1988a) compared the effect of a 1.5 minute rest period halfway through the examination of a given eye. Those subjects given a rest period demonstrated a greater sensitivity in the second half of the test compared with those subjects not given a break. The improvement was greater towards the periphery and was similar between normals and glaucoma patients. Rest periods, however, reduce the decline in sensitivity rather than arrest the process entirely. Indeed, some studies have reported continued within-eye within-examination and between-eye fatigue effects despite the provision of rest

periods both within- and between- the examination of the two eyes (Johnson et al 1988a; Searle et al 1991a, b; Wild et al 1989c, 1991b; Hudson et al 1994).

The fatigue effect is dependent on the duration of the perimetric examination. Gaspar et al (1994) discussed the factors influencing the duration of the perimetric examination. They examined 105 glaucoma patients with the Octopus automated perimeter. The test duration was compared with respect to the standard perimetric indices and reliability indices. The duration of the examination correlated well with MS, MD, LV and SF. The age of the patient had no influence on the test duration. The duration of the test is also dependent on the type of perimetric strategy employed. The development of faster strategies to estimate threshold and to reduce testing time have been discussed in Chapter 3; however, the assessment of the fatigue effect with such algorithms remains unknown.

The fatigue effect can be reduced to some extent by improving the vigilance of the patient (Coren and Ward 1989). Coman et al (1994) performed 7 sessions of automated perimetry with program 24-2 of the Humphrey Field Analyser on both eyes of 21 normal subjects. Five of the sessions involved the use of different procedures designed to improve vigilance: including visual (presentation of a flickering fixation light) and auditory cues, rest periods and simple encouragement. Performance declined over the duration of the examination particularly for the second eye to be examined. No significant improvement was observed for any of the vigilance enhancing procedures. Conversely, Mills et al (1994) demonstrated an improvement in threshold and a decrease in SF with auditory cueing but at the expense of increased fixation losses. This study examined one eye only and the effect of experience was not addressed.

5.3. Learning effects in present colour vision testing

All psychophysical methods provide threshold estimations that are contaminated by non-sensory factors such as criterion effects. Learning effects have been documented in colour vision testing (Aspinall 1974; Verriest et al 1982; Breton et al 1988). Aspinall (1974) employed the Farnsworth-Munsell 100-hue test to measure performance in two groups of normal subjects: one group had

been previously trained in the test procedure whilst the other had not. The trained group exhibited an improved performance and a reduced between-subject variability compared to the untrained group. These findings were later confirmed by Verriest et al (1982). Breton et al (1988) studied the effect of repeated testing on the outcome of the 100-Hue test using three groups of subjects. Group A were given 4 successive tests at 3 different illuminance levels without prior training. Group B received prior training followed by three successive tests at a standard illuminance of 160 lux. Group C also received prior training and were then tested with successive presentations each at 5 different illuminance levels. A significant improvement in performance was demonstrated by the untrained group A, irrespective of illuminance level, while the trained groups B and C, exhibited no clear trend towards improvement. After further questioning of both trained and untrained groups regarding performance in the tests it was hypothesized that the source of the learning effect was cognitive rather than a neural-based change in colour discrimination.Such learning effects may continue over several months (Hardy et al 1994).

5.4. Learning effects in Blue-Yellow perimetry

5.4.1. Aim of the study

It can be anticipated that B-Y perimetry will be applied to patients naive to any form of perimetric technique and also to patients previously experienced in W-W automated perimetry. The extent of the within- and between-eye learning effects for B-Y perimetry in naive patients is unknown. Furthermore, the extent to which the learning effects might be present in patients already experienced in W-W perimetry is also unknown. The purpose of the study therefore was to investigate the B-Y within- and between-eye learning effect in two groups of normal subjects: those experienced in W-W perimetry and those naive to any form of perimetry.

5.4.2. Materials and Methods

Sample

The sample comprised 61 clinically normal subjects assigned to one of four groups based upon age and previous experience in W-W automated threshold perimetry. The first group consisted of 11 young subjects (mean age 24.0 years, SD 4.2, range 20-34 years; 7 males, 4 females) naive to any form of perimetric technique. The second group consisted of 10 young subjects (mean age 27.0 years, SD 3.8, range 22-33 years; 8 males, 2 females) who had undergone at least 4 previous full threshold automated perimetric examinations (Humphrey Field Analyser 640 Programs 30-2 or 24-2) over the previous 6 months. The third group consisted of 22 elderly subjects (mean age 61.9 years, SD 8.3, range 51-79 years; 15 males, 7 females) naive to any form of perimetric technique. The fourth group consisted of 18 elderly subjects (mean age 66.9 years, SD 6.3, range 52-80 years; 9 males, 9 females) who had undergone at least 4 previous full threshold automated perimetric examinations (Humphrey Field Analyser 640 Programs 30-2 or 24-2) over the previous 6 months. Informed consent was obtained from each subject. Subjects were recruited on the basis of consecutive presentation. The experienced group had previously taken part in an earlier perimetric clinical trial and were age-matched to the naive group as closely as possible.

All subjects conformed to rigid inclusion criteria: a corrected visual acuity of at least 6/9 in both eyes, distance refractive error of within ±5 dioptres sphere and within ±3 dioptres cylinder, clear ocular media as classified by the Lens Opacity Classification system LOCS II (Chylack et al 1989), intraocular pressure of less than 22mmHg, normal optic nerve head appearance, no family history of glaucoma or diabetes, no history of ocular disease or trauma, no neurological history or systemic disease, no systemic medication known to influence the visual field and no history of any congenital colour vision defect.

Perimetry

The B-Y visual field was examined using a modified Humphrey Field Analyser (HFA) 640. The modified perimeter has been described in detail in Chapter 4 (Section 4.10.1). The modifications

became operative after the instrument had performed its standard internal calibration routine. The yellow adapting background was produced by a Schott OG530 filter (background luminance 330cdm^{-2} and the blue stimulus filter by a OCLI blue dichroic filter.

The learning effect can be studied for any number of examinations and for any interval between examinations. Clearly, the ideal study design should reflect that of standard clinical practice. However, the particular regime of clinical management varies from patient to patient and indeed from clinician to clinician. A short interval between examinations was used in this study for two reasons. Firstly, since two or three baseline fields performed within a short time period provide a better starting point for the recognition of change (Hoskins et al 1988), it is expedient to elucidate the learning effect over such a period. Secondly, the relatively optimum conditions of a short interval between examinations can accentuate the learning effect and can provide an indication of the potential improvement in the visual field over longer intervals. Indeed, similar experimental designs have been used previously (Wood et al 1987a; Wild et al 1989c, 1991b; Searle et al 1991a, b).

Blue-on-Yellow perimetry (Goldmann size V, stimulus duration 200ms) was performed on three consecutive days and at day 10, ie after an interval of one week, using Program 30-2. The examination at day 10 was intended to determine the extent of the retention of any learning effect. Both eyes were examined at each visit, the right eye was always examined first. Rest periods of 2-3 minutes were given at 5-7 minute intervals during the examination of each eye and a further rest of 5 minutes was given prior to the examination of the second eye in order to minimise fatiguing effects. Each subject was given the same instructions for the examination, regardless of perimetric experience, in order to minimize the effects of operator bias. The distance refraction was used where necessary together with the near correction if appropriate. The eye not examined was occluded with an opaque patch. Fixation losses were less than 20%, and false-negative and false-positive responses less than 33% for each subject in both the trained and untrained groups. For the reasons outlined in Chapter 4 (Section 4.10.1.), fixation was also constantly monitored using the video monitor.

5.4.3. Analysis

Using the procedures outlined in Chapter 4 (Section 4.10.1.), the B-Y sensitivities were re-calculated with respect to the maximum stimulus luminance of the blue stimulus and the yellow background luminance.

The primary analysis was concerned with the identification of any improvement in sensitivity over the three days rather than with differences in the absolute measurement of sensitivity between the four groups. Furthermore, having identified any such improvement in sensitivity over the three days, the primary analysis was required to identify whether the improvement was different between the two eyes of any given group, was different between the naive and experienced groups or was different between the two age groups. The secondary analysis was required to identify whether any such increase in sensitivity over the three days was different across the various regions of the field.

The global mean sensitivity (MS) based upon 74 of the 76 stimulus locations of Program 30-2, was calculated for each eye of each subject for each visit. The two stimulus locations above and below the blind spot were not included in the analysis. The unweighted short-term fluctuation (SF) (Flammer 1986; Heijl et al 1987c; Flanagan et al 1993a) was similarly calculated for each eye of each subject for each visit and was based upon the conventional ten standard stimulus locations employed for calculation of the SF in conventional W-W perimetry. The MS was also calculated for each of the superior and inferior hemifields and for the central and peripheral annular zones for each eye of each subject at each visit. The annular zones were approximately equally divided such that there were 38 stimulus locations in the central zone and 36 in the peripheral zone.

The primary analysis was considered to be the analysis of global MS and global SF. The data for the global MS and SF over days one to three were analysed by separate repeated measures ANOVAs. Perimetric experience and age group together with their interaction were considered as between-subjects factors. The eye examined, the examination day and any interaction involving

these were considered as within-subjects factors. Where appropriate, the Greenhouse-Geiser correction was used for the lack of compound symmetry due to the serial correlation between the repeated measures. A similar analysis was performed between days 3 and 10. To account for accumulating Type I errors (the possibility of finding a significant difference for a particular parameter when no such difference actually exists) a Bonferroni correction was applied to each significance level. The conventional 0.05 level was divided by the number of analyses (two) and the outcome of the statistical testing was considered to be significant only at the $p \leq 0.025$ level.

The secondary analysis was considered to be the analysis of the superior and inferior hemifield MSs and of the central and peripheral MSs. A repeated measures ANOVA similar to the primary analysis was undertaken with the given hemifield or annulus considered as a within-subjects factor. A Bonferroni correction was similarly applied to the hemifield and annulus analyses and the level of the statistical testing was again considered to be significant only at the $p \leq 0.025$ level. The Bonferroni correction is only appropriate if the analyses are independent of each other. Some dependency was present, however, between the analyses in that the global MS was highly correlated with those from each of the hemifields and from each of the annuli and the MS of one hemifield was correlated with that of the opposite hemifield. The number of false-positive and false-negative responses was minimal and insufficient to perform any statistical analysis.

5.4.4. Results

Primary Analysis - Global MS

Group mean MS is illustrated in Table 5.1 for each eye at each day for the four subject groups. As would be expected, the global MS for days one to three, combined, was greater for the younger age group ($p<0.001$). It was also greater in the first eye examined ($p=0.021$) and greater for the naive group ($p=0.023$). For days 3 and 10, combined, the global MS was similarly greater for the younger age group ($p<0.001$) and in the first eye examined ($p<0.001$) but was independent of perimetric experience ($p=0.129$).

The global MS increased over the three days ($p<0.001$) by 0.7dB (approximately three percent) from baseline averaged across eyes and groups. This increase was irrespective of perimetric experience ($p=0.109$), the eye examined ($p=0.029$) and age ($p=0.190$). The ANOVA for the global MS over the three days is displayed in Table 5.2.

The global MS was greater for day 10 compared to day 3 but this difference did not reach statistical significance overall ($p=0.034$). Specifically, however, the increase at day 10 was greater for the elderly group (1.0dB) compared to the younger group who on average exhibited no further improvement ($p=0.015$) from day 3. The ANOVA for the global MS between days 3 and 10 is displayed in Table 5.3.

The proportionate change in MS at days 2, 3 and 10 relative to the baseline at day one is shown in Figure 5.1. The standardisation of the data in this way facilitates direct comparison across all groups regardless of age. The improvement in global MS between days 1 and 10, averaged across both eyes of all 4 groups, was equivalent to 1.2dBs or 6.5% of the baseline sensitivity with the increase being greater for the first eye examined (8.2% compared to 4.9%). The extent of the improvement in MS varied considerably between subjects with improvements of between 20% and 30% not uncommon.

		Day 1		Day 2		Day 3		Day 10	
Group	Eye	Mean	SD	Mean	SD	Mean	SD	Mean	SD
Young Naive	R	2.52	0.27	2.66	0.18	2.66	0.19	2.63	0.27
	L	2.52	0.24	2.67	0.27	2.62	0.19	2.51	0.35
Young Experienced	R	2.44	0.19	2.48	0.22	2.54	0.26	2.60	0.20
	L	2.41	0.27	2.44	0.26	2.51	0.26	2.55	0.23
Elderly Naive	R	1.99	0.44	2.12	0.40	2.11	0.37	2.16	0.40
	L	2.05	0.44	2.07	0.42	2.03	0.38	2.08	0.42
Elderly Experienced	R	1.83	0.40	1.86	0.38	1.86	0.40	1.99	0.39
	L	1.78	0.35	1.82	0.37	1.79	0.40	1.96	0.39

Table 5.1. Group mean global mean sensitivity (log units) for each eye of the four subject groups at days 1-3 and 10. One log unit is equivalent to 10dB.

Source	Degrees of Freedom	Sums of Squares	Mean Square	F value	P value
Age	1	31.800	31.800	46.20	p<0.001
Experience	1	3.800	3.800	5.50	p=0.023
Age x Experience	1	0.500	0.500	0.70	p=0.417
Error	57	39.00	0.700		
Eye	1	0.050	0.050	5.66	p=0.021
Eye x Age	1	0.000	0.000	0.01	p=0.624
Eye x Experience	1	0.020	0.020	2.21	p=0.275
Eye x Age x Experience	1	0.002	0.002	0.26	p=0.957
Error	57	0.505	0.009		
Day	1	0.262	0.262	12.04	p<0.001
Day x Age	1	0.066	0.066	3.03	p=0.095
Day x Experience	1	0.017	0.017	0.80	p=0.109
Day x Age x Experience	1	0.000	0.000	0.01	p=0.484
Error	57	1.240	0.022		
Eye x Day	1	0.051	0.051	10.07	p=0.029
Eye x Day x Age	1	0.006	0.006	1.11	p=0.190
Eye x Day x Experience	1	0.034	0.034	6.69	p=0.063
Eye x Day x Age x Experience	1	0.003	0.003	0.64	p=0.128
Error	57	0.287	0.005		

Table 5.2. Summary table for the repeated measures analysis of variance for the global mean sensitivity across days 1 to 3.

Source	Degrees of Freedom	Sums of Squares	Mean Square	F value	P value
Age	1	19.200	19.200	42.10	p<0.001
Experience	1	1.100	1.100	2.40	p=0.129
Age x Experience	1	0.400	0.400	1.00	p=0.332
Error	53	26.500	0.500		
Eye	1	0.226	0.226	16.82	p<0.001
Eye x Age	1	0.000	0.000	0.001	p=0.873
Eye x Experience	1	0.024	0.024	1.82	p=0.209
Eye x Age x Experience	1	0.002	0.002	0.13	p=0.807
Error	53	0.712	0.013		
Day	1	0.113	0.113	2.42	p=0.034
Day x Age	1	0.197	0.197	4.22	p=0.015
Day x Experience	1	0.143	0.143	3.05	p=0.039
Day x Age x Experience	1	0.005	0.005	0.10	p=0.792
Error	53	2.476	0.047		
Eye x Day	1	0.004	0.004	0.50	p=0.512
Eye x Day x Age	1	0.010	0.010	1.23	p=0.305
Eye x Day x Experience	1	0.009	0.009	1.10	p=0.333
Eye x Day x Age x Experience	1	0.001	0.001	0.08	p=0.792
Error	53	0.423	0.423		

Table 5.3. Summary table for the repeated measures analysis of variance for the mean sensitivity across days 3 to 10.

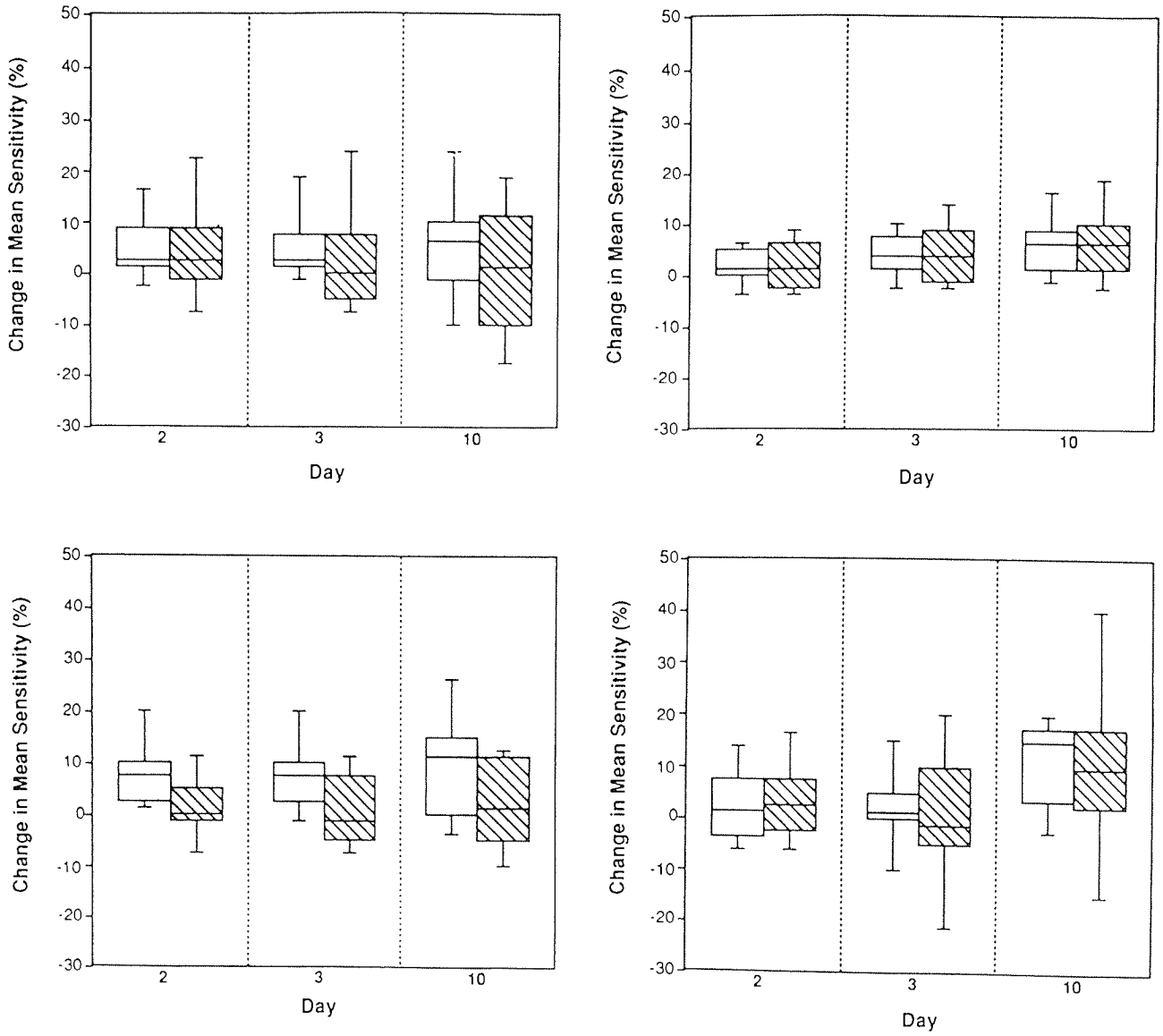

Figure 5.1 Proportionate change in mean sensitivity for days 2, 3 and 10 relative to the baseline at day 1 (Top left young naive; top right young experienced; bottom left elderly naive; bottom right elderly experienced). The open boxplots represent the right eye and the hatched boxplots the left eye. The box indicates the 15, 50 and 85 percentiles of the range of sensitivity change of the given eye for the given group whilst the lower and upper extremities of the whiskers represent the 0 and 100 percentiles respectively.

Primary Analysis - Global SF

Group mean SF is illustrated in Table 5.4 for each eye at each day for the four subject groups. The global SF considered over days one to three, combined, was greater for the elderly groups ($p=0.011$) but was independent of previous perimetric experience ($p=0.944$). It was larger in the second eye of the experienced group ($p=0.007$). For days 3 and 10, combined, the global SF was greater for the older age group ($p=0.010$).

The global SF decreased on average by 0.15dB (9.9%) over the three days ($p<0.001$) irrespective of perimetric experience ($p=0.944$) and this decrease was more pronounced for the younger age group (0.35dB) compared to the older group who overall showed no reduction ($p=0.023$). The ANOVA for the global SF over the three days is displayed in Table 5.5. The decrease in the SF was more pronounced for the first eye examined (0.37dB) compared to the second eye examined (0.1dB) but the difference did not reach statistical significance ($p=0.028$).

There was no statistically significant changes in SF between days 3 and 10 for any of the groups. The ANOVA for the global SF between days 3 and 10 is displayed in Table 5.6.

The proportionate change in SF for days 2, 3 and 10 relative to the baseline at day one is shown in Figure 5.2. The reduction in the Global SF between days 1 and 10 averaged across both eyes of all 4 groups was equivalent to 0.25dB (16.0%) and the extent of the improvement again varied considerably between subjects with improvements present of between 30% and 40%.

		Day 1		Day 2		Day 3		Day 10	
Group	Eye	Mean	SD	Mean	SD	Mean	SD	Mean	SD
Young Naive	R	0.22	0.07	0.15	0.05	0.14	0.03	0.16	0.05
	L	0.13	0.04	0.14	0.05	0.15	0.04	0.14	0.04
Young Experienced	R	0.19	0.04	0.13	0.04	0.16	0.04	0.15	0.03
	L	0.19	0.08	0.16	0.06	0.14	0.04	0.16	0.04
Elderly Naive	R	0.20	0.06	0.19	0.04	0.18	0.05	0.14	0.03
	L	0.18	0.05	0.17	0.05	0.19	0.07	0.18	0.07
Elderly Experienced	R	0.18	0.40	0.17	0.04	0.16	0.06	0.17	0.05
	L	0.18	0.07	0.18	0.04	0.18	0.04	0.17	0.07

Table 5.4. Group mean global short-term fluctuation (log units) for each eye of the four subject groups at days 1-3 and 10. One log unit is equivalent to 10dB.

Source	Degrees of Freedom	Sums of Squares	Mean Square	F value	P value
Age	1	0.039	0.039	6.95	p=0.011
Experience	1	0.001	0.001	0.00	p=0.944
Age x Experience	1	0.007	0.007	1.17	p=0.284
Error	57	0.342	0.006		
Eye	1	0.012	0.012	3.38	p=0.169
Eye x Age	1	0.006	0.006	1.54	p=0.153
Eye x Experience	1	0.004	0.004	1.13	p=0.007
Eye x Age x Experience	1	0.004	0.004	1.12	p=0.505
Error	57	0.207	0.004		
Day	1	0.019	0.019	5.89	p<0.001
Day x Age	1	0.018	0.018	5.66	p=0.023
Day x Experience	1	0.000	0.000	0.07	p=0.944
Day x Age x Experience	1	0.002	0.002	0.68	p=0.505
Error	57	0.183	0.183		
Eye x Day	1	0.006	0.006	2.24	p=0.028
Eye x Day x Age	1	0.007	0.007	2.29	p=0.067
Eye x Day x Experience	1	0.018	0.018	6.50	p=0.055
Eye x Day x Age x Experience	1	0.004	0.004	1.45	p=0.102
Error	57	0.162	0.003		

Table 5.5. Summary table for the repeated measures analysis of variance for the short-term fluctuation across days 1 to 3.

Source	Degrees of Freedom	Sums of Squares	Mean Square	F value	P value
Age	1	0.026	0.021	7.09	p=0.010
Experience	1	0.001	0.001	0.10	p=0.752
Age x Experience	1	0.001	0.004	0.23	p=0.635
Error	53	0.212	0.004		
Eye	1	0.013	0.013	0.93	p=0.339
Eye x Age	1	0.025	0.025	1.81	p=0.184
Eye x Experience	1	0.008	0.008	0.55	p=0.462
Eye x Age x Experience	1	0.041	0.041	2.94	p=0.092
Error	53	0.732	0.014		
Day	1	0.009	0.009	0.63	p=0.856
Day x Age	1	0.051	0.051	3.58	p=0.215
Day x Experience	1	0.017	0.017	1.20	p=0.408
Day x Age x Experience	1	0.022	0.022	1.53	p=0.329
Error	53	0.752	0.014		
Eye x Day	1	0.008	0.008	0.73	p=0.397
Eye x Day x Age	1	0.031	0.031	2.69	p=0.107
Eye x Day x Experience	1	0.027	0.027	2.39	p=0.128
Eye x Day x Age x Experience	1	0.046	0.046	3.98	p=0.051
Error	53	0.607	0.011		

Table 5.6. Summary table for the repeated measures analysis of variance for the short-term fluctuation across days 3 to 10.

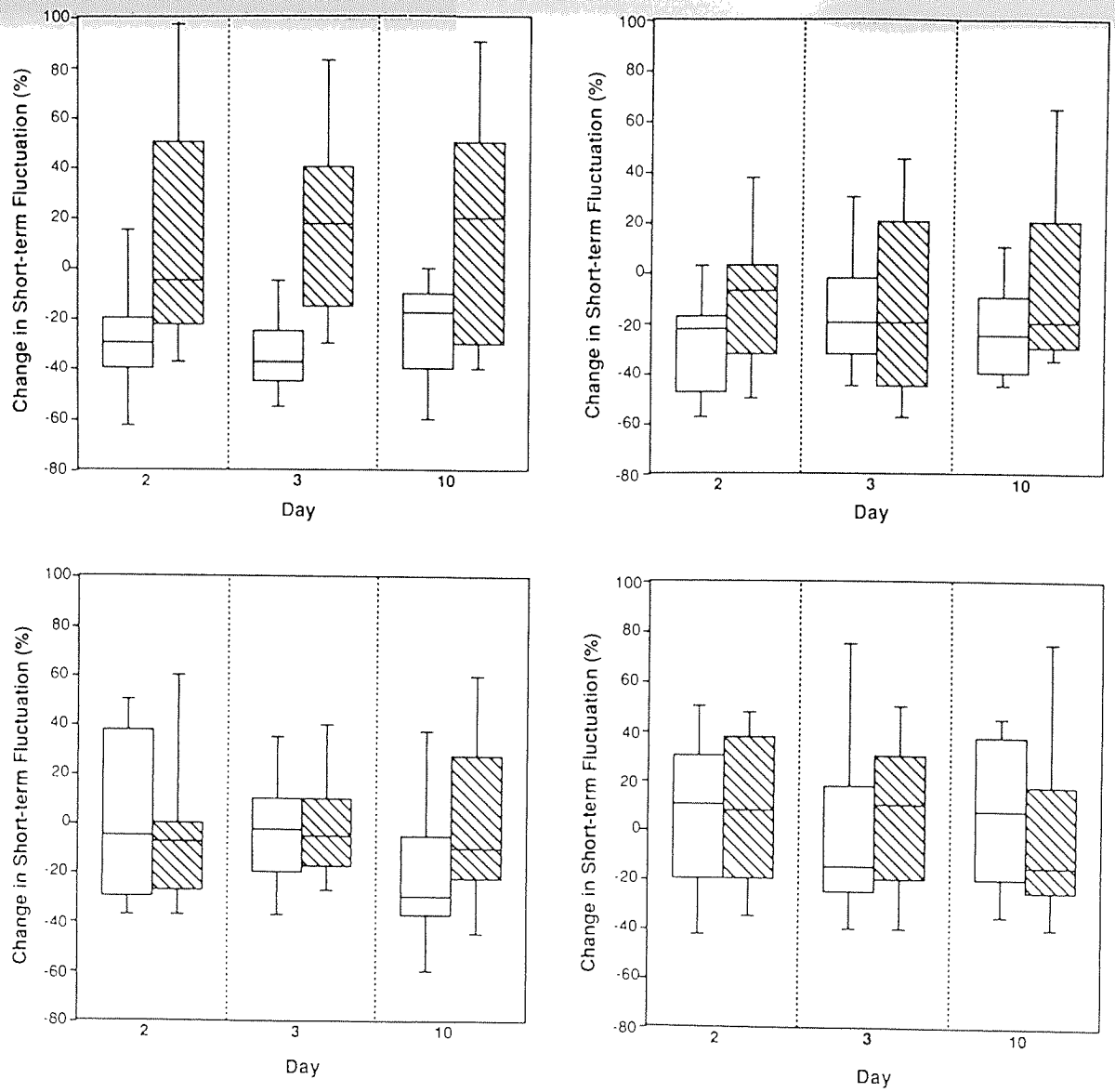

Figure 5.2 Proportionate change in short-term fluctuation for days 2, 3 and 10 relative to the baseline at day 1 (Top left young naive; top right young experienced; bottom left elderly naive; bottom right elderly experienced). The open boxplots represent the right eye and the hatched boxplots the left eye. The box indicates the 15, 50 and 85 percentiles of the range of short-term fluctuation change of the given eye for the given group whilst the lower and upper extremities of the whiskers represent the 0 and 100 percentiles respectively. Note a reduction in the short-term fluctuation is indicated by a negative value. Note also the scaling of the vertical axis is different from that of Figure 5.1.

Secondary analysis - Superior and Inferior MS

Group mean superior and inferior MS is illustrated in Table 5.7 for each eye at each day for the four subject groups. The superior and inferior MSs increased over the three days ($p<0.001$). The increase was more pronounced for the superior field than the inferior field ($p=0.006$) and also for the first eye ($p=0.005$) and for the naive group ($p=0.011$). The greater improvement in the superior hemifield was more pronounced for the naive group ($p=0.001$) particularly for the young naive group ($p=0.021$) and was also greater for the first eye ($p=0.015$). The ANOVA for the superior and inferior MSs over the three days is displayed in Table 5.8.

The superior and inferior MSs were also greater for day 10 compared to day 3 ($p=0.025$) and this difference was more pronounced for the older age group ($p=0.017$). The improvement, however, was similar between the two hemifields ($p=0.136$). The ANOVA for the superior and inferior MSs between days 3 and 10 is displayed in Table 5.9.

Secondary Analysis - Central and Peripheral MS

Group mean central and peripheral MS is illustrated in Table 5.10 for each eye at each day for the four subject groups. The central and peripheral annulus MSs increased over the three days ($p<0.001$) particularly for the first eye ($p=0.010$) although the increase was similar for both annuli ($p=0.664$) regardless of age ($p=0.630$), perimetric experience ($p=0.492$) or eye examined ($p=0.967$). The ANOVA for the central and peripheral MSs over the three days is displayed in Table 5.11.

The MSs for the two annuli were similar between days 3 and 10 overall ($p=0.653$) but an increase in sensitivity at day 10 was present for the older age group ($p=0.021$). The ANOVA for central and peripheral MSs between days 3 to 10 is displayed in Table 5.12.

			Day 1		Day 2		Day 3		Day 10	
Group	Eye	Hemifield	Mean	SD	Mean	SD	Mean	SD	Mean	SD
Young Naive	R	Superior	2.41	0.38	2.57	0.24	2.57	0.26	2.55	0.33
		Inferior	2.63	0.18	2.74	0.14	2.74	0.12	2.71	0.22
	L	Superior	2.42	0.32	2.57	0.32	2.50	0.29	2.40	0.40
		Inferior	2.63	0.18	2.73	0.22	2.69	0.13	2.61	0.31
Young Experienced	R	Superior	2.36	0.25	2.39	0.26	2.43	0.33	2.52	0.25
		Inferior	2.52	0.16	2.57	0.20	2.66	0.20	2.67	0.16
	L	Superior	2.34	0.33	2.39	0.33	2.44	0.34	2.51	0.31
		Inferior	2.46	0.22	2.50	0.21	2.57	0.19	2.60	0.17
Elderly Naive	R	Superior	1.89	0.50	2.05	0.45	2.34	0.33	2.34	0.33
		Inferior	2.08	0.41	2.19	0.40	2.46	0.22	2.46	0.22
	L	Superior	1.96	0.47	1.98	0.48	1.91	0.46	1.98	0.50
		Inferior	2.15	0.41	1.98	0.48	2.14	0.33	2.16	0.36
Elderly Experienced	R	Superior	1.76	0.42	1.75	0.41	1.76	0.45	1.91	0.42
		Inferior	1.88	0.40	1.95	0.39	1.94	0.38	2.09	0.41
	L	Superior	1.73	0.32	1.76	0.32	1.72	0.33	1.88	0.37
		Inferior	1.81	0.43	1.84	0.48	1.81	0.53	1.98	0.50

Table 5.7. Group mean hemifield mean sensitivity (log units) for each eye of the four subject groups at days 1-3 and 10. One log unit represents 10dB.

Source	Degrees of Freedom	Sums of Squares	Mean Square	F value	P value
Age	1	65.590	65.590	46.35	p<0.001
Experience	1	7.125	7.125	5.04	p=0.029
Age x Experience	1	0.967	0.967	0.68	p=0.412
Error	57	80.656	1.415		
Hemifield	1	4.004	4.004	37.79	p<0.001
Hemifield x Age	1	0.041	0.041	0.39	p=0.537
Hemifield x Experience	1	0.029	0.029	0.28	p=0.600
Hemifield x Age x Experience	1	0.000	0.000	0.00	p=0.955
Error	57	6.040	0.106		
Eye	1	0.303	0.303	10.53	p=0.002
Eye x Age	1	0.029	0.029	1.00	p=0.321
Eye x Experience	1	0.005	0.005	0.19	p=0.664
Eye x Age x Experience	1	0.000	0.000	0.00	p=0.948
Error	57	1.642	0.029		
Day	2	0.591	0.295	9.05	p<0.001
Day x Age	2	0.167	0.084	2.56	p=0.086
Day x Experience	2	0.050	0.025	0.76	p=0.461
Day x Age x Experience	2	0.114	0.057	1.74	p=0.183
Error	114	3.722	0.029		

Table 5.8. Summary table for the repeated measures analysis of variance for the superior and inferior mean sensitivity across days 1 to 3.

Source	Degrees of Freedom	Sums of Squares	Mean Square	F value	P value
Hemifield x Eye	1	0.089	0.089	2.31	p=0.135
Hemifield x Eye x Age	1	0.002	0.002	0.05	p=0.823
Hemifield x Eye x Experience	1	0.047	0.047	1.22	p=0.274
Hemifield x Eye x Age x Experience	1	0.001	0.001	0.02	p=0.882
Error	57	2.195	0.039		
Hemifield x Day	2	0.058	0.029	5.41	p=0.006
Hemifield x Day x Age	2	0.008	0.004	0.71	p=0.492
Hemifield x Day x Experience	2	0.076	0.038	7.11	p=0.001
Hemifield x Day x Age x Experience	2	0.043	0.021	4.01	p=0.021
Error	114	0.610	0.005		
Eye x Day	2	0.120	0.060	5.70	p=0.005
Eye x Day x Age	2	0.007	0.037	3.47	p=0.037
Eye x Day x Experience	2	0.103	0.051	4.86	p=0.011
Eye x Day x Age x Experience	2	0.074	0.037	3.52	p=0.036
Error	114	1.203	0.011		
Hemifield x Eye x Day	2	0.037	0.019	4.35	p=0.015
Hemifield x Eye x Day x Age	2	0.030	0.015	3.53	p=0.033
Hemifield x Eye x Day x Experience	2	0.022	0.011	2.60	p=0.079
Hemifield x Eye x Day x Age x Experience	2	0.004	0.002	0.51	p=0.602
Error	114	0.488	0.004		

Table 5.8 (cont). Summary table for the repeated measures analysis of variance for the superior and inferior mean sensitivity across days 1 to 3.

Source	Degrees of Freedom	Sums of Squares	Mean Square	F value	P value
Age	1	39.049	39.049	42.51	p<0.001
Experience	1	2.254	2.254	2.45	p=0.123
Age x Experience	1	1.074	1.074	1.17	p=0.284
Error	53	48.688	0.919		
Hemifield	1	2.907	2.907	30.64	p<0.001
Hemifield x Age	1	0.001	0.001	0.01	p=0.907
Hemifield x Experience	1	0.041	0.041	0.43	p=0.515
Hemifield x Age x Experience	1	0.000	0.000	0.00	p=0.962
Error	53	5.028	0.095		
Eye	1	0.528	0.528	19.69	p<0.001
Eye x Age	1	0.005	0.005	0.17	p=0.678
Eye x Experience	1	0.028	0.028	1.06	p=0.308
Eye x Age x Experience	1	0.010	0.010	0.36	p=0.553
Error	53	1.422	0.027		
Day	1	0.283	0.283	5.27	p=0.026
Day x Age	1	0.324	0.324	6.03	p=0.017
Day x Experience	1	0.239	0.239	4.45	p=0.400
Day x Age x Experience	1	0.003	0.003	0.06	p=0.803
Error	53	2.844	0.054		

Table 5.9. Summary table for the repeated measures analysis of variance for the superior and inferior mean sensitivity across days 3 to 10.

Source	Degrees of Freedom	Sums of Squares	Mean Square	F value	P value
Hemifield xEye	1	0.018	0.018	0.63	p=0.430
Hemifield xEye x Age	1	0.000	0.000	0.01	p=0.942
Hemifield xEye x Experience	1	0.091	0.091	3.21	p=0.079
Hemifield xEye x Age x Experience	1	0.001	0.001	0.02	p=0.878
Error	53	1.509	0.028		
Hemifield x Day	1	0.014	0.014	2.29	p=0.136
Hemifield x Day x Age	1	0.005	0.005	0.83	p=0.367
Hemifield x Day x Experience	1	0.000	0.000	0.02	p=0.899
Hemifield x Day x Age x Experience	1	0.014	0.014	2.36	p=0.130
Error	53	0.316	0.006		
Eye x Day	1	0.007	0.007	0.36	p=0.552
Eye x Day x Age	1	0.018	0.018	0.93	p=0.339
Eye x Day x Experience	1	0.023	0.023	1.18	p=0.283
Eye x Day x Age x Experience	1	0.002	0.002	0.11	p=0.740
Error	53	1.028	0.019		
Hemifield x Eye x Day	1	0.001	0.001	0.23	p=0.637
Hemifield x Eye x Day x Age	1	0.008	0.008	2.18	p=0.146
Hemifield x Eye x Day x Experience	1	0.001	0.001	0.17	p=0.683
Hemifield x Eye x Day x Age x Experience	1	0.000	0.000	0.09	p=0.763
Error	53	0.187	0.004		

Table 5.9 (cont). Summary table for the repeated measures analysis of variance for superior and inferior mean sensitivity (MS) across days 3 to 10.

			Day 1		Day 2		Day 3		Day 10	
Group	Eye	Location	Mean	SD	Mean	SD	Mean	SD	Mean	SD
Young Naive	R	Central	2.68	0.25	2.83	0.15	2.83	0.12	2.81	0.22
		Peripheral	2.36	0.31	2.48	0.23	2.47	0.23	2.45	0.34
	L	Central	2.69	0.20	2.82	0.24	2.76	0.16	2.67	0.30
		Peripheral	2.35	0.32	2.46	0.29	2.43	0.25	2.32	0.41
Young Experienced	R	Central	2.64	0.16	2.68	0.19	2.75	0.22	2.80	0.16
		Peripheral	2.23	0.25	2.26	0.26	2.33	0.31	2.38	0.24
	L	Central	2.56	0.22	2.61	0.22	2.67	0.23	2.71	0.21
		Peripheral	2.23	0.32	2.28	0.32	2.34	0.30	2.39	0.26
Elderly Naive	R	Central	2.16	0.48	2.30	0.48	2.26	0.45	2.30	0.46
		Peripheral	1.81	0.41	1.94	0.41	1.94	0.38	2.00	0.38
	L	Central	2.23	0.45	2.26	0.44	2.23	0.42	2.26	0.43
		Peripheral	1.87	0.43	1.87	0.43	1.82	0.37	1.87	0.43
Elderly Experienced	R	Central	2.03	0.36	2.04	0.38	2.07	0.39	2.18	0.41
		Peripheral	1.60	0.46	1.65	0.41	1.64	0.41	1.77	0.44
	L	Central	1.98	0.31	2.01	0.34	1.98	0.38	2.14	0.37
		Peripheral	1.56	0.41	1.59	0.44	1.54	0.44	1.72	0.48

Table 5.10. Group mean central and peripheral mean sensitivity (log units) for each eye of the four subject groups at days 1-3 and 10. One log unit is equivalent to 10dB.

Source	Degrees of Freedom	Sums of Squares	Mean Square	F value	P value
Age	1	65.590	65.590	46.35	p<0.001
Experience	1	7.125	7.125	5.04	p=0.029
Age x Experience	1	0.967	0.967	0.68	p=0.412
Error	57	80.656	1.415		
Annulus	1	23.274	23.274	340.60	p<0.001
Annulus x Age	1	0.051	0.051	0.74	p=0.393
Annulus x Experience	1	0.071	0.071	1.05	p=0.311
Annulus x Age x Experience	1	0.008	0.008	0.11	p=0.738
Error	57	3.895	0.068		
Eye	1	0.207	0.207	7.22	p=0.009
Eye x Age	1	0.008	0.008	0.27	p=0.603
Eye x Experience	1	0.035	0.035	1.22	p=0.274
Eye x Age x Experience	1	0.013	0.013	0.45	p=0.504
Error	57	1.639	0.029		
Day	2	0.683	0.342	10.16	p<0.001
Day x Age	2	0.152	0.076	2.26	p=0.113
Day x Experience	2	0.128	0.064	1.90	p=0.156
Day x Age x Experience	2	0.035	0.018	0.52	p=0.586
Error	114	3.834	0.034		

Table 5.11. Summary table for the repeated measures analysis of variance for the central and peripheral mean sensitivity across days 1 to 3.

Source	Degrees of Freedom	Sums of Squares	Mean Square	F value	P value
Annuli x Eye	1	0.002	0.002	0.09	p=0.763
Annuli x Eye x Age	1	0.042	0.042	1.75	p=0.191
Annuli x Eye x Experience	1	0.043	0.043	1.81	p=0.184
Annuli x Eye x Age x Experience	1	0.007	0.007	0.27	p=0.603
Error	57	1.352	0.024		
Annuli x Day	2	0.004	0.002	0.40	p=0.664
Annuli x Day x Age	2	0.004	0.002	0.45	p=0.630
Annuli x Day x Experience	2	0.006	0.003	0.71	p=0.492
Annuli x Day x Age x Experience	2	0.001	0.001	0.11	p=0.889
Error	114	0.521	0.005		
Eye x Day	2	0.100	0.050	4.80	p=0.010
Eye x Day x Age	2	0.041	0.021	1.99	p=0.143
Eye x Day x Experience	2	0.051	0.026	2.48	p=0.090
Eye x Day x Age x Experience	2	0.019	0.010	0.93	p=0.395
Error	114	1.179	0.010		
Annuli x Eye x Day	2	0.000	0.000	0.03	p=0.967
Annuli x Eye x Day x Age	2	0.013	0.006	1.66	p=0.197
Annuli x Eye x Day x Experience	2	0.000	0.000	0.05	p=0.946
Annuli x Eye x Day x Age x Experience	2	0.005	0.002	0.59	p=0.550
Error	114	0.439	0.004		

Table 5.11 (cont). Summary table for the repeated measures analysis of variance for the central and peripheral mean sensitivity across days 1 to 3.

Source	Degrees of Freedom	Sums of Squares	Mean Square	F value	P value
Age	1	39.272	39.272	42.15	p<0.001
Experience	1	2.218	2.218	2.38	p=0.129
Age x Experience	1	1.039	1.039	1.11	p=0.296
Error	53	49.379	10.932		
Annulus	1	14.575	14.575	289.38	p<0.001
Annulus x Age	1	0.018	0.018	0.35	p=0.557
Annulus x Experience	1	0.053	0.053	1.05	p=0.311
Annulus x Age x Experience	1	0.022	0.022	0.44	p=0.509
Error	53	2.669	0.050		
Eye	1	0.498	0.498	17.57	p<0.001
Eye x Age	1	0.004	0.004	0.14	p=0.712
Eye x Experience	1	0.023	0.023	0.82	p=0.370
Eye x Age x Experience	1	0.015	0.015	0.54	p=0.464
Error	53	1.502	0.029		
Day	1	0.256	0.256	4.78	p=0.033
Day x Age	1	0.303	0.303	5.66	p=0.021
Day x Experience	1	0.228	0.228	4.28	p=0.044
Day x Age x Experience	1	0.004	0.004	0.08	p=0.777
Error	53	2.832	0.053		

Table 5.12. Summary table for the repeated measures analysis of variance for the central and peripheral mean sensitivity across days 3 to 10.

Source	Degrees of Freedom	Sums of Squares	Mean Square	F value	P value
Annuli x Eye	1	0.000	0.000	0.01	p=0.922
Annuli x Eye x Age	1	0.068	0.068	2.61	p=0.111
Annuli x Eye x Experience	1	0.043	0.043	1.65	p=0.205
Annuli x Eye x Age x Experience	1	0.000	0.000	0.00	p=0.970
Error	53	1.376	0.026		
Annuli x Day	1	0.000	0.001	0.20	p=0.653
Annuli x Day x Age	1	0.000	0.000	0.09	p=0.765
Annuli x Day x Experience	1	0.001	0.001	0.29	p=0.594
Annuli x Day x Age x Experience	1	0.000	0.000	0.03	p=0.865
Error	53	0.185	0.003		
Eye x Day	1	0.003	0.003	0.19	p=0.665
Eye x Day x Age	1	0.029	0.029	1.60	p=0.211
Eye x Day x Experience	1	0.032	0.032	1.72	p=0.195
Eye x Day x Age x Experience	1	0.000	0.000	0.02	p=0.900
Error	53	0.972	0.018		
Annuli x Eye x Day	1	0.000	0.000	0.04	p=0.835
Annuli x Eye x Day x Age	1	0.000	0.000	0.06	p=0.805
Annuli x Eye x Day x Experience	1	0.001	0.001	0.15	p=0.696
Annuli x Eye x Day x Age x Experience	1	0.000	0.000	0.02	p=0.886
Error	53	0.218	0.004		

Table 5.12 (cont). Summary table for the repeated measures analysis of variance for the central and peripheral mean sensitivity across days 3 to 10.

5.4.5. Discussion

The study has documented changes in B-Y sensitivity over a period of time relative to a recorded baseline value. The improvements in the group mean MS although clearly present, are on average at the lower end of the range for the normal eye in W-W perimetry which lie between 1dB and 10dB (Heijl et al 1989a; Wood et al 1987a; Searle et al 1991a, b).

For a between-visit improvement in sensitivity to be manifest, the learning effect at the subsequent follow-up examination has to be greater than the fatiguing component. An improvement in sensitivity can result from either an increase in the learning component with a constant fatigue component or from a decrease in the fatigue component with a constant learning component or from an alteration in both. The apparently small overall between-visit learning effect reported in this study could be explained on the basis that B-Y perimetry is an easier task than W-W perimetry requiring less training. Alternatively, the magnitude of the effect can be explained on the basis that B-Y perimetry is a more difficult task which may also involve a sizeable within-eye fatiguing component which would mask the magnitude of the learning component. Indeed, evidence for the difficulty of the task can be seen in the continued improvement in sensitivity at day 10 for the elderly groups. This indicates that the B-Y learning effect is still present at the fourth session of perimetry and contrasts with the time course for W-W perimetry which suggests that in the majority of cases the learning effect is completed after the first two or three examinations (Heijl et al 1989a; Wood et al 1987a; Wild et al 1989c, 1991b; Werner et al 1991; Marchini et al 1991). Furthermore, the higher sensitivity in the first eye for the three days as a whole, together with the tendency to a greater improvement in the MS of the first eye over the three day period is indicative of a fatiguing effect for the second eye and is in accord with other studies (Searle et al 1991a, b; Wild et al 1989c, 1991b; Hudson et al 1994).

The Ganzfeld or Troxler effect has been suggested as a possible mechanism for the fatigue effect in automated perimetry (Searle et al 1991b; Hudson et al 1994). Ganzfeld blankout, whereby an intermittent darkening of the visual field is perceived, occurs as a result of the suppression of eye movements and the formation of a stabilised retinal image (Hart 1987; Davson 1986). The

stimulus gradually disappears until the stimulus is moved or fixation changes. The phenomenon is considered to be of neural origin rather than due to photochemical bleaching since the disappearance occurs before a significant amount of bleaching can take place and can also be quickly reversed (Clarke and Belcher 1962; Pirenne and Marriott 1986). The Troxler effect is thought to arise from an enlargement of the receptive field size which adapts to the current visual scene (Gilbert and Wiesel 1991; Campbell and Andrews 1992). The enlargement arises from the activation of dendrites which accept a innervation from outside the image-stabilised region.

Two Ganzfeld components have been described (Gur 1991): a 'fade-out' which is a gradual loss of perceived brightness under both monocular and binocular conditions and is affected by the intensity (Gur 1989) and the wavelength (Hochberg et al 1951; Gur 1989) of the adapting field and a 'black-out or blankout' involving a brief complete loss of vision under monocular conditions, irrespective of light intensity and wavelength (Bolanowski and Doty 1987). The blankout effect occurs when there is a approximately 0.75 log units intensity difference between the two eyes (Bolanowski and Doty 1987). Gur (1991) suggests that fade-out is retinal in origin whilst blankout results from an inhibition of cortical visual processing. Fuhr et al (1990) studied the 'blankout' effects in conventional W-W perimetry. Ten subjects viewed the Humphrey Field Analyser bowl for 2 minutes. The non-tested eye was occluded with either an opaque or translucent occluder. The bowl was additionally viewed under binocular conditions. Subjects were asked to comment upon the appearance of the perimeter bowl over the testing period. No intermittent darkening or 'blankout effect' were reported when the bowl was viewed binocularly. Eight of the 10 subjects reported intermittent darkening with the opaque occluder; the darkening lasted approximately for 11 seconds and occurred about 3 times per minute. No darkening was reported for the translucent occluder. Furthermore, when conventional W-W perimetry was performed using a custom program; sensitivity with the opaque occluder was reduced by 0.7dB and variability increased by 19% (approximately 2dB) relative to the translucent occluder.

The high background luminance employed for B-Y perimetry will exacerbate the 'blankout' effect. The relative logarithmic difference in illumination between the two eyes for the 300 cdm^{-2} bowl

luminance would be 2.48 log units compared to 1.0 log unit for the standard 10cdm^{-2} W-W bowl luminance. In addition, the recently commercially available B-Y upgrade to the HFA which utilises a 440nm narrow band filter and a bowl luminance of 100 cdm^{-2} will also result in a difference of 2.0 log units between the two eyes. Therefore, it would be expected that, at the background luminance levels of 100-300cdm^{-2} currently utilized in B-Y perimetry, the blankout effect would be more pronounced than at the standard 10cdm^{-2}. Indeed, patients commented that darkened patches appeared as the test was performed and that these were alleviated by an increase in the blink rate. The Ganzfeld effect may also explain why the learning effect was relatively small, overall, and may also explain the increased SF which has been reported for B-Y perimetry compared to W-W perimetry (Nelson- Quigg et al 1991; Sample et al 1993a; Johnson et al 1993d). Therefore, it may be prudent to perform B-Y perimetry with a translucent occluder in front of the non-tested eye to reduce the blankout effects. However, the monocular effects of fade-out would still be present. The magnitude of any differences in B-Y sensitivity as a result of both blankout and fade-out effects require further study.

Since the perimeter bowl is yellow in colour, it is important to consider any differential effect of wavelength on these adaptational effects. Hochberg et al (1951) reported that red adapting fields were perceived to be achromatic in less than 3 minutes, whilst green adapting fields disappeared after 6 minutes. Cohen (1958), however, demonstrated that the majority of subjects reported desaturation for both red and green fields after only 1 minute. The differences in these studies are thought to exist due to both intensity and wavelength differences in the experimental design (Gur 1989). Gur (1989) tested wavelengths between 440nm and 620nm in 20nm intervals at each of 5 intensity levels. Subjects were required to report when the field firstly became desaturated and secondly dark. Fading times were shorter for long wavelength fields; at all wavelengths the magnitudes were linearly related to the logarithm of the field intensity. It would be expected for the yellow background (λ=550nm) employed in colour perimetry, that the background would be perceived to be achromatic in less than 1 minute, the magnitude of the fading time would depend on the background luminance. The significance of these background wavelength and intensity effects upon B-Y sensitivity requires further study.

The secondary analysis suggests that the improvement in B-Y MS was independent of eccentricity. This finding is contrary to that reported for W-W automated perimetry which suggests that the improvement in sensitivity increases with increase in eccentricity (Wood et al 1987a; Searle et al 1991a, b; Heijl et al 1989a; Wild et al 1989c). The analysis also suggests that the improvement in MS was regionally dependent being greater in the superior hemifield compared to the inferior hemifield. This finding may be associated with a progressive increase in the palpebral aperture as the patient becomes more tolerable of the high bowl luminance. However, no changes in the palpebral aperture were observed with the HFA video monitor at any time during the examination. A reduction in the palpebral aperture size has also been suggested for the greater within-test fatigue effect in the superior field (Hudson et al 1994).

The results indicate that the learning effect for B-Y perimetry was independent of experience in W-W perimetry. Conventional W-W perimetry is undertaken using stimulus size III and a background luminance of 10cdm^{-2}, whilst B-Y perimetry is undertaken with a size V blue stimulus and a high luminance background. The interaction of stimulus size and threshold luminance for the SWS pathway is not known. Aspinall (1974) suggested that improvements in performance of the 100-Hue test were as a result of an increasing familiarity with the task required. Those experienced in W-W perimetry were required to adopt new criteria for detecting the presence of B-Y stimuli. This may also explain the surprising finding that the baseline mean sensitivities of both the young and elderly experienced subjects were lower for both eyes compared to the corresponding naive groups. The reason for this unexpected finding is not totally clear. Both the experienced groups were slightly older than the naive groups by approximately 5 years but the difference in age is unlikely to account completely for the differences in the baseline sensitivity between the two groups. Indeed, the increase in ocular media absorption for short wavelengths with increase in age is 0.03-0.06 log units per decade (Pokorny et al 1987; Johnson et al 1988b) whilst the reduction in SWS sensitivity with age is 0.05-0.09 log units per decade (Johnson et al 1988b; Werner and Steele 1988; Haegestrom-Portnoy et al 1989). The difference between the absolute sensitivity of the naive and experienced groups might partially be explained by a

difference in the criterion for the detection of the two types of stimulus. The criterion for the detection of the white stimulus at threshold is based mostly upon the edge contrast between the white stimulus and white background whilst that of the blue stimulus at threshold is based more upon the chromatic content of the stimulus than upon edge detection. Indeed, the response to B-Y stimuli has been shown to be more resistant to defocus than the response to W-W stimuli (Johnson et al 1993d) and was explained in part by the poor resolution characteristics of the SWS pathway (Swanson 1991). It can reasonably be hypothesized that when first undertaking B-Y perimetry, individuals experienced in W-W perimetry may inappropriately employ the criterion for W-W detection. In contrast, individuals naive to any form of perimetry are free of contamination by the W-W criterion effect and immediately begin to learn and apply the B-Y criterion. Nevertheless, the rate of improvement in B-Y sensitivity was similar between the experienced and naive groups.

Short wavelength stimuli such as that used in B-Y perimetry are preferentially absorbed by the ocular media (Pokorny et al 1987; Sample et al 1988b, 1989, 1991a; Johnson et al 1988b, 1989b, 1993c; Savage et al 1993; Hudson and Wild 1993). This has been discussed fully in Chapter 4. The current perimetric measurement of wavelength dependent ocular media absorption is based upon the deviation of scotopic sensitivity from the absorption spectrum of rhodopsin and requires the patient to be fully dark adapted (Adams et al 1991; Johnson et al 1988b, c, 1989a, 1993a, b, d; Lewis et al 1993; Casson et al 1993b; Sample et al 1986b, 1988a, 1989, 1993a, b; Sample and Weinreb 1989, 1990, 1992; Weinreb and Sample 1991; Hudson and Wild 1993). Wavelength dependent ocular media absorption was not measured since the aim of the study was to identify any relative change in sensitivity over the 10 day period rather than to quantify the sensitivity in absolute terms. It is unlikely that ocular media absorption within a given subject would have altered over the time period of the study.

B-Y sensitivity is also attenuated within a maximum of 8° eccentricity by the macular pigment (Hudson and Wild 1993; Wild and Hudson 1995). The effects of macular pigmentation have been discussed in Chapter 4. The perimetric measurement of macular pigment absorption is also a lengthy and complex procedure. It involves measurement of the difference in sensitivity for a size

V stimulus, between the fovea and 10° eccentricity, to narrow band interference filters of 570nm and 460nm presented on a red background (Pease et al 1983, 1987; Bone et al 1985). The red background serves to adapt the LWS system and the stimulus is flickered at 25Hz to exclude detection by the rods and the blue cones. Measurement of macular pigment absorption was similarly not considered necessary since the aim of the study was to identify only the relative change in sensitivity over the 10 day period.

The magnitude of B-Y isolation is primarily governed by the combination of stimulus wavelength and background luminance and their interaction together. The magnitude of B-Y isolation in the present study is approximately 1.4 log units. The B-Y perimetric response at any given stimulus location with pre-existing glaucomatous field loss deeper than the degree of SWS isolation would no longer be controlled by the SWS pathway and would be mediated by the MWS pathway. Such patients may not benefit from examination with B-Y perimetry and these areas of the visual field might be more appropriately examined with conventional W-W perimetry. The extent of any further learning effect when conventional W-W perimetry is undertaken in those patients experienced in B-Y perimetry but undergoing W-W perimetry for the first time is difficult to predict and requires further study.

Care must therefore be exercised in the interpretation of initial B-Y visual fields since the initial fields will either simulate or exacerbate a shallow general reduction in sensitivity. This apparent reduction in sensitivity, however slight, would contaminate the early B-Y diffuse loss which has been reported to occur in primary open angle glaucoma (Johnson et al 1988c, 1989a, 1993a, b, d; Lewis et al 1993; Flanagan et al 1991a; deJong et al 1991, 1993; Heron et al 1988; Hart et al 1990; Sample et al 1986b, 1988b; 1993b, c, d, 1994; Sample and Weinreb 1989, 1990, 1992; Weinreb and Sample 1991; Casson et al 1993b) and would also underestimate the depth of any focal loss.

CHAPTER 6: THE DETECTION OF BLUE-YELLOW GLAUCOMATOUS VISUAL FIELD LOSS

6.1. Colour vision and glaucoma

6.1.1. Central colour vision tests

Colour vision abnormalities in glaucoma is well documented (Fishman et al 1974; Lakowski and Drance 1978; Drance 1981; Adams and Rodic 1982; Adams et al 1982; Adams 1982; Motolko et al 1982b; Drance and Lakowski 1983; Airaksinen et al 1986; Flammer and Drance 1984; Drance et al 1987a; Lachenmayr et al 1991a; Lachenmayr and Drance 1992b). The colour deficit appears to be mainly of the Blue-Yellow type; however, Red-Green loss has also been reported (Verriest 1963). A blue-yellow, or tritan, loss of central colour vision has also been reported in OHT patients prior to the development of conventional W-W visual field loss (Lakowski and Drance 1978; Drance et al 1987a; Drance and Lakowski 1983; Motolko et al 1982b).

The ability of the D-15 test and the 100-Hue test to detect early glaucomatous visual field loss is equivocal (Poinoosawmy et al 1980; Adams and Rodic 1982; Adams et al 1982; Flammer and Drance 1984; Drance et al 1987a, c; Lakowski and Drance 1978; Trick et al 1988; Lachenmayr and Drance 1992b; deJong et al 1993). Flammer and Drance (1984) measured colour vision with the 100-Hue test and the visual field with the Octopus automated perimeter in a sample of 25 OHTs and 10 glaucoma patients. Colour vision disturbances correlated with a reduction in the global MS. Poinoosawmy et al (1980) also found a correlation between colour vision deficiency and visual field loss. Furthermore, Trick et al (1988) demonstrated colour vision defects in 23% of 130 OHTs examined with the D-15 test; however, only 11.5% of the 130 patients exhibited Pattern Electroretinogram (PERG) defects. Conversely, Drance et al (1987c) reported a greater sensitivity in the detection of glaucomatous field loss with the PERG than with the 100-Hue test. Breton and Krupin (1987), however, failed to find a significant correlation between the 100-Hue error score and the severity of visual field loss when the colour vision results were corrected for age. Furthermore, the poor correlation between the results of the 100-Hue test and the integrity of the retinal nerve fibre layer further suggests a lack of sensitivity for the 100-Hue test in the

detection of glaucoma (Airaksinen et al 1986; Lachenmayr et al 1991a). Indeed, Hamill et al (1984) found no clear association between early glaucomatous optic disc cupping and colour vision scores.

Unfortunately, these simple central colour vision tests have three major disadvantages: the stimuli are foveally presented and peripheral retinal locations are therefore not assessed; the tests are designed to assess congenital colour vision defects; and the influence of age, ocular media absorption and pupil size on these tests remain unknown (Adams et al 1982; Sample 1986a, 1988a; Weinreb and Sample 1991).

Laboratory based increment-threshold spectral sensitivity (ITSS) functions (whereby sensitivity to a variety of narrowband spectral stimuli is measured against either white or chromatic adapting fields) and threshold versus intensity (TVI) curves (whereby the increment threshold is measured at various intensities of adapting field for a given set of stimulus parameters) have demonstrated a preferential reduction in the short-wavelength region of the spectrum in glaucoma and in OHT (Lakowski et al 1976;Verriest and Uvijls 1977; Steinschneider et al 1984; Adams et al 1982; Adams 1982; Adams et al 1987a, b; Alvarez and Mills 1985; Sucs and Verriest 1989; Greenstein et al 1989; Lachenmayr and Drance 1992b; Kalloniatis et al 1993; Kalloniatis and Harwerth 1993). The chromatic adaptation techniques employ a background of a particular wavelength and luminance which isolates a single cone mechanism (Wald 1964). In addition to the psychophysical measurement of short wavelength deficiencies, a loss of blue spectral sensitivity has been demonstrated in both OHT and glaucoma using electrophysiologcal investigation (Bielik et al 1991; Korth et al 1993, 1994).

6.1.2. Manual colour perimetry

Manual colour perimetry permits the examination of chromatic function in the peripheral visual field. Studies using manual colour perimetry to selectively examine the cone mechanisms, have demonstrated the potential for examination of the peripheral field in a quantitative manner (Greve et al 1974; Heidin and Verriest 1981; King-Smith et al 1984; Lakowski et al 1977; Dunn and

Lakowski 1981; Maione et al 1976; Marre and Marre 1978; Genio and Friedmann 1981; Zwas et al 1982, Zwas and Shin 1987; Sucs and Verriest 1988; Hugkulstone and Vernon 1992).

Selective defects to blue stimuli have been reported in early glaucoma (Marré and Marré 1978; Zwas et al 1982; Zwas and Shin 1987; Sucs and Verriest 1988; Heron et al 1988; Yamazaki et al 1989). Marré and Marré (1978) using a modified Goldmann perimeter, demonstrated glaucomatous visual field defects by colour perimetry which were not evident by conventional perimetry. Furthermore, in established visual field defects the loss was more extensive with the chromatic stimulus than that recorded with conventional white stimuli. Use of a blue filter in conjunction with the Friedmann Visual Field Analyser has identified early loss in OHT prior to the development of W-W visual field loss (Hugkulstone and Vernon 1992) and an increase in the size and depth of focal loss (Genio and Friedmann 1981). The degree of blue cone (SWS) isolation using a blue stimulus without an adapting background, however, remains unknown. Furthermore, the effects of between-subject differences in ocular media absorption upon the blue stimulus were not adressed in these studies. Using a purpose built projection system, Heron et al (1988) compared increment thresholds for blue stimuli presented on a high luminance yellow background and yellow stimuli presented on the same yellow background out to 15° eccentricity in a sample of OHTs and POAG patients. A diffuse reduction in B-Y sensitivity was found in both the OHT and POAG groups compared to an age-matched normal sample. Furthermore, 6 of the 31 OHTs also had localised defects in B-Y sensitivity compared with normal Y-Y sensitivity. Using a Goldmann perimeter, Yamazaki et al (1989) compared the spectral and achromatic sensitivities in POAG and NTG patients. A greater loss of blue sensitivity was found in the POAG group compared to the NTG group. It was suggested that different mechanisms of damage might result in different types of field loss in glaucoma. Unfortunately, no correction was again made for the reduction in B-Y sensitivity resulting from lenticular absorption in any of these studies of B-Y sensitivity.

Other studies have been unable to demonstrate any significant advantage of manual colour perimetry over conventional manual W-W perimetry in the evaluation of glaucomatous field loss

(Logan and Anderson 1983; Drum et al 1989). Indeed, Drum et al (1989) highlighted the distinction between attenuation arising from preretinal absorption and that from neural damage.

6.1.3. Automated colour perimetry

Colour contrast perimetry has been studied by Hart et al 1984; Hart and Gordon 1984; Hart 1989; and Hart et al 1991. Coloured stimuli of varying saturation were presented on an equiluminous white adapting background; detection of the coloured stimuli was based upon the difference in colour contrast rather than upon the difference in luminance contrast (King-Smith et al 1983). Hart and co-workers considered that colour contrast perimetry with either kinetic or static methods of stimulus presentation offered no useful diagnostic advantage in established cases of glaucoma (Hart et al 1984; Hart and Gordon 1984; Hart 1989; Hart et al 1991). However, Vingrys et al (1988) demonstrated a chromatic loss of sensitivity in two selected patients using equiluminous red and blue static stimuli which occurred in advance of any loss of achromatic sensitivity.

Presentation of perimetric stimuli using high resolution display monitors has been criticised because of the inability to directly compare results to those recorded using standard W-W automated perimetry (Vingrys et al 1990). However, the modification of a conventional Humphrey Field Analyser to perform B-Y perimetry has allowed direct comparison of the B-Y visual field with the conventional W-W field (Sample et al 1986b, 1988a; Sample and Weinreb 1989; Johnson et al 1988b, c, 1989a; Hart et al 1990). Furthermore, automated B-Y perimetry also allows a large number of stimulus locations to be evaluated within a single examination using standard perimetric strategies (Johnson et al 1989a). Sample and Weinreb (1990) performed B-Y perimetry in ten normal subjects, fourteen OHTs and sixteen POAG patients. The B-Y results were corrected for lenticular absorption using the perimetric technique of Sample et al (1988b, 1989). Surprisingly, losses in B-Y sensitivity were apparent in 43% of the OHT patients despite demonstrating normal W-W visual fields; furthermore 81% of the POAG group demonstrated more extensive B-Y loss ie greater area and / or depth of defect when compared to the W-W field. Similar qualitative findings were reported by Johnson et al (1989a); however, only 7% of the OHT group and 15% of the POAG group demonstrated a greater B-Y field loss.

The need to establish specific isolation of the SWS pathway before B-Y perimetry can be evaluated was stressed by Weinreb and Sample (1991) who also considered a coloured adapting background was required to isolate the SWS pathway. However, Harwerth et al (1993) demonstrated isolation of the SWS mechanisms using a $10cdm^{-2}$ white background and a size V narrowband blue stimulus. Interestingly, Friedmann (1991) considered that the inability by Hart et al (1984, 1989, 1991) to differentiate differences in chromatic and achromatic sensitivity loss was attributable to the kinetic stimuli employed which fail to selectively stimulate the SWS pathway. The SWS cones are thought to provide little contribution in the detection of movement by the visual system (Lee and Stromeyer 1989).

6.1.4. Patterns of Glaucomatous visual field loss

Drance (1992); Flammer (1985) and Spaeth (1994) have outlined two distinct types of glaucomatous damage: diffuse damage and focal damage. Diffuse and focal defects have been observed in the nerve fibre layer (Hoyt et al 1972, 1973; Sommer et al 1977;1991 Quigley et al 1980, 1993; Airaksinen et al 1981, 1983, 1984, 1985c; Hitchings et al 1987; Caprioli 1989, 1990; Chihara and Honda 1992; Tuulonen et al 1993; Jonas and Schiro 1994) and across the optic nerve head (Airaksinen et al 1984; Quigley et al 1979, 1982, 1987; Radius 1987; Dandona et al 1991). In addition, different mechanisms of glaucomatous damage have been suggested which may account for diffuse and focal damage (Flammer 1985; Drance 1981, 1985b, 1992; Levene 1980; Quigley 1987a, 1993; Radius 1987; Fechtner and Weinreb 1994). The mechanisms may be either independent of, or related to, each other.

The concept of diffuse and focal changes is also applicable to functional change, particularly visual field loss. Diffuse loss is characterised by a generalised depression in sensitivity across the entire field (Aulhorn and Harms 1967; Armaly 1972; Anctil and Anderson 1984; Drance 1985a; Flammer 1984, 1985; Feur and Anderson 1989) which may occur independently of, or be associated with, localised defects (Lachenmayr et al 1991c; Zeiter et al 1992; Samuelson and Spaeth 1993). Glaucomatous field loss defined by conventional W-W perimetry is thought to be

more localised in NTG (Hitchings and Anderton 1983; Caprioli and Spaeth 1984; Caprioli et al 1987b; Flammer et al 1985; Funkhouser 1991; Zeiter et al 1992; Araie et al 1993; Samuelson and Spaeth 1993) and more diffuse in high tension glaucoma (Flammer 1984; Anctil and Anderson 1984; Feur and Anderson 1989; Glowazki and Flammer 1987; Drance et al 1987b; Chauhan et al 1989a; Lachenmayr et al 1991a; Lachenmayr and Drance 1992a, b). Visual field defects in NTG may be of sudden onset (Levene 1980), closer to fixation (Levene 1980; Hitchings and Anderton 1983; Caprioli and Spaeth 1984) and of greater depth (Levene 1980; Hitchings and Anderton 1983; Caprioli and Spaeth 1984). Other reports have failed to identify any differences in field loss between the two types of glaucoma (Motolko et al 1982a; Lewis et al 1983; Phelps et al 1983; King et al 1986a). Differences in the findings between studies have been attributed to differences in patient selection for each study, the depth of scotomata and in the chosen method of data comparison (Phelps et al 1984; Caprioli et al 1986a). Although, diffuse visual field loss may represent an early stage in the course of the glaucomatous process it is considered to lack the diagnostic specificity achieved when focal defects are present (Hart et al 1990).

The visual field indices have also been compared to structural measurements of the retinal nerve fibre layer and of the optic nerve head. Airaksinen et al (1985a, b, c) demonstrated a moderate correlation between the W-W visual field indices MD and CPSD and the retinal nerve fibre layer loss. Identification of diffuse loss using the Bebié curve also shows good agreement with the nerve fibre layer loss (Lachenmayr et al 1992a). The relationship between the visual field and characteristics of the optic nerve head will be discussed fully in Chapter 8.

Other reports have questioned the extent to which diffuse loss is a component of glaucomatous damage since it resembles the non-specific finding caused by media opacities (Werner et al 1982; Heijl 1989, 1991; Langerhorst et al 1989b; Asman and Heijl 1994) (see Chapter 4). Furthermore, studies demonstrating the presence of diffuse loss in glaucoma have been criticised because of their approach to the statistical interpretation of the visual field (Asman and Heijl 1994).

Diffuse and focal types of field loss have also been reported in the preliminary studies of B-Y perimetry (Heron et al 1988; Sample and Weinreb 1989, 1990; Johnson et al 1988c, 1989a; Hart et al 1990). Interestingly, Hart and co-workers (1990) suggested that a diffuse loss of B-Y sensitivity occurs across the entire central field prior to the development of W-W field loss and focal B-Y loss occurred simultaneously with the development of W-W field loss. The statistical analysis of previously reported B-Y visual field loss has not been as robust as that for W-W loss. B-Y abnormality has been defined globally in terms of the mean deviation (Heron et al 1988; Adams et al 1991; Flanagan et al 1991a; Hart et al 1990; Johnson et al 1988c, 1989a, 1993a, b, d; deJong et al 1990, 1993; Lewis et al 1993; Sample et al 1986b, 1988a, 1993b, c, d, 1994; Sample and Weinreb 1989, 1990, 1992; Weinreb and Sample 1991); on a pointwise basis in terms of a constant defect depth, regardless of any differences in the normal variability across the visual field (Sample et al 1986b, 1988a, 1993b, c, d, 1994; Sample and Weinreb 1989, 1990, 1992; Weinreb and Sample 1991); and with respect to the 95% and 99% confidence limits for normality based upon the overall height of the hill of vision (Adams et al 1991; Johnson et al 1988c, 1989a, 1993a, b, d; Casson et al 1993b). No attempt has been made to separate the localised B-Y loss from the generalised component of sensitivity by adjusting for the height of the B-Y hill of vision in a manner similar to that of the W-W pattern probability plots. As such the true nature of the focal loss has not been identified.

6.2 B-Y Perimetry in the detection of glaucomatous visual field loss

6.2.1. Aim of the study

Prior to the undertaking of this study in 1991, preliminary evaluation of B-Y perimetry for the detection of glaucomatous visual field loss had originated from only two research centres (Sample et al 1986b, 1988a; Sample and Weinreb 1989, 1990; Johnson et al 1988c, 1989a) The major aim of the study was to independently corroborate the findings of these studies and to further develop the clinical technique of B-Y perimetry in the detection of glaucomatous field loss. During the collection of data for this study, further reports investigating B-Y perimetry were published and are thus referred to in context with the findings from this study.

The study was subdivided into four parts: Firstly, to determine the magnitude of the between-subject normal variability of B-Y perimetry with respect to eccentricity and to age and to compare the findings with those for W-W perimetry. Secondly, to evaluate the sensitivity and specificity of B-Y perimetry in the detection of glaucomatous field loss using the total and pattern deviation probability analyses. Thirdly, to investigate the use of B-Y perimetry for the examination of those areas within the glaucomatous visual field exhibiting normal sensitivity to W-W perimetry. Fourthly, to apply the statistical procedures to a sample of OHTs.

6.2.2 Materials and methods

Sample

The study comprised four separate samples: a normal age-matched control group, a separate sample of normals, a POAG sample and an OHT sample.

Normal age-matched control group

The normal control group comprised 50 age-matched normal subjects randomly recruited from local old aged pensioner associations and stratified by age over two decades. Twenty-five subjects were aged between 60-69 years (mean age 64.9 years SD 4.0) and 25 subjects were aged between 70-82 years (mean age 75.1 years SD 4.0). Inclusion criteria comprised an IOP of

less than 21mmHg, normal optic nerve head appearance, normal HFA W-W Program 24-2 field, refractive error in the examined eye of less than ± 5 dioptres sphere and less than 3 dioptres cylinder, visual acuity of better than 6/9, minimal lenticular changes not greater than NI, CII or PI by LOCS II (Chylack et al 1989), no history of a congenital colour vision defect, no systemic medication known to influence the visual field, no ocular surgery or trauma, no history of diabetes mellitus and a negative family history of glaucoma or diabetes mellitus. One eye, only, of each age-matched normal subject was selected for the study.

Normal Group

The additional normal sample comprised 20 subjects, aged between 60-78 years with identical inclusion criteria to that of the normal age-matched control group (mean age 66.5 years SD 5.8) together with an additional 7 subjects with NIII, PIII, CIII cataract or worse as classified by LOCS II (Chylack et al 1989). The 20 subjects were known to exhibit normal W-W visual fields by both total and pattern deviation plots. The visual acuities in the cataract group ranged from 6/12 to 6/36. Subjects with clinically significant cataract were deliberately included in the sample to test the efficacy of the subsequent B-Y total and pattern deviation analysis. All 7 cataract patients exhibited an abnormal B-Y total deviation plot but a normal pattern deviation plot. One eye of each normal subject was selected at random for examination unless there was a marked difference in the severity of the cataract between the two eyes in which case the eye with the more advanced cataract was selected.

POAG group

The POAG sample comprised 24 patients aged between 60-83 years and consecutively recruited from the Glaucoma Department of the Birmingham and Midland Eye Hospital (mean age 69.2 years SD 8.7). Patients with POAG were treated with topical ß-blockers only, and exhibited characteristic optic nerve head abnormalities, a presenting IOP of greater than 22 mmHg and characteristic W-W field loss. The sample was deliberately structured to include the widest range of glaucomatous visual field loss. The mean IOP on presentation to the hospital was 27.78 mmHg (SD 4.0).

OHT group

The OHT sample comprised 27 patients, aged between 60-82 years, also consecutively recruited from the Glaucoma Department of the Birmingham and Midland Eye Hospital (mean age 68.2 years (SD 6.4)). Ocular hypertension was defined as a pressure greater than 22mmHg and normal W-W fields. The OHTs were classified into risk categories originally defined by Hart et al (1978). Of the 27 OHT's, 9 were classified as low risk (IOP of <28mmHg and vertical C/D ratio <0.6) and 14 as medium risk (IOP of <28mmHg and vertical C/D ratio <0.6 with a positive family history of POAG; or IOP >28mmHg and/or C/D >0.6 but not both and a positive family history of POAG). The remaining 4 OHTs were classified as high risk (IOP≥28mmHg and C/D ≥0.6) and were receiving topical ß-blockers. The mean IOP on presentation to the Hospital was 24.7 mmHg (SD 2.9).

The field characteristics at the start of data collection of the patient sample in terms of the W-W visual field indices mean deviation and corrected pattern standard deviation are displayed in Figure 6.1. All the OHT and POAG patients conformed to identical inclusion criteria as the age-matched normal control group with the exception of the criteria for IOP, optic nerve head appearance, visual field and family history of glaucoma. One eye, only, of each patient was examined. For the POAG group the eye with the least field loss was selected whilst for the OHT group, the eye with the highest IOP was examined.

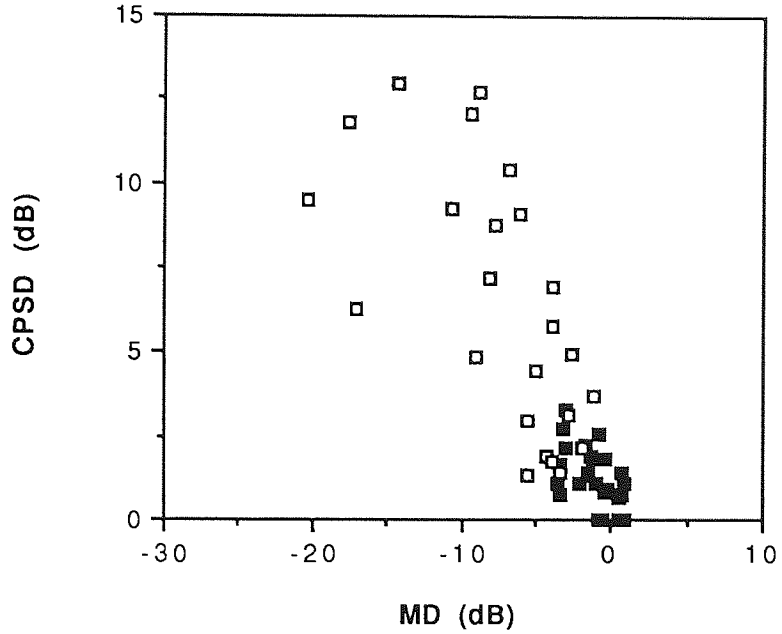

Figure 6.1 The corrected pattern standard deviation (CPSD) plotted against the mean deviation for the Humphrey Field Analyser Program 24-2 (stimulus size III), illustrating the type of W-W field loss exhibited by the patient sample. Closed symbols represent the OHT group and open symbols the POAG group.

Perimetry

Perimetry was performed using Program 24-2 of the modified Humphrey Field Analyser 640 (Hudson et al 1993). The modifications and the associated calibrations necessary for B-Y perimetry have been described in Section 4.10.1. Each subject and patient attended for three separate perimetric examinations performed at the Department of Vision Sciences, Aston University. The first visit comprised a training session involving standard W-W perimetry (Goldmann size III; background luminance 10 cdm^{-2}) and B-Y perimetry (Goldmann size V; background luminance 330 cdm^{-2}). The first session was to minimise the learning effects present in both W-W and B-Y perimetry (Chapter 5) and the results were discarded. The same perimetric protocol was utilised at the second visit. The order of perimetric test within a session was randomised between patients in order to minimise order effects. A size III white stimulus was chosen since it is the clinical standard. A size V blue stimulus was used for compatibility with other preliminary B-Y studies (Heron et al 1988; Hart et al 1990; Sample et al 1986b, 1988a; Sample and Weinreb 1990; Johnson et al 1988b, c, 1989a).

Appropriate refractive correction was used for the viewing distance of the perimeter bowl. Fixation losses were less than 20% and false-negative and false-positive responses less than 33% for all subjects. The efficiency of fixation was constantly monitored with the video monitor of the HFA. Extensive rest periods were given both within- and between-tests to minimise fatigue effects (Searle et al 1991a, b; Hudson et al 1994; Wild et al 1989c, 1991b; Johnson et al 1988a; Heijl and Drance 1983) and no single visit lasted more than 60 minutes in total.

Ocular media characteristics and forward light scatter

At the third visit, measurements were undertaken of ocular media absorption and forward light scatter on all subjects and patients. Both techniques have been described in Section 4.10.1. When field loss was present at 15° eccentricity in a given quadrant for a specific patient the thresholds at that location were not included in the calculation of the grand mean for lenticular absorption.

6.2.3. Analysis

The perimetric sensitivities for the W-W and B-Y stimuli were each calculated in log units relative to the maximum stimulus intensity of the given stimulus (see Section 4.10.1). Left eye data was converted to right eye data where necessary. The B-Y sensitivity at each stimulus location for each age-matched normal subject was corrected for the individual measure of ocular media absorption. Similarly, the B-Y sensitivity at each stimulus location for each subject in the second normal sample and for each POAG or OHT patient was individually corrected for ocular media absorption. Stimulus locations at which the B-Y threshold exceeded the maximum available stimulus intensity (ie 0.0 log units) were not corrected for absorption.

The group mean and standard deviation of the sensitivities at each of the 52 stimulus locations of Program 24-2 for each age group of the normal age-matched control group were separately calculated for both the W-W and B-Y stimulus combinations. The two stimulus locations above and below the blind spot were omitted from the analysis. The distributions of W-W and B-Y

sensitivities at each stimulus location were tested for normality using a one-tailed Kolmogorov-Smirnov test. The Kolmogorov-Smirnov test is used to test the deviations of an observed frequency distribution from an expected normal distribution. A critical value, defined as the absolute value of the largest difference between the observed and expected frequency distributions, is calculated. A probability is assigned to the magnitude of the critical value using standard mathematical tables. The distributions of normal sensitivities at each of the 52 stimulus locations exhibited a Gaussian distribution for both the W-W and B-Y stimulus combinations. Pointwise deviations from the normal sensitivity for each age group corresponding to 95%, 98% and 99% probabilities were then calculated for both the W-W and B-Y fields. The calculation of normal probability limits was based upon the group mean sensitivity and respective standard deviation at each stimulus location in each age group for each stimulus combination. For a given probability level a value, z, can be obtained from standard statistical tables; where z can be defined as:

$$z = (y - \mu) / \sigma$$

where μ and σ are the mean and standard deviation, respectively, of the particular variable and y is the unknown variable lying within the normal distribution.

Thus to calculate a value of sensitivity, y, with a known probability level within a given normal distribution eg p=0.05, p=0.01 and p=0.005, the formula above can be applied:

$$z = \left\{ y - \mu / \sigma \right\} \text{ (i)}$$

where y is the unknown pointwise sensitivity found in 95%, 99% and 99.5% of the normal population, μ is the group mean sensitivity for a given stimulus location, i, and σ is the standard deviation of the group mean sensitivity at location i.

Furthermore, $y - \mu = D$ where D is the pointwise local deviation in sensitivity compared to the age-matched normal value.

$$z = \{ D / \sigma \} \quad (i)$$

By manipulation $D = z \times \sigma$

Pointwise deviations (D) from the normal sensitivity at each stimulus location for each age group corresponding to p=0.05, p=0.01 and p=0.005 probabilities for a normal population are then calculated from known values of z and σ.

The W-W and B-Y fields of each subject and patient were then compared to the respective age-matched normal groups. The unweighted global indices mean deviation (MD), short-term fluctuation (SF) and corrected pattern standard deviation (CPSD) were calculated for each stimulus combination using the formulae of Heijl et al (1987c). Total and pattern probability maps were produced for each W-W and B-Y field of each patient. The height of the field was calculated in an identical manner to that of Heijl et al (1987c, 1989c) by ranking the magnitude of the deviation from the normal value of sensitivity at each stimulus location and then subtracting the seventh highest ranked deviation from each of the 52 deviations. The corresponding W-W indices and probability maps derived from the W-W STATPAC printout were also utilised to compare the sensitivity and specificity of the normal age-matched control W-W data base.

The resulting indices and probability plots derived for the W-W and B-Y fields of both the normal group and the patient group were then evaluated. The visual field was considered abnormal if a cluster of three or more stimulus locations exhibited a defect depth of <5% (ie p<0.05) on the pattern probability plot. It was then further evaluated with respect to the total deviation plot and as to whether the abnormality was typical of that in glaucoma.

6.2.4. Follow-up

The study of the patient group was prospective in nature. The mean duration of follow-up was 11 months (range from 4 to 14 months) and the mean number of examinations per patient was 2.3. The rationale for the frequency of follow-up was governed by a number of factors including an increase in IOP, the risk category of the given OHT patient, a discrepant field, and an apparently progressing W-W or B-Y field or both.

6.2.5 Results

The group mean ocular media absorption for the normal age-matched controls was 0.98 log units (SD 0.12) and 1.13 log units (SD 0.10) for the 60-69 and 70-82 year old age groups respectively. Repeated measures ANCOVA with sample type as a between-subjects factor and age as a covariate showed that lenticular absorption increased with increase in age ($p<0.001$) but that the magnitude of the absorption was similar across all sample types ($p=0.40$) (Table 6.1).

Variable	dF	Sums of Squares	Mean Square	F value	P value
Age	1	0.554	0.554	43.988	$p<0.001$
Sample Type	1	0.040	0.040	0.854	$p=0.395$
Age x Sample Type	1	0.011	0.011	0.879	$p=0.351$
Error	96	1.208	0.013		

Table 6.1. Summary table for the repeated measures analysis of covariance for the ocular media absorption.

The group mean straylight parameter for the normal age-matched controls was 1.07 log units (SD 0.22) and 1.46 log units (SD 0.32) for the 60-69 and 70-82 year old age groups respectively. Repeated measures ANCOVA with sample type as a between-subjects factor and age as a covariate showed that straylight increased with increase in age ($p<0.001$), irrespective of the sample type ($p=0.150$) and that the magnitude of the straylight was similar across all sample types ($p=0.10$) (Table 6.2).

Variable	dF	Sums of Squares	Mean Square	F value	P value
Age	1	1.164	1.164	19.949	p<0.001
Sample Type	1	0.241	0.241	4.017	p=0.104
Age x Sample Type	1	0.201	0.201	3.350	p=0.150
Error	96	5.770	0.060		

Table 6.2. Summary table for the repeated measures analysis of covariance for the log (straylight parameter).

The group mean MS and SF of the normal age-matched control group for each of the two stimulus combinations as a function of the two age groups is given in Table 6.3. A repeated measures ANCOVA with stimulus combination as a within-subjects factor and age as a covariate showed that, overall, the B-Y SF was larger than the W-W SF (p=0.002) regardless of patient age (p=0.96) (Table 6.4).

Stimulus / Background combination	60-69 yrs age group		70-82 yrs age group	
	MS	SF	MS	SF
W-W	2.71 (0.22)	0.13 (0.04)	2.61 (0.27)	0.15 (0.03)
B-Y	1.91 (0.27)	0.17 (0.05)	1.87 (0.37)	0.17 (0.05)

Table 6.3. Group mean mean sensitivity (MS) and short-term fluctuation (SF) for the two stimulus combinations for each of the two age groups of normal age-matched control groups. Values are expressed in log units. One log unit is equivalent to 10dB. One standard deviation is given in parenthesis.

Variable	dF	Sums of Squares	Mean Square	F value	P value
Age	1	0.000	0.000	0.003	p=0.959
Error	48	0.129	0.003		
Stimulus combination	1	0.023	0.023	10.586	p=0.002
Age x Stimulus combination	1	0.001	0.001	0.601	p=0.442
Error	48	0.102	0.002		

Table 6.4. Summary table for the repeated measures analysis of covariance for the normal short-term fluctuation.

The standard deviation of the group mean sensitivity at each stimulus location (demonstrating the within-test between-subject variability) of the normal age-matched control group for each of the two stimulus combinations as a function of the two age groups is given in Figure 6.2 and Figure 6.3. A repeated measures ANOVA with age as a between-subjects factor and eccentricity and stimulus combination as within-subjects factors showed that, overall, the variability increased with increase in age ($p=0.002$) and with increase in eccentricity ($p<0.001$) for both stimulus combinations (Table 6.5). The variability was greater for the B-Y stimulus combination compared to the W-W ($p<0.001$) particularly across the visual field ($p<0.001$) and with increase in age ($p=0.032$). There was no difference in the magnitude of the variability between the B-Y data corrected for absorption and that not corrected for absorption ($p=0.24$) (Figure 6.4).

60-69 Years

		0.55	0.57	0.49	0.45		
	0.42	0.34	0.31	0.27	0.29	0.40	
	0.36	0.27	0.22	0.31	0.32	0.37	0.34	0.31
0.38	0.28	0.19	0.21	0.21	0.21	0.25		0.34
0.50	0.42	0.19	0.22	0.17	0.17	0.21		0.27
	0.36	0.25	0.20	0.18	0.19	0.18	0.21	0.24
		0.30	0.26	0.31	0.23	0.19	0.25	
			0.29	0.30	0.29	0.32		

70-82 Years

		0.67	0.74	0.65	0.91		
	0.38	0.41	0.46	0.48	0.67	0.61	
	0.34	0.31	0.32	0.28	0.31	0.27	0.42	0.51
0.44	0.26	0.27	0.26	0.27	0.24	0.35		0.43
0.31	0.27	0.22	0.14	0.22	0.24	0.23		0.31
	0.27	0.23	0.16	0.16	0.18	0.21	0.34	0.32
		0.29	0.31	0.16	0.28	0.21	0.25	
			0.28	0.30	0.32	0.43		

W-W PERIMETRY

Figure 6.2. The standard deviation of the group mean W-W sensitivity of the normal age-matched control group at each stimulus location for program 24-2 of the Humphrey Field Analyser. Top 60-69 years; bottom 70-82 years. The values are in log units.

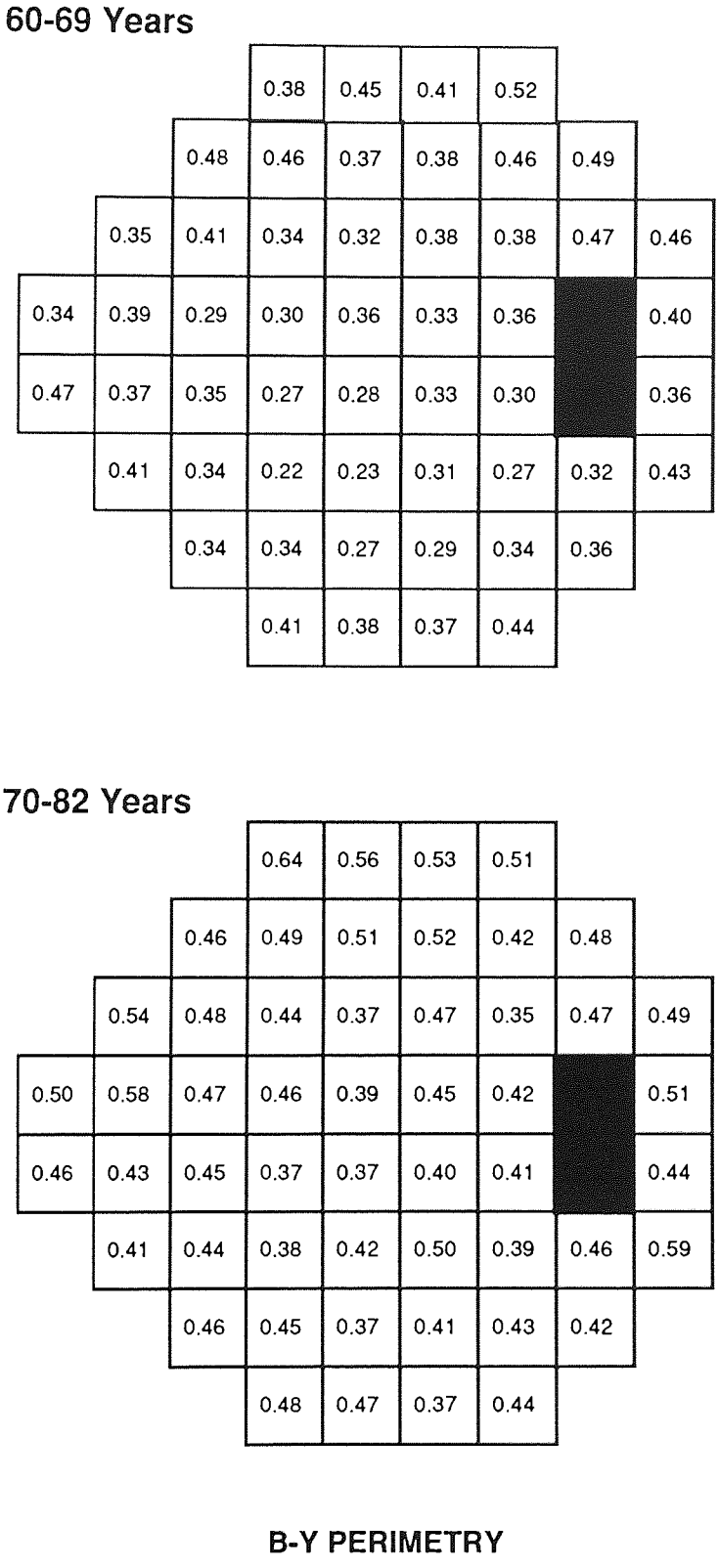

Figure 6.3. The standard deviation of the group mean B-Y sensitivity, corrected for individual ocular media absorption, of the normal age-matched control group at each stimulus location for program 24-2 of the Humphrey Field Analsyer. Top 60-69 years; bottom 70-82 years. The values are in log units.

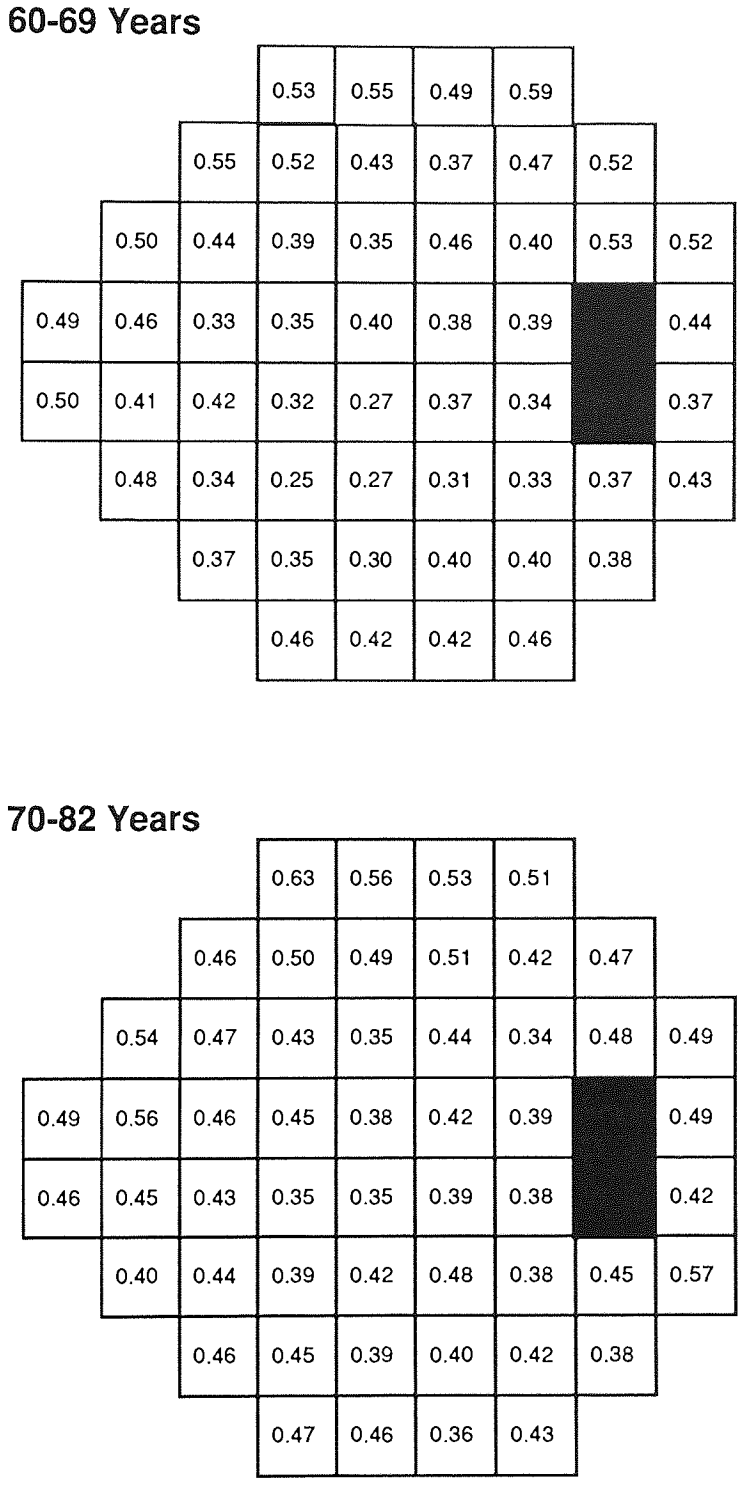

Figure 6.4. The standard deviation of the group mean B-Y sensitivity, uncorrected for individual ocular media absorption, of the normal age-matched control group at each stimulus location for program 24-2 of the Humphrey Field Analsyer. Top 60-69 years; bottom 70-82 years. The values are in log units.

Twenty-five of the 27 normal subjects exhibited a normal B-Y field. The remaining two subjects each exhibited one cluster of three abnormal pattern deviation points at the 5% level: one cluster corresponded to an upper lid artefact whilst the second was situated in the arcuate area. All 7 cataract patients exhibited abnormalities of the B-Y total deviation plot but normal B-Y pattern deviation plots. Three cases of cataract are illustrated in Figures 6.5 - 6.7. All 24 POAG patients manifested abnormal B-Y fields.

The level of agreement in terms of the severity of the field loss between the B-Y and W-W stimulus combinations for the POAG group, based upon the probability plots alone, is summarised in Figure 6.8. Of the 24 patients, 12 had a similar level of field loss for the B-Y compared to each of the two W-W methods of analysis. Six patients, however, exhibited wider B-Y focal loss; an example of such loss is illustrated in Figure 6.9. A further 5 patients demonstrated a substantially greater B-Y diffuse loss on the total deviation plot but exhibited similar W-W and B-Y pattern probability plots; an example of such loss is illustrated in Figure 6.10. The nature of the loss is also displayed in the form of Bebié curves for both the W-W and B-Y fields (Figure 6.10). No patients exhibited new scotomata. One patient consistently exhibited a different B-Y field to that of the corresponding W-W field (Figure 6.11).

The degree of agreement in the number of abnormal fields between the B-Y and W-W stimulus combinations for the OHT group is summarised in Figure 6.12. Of the 27 OHTs, 20 exhibited a normal B-Y field at the first examination together with normal W-W fields evaluated with respect to both the normal control group and to the STATPAC analysis. Two patients were borderline on B-Y and W-W analyses, the loss however was not consistent with that of a glaucomatous field defect. Five individuals, all at medium risk, exhibited a repeatable abnormal B-Y focal defect at the outset and normal W-W fields with respect to both the normal control group and to the STATPAC analysis although in one of these cases, the W-W field relative to that of the normal age-matched control group was borderline. Subsequent follow-up of these 5 patients revealed a confirmed W-W focal loss in 2 cases (Figures 6.13 and 6.14). No patients had evidence of a diffuse type of loss.

Source	dF	Sums of Squares	Mean Square	F value	P value
Age	1	0.166	0.166	11.848	p=0.002
Error	22	0.308	0.014		
Stimulus combination	2	0.140	0.070	9.872	p<0.001
Age x Stimulus combination	2	0.028	0.014	1.999	p=0.148
Error	44	0.311	0.007		
Eccentricity	2	0.667	0.334	58.331	p<0.001
Age x Eccentricity	2	0.009	0.004	0.771	p=0.469
Error	44	0.252	0.006		
Stimulus combination x eccentricity	4	0.069	0.017	6.485	p<0.001
Age x Stimulus comb x eccentricity	4	0.029	0.007	2.771	p=0.032
Error	88	0.233	0.003		

Table 6.5. Repeated measures analysis of covariance for the pointwise Standard Deviation.

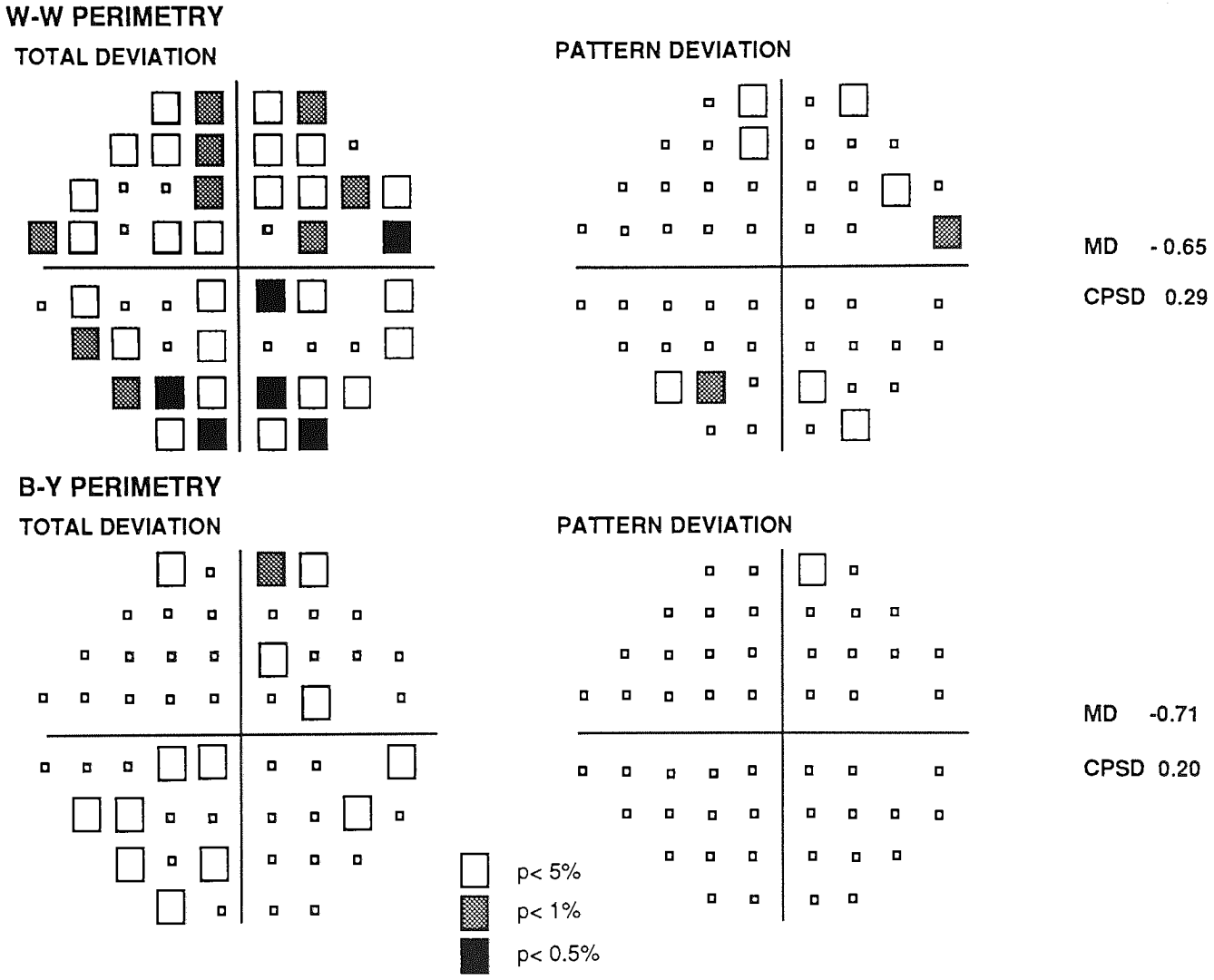

Figure 6.5 Total and pattern deviation plots for W-W (top) and B-Y (bottom) illustrating a patient with anterior cortical cataract (LOCS grade CIV). Indices are represented are in log units.

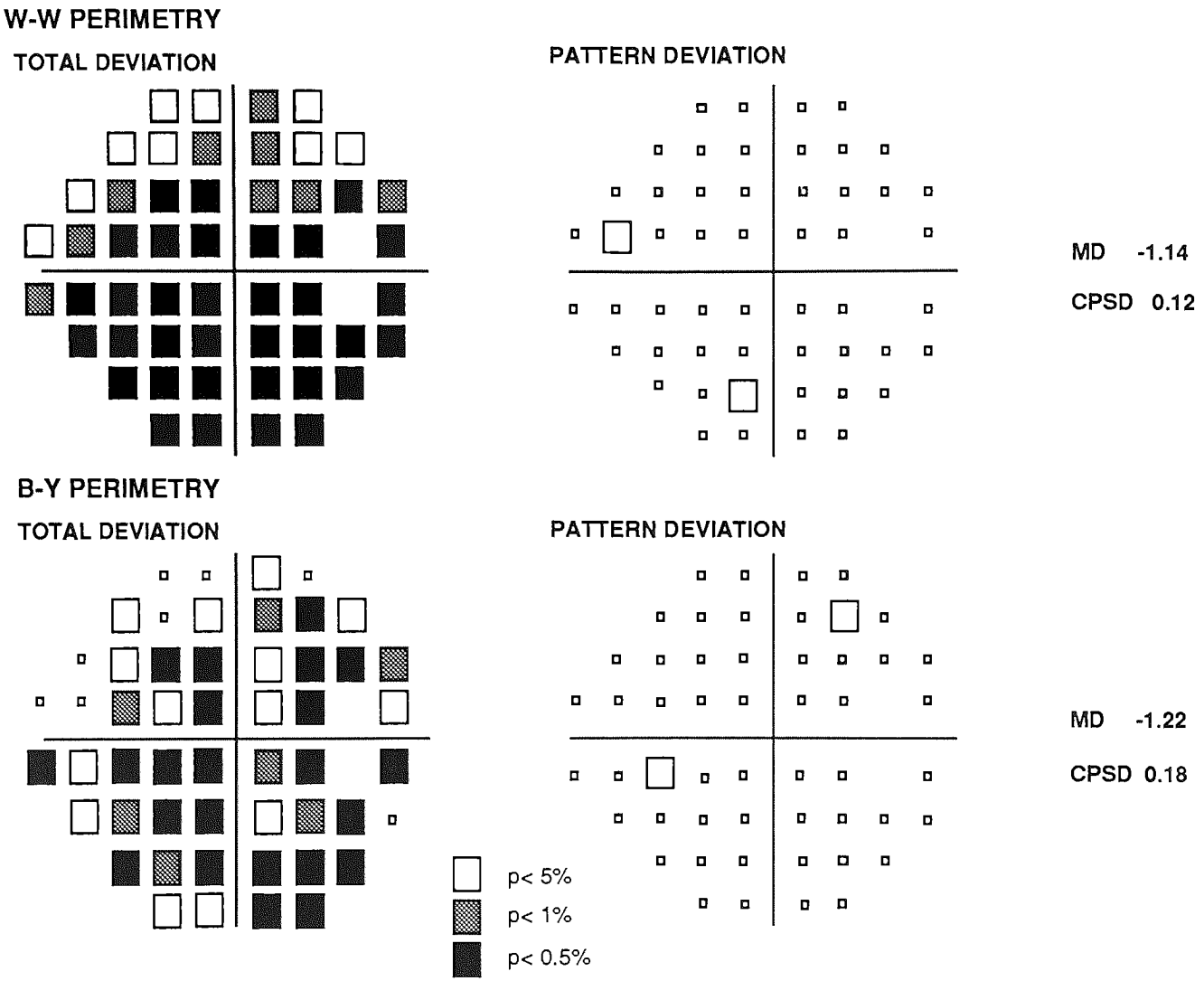

Figure 6.6. Total and pattern deviation plots for W-W (top) and B-Y (bottom) illustrating a patient with nuclear cataract (LOCS grade NIV). Indices are represented are in log units.

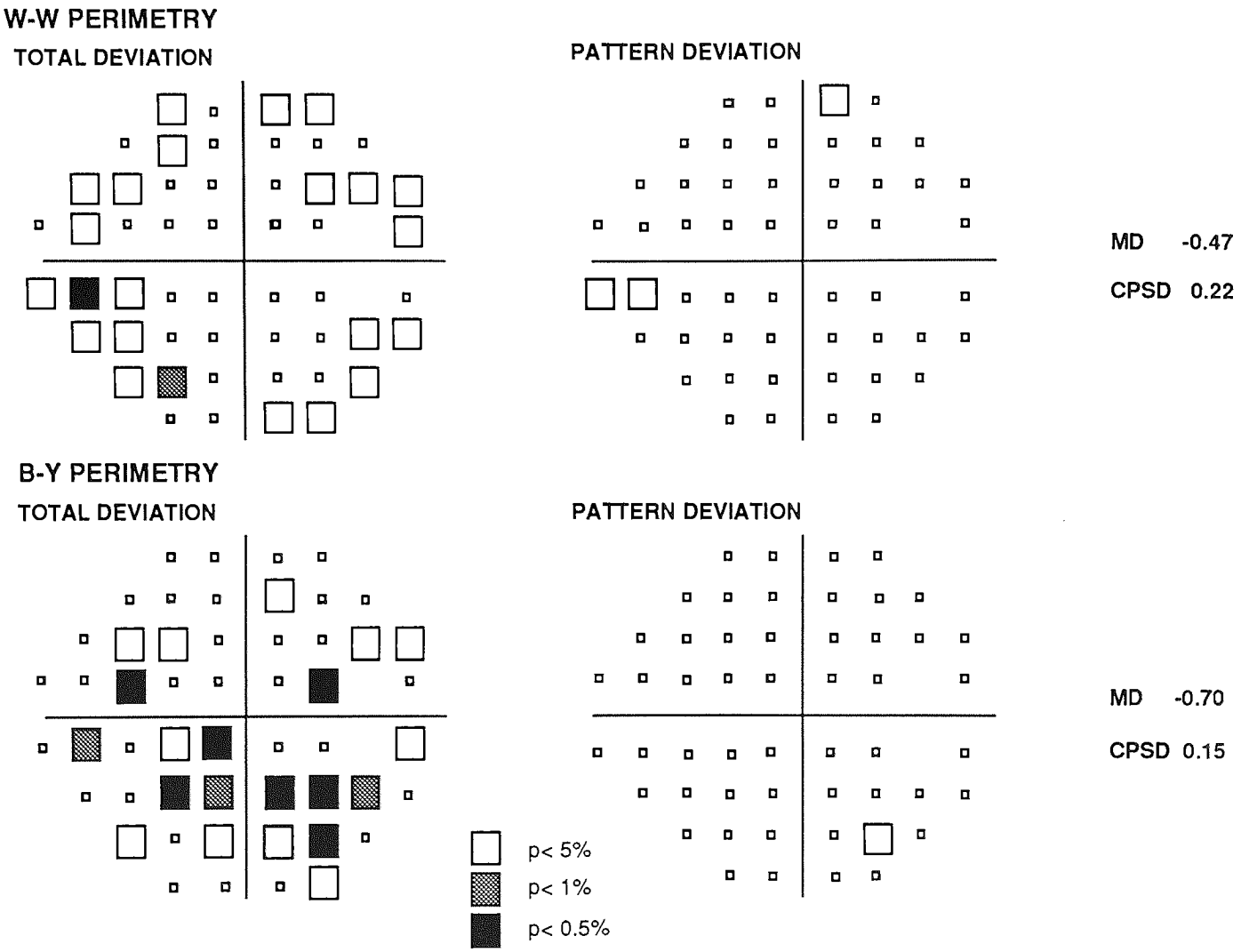

Figure 6.7. Total and pattern deviation plots for W-W (top) and B-Y (bottom) illustrating a patient with posterior subcapsular cataract (LOCS grade PII). Indices are represented are in log units.

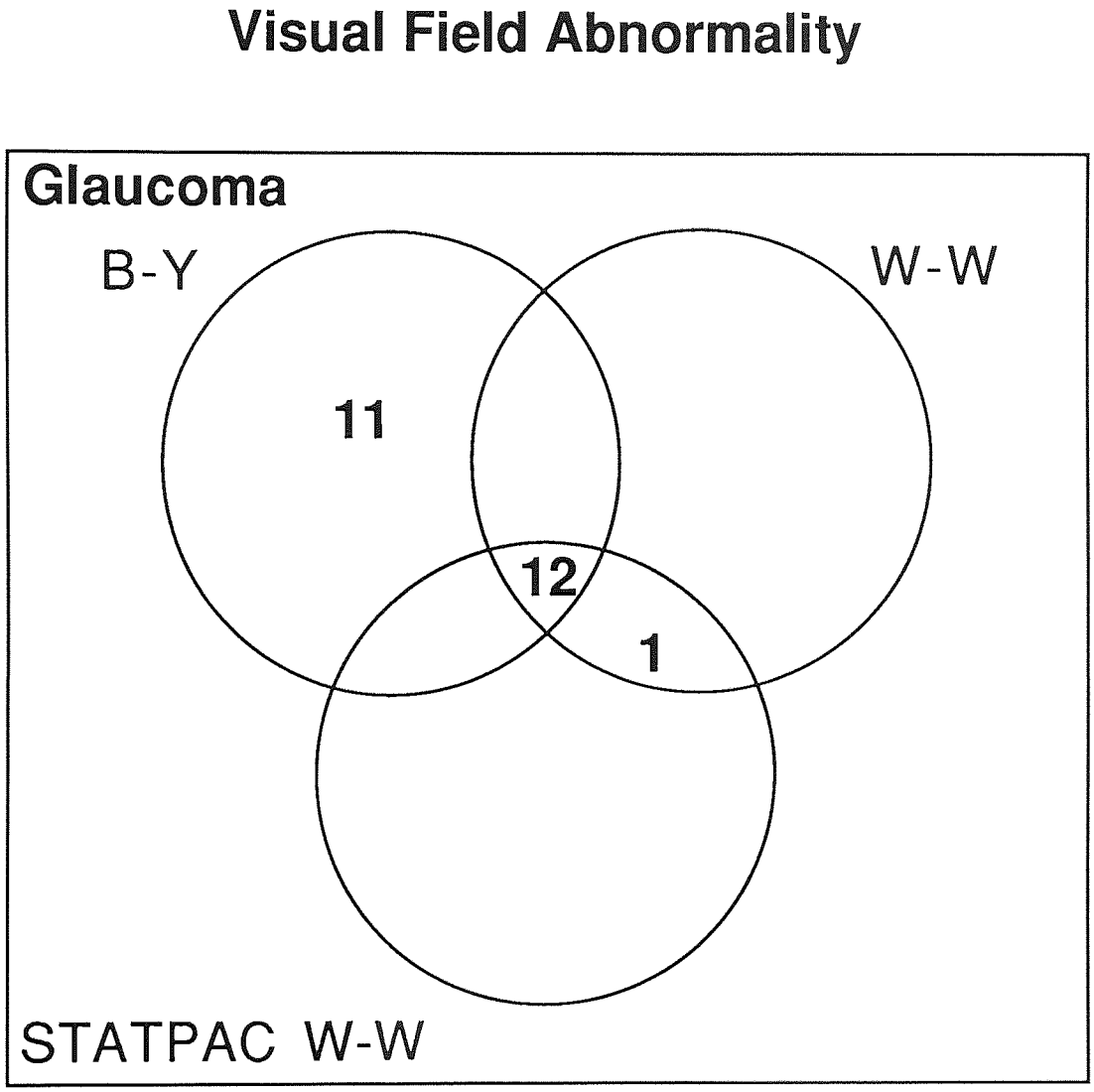

Figure 6.8. Venn diagram illustrating the level of agreement in field loss between the B-Y and W-W stimulus combinations for the POAG group.

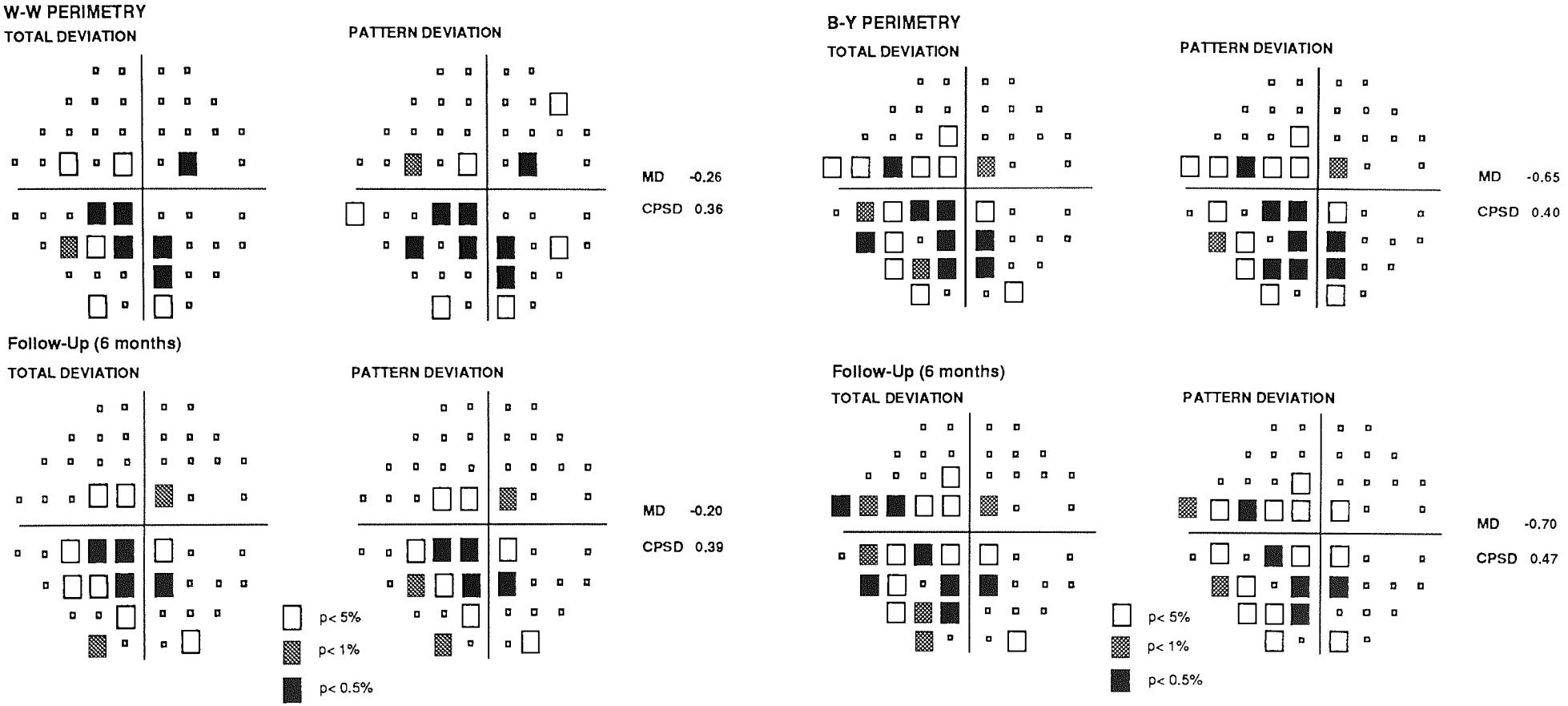

Figure 6.9 Total and pattern deviation plots for W-W (left) and B-Y (right) illustrating a POAG patient with greater B-Y loss at the outset and at the 6 month follow-up. The indices are in log units. (Presenting IOP 23mmHg, vertical C / D ratio 0.7, negative family history of glaucoma, current treatment Timolol 0.5% bd).

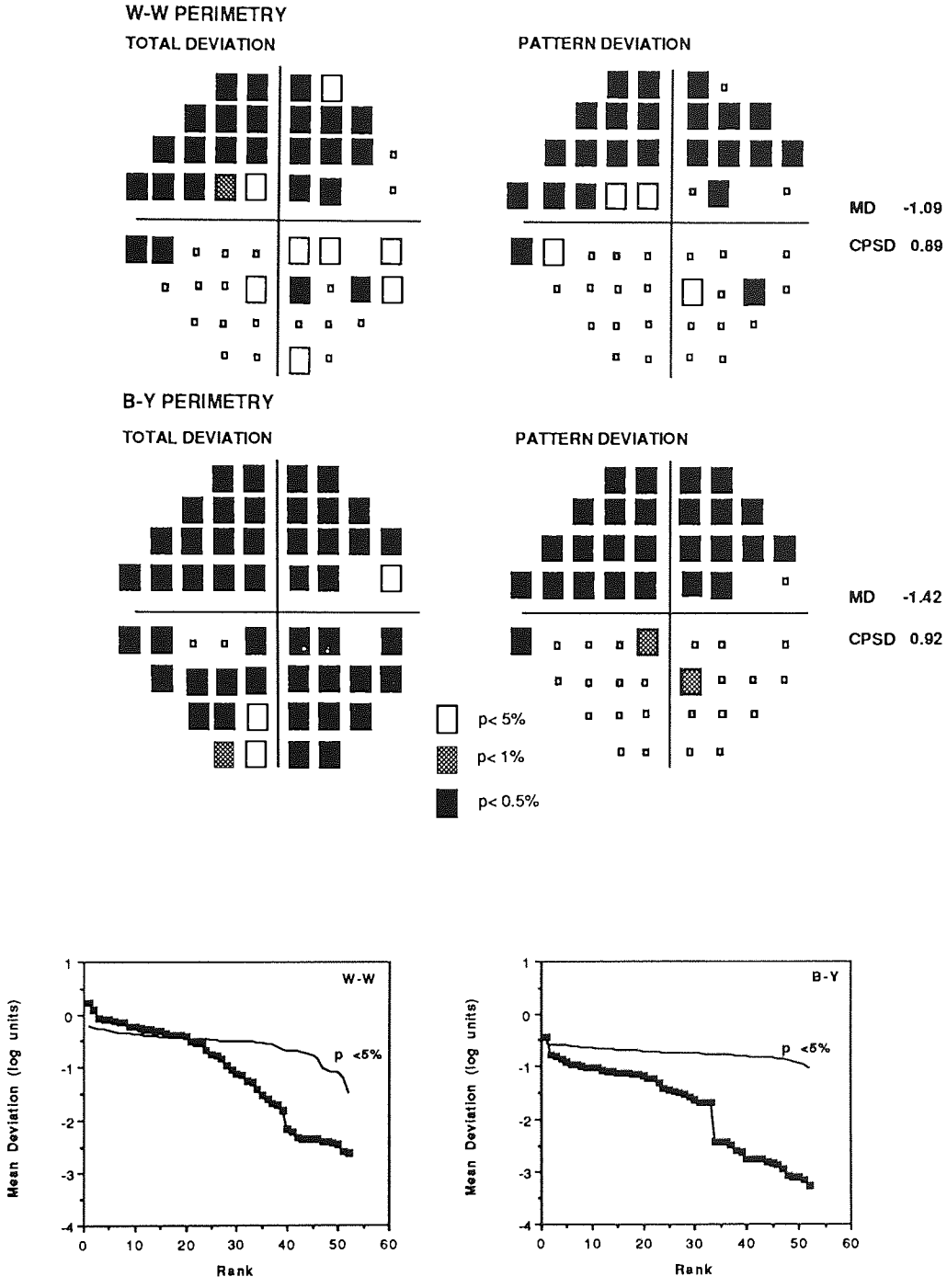

Figure 6.10. Total and pattern deviation plots (top) and associated Bebié curves (bottom) for W-W (left) and B-Y (right) illustrating a POAG patient with greater diffuse B-Y loss. The indices are in log units. The upper slope of each Bebié curve for each stimulus combination represents the 95% confidence limit. (Presenting IOP 30mmHg, vertical C / D ratio 0.8, negative family history of glaucoma, current treatment Timolol 0.5% bd).

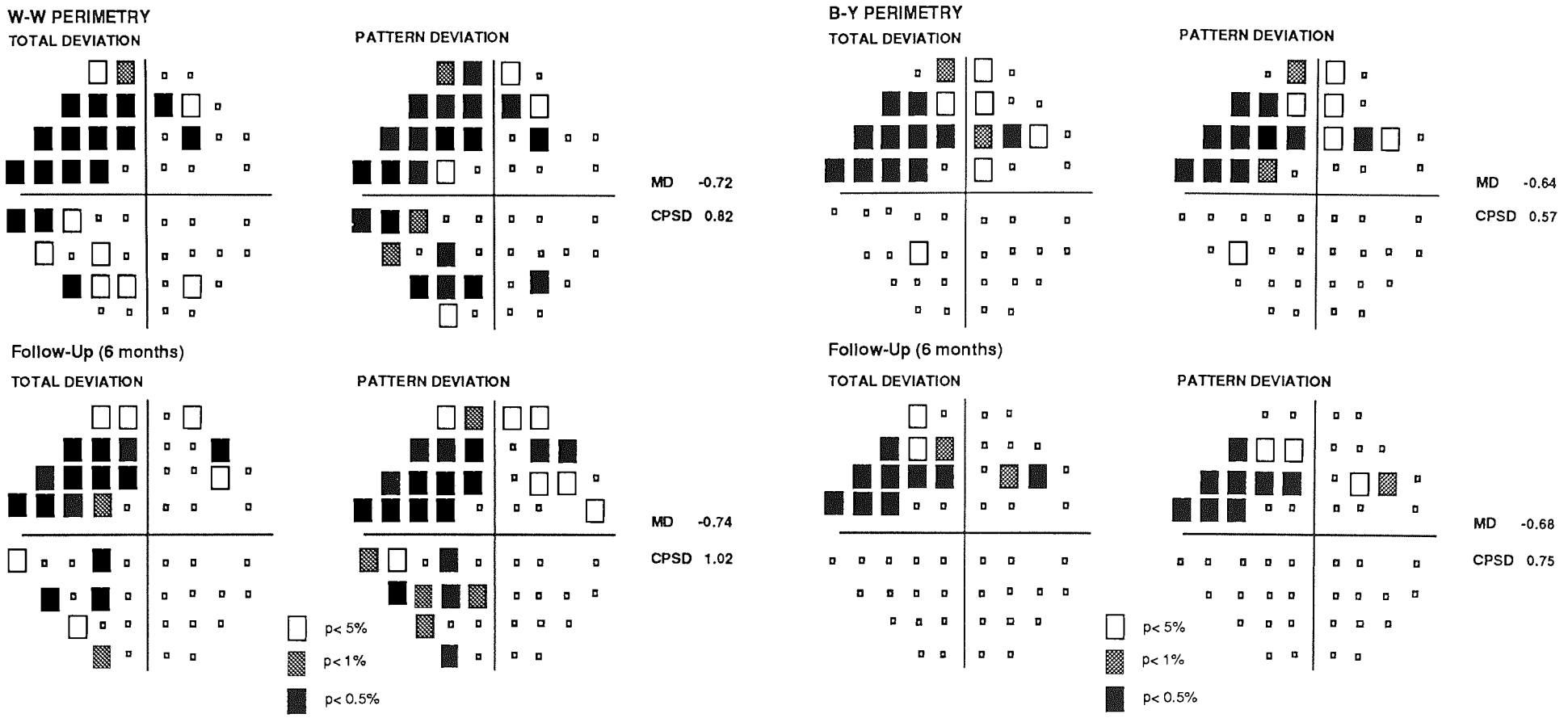

Figure 6.11. Total and pattern deviation plots for W-W (left) and B-Y (right) illustrating a POAG patient with greater W-W loss at the outset and at the 6 month follow-up. The indices are in log units. (Presenting IOP 30mmHg, vertical C / D ratio 0.8, positive family history of glaucoma, current treatment Timolol 0.5% bd).

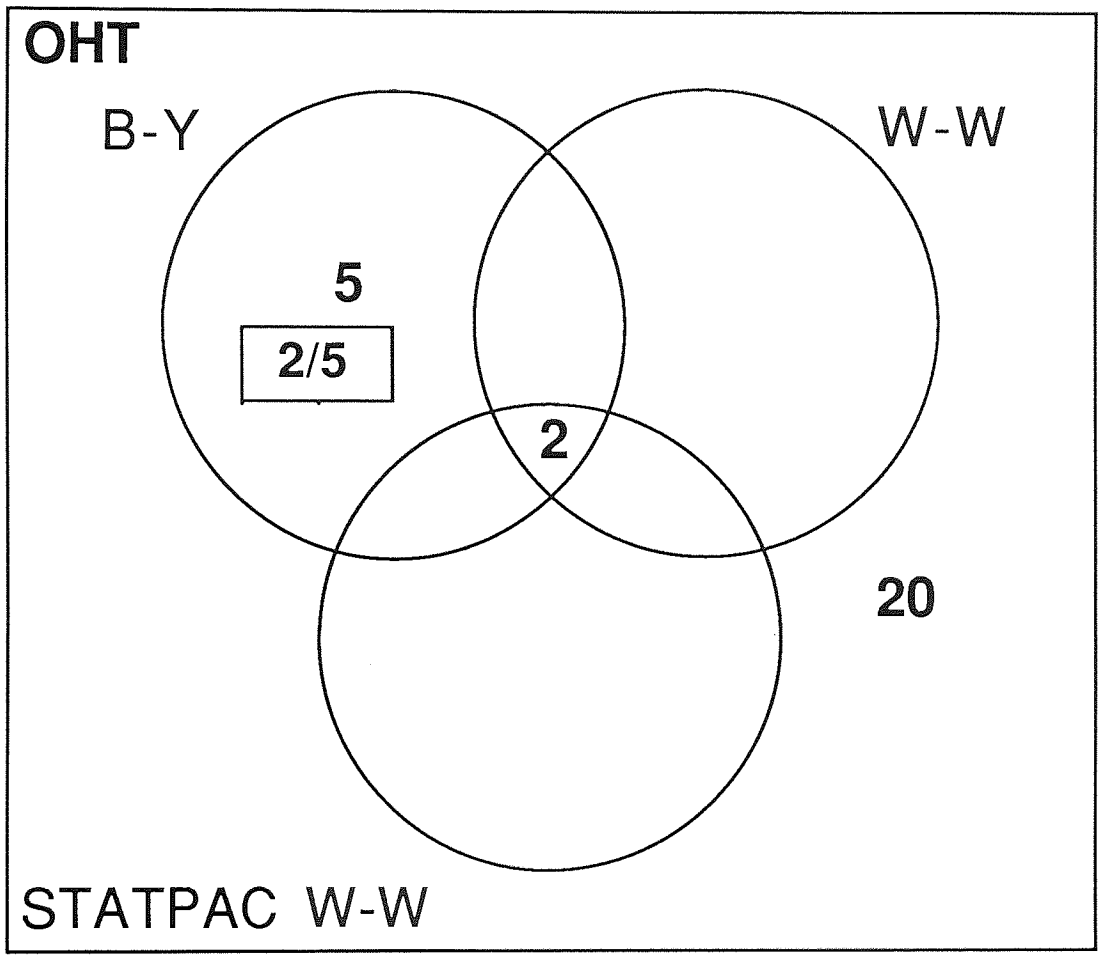

Figure 6.12. Venn diagram illustrating the presence of field loss between the B-Y and W-W stimulus combinations for the OHT group. The value outside the circles indicates the number of patients with normal fields for the B-Y and both the W-W analyses. The boxed number within the circle representing the B-Y stimulus combination indicates the number of patients subsequently manifesting a repeatable W-W loss.

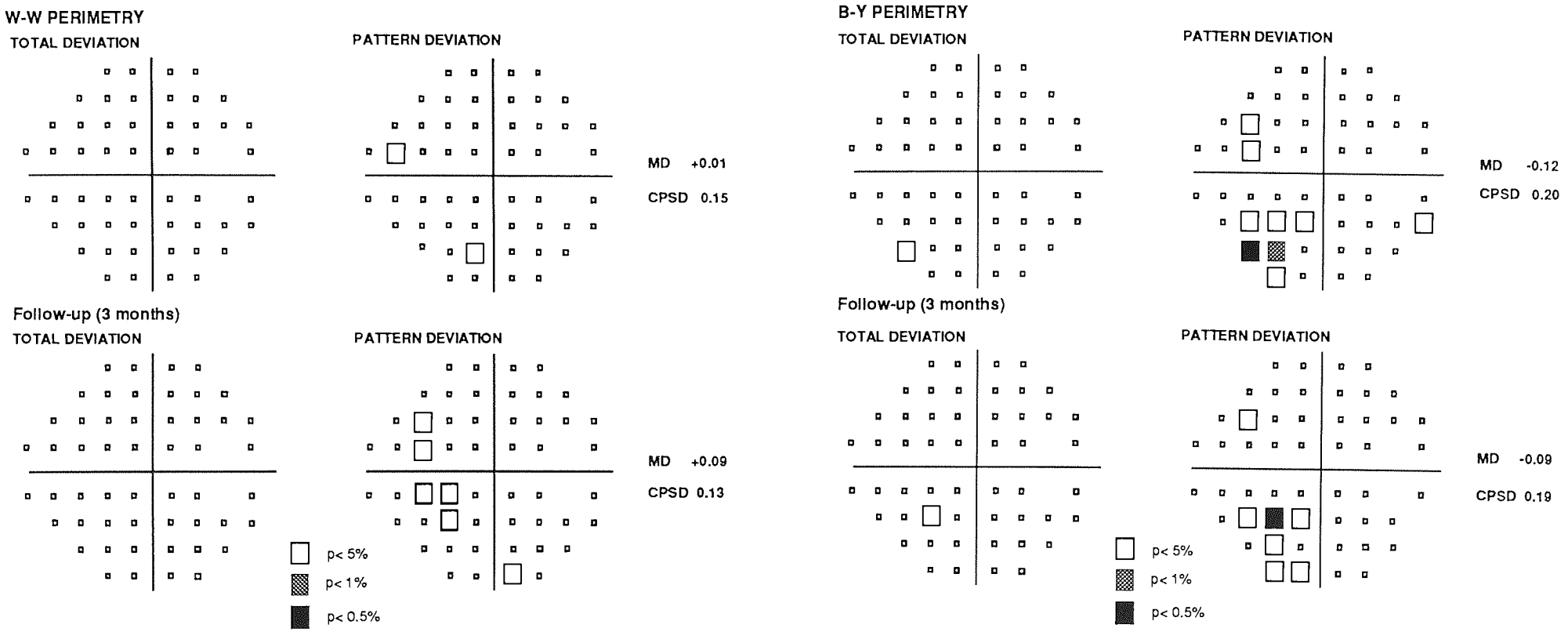

Figure 6.13a. Total and pattern deviation plots for W-W (left) and B-Y (right) illustrating an OHT patient with a normal W-W field but abnormal B-Y field at the outset and the appearances at the 3 month follow-up. The indices are in log units. (Medium risk category: presenting IOP 27mmHg, vertical C / D ratio 0.6, positive family history of glaucoma).

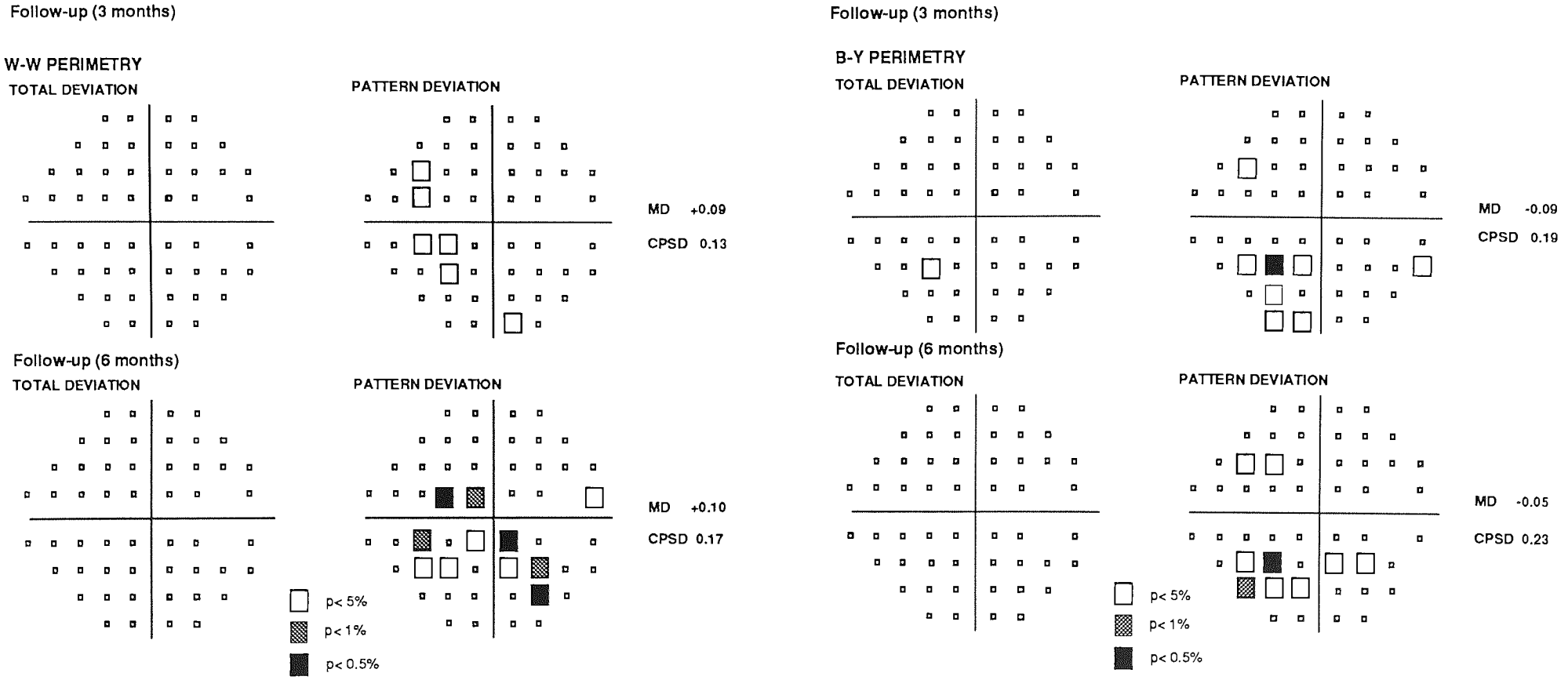

Figure 6.13b. Total and pattern deviation plots for W-W (left) and B-Y (right) illustrating the case in Figure 6.13a at the 6 month follow-up.The indices are in log units.

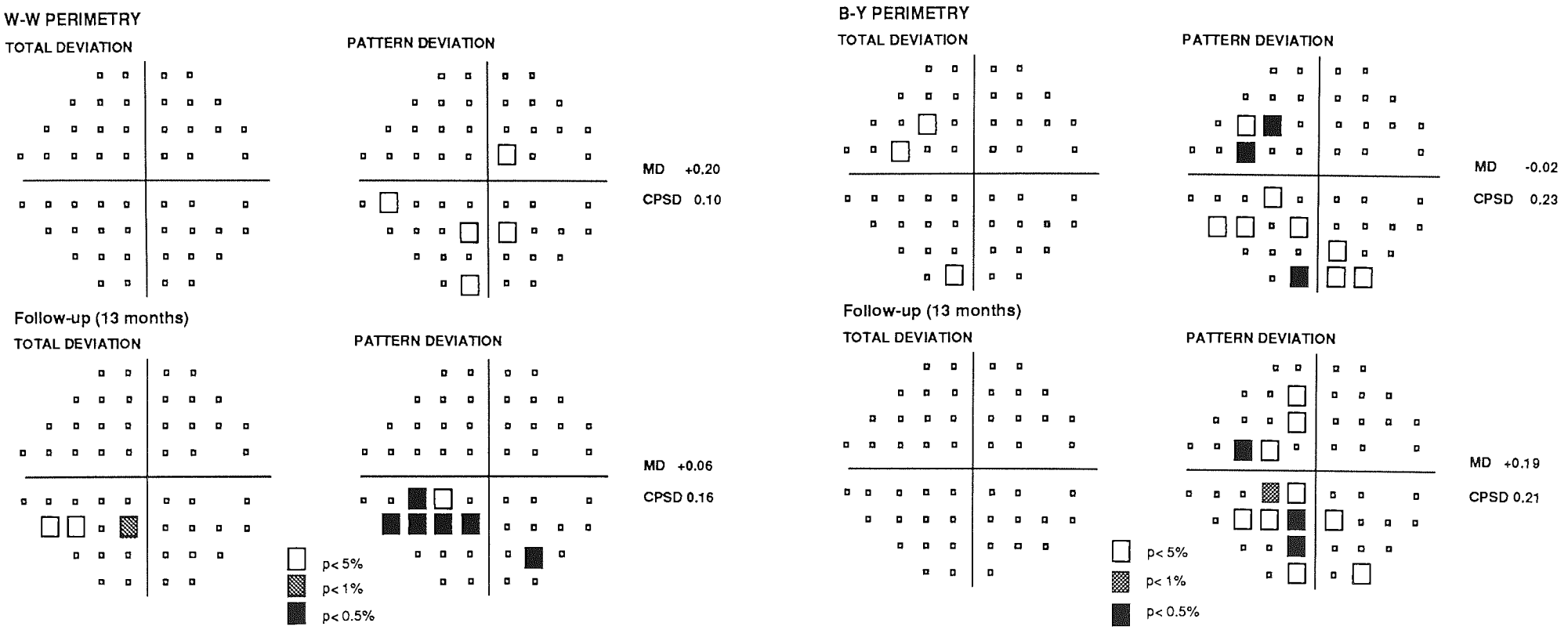

Figure 6.14a. Total and pattern plots for W-W (left) and B-Y (right) illustrating an OHT patient with a suspicious W-W field but abnormal B-Y field at the outset and the appearances at the 13 month follow-up. The indices are in log units. (Medium risk category: presenting IOP 22mmHg, vertical C / D ratio 0.6, positive family history of glaucoma).

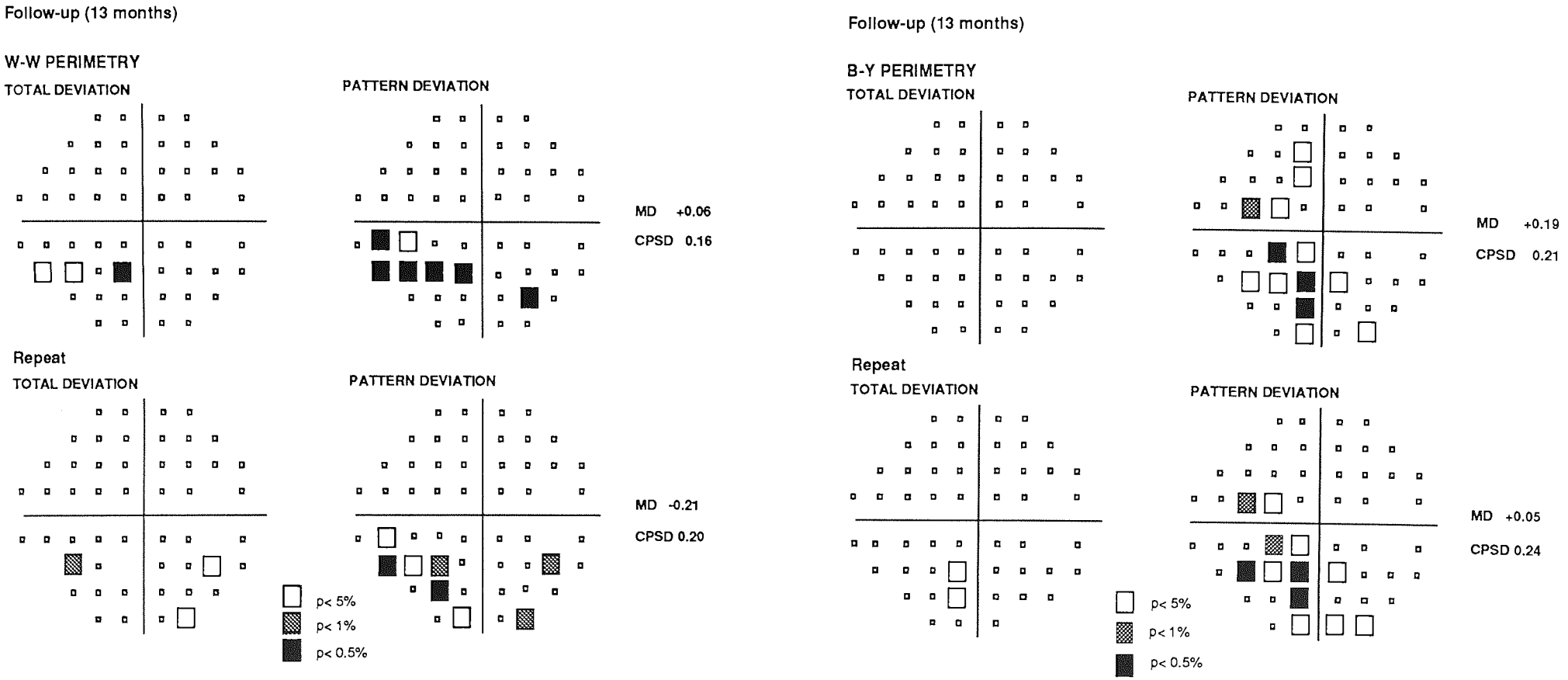

Figure 6.14b. Total and pattern plots for W-W (left) and B-Y (right) illustrating the OHT patient illustrated in Figure 6.14a at the 13 month follow-up and the corresponding repeat field after 2 weeks. The indices are in log units.

A repeated measures ANCOVA with diagnostic category (ie OHT or POAG) as a between-subjects factor, stimulus type as a within-subjects factor and age as a covariate was separately carried out for each of the visual field indices, MD, SF and CPSD (Tables 6.6-6.8). As would be expected, overall, the MD was more negative for the POAG group ($p<0.001$) compared to the OHT group and this difference increased with age ($p=0.041$). The B-Y MD was more negative than the W-W MD ($p=0.002$) irrespective of diagnosis ($p=0.36$) and age ($p=0.36$). The SF was greater for the POAG group ($p=0.001$) compared to the OHT group but there was no difference between the W-W and B-Y combinations ($p=0.59$) regardless of age ($p=0.32$). Not surprisingly the CPSD was greater for the POAG group than the OHT group ($p<0.001$) but this difference was independent of age ($p=0.08$) and stimulus combination ($p=0.85$). The group mean MD, SF and CPSD for the OHT and POAG groups is illustrated in Table 6.9.

Source	dF	Sums of Squares	Mean Square	F value	P value
Age	1	2.649	2.649	9.522	p=0.003
Diagnosis	1	8.446	8.446	30.360	p<0.001
Age x Diagnosis	1	1.226	1.226	4.406	p=0.041
Error	47	13.075	0.278		
Stimulus combination	1	0.501	0.501	10.724	p=0.002
Stimulus combination x Age	1	0.040	0.040	0.855	p=0.360
Stimulus combination x Diagnosis	1	0.040	0.040	0.860	p=0.359
Stimulus comb x Age x Diagnosis	1	0.088	0.088	1.891	p=0.176
Error	47	2.198	0.047		

Table 6.6. Repeated measures analysis of covariance for the mean deviation (MD).

Source	dF	Sums of Squares	Mean Square	F value	P value
Age	1	0.009	0.009	1.001	p=0.322
Diagnosis	1	0.100	0.100	11.665	p=0.001
Age x Diagnosis	1	0.001	0.001	0.105	p=0.748
Error	47	0.404	0.009		
Stimulus combination	1	0.001	0.001	0.313	p=0.579
Stimulus combination x Age	1	0.014	0.014	3.205	p=0.080
Stimulus combination x Diagnosis	1	0.013	0.013	2.856	p=0.100
Stimulus comb x Age x Diagnosis	1	0.002	0.002	0.538	p=0.467
Error	47	0.209	0.004		

Table 6.7. Repeated measures analysis of covariance for the short-term fluctuation (SF).

Source	dF	Sums of Squares	Mean Square	F value	P value
Age	1	0.512	0.512	5.049	p=0.029
Diagnosis	1	3.855	3.855	38.000	p<0.001
Age x Diagnosis	1	0.324	0.324	3.190	p=0.081
Error	47	4.768	0.101		
Stimulus combination	1	0.002	0.002	0.229	p=0.634
Stimulus combination x Age	1	0.001	0.001	0.105	p=0.747
Stimulus combination x Diagnosis	1	0.000	0.000	0.037	p=0.849
Stimulus comb x Age x Diagnosis	1	0.004	0.004	0.604	p=0.441
Error	47	0.341	0.007		

Table 6.8. Repeated measures analysis of covariance for the corrected pattern standard deviation (CPSD).

Stimulus / Background combination	OHT			POAG		
	MD	SF	CPSD	MD	SF	CPSD
B-Y	-0.18 (0.30)	0.17 (0.04)	0.18 (0.07)	-0.69 (0.46)	0.21 (0.10)	0.43 (0.23)
W-W	-0.08 (0.18)	0.14 (0.04)	0.17 (0.11)	-0.68 (0.51)	0.23 (0.12)	0.57 (0.33)

Table 6.9. Group mean mean deviation (MD), group mean short-term fluctuation (SF) and group mean corrected pattern standard deviation (CPSD) for each of the B-Y and W-W stimulus combinations for the OHT and glaucoma patients. Values are expressed in log units. One log unit is equivalent to10dB. One standard deviation is given in parenthesis.

6.2.6. Discussion

Normal Subjects

The evaluation of conventional W-W visual field abnormality is based upon rigid statistical procedures such as the global indices (Flammer 1986; Heijl et al 1987c) and the total and pattern probability plots (Heijl and Asman 1989; Heijl et al 1987c, 1989c). The findings of this study demonstrate an increase in the standard deviation of the group mean normal pointwise B-Y and W-W sensitivities with increase in eccentricity and with increase in age; this is in agreement with the findings of Heijl et al (1987b, 1988) for W-W perimetry. The data of the present study was normally distributed at all locations for both the W-W and B-Y stimulus combinations and the 1% and 0.5% probability levels were obtained from calculations based on this Gaussian distribution rather than from empirical derivations. The normal distribution of the W-W data is in contrast to the W-W data of Heijl et al (1987b) who found a non-Gaussian distribution. The reason for the difference in the type of W-W distribution between the two studies is unclear particularly since the experimental protocols were similar. However, the Heijl study involved the collection of data from both eyes at the same visit. It is known that the fatigue effect is greater for the second eye (Searle et al 1991a, b; Wild et al 1989c, 1991b; Hudson et al 1994) and it is possible that this may have influenced the outcome of their distribution. Nevertheless, the standard deviation of the group mean age-matched normal W-W sensitivities was similar at all locations to those of Heijl et al (1987b, 1988).

The finding of an increased within-examination variability in the age-matched normal group for the B-Y compared to the W-W is in agreement with Sample et al (1993a) who found that the SF was higher for B-Y in normal eyes although the difference was not statistically significant. The similarity of the B-Y and W-W SF in the patient groups is also in agreement with Sample et al (1993a) who also failed to find a statistically significant difference. The results and those of Sample et al (1993a), are also compatible with Nelson-Quigg et al (1990) who reported a 25-30% greater B-Y SF. The apparent increased variability of the B-Y SF in the age-matched normal group may have been artifactual due to a decreased W-W SF arising from the requirement of a

normal W-W field. However the SF was also higher (mean 1.67dB; SD 0.43) than the W-W SF (mean 1.32dB; SD 0.38) in the normal group of 20 subjects and this also reached statistical significance (p=0.007). Nevertheless, the magnitude of the B-Y SF still lies within the normal range of the W-W SF. The increase in within-test between-subject variability for B-Y perimetry is also in agreement with the general comments of Johnson et al (1989a). A consequence of the increased magnitude of the B-Y pointwise standard deviations is that, for a given probability level, the deviation of the measured B-Y sensitivity from that of the normal value is larger than the equivalent W-W deviation. Furthermore, the consequence of this within- and between-subject normal variability in B-Y sensitivity for the new faster testing algorithms developed for W-W perimetry and discussed in Chapter 3 remain unknown.

The technique of B-Y perimetry has been criticised as time-consuming due the requirement of an individual measurement of lenticular absorption requiring approximately 45 minutes (Johnson et al 1993c; Sample et al 1993c). Johnson et al (1993c) have recently developed a Lens Absorption Meter (LAM) to rapidly assess the correction required for individual ocular media absorption in B-Y perimetry. Alternatively, Sample et al (1993c) have compared stimulus locations in the opposite hemifield which overcomes the necessity for the measurement of lenticular absorption. The correction of the B-Y data for lenticular absorption resulted in an increase in the mean sensitivity at each stimulus location. However, surprisingly, the magnitudes of the standard deviations of the mean sensitivities remained unchanged compared to those without correction indicating that the between-subject variability is unaffected by correction for lenticular absorption. Interestingly, Johnson et al (1988b) demonstrated an increased between-subject variability after correction for lenticular absorption. The similarity of the standard deviations implies that the assessment of lenticular absorption on an individual basis could be avoided when using a broadband blue stimulus since the magnitude of the deviation from normality required for a given probability level would not be affected. Any individual difference from the height of the average age-matched normal uncorrected field could be removed using the pattern deviation approach (ie an elevation of the field). Such an approach would ignore any diffuse component due to optical factors such as forward light scatter (Chapter 4) or due to neural damage. The difficulty in separating such

components in W-W perimetry (Funkhouser et al 1993), however, would also be present in B-Y perimetry. Ignoring the reduction in the height of the B-Y visual field would also reduce the range of sensitivity over which any given focal loss could be evaluated. The general height reduction attributable to the magnitude of lenticular absorption increases as the wavelength of the stimulus decreases (Savage et al 1993; Hudson and Wild 1993; Pokorny et al 1987; Sample et al 1988b). As a result of an increase in absorption at shorter wavelengths the use of a 440nm narrowband stimuli employed by Sample and Weinreb (1989, 1990, 1992) may result in a different general height reduction compared to that obtained with the broadband OCLI filter. Nevertheless, the magnitude and trend of the pointwise SDs across the field of the broadband filter are in general agreement with the 440nm narrow band filter employed by Sample and Weinreb (1992).

Sensitivity and Specificity

The probability maps indicate the frequency with which the given pointwise sensitivity is seen in a normal population. The model and limits assigned in the B-Y maps gave good specificity for a separate sample of 20 normal individuals and 7 patients with cataract. Eighteen out of 20 normal subjects yielded normal fields whilst all 7 individual with cataract exhibited a normal pattern probability map. This finding is in good agreement with the specificity of STATPAC of approximately 90% (Heijl and Asman 1989). Furthermore, the finding that all 24 POAG eyes were abnormal on B-Y pattern probability maps is also in agreement with the sensitivity of STATPAC (Heijl and Asman 1989).

OHT and POAG patients

Since the initiation of this study, longitudinal studies over a five year period suggest that B-Y visual field defects occur prior to conventional W-W field loss in POAG and exhibit progression in advance of that when recorded with conventional W-W perimetry by approximately 3 years (Sample and Weinreb 1992; Johnson et al 1993a, b, d; Casson et al 1993b). The SWS loss is believed to have both diffuse and focal components (Heron et al 1988; deJong et al 1990, 1993; Flanagan et al 1991a; Hart et al 1990; Adams et al 1991; Sample et al 1986b, 1988, 1993b, c, d, 1994; Sample and Weinreb 1989, 1990, 1992; Weinreb and Sample 1991; Johnson et al 1988c,

1989a, 1992, 1993a, b, d; Lewis et al 1993) with the focal loss corresponding to nerve fibre bundle patterns (Adams et al 1991). The diffuse reduction of B-Y sensitivity may be related to the degree of IOP (Lewis et al 1993), nevertheless B-Y deficits have also been recorded in low tension glaucoma (Sample et al 1994).

In cases of early to moderate glaucomatous loss, the results of the current study show that compared to W-W perimetry, B-Y perimetry identifies a wider, and to some extent deeper, area of focal loss. The development of new B-Y scotomata was not present. The findings are compatible with the total deviation plots of Johnson and associates (Johnson et al 1988c, 1989a, 1993a, b, d; Adams et al 1991; Casson et al 1993b) who found that B-Y perimetry identified field progression prior to that of W-W perimetry. The results of the pattern probability analysis for 5 patients in the OHT group is consistent with the concept that B-Y perimetry is capable of detecting glaucomatous visual field loss in ocular hypertension earlier than that identified by W-W perimetry (Adams et al 1991, Flanagan et al 1991a; Johnson et al 1988c, 1989a, 1993a, b, d; deJong et al 1991, 1993; Hart et al 1990; Lewis et al 1993; Casson et al 1993b; Sample et al 1986b, 1988a, 1993b, c, d, 1994). Caution needs to be exercised, however, in distinguishing between variability and progression on the basis of 2-3 fields obtained within the one year time period of the study. Interestingly, however, none of the 4 high risk OHTs, all of whom were being treated with ß-blockers, manifested a B-Y field defect. Several unpublished studies have found cases in which patients have manifested a normal B-Y field with an abnormal W-W field (Drance SM, Flanagan JG; personal communications). No cases were present in the current study. However, one glaucoma patient demonstrated a consistently worse W-W field than the corresponding B-Y field (Figure 6.11). It could be hypothesized that different mechanisms of damage in glaucoma which result in different patterns of glaucomatous loss may explain this finding; however this requires further investigation. In the present study neither diffuse B-Y or W-W loss on the total deviation maps was evident amongst any of the OHTs. However, 5 POAG patients with advanced glaucoma showed greater diffuse loss on the B-Y total deviation plot compared to that of W-W despite equivalence of the W-W and B-Y pattern deviation plots. These latter findings were not considered to be due to cataract or pupil size.

Recognition of differences in the depth of focal loss by comparison of pattern deviation probability plots between B-Y and W-W is limited in that a given probability symbol covers a particular range of defect depths. Furthermore, the range of probability levels for both the W-W and B-Y is truncated at a probability level of 0.5%. In addition, the depth of B-Y loss required to attain significance is greater due to the increased normal between-subject variability such that at a probability level of $p<0.5\%$ the deviation from the B-Y normal response approaches the degree of isolation of 1.4 log units. When the defect depth exceeds the value of isolation, the perimetric response is no longer solely mediated by the SWS pathway and the response is most likely governed by the MWS pathway (Johnson et al 1993a; Hart et al 1990). In such a case, the use of the B-Y stimulus combination would also be limited by the available dynamic range.

The value of B-Y perimetry compared to W-W perimetry at stimulus locations in which SWS isolation is lost warrants further study. Statistical elevation or depression of the hill of vision can markedly alter the apparent depth of focal loss displayed by the pattern deviation plot for both W-W and B-Y stimuli. The magnitude of the defect depth in relation to the available SWS isolation should therefore be evaluated by inspection of the total deviation plot alone. An additional problem may arise in the calculation of the global short-term fluctuation and the corrected pattern standard deviation whereby, as a result of the local short-term fluctuation, a stimulus location may exhibit an initial threshold apparently mediated by the SWS pathway and a second threshold apparently mediated by the MWS pathway. Until the relationship is known between the W-W sensitivity and the B-Y sensitivity at a location where the B-Y defect depth is beyond the level of isolation, any analytical package for B-Y perimetry should identify those stimulus locations which lie outside the limits of SWS isolation.

The inherent increase in between-subject variability for B-Y perimetry must be accounted for in the determination of abnormality. Failure to do so will result in a large number of false-positive defects. This may answer the question posed by Sample and Weinreb (1990) as to why 43% of OHTs demonstrated B-Y abnormality. Nevertheless, the technique gives good specificity and can

produce a wider loss compared with W-W perimetry in POAG. The data is consistent with the concept that B-Y perimetry provides an earlier indication of field loss in OHT compared to W-W perimetry. However, the interaction of the wider limits for B-Y abnormality together with the magnitude of SWS isolation can limit the range over which B-Y defects can be detected and monitored.

CHAPTER 7: ISOLUMINANCE COLOUR CONTRAST SENSITIVITY IN NORMAL SUBJECTS AND OHT PATIENTS

7.1 Introduction

Automated perimetry involves measurement of threshold at locations in the visual field for static or kinetic stimuli presented on a defined background of known luminance. The measurement of a threshold at a variety of spatial and / or temporal frequencies produces a classic bell-shaped function, the Contrast Sensitivity Function (CSF), originally described by Campbell and Green (1965). Spatial contrast sensitivity (CS) measures the ability of a subject to detect a grating stimulus, which may vary in luminance, colour and / or a combination of both across a spatial domain. Temporal contrast sensitivity involves the measurement of contrast or modulation depth at a variety of temporal frequencies.

7.2 Contrast Sensitivity and Glaucoma

The utility of luminance CS measurements for the investigation of OHT and glaucoma is equivocal (Arden and Jacobsen 1978; Hitchings et al 1981; Motolko et al 1982b; Ross et al 1984, 1985; Singh et al 1981; Sokol et al 1980; Stamper et al 1982; Vaegan and Halliday 1982; Drance et al 1987c; Korth et al 1989; Lustgarten et al 1990; Sample et al 1991b; Mantyjarvi and Terasvirta 1993). Significant reductions of CS in glaucoma patients with normal visual acuity have been reported using the Arden grating test which measures sensitivity at low spatial frequencies (Arden and Jacobsen 1978). The sensitivity of the Arden grating test can also be improved by the use of a forced-choice testing paradigm (Vaegan and Halliday 1982). However, a considerable overlap in the scores of the Arden test between normal and glaucomatous eyes has been found (Hitchings et al 1981; Singh et al 1981; Stamper et al 1982), particularly in patients over the age of 50 years (Sokol et al 1980), which limits the diagnostic capability of the test. Such overlap between normal and abnormal eyes has also been reported using a Nicolet CS 2000 monitor-based system (Drance et al 1987c; Korth et al 1989) and the Vistech 6500 test (Maudgal et al 1988; Adams et al 1987a; Sponsel et al 1991; Mantyjarvi and Terasvirta 1993). Conversely, using an oscilloscope-based technique, Ross et al (1984, 1985b) found that 47 of 50 glaucoma patients

and 31 of 50 OHTs exhibited an abnormal CS. Furthermore, the CS loss increased as the degree of W-W visual field loss increased (Ross et al 1984).

Korth et al (1989) stressed the importance of patient age in the differentiation of abnormal from normal eyes: they demonstrated little difference in the CS at all spatial frequencies between normal age-matched subjects and glaucoma patients over 50 years. Indeed, the decline in CS with age (Singh et al 1981; Sokol et al 1980; Stamper et al 1982; Mantyjarvi and Terasvirta 1993) together with the greater incidence of media opacities, which also reduces CS particularly for higher spatial frequencies (Hess and Woo 1978), may limit the ability of CS to clearly differentiate normal eyes from abnormal eyes.

A number of studies have reported a preferential loss of CS at high spatial frequencies in glaucoma (greater than 10 cycles per degree (cpd)) (Ross et al 1984; Korth et al 1989; Lustgarten et al 1990; Sample et al 1991b). This preferential loss has been suggested to be the reason for the poor diagnostic sensitivity of the Arden test, which tests at spatial frequencies less than 6.4 cpd (Sample et al 1991b). Korth et al (1989) demonstrated a preferential loss of sensitivity at high spatial frequencies in glaucoma patients below 50 years of age compared to age-matched normal groups. Interestingly, Sample et al (1991b) using the Vistech 6000 test, demonstrated an overall loss of CS in glaucoma patients but a greater reduction in sensitivity specifically at 12cpd. The results of the OHTs were not significantly different from those of normal subjects. Using an oscilloscope-based technique and a number of clinical-based contrast sensitivity charts, Wood and Lovie-Kitchin (1992, 1993) were also unable to demonstrate any significant differences in the mean contrast sensitivity between normals and OHTs. The highest diagnostic sensitivity and specificity for the tests was achieved when the CS was measured at the peak of the CSF (4cpd). Although Phelps and Motolko (1982) found considerable overlap between age-matched normals and glaucoma patients, an asymmetric CS was also demonstrated in some OHT patients which was a first indication of early unilateral glaucoma. A mid-frequency loss (6-10cpd) in glaucoma was also demonstrated using a laser system to by-pass the optical components of the eye (Shokoohi et al 1994); 13 of 21 glaucoma patients demonstrated an abnormal CS. Interestingly,

Ross et al (1984) identified three categories of CS loss in glaucoma: Type I involved a loss at all spatial frequencies and generally occurred in eyes with advanced field loss, Types II and III involved loss only at medium or high spatial frequencies respectively and were present in eyes with mild field loss.

Temporal CS has also been used in the early detection of glaucoma (Atkin et al 1979, 1980; Tyler 1981; Tyler et al 1984; Korth et al 1989; Breton et al 1991). Tyler et al (1981) and Atkin et al (1979, 1980) using flickering stimuli and counter-phase reversing patterns, demonstrated a categorical reduction of the central CS in glaucoma patients when compared to normals. The reduction in CS compared to the normal increased when the peripheral retina was examined (Tyler et al 1981; Korth et al 1989; Falcao-Reis et al 1990). The temporal frequency at which the reduction in sensitivity can be detected is equivocal. Indeed, Tyler et al (1981) showed that 36 of a mixed sample of 41 glaucoma and OHT patients demonstrated reductions in temporal CS outside the foveal region at a frequency in the region of 35Hz. Furthermore, the OHT patients had little or no field loss measured by Goldmann perimetry. Breton et al (1991) demonstrated a frequency- specific sensitivity loss at 15Hz in addition to a generalised loss, when the temporal CS of 52 glaucoma patients was measured at temporal frequencies between 5-30Hz. Furthermore, 6 of the 51 OHTs with no conventional W-W field loss demonstrated similar reductions in CS to that of the glaucoma patients. However, Korth et al (1989) also demonstrated a reduction in the spatiotemporal CS at spatial frequencies ranging from 0.5 to 6.0cpd with a temporal frequency of 10Hz at an eccentricity of 11° in glaucoma patients below 50 years of age. Furthermore 41 patients with either OHT or glaucoma involving minimal field loss using a monitor display (spatial frequency 1.6cpd, flicker frequency 1Hz) revealed significant losses in the inferior field particularly at eccentricities greater than 15° for the glaucoma group and for 11 OHTs, particularly the high risk patients (Falcao-Reis et al 1990).

The influence of the IOP upon CS is equivocal (Atkin et al 1979; Tyler et al Stamper 1984; Hitchings et al 1981; Buncic et al 1986; Wood and Lovie-Kitchin 1993). An elevated IOP has been found to be associated with a reduction in the temporal CS (Tyler et al 1984). Similarly, an

improvement of temporal CS has been reported when OHT patients have undergone topical β-blocker therapy (Buncic et al 1986; Tytla et al 1990). An improvement in the spatial CS of normal tension glaucoma patients has been reported following treatment with the calcium-channel blocker, nimodipine (Piltz et al 1993). Furthermore, an improvement in CS has also been demonstrated after laser trabeculoplasty (Nordmann et al 1992). The ability of CS to monitor visual field progression is poor (Nordmann et al 1992). Other studies of spatial CS, however, have failed to demonstrate any relationship between the magnitude of IOP and the CS (Atkin et al 1979, 1980; Hitchings et al 1981; Wood and Lovie-Kitchin 1993).

The structural characteristics of the optic nerve have also been compared with contrast sensitivity. Atkin et al (1980) found a reduction in the temporal CS with increase in the cup / disc ratio. In addition, a reduced temporal CS has been found in eyes in which the neuroretinal rim area is reduced (Korth et al 1989). A similar relationship, however, has not been demonstrated for spatial CS. Nevertheless, Mizokami and Asai (1989) have reported a good relationship between the spatial CS and the loss of retinal nerve fibres in the macular region. No relationship was present between the W-W visual field index MD and the CS.

The study of colour contrast sensitivity, involving stimuli of varying colour contrast is becoming increasingly popular (Arden et al 1988a, b; Gunduz et al 1988; Falcao-Reis et al 1991; Yu et al 1991; Geier et al 1993). Hues are modulated along the colour confusion lines for trichromatic vision. Furthermore, the stimulus configuration involves only spatial variations in colour contrast rather than variations in luminance contrast, hence the term isoluminance colour contrast sensitivity. Colour CS has been investigated in OHT and in glaucoma by modulating the colour along the tritan, protan and deutan colour confusion axes (Gunduz et al 1988; Falcao-Reis et al 1991; Yu et al 1991). A greater loss along the tritan axis was evident in both OHT and glaucoma compared to the normal age-matched controls when the gratings are presented in the central field (Gunduz et al 1988; Falcao-Reis et al 1991). Falcao-Reis et al (1991) also considered the importance of patient risk factors in the determination of abnormality. They classified patients as low-risk, medium-risk and high-risk OHT based upon presenting IOP and cup / disc ratio. A

considerable overlap existed between the colour CS of the patients and the normals particularly in the case of the low risk OHTs. However, 54 of the 170 OHTs had a significantly greater tritan threshold than the normal particularly in the case of the high risk OHTs. The tritan thresholds of the OHTs were higher compared to the normal than were those of the protan and deutan axes. The glaucoma group demonstrated a significant reduction for all three colour axes; however 7 of the 32 glaucoma patients were also normal (Falcao-Reis et al 1991). Falcao-Reis et al (1991) considered that the apparent lack of sensitivity of the test did not reflect the limitations of the test, itself, but rather the type of glaucomatous damage. Diffuse glaucomatous loss resulted in defective foveal colour vision; however, localised loss beyond the fovea was not detectable with a foveal based test of colour CS. The sensitivity and specificity of this type of test could be improved by the examination of the extrafoveal field. Interestingly, Yu et al (1991) assessed the peripheral tritan CS in 157 OHTs and 84 glaucoma patients. The stimulus comprised an annulus of 12.5° radius and of 1° width, of which a random 45° quadrant of the annulus was removed. Using a forced-choice procedure the patient identified the quadrant which was free of the annulus. All glaucoma patients exhibited a sensitivity which was significantly different from the normal in at least one area of the field. This difference increased with increasing W-W field loss. Of the 77 high risk OHTs, 38 patients demonstrated tritan thresholds which were three SDs above the mean threshold of the normal age-matched group.

Studies of isoluminance colour CS have originated from a limited number of research groups. There is a need to independently corroborate the findings of the published studies using a different testing protocol. Furthermore, no study has compared the results of B-Y perimetry to those of isoluminance B-Y CS and R-G CS in the detection of early glaucomatous visual field loss.

7.3.1. Aim of the Study

The aim of the study was twofold: firstly to compare the R-G and B-Y isoluminance colour contrast sensitivity in a sample of normals and secondly to evaluate the technique for the detection of glaucomatous visual field loss using the sample of OHTs who had previously undergone W-W and B-Y perimetry.

7.3.2 Materials and methods

The study comprised two samples: a normal age-matched control group and a group of OHT patients. All the subjects and patients formed part of the study described previously in Chapter 6.

Normal age-matched control group

The normal control group comprised 43 of the 50 age-matched normal subjects randomly recruited from local old-aged pensioner associations and stratified by age. Twenty-three subjects were aged between 60-69 years (mean age 64.3 years SD 4.9) and 20 subjects were aged between 70-82 years (mean age 75.0 years SD 3.9). All subjects conformed to the inclusion criteria described in Section 6.2.2. One eye, only, of each age-matched normal subject was selected for the study.

OHT group

The OHT sample comprised 20 of the 27 patients described in Section 6.2.2.

Contrast Sensitivity

All subjects and patients underwent two testing paradigms, namely the measurement of isoluminance red-green and blue-yellow colour contrast sensitivity. The stimuli were generated by a Venus Visual Stimulator (Neuroscientific Ltd, USA) using software written in Microsoft C and were presented on a colour monitor. The stimuli consisted of gratings modulated either along a R-G axis or along a blue-yellow B-Y axis. Modulation along the R-G confusion line results in the sensitivity of the SWS mechanism remaining constant. Similarly, modulation of the B-Y grating along the tritanopic confusion line results in an equal stimulation of the R-G mechanisms

(Krauskopf et al 1982). Based upon a knowledge of the chromaticity coordinates of the CIE (1931) standard colorimetric system (Wyszecki and Stiles 1964), the extent of the colour modulation was limited by the phosphors of the TV monitor which were derived from spectroradiographic measurements (Figure 7.1). The colour coordinates to achieve the required modulation along the R-G and B-Y axes were derived by firstly defining the limits of the monitor phosphor triangle within the CIE colour triangle and secondly determining the proportions of individual red, green and blue phosphors necessary to achieve the required CIE colour coordinates.

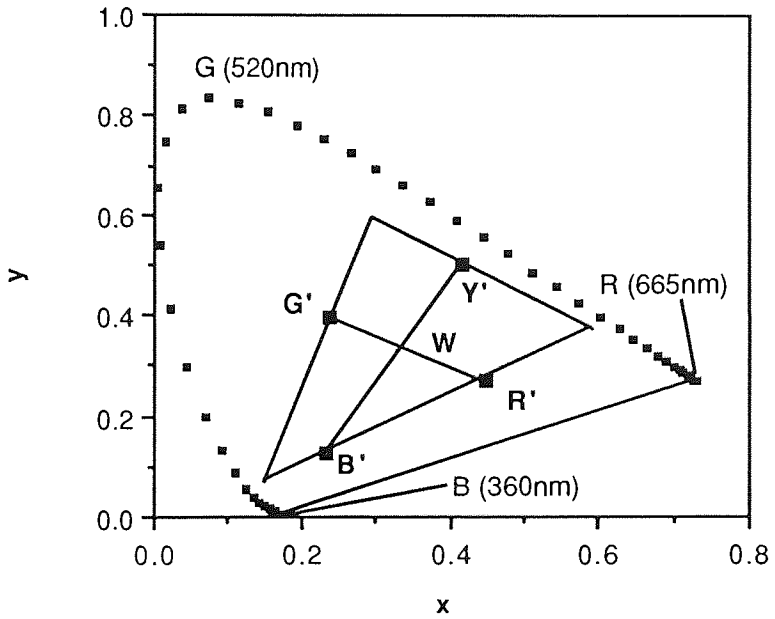

Figure 7.1 The CIE (1931) chromaticity diagram in relationship to the monitor phosphor triangle and the modulation axes for the colour contrast gratings. Maximum available modulation for the blue-yellow and red-green stimuli varied between the lines **B'** and **Y'**, **R'** and **G'** respectively. **W** represents the white point of the CIE colour triangle positioned at coordinates (0.33, 0.33).

The chromaticity coordinates for the three phosphors of the TV monitor were measured using the Bentham spectroradiometer (Bentham Instruments, Reading, UK):

Green (0.297,0.596)

Red (0.591, 0.374)

Blue (0.150, 0.072)

The red, green and blue coordinates defined a phosphor triangle within the CIE triangle, such that the colour coordinates for the required stimuli on the TV monitor were constrained within the limits of both these triangles. It was also assumed that both the R'-G' and B'-Y' modulation axes passed through the white point (W) defined by chromaticity coordinates (0.33, 0.33).

Using the CIE triangle and phosphor triangle coordinates, two sides of the phosphor triangle (Red-Green, Blue-Red) were defined:

Along the Red-Green phosphor line $y = 0.821 - 0.757x$

Along the Blue-Red phosphor line $y = -0.103 + 0.8067x$

Furthermore, using the CIE triangle and the phosphor triangle, the tritanopic confusion (B'-Y') axis were defined:

$$y = -0.355 + 2.076x$$

The B'-Y' axis intersects the Blue-Red region of the phosphor triangle, such that the colour coordinates can be derived by simple manipulation of the equation of their respective lines:

Equation for the Blue-Red phosphor line $y = 0.807x - 0.103$

Equation for the B'-Y' tritanopic line $y = 2.076x - 0.355$

$$0.807x - 0.103 = 2.076x - 0.355$$

$$0.25198 = 1.26946x$$

$$x = 0.199 \text{ and } y = 0.057$$

The B'-Y' axis also intersects the Red-Green region of the phosphor triangle. The colour coordinates were derived by simple manipulation of the equation of their respective lines:

Equation for the Red-Green phosphor line $y = 0.821 - 0.757x$

Equation for the B'-Y' tritanopic line $y = 2.076x - 0.355$

$$2.076x - 0.355 = -0.757x + 0.821$$

$$2.834x = 1.176$$

$$x = 0.415 \text{ and } y = 0.507$$

The two sets of theoretical coordinates (0.199, 0.057) and (0.415, 0.507) were those which lay within the phosphor triangle and identify the extremities of the B'-Y' tritanopic confusion line. Various proportions of each of the Red (R) and Blue (B) monitor phosphors were required to produce these stimulus coordinates. Using various phosphor combinations (%B, %R and %G), the resulting CIE coordinates were measured using the spectroradiograph until a match to the theoretical equation was found.

0% B	-40%	R (0.206, 0.109)	Error from equation	0.036
	-50%	R (0.195, 0.101)		0.051
	-30%	R (0.218, 0.116)		0.018
	-35%	R (0.212, 0.113)		0.028
	-20%	R (0.228, 0.123)		0.004
	-15%	R (0.233, 0.126)		-0.003

The equation of the line representing the proportion of red phosphor, %R, plotted as a function of the residual error was calculated:

$$y = 25.475 + 1.479x$$

where y represents the residual error and x represents the %R

For the minimum residual error y=0

$$x = -17.22$$

Therefore, the %R required to achieve the coordinates of the tritanopic confusion line of the Red-Blue region which resulted in the least error from the equation is -17.22%

At 0% B -17.22% R the CIE coordinates on the monitor were (0.233, 0.126)

A similar process was performed to calculate the actual coordinates which resulted in the least error of the Red-Green intersection from the B'-Y' tritanopic confusion line:

At 0% R, and -21.1% B, the CIE coordinates on the monitor were (0.417, 0.503)

The B'-Y' stimulus therefore varied between the coordinates (0.233, 0.126) and (0.417, 0.503).

The R'-G' confusion axis also has two theoretical extremities (based upon the CIE triangle and the TV phosphor triangle) and is orthogonal to the B-Y axis (Krauskopf et al 1982).

The equation of the R'-G' confusion axis was derived:

$$y = 0.493 - 0.482x$$

Various proportions of each of the Red and Blue TV phosphors were required to produce the correct stimulus coordinates. Combinations of Red and Blue phosphors were thus selected; the resulting CIE coordinates were measured using the spectroradiograph until a match to the theoretical equation was found.

0% R -80%	B (0.467, 0.288)	Error from equation	0.019
-70%	B (0.412, 0.248)		-0.146

The equation of the line representing the proportion of blue phosphor, %B, plotted as a function of the residual error was calculated:

$$y = -0.503 - 0.007x$$

where y represented the residual error and x represented the %B

For the minimum residual error y=0

$$x = -77.01$$

Therefore, the %B required to achieve the coordinates of the R'-G' confusion line of the Red-Blue region which resulted in the least error from the equation was -77.01%

At 0% R, -77.01% B, the CIE coordinates on the monitor were (0.451, 0.269)

A similar process was performed to calculate the actual coordinates which resulted in the least error of the Blue-Green intersection from the R'-G' confusion line:

At -50% B and -7.0% G the CIE coordinates on the monitor were (0.237, 0.379)

The R'-G' stimulus therefore varied between the coordinates (0.451, 0.269) and (0.237, 0.379).

The derived coordinates were based upon 100% of the maximum modulation. The colour contrast of the B'-Y' and R'-G' stimuli were therefore defined as a fraction of the maximum modulation along each of the two confusion axes. Furthermore, the colour contrast threshold was defined as the smallest detectable modulation along the two axes.

Before the measurement of colour contrast sensitivity was performed, the R-G and B-Y isoluminant points for each individual was measured. The determination of isoluminance on an individual basis ensured that later contrast sensitivity measurements were based upon purely chromatic discrimination rather than upon detection using luminance cues. The isoluminance point for all subjects and patients for each of the R'-G' and B'-Y' stimuli was separately measured using a modification of the minimum motion technique of Mullen (1985, 1991). Isoluminance was assumed to exist at the luminance ratio resulting in the largest difference in sensitivity from that recorded with an achromatic luminance modulated stimulus. Sinusoidal gratings of 1cpd, were presented on the monitor at a viewing distance of 1.25 metres. A low spatial frequency was selected to reduce luminance artifacts resulting from chromatic aberration (Mullen 1985; Thibos et al 1990; Bradley et al 1992) and was also considered optimal for the stimulation of the SWS pathways (Green 1968; Kelly 1974; Humanski and Wilson 1992). One eye only was examined in the study. Appropriate refractive correction for the testing distance was worn by all subjects and patients. The entire screen subtended 15° square to the eye. Using a transparent template, the screen was divided equally into eight equal vertical strips. The luminance ratio of the blue-yellow grating varied across the eight separate strips. Photometrically, the luminance of the screen varied from 0.3 log units below the isoluminant point to 0.3 log units above the isoluminant point. In addition, the stimulus flickered in counterphase at a temporal frequency of 10Hz. Those areas of the screen where luminance modulation was reduced were perceived either as stationary or at a minimum flicker. Subjects and patients were requested to select one of the eight strips of the B-Y grating where flicker was at a minimum. The selection indicated the isoluminant point of that individual. After selection, the procedure was repeated and the grating pattern was presented

again to the eye. The grating was photometrically positioned around the subjective isoluminant point; the range of luminance ratios extended from 0.15 log units below photometric isoluminance to 0.15 log units above photometric isoluminance. The selected luminance ratio resulting in minimum flicker indicated the isoluminant point. This procedure was repeated in an identical fashion for the red-green gratings. Both isoluminance ratios were used for the subsequent colour contrast threshold measurements. The use of individual isoluminance points reduced the influence of artifacts on the B-Y contrast threshold measurements which could have arisen from lenticular absorption and macular pigmentation.

Contrast threshold measurements were determined using a split-screen forced-choice method of stimulus presentation. Horizontal gratings (1 cpd) were presented and the individual was required to indicate whether the grating was in the upper or lower half of the screen. The luminance of the screen remained constant at $10cdm^{-2}$. Threshold was measured using an up- and down-staircase approach. The initial step size was 0.15 log units, which decreased to 0.075 log units after the first reversal. Threshold was estimated after a total of 5 reversals had been completed. The algorithm required two successive correct responses before the contrast was further reduced compared to an increase in contrast which required a single incorrect response. Threshold was repeated four times for each R-G and B-Y grating. The order of R-G and B-Y presentation was randomised within a given individual and also between individuals. The first threshold measurement recorded with each grating was discarded to minimise any learning effects. All CS measurements were performed on a separate occasion after all the visual field measurements had been completed. The monitor and colour generator were switched on at least one hour before the collection of data to ensure stability of the TV phosphors (Metha et al 1993). The glaucoma patients were not included in this study due to the difficulty in achieving isoluminance in areas of existing glaucomatous visual field loss (Yu et al 1991).

7.3.4. Analysis

Mean B-Y and R-G thresholds were calculated for each subject and patient from each of the three separate threshold measurements. A group mean mean contrast sensitivity and a group mean

isoluminance ratio was calculated for the B-Y and R-G gratings for both normal age groups. The B-Y and R-G sensitivities and the B-Y and R-G isoluminance ratios all exhibited normal distributions allowing standard parametric statistics to be applied to the data. The B-Y and R-G CS measurements for each patient were compared with respect to the mean age-matched normal CS values and the 95% confidence limits.

7.3.5 Results

The group mean contrast sensitivity and isoluminance ratios for the B-Y and R-G gratings for both the 60-69 and 70-82 year age groups are displayed in Table 7.1.

Contrast Sensitivity	60-69 yrs age group		70-82 yrs age group	
	Sensitivity	Isoluminance Ratio	Sensitivity	Isoluminance Ratio
B-Y	1.57 (0.13)	0.89 (0.12)	1.35 (0.15)	0.94 (0.12)
R-G	2.02 (0.14)	0.91 (0.13)	1.87 (0.14)	0.84 (0.11)

Table 7.1. Group mean colour contrast sensitivity and isoluminance ratios for the B-Y and R-G gratings for each of the two age groups of normal subjects. Values are expressed in log units. One standard deviation is given in parenthesis.

A repeated measures ANCOVA with grating colour as a within-subjects factor, diagnosis (ie normal or OHT) as a between-subjects factor and age as a covariate revealed that contrast sensitivity declined with age ($p<0.001$) and that the decline with age was greater for the B-Y grating ($p=0.008$) regardless of diagnosis ($p=0.140$) (Table 7.2). Furthermore, the B-Y CS was significantly lower than the R-G CS ($p<0.001$) irrespective of the diagnosis ($p=0.104$). The distribution of the B-Y and R-G CS as a function of age for the normal group is displayed in Figure 7.2.

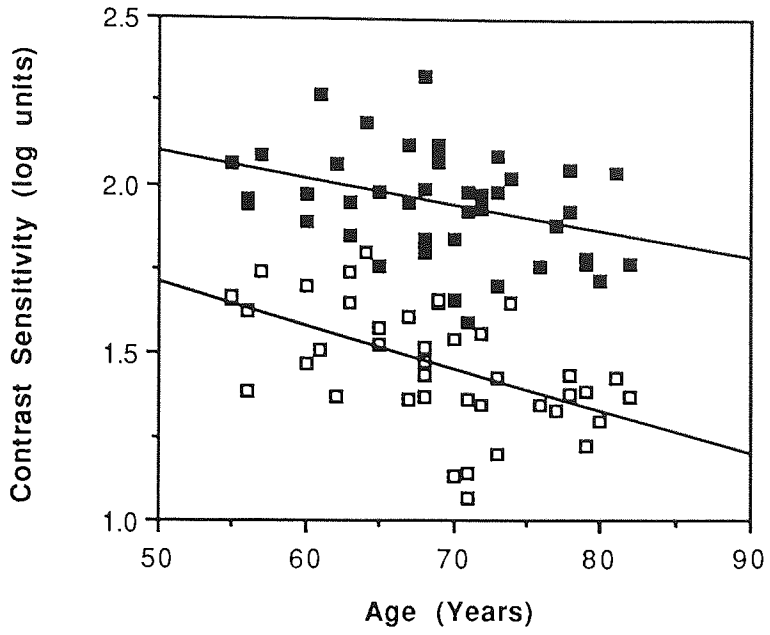

Figure 7.2 Colour contrast sensitivity plotted as a function of age for the normal subjects. Closed squares represent the sensitivity for R-G gratings, Open squares represents the sensitivity for B-Y gratings.

The individual distribution of B-Y and R-G sensitivities for the normal subjects and OHT patients in each age group is displayed in Figure 7.3. The B-Y and R-G sensitivities for the OHT patients were within the normal range for all individuals.

A repeated measures ANCOVA with grating colour as a within-subjects factor, diagnosis (ie normal or OHT) as a between-subjects factor and age as a covariate revealed that the isoluminance ratio did not alter with age ($p=0.316$) and was independent of the diagnosis ($p=0.770$) (Table 7.3). Overall, the magnitude of the B-Y isoluminance ratio was similar to that for the R-G grating ($p=0.132$) and this difference was independent of the diagnosis ($p=0.775$). In addition, the B-Y ratio increased with increase in age ($p<0.001$) particularly for the normal group ($p=0.026$). There was no relationship between the B-Y colour contrast sensitivity and the visual field B-Y mean sensitivity (Figure 7.4).

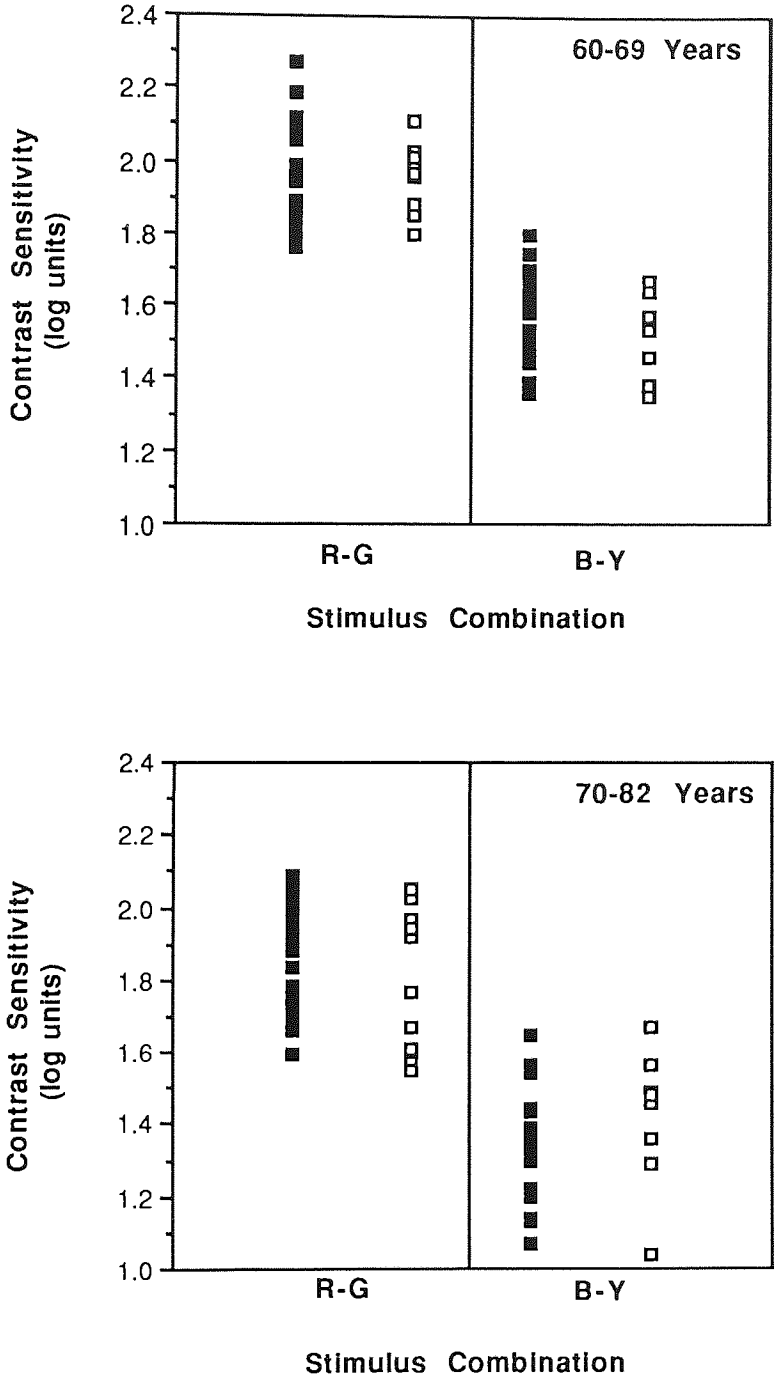

Figure 7.3. The distribution of individual contrast sensitivity measurements for the R-G and B-Y stimuli in the normal control group (closed squares) and the OHT group (open squares) for the 60-69 years age group (top) and 70-82 years age group (bottom).

Variable	dF	Sums of Squares	Mean Square	F value	P value
Age	1	1.682	1.682	43.759	p<0.001
Diagnosis	1	0.020	0.020	0.515	p=0.476
Age x Diagnosis	1	0.030	0.030	0.793	p=0.377
Error	65	2.499	0.038		
Colour	1	6.568	6.568	586.345	p<0.001
Age x Colour	1	0.085	0.085	7.588	p=0.008
Colour x Diagnosis	1	0.030	0.030	2.712	p=0.104
Age x Colour x Diagnosis	1	0.025	0.025	2.231	p=0.140
Error	65	0.728	0.011		

Table 7.2. Summary table for the repeated measures analysis of covariance of the colour contrast sensitivity.

Variable	dF	Sums of Squares	Mean Square	F value	P value
Age	1	0.015	0.015	1.020	p=0.316
Diagnosis	1	0.001	0.001	0.086	p=0.770
Age x Diagnosis	1	0.008	0.008	0.527	p=0.471
Error	65	0.956	0.015		
Colour	1	0.021	0.021	2.325	p=0.132
Colour x Diagnosis	1	0.001	0.001	0.083	p=0.775
Colour x Age	1	0.149	0.149	16.514	p<0.001
Age x Colour x Diagnosis	1	0.047	0.047	5.189	p=0.026
Error	65	0.585	0.009		

Table 7.3. Summary table for the repeated measures analysis of covariance of the isoluminance ratio.

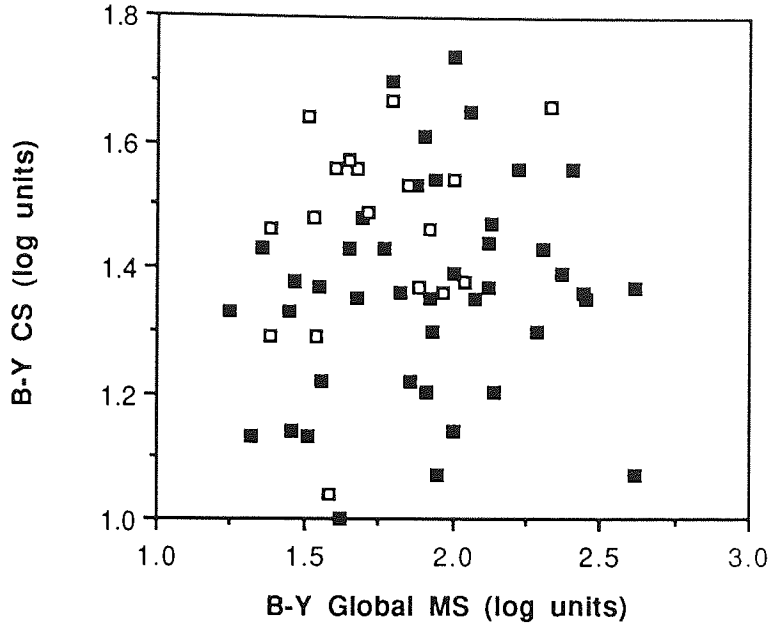

Figure 7.4. B-Y contrast sensitivity (CS) plotted as a function of B-Y global mean sensitivity (MS) for the normal subjects (closed squares) and OHT patients (open squares).

7.3.6. Discussion

The results of the study demonstrate that the normal B-Y CS is significantly lower than the corresponding R-G CS. However, the absolute sensitivity cannot be directly compared since the blue stimulus at 100% modulation has a reduced saturation compared to the R-G stimulus as a consequence of the smaller excitation range of the blue phosphor.

The increase in the B-Y isoluminance ratio with increasing age can be explained by an increase in the absorption of short wavelength stimuli with increase in age. The increased short wavelength absorption with age has been reported in previous studies (Pokorny et al 1987; Sample et al 1988b; Johnson et al 1988b; Savage et al 1993; Hudson and Wild 1993) and was demonstrated in Chapter 4. Interestingly, a moderate correlation was present between the individual ocular media absorption and the B-Y isoluminance ratio ($r=0.54$, $p<0.001$) (Figure 7.5).

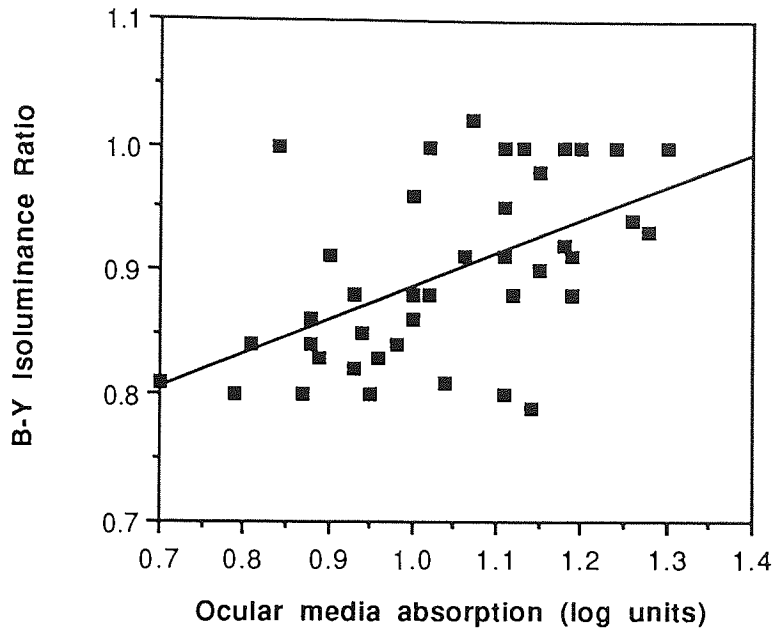

Figure 7.5 Individual ocular media absorption plotted as a function of the B-Y isoluminance ratio for the normal group. The slope represents the least squares linear regression function.

The colour CS for the R-G and B-Y gratings also shows a reduction with increase in age. This decline is consistent with the reduction in luminance contrast sensitivity with increase in age (Owsley et al 1983; Sekuler et al 1980; Ross et al 1985b; Elliott 1987; Tulunary et al 1988; Nameda et al 1989). The decline in B-Y sensitivity with increase in age was greater than that for the R-G sensitivity. A decline in B-Y sensitivity with age has been reported in other studies (Lakowski 1958; Pinckers 1980; Moreland 1972) and has been attributed to the yellowing of the crystalline lens (Said and Weale 1959; Ruddock 1965). The findings in the current study cannot be explained on the basis of ocular media yellowing since the individual measurement of the B-Y isoluminance ratio compensated for both ocular media and macular pigment absorption. In addition, macular pigmentation is independent of age (Ruddock 1965; Bone and Sparrock 1971; Pease et al 1987; Werner et al 1987; Bone et al 1988). Although the influence of forward light scatter has been demonstrated to preferentially reduce B-Y perimetric sensitivity in eyes with varying degrees of cataract, the influence of forward light scatter on the R-G isoluminance ratio and on R-G CS is greater than on the B-Y isoluminance ratio and B-Y CS (Steen et al 1994). In addition, since the sample demonstrated an absence of clinically significant cataract (LOCS <NI, <CII or <PI), forward light scatter was not considered to influence the findings. The decline in B-Y

CS with age could be attributed to a reduction in retinal luminance with age (Werner et al 1990) since a preferential loss of blue colour discrimination occurs when the retinal illuminance is reduced (Knoblach et al 1987). Furthermore, a reduction in CS with age has been attributed to a reduction in pupil size with age which also serves to reduce the retinal illuminance (Owsley et al 1983). The differential effect between the B-Y and R-G gratings is unlikely to be as a result of changes in pupil size since the monitor screen was maintained at a constant luminance of 10 cdm^{-2}.

Alternatively, the preferential reduction of SWS sensitivity with age compared to the other cone mechanisms could be explained on a neural basis. Such a theory has been proposed by Haegestrom-Portnoy et al (1989) who also demonstrated a greater decline in SWS sensitivity compared to LWS cone sensitivity. In the older groups approximately 0.2 log units of SWS loss was attributable to neural ageing (-0.05 log unit per decade) compared to a decline of only 0.01 log unit per decade in LWS sensitivity. The decline of B-Y sensitivity is also in agreement with the findings of other studies (Eisner et al 1987; Johnson et al 1988b; Schneck and Adams 1988). Functional losses of sensitivity with age have also been demonstrated in histological studies, particularly losses in the photoreceptors (Gartner and Henkind 1981; Yuodelis and Hendrickson 1986; Farber et al 1985; Marshall 1979; Marshall and Laties 1985). The neural loss of SWS sensitivity is also believed to be eccentricity dependent such that, due to the protective role of the macular pigment, SWS loss with age at the fovea is reduced compared to that in the extrafoveal region (Haegestrom-Portnoy et al 1988). The SWS pathways have also been suggested to be more vulnerable to damage than the other colour pathways (Harwerth and Sperling 1975; Sperling et al 1980; Hood et al 1984; Gunduz and Arden 1989). However, a similarity of the slope functions of the SWS and MWS / LWS pathways with age has also been reported (Werner and Steele 1988). The difference in the results between studies may be attributed to different testing protocols (Werner et al 1990). Indeed, Higgins and Jaffe (1988) reported a lower rate of decline in spatial luminance CS measured with a forced-choice technique than for the method of adjustments. Furthermore, Yu et al (1991) using isoluminance colour contrast sensitivity were

unable to demonstrated a decline in sensitivity with age along either the protan, deutan or tritan colour axes.

The results for the study are also in agreement with the findings of Falcao-Reis et al (1991) who demonstrated a considerable overlap between the central colour CS of OHT patients and the age-matched control group. Indeed, all of the OHT patients in the current study were inside the 95% limits for normality (Figure 7.3). Such an overlap in sensitivities between normals, OHT and glaucoma patients has also been reported for luminance CS (Sokol et al 1980; Hitchings et al 1981; Singh et al 1981; Stamper et al 1982; Phelps and Motolko 1982; Drance et al 1987c; Korth et al 1989; Maudgal et al 1988; Adams et al 1987a; Sample et al 1991b; Sponsel et al 1991; Mantyjarvi and Terasvirta 1993; Wood and Lovie-Kitchen 1992, 1993). Conversely, Yu et al (1991) reported a reduction of peripheral B-Y CS in 50% of high-risk OHTs prior to the development of W-W visual field loss. Although the sample in the current study comprised only 4 high-risk OHTs, all 4 patients were undergoing hypotensive therapy prior to inclusion to the study. The role of IOP control upon the mechanisms of central colour vision loss in glaucoma remain largely unknown. Lewis et al (1993), however, have reported an asymmetric reduction of central B-Y sensitivity in the eye with the highest pressure in patients with asymmetric IOP and normal conventional W-W fields. Falcao-Reis et al (1991) also discussed different types of colour vision loss in glaucoma: one type resulted in diffuse damage including the macular region whilst the other type was more focal in nature and did not involve the macula. Nevertheless, diffuse damage resulting in early central colour vision disturbances has been suggested to occur prior to any focal damage (Flammer 1985; Drance et al 1987c; Hart et al 1990). Interestingly, the results for the study described in Chapter 6 also indicate an absence of a diffuse reduction in B-Y sensitivity in the OHT group. This finding and the results recorded for colour CS may indicate an absence of diffuse loss in glaucoma. However, the sample used in the study may not be of the type considered to be at risk of the diffuse pattern of glaucomatous field loss.

Although the relatively small sample size may limit the impact of the findings of the study, the outcome of B-Y colour contrast sensitivity as a function of age in the normal eye and in the detection of early glaucoma remains equivocal.

CHAPTER 8: ASSESSMENT OF OPTIC NERVE HEAD TOPOGRAPHY WITH THE HEIDELBERG RETINAL TOMOGRAPH

8.1. Topographical assessment of the optic nerve head

An accurate and repeatable measurement procedure for topographical analysis of the optic nerve head is an essential requirement for the efficient detection and follow-up of glaucoma.

Quantitative documentation of the topography of the optic nerve head by ophthalmoscopy is principally limited to estimation of the cup / disc ratio (Lichter 1976; Sommer et al 1979; Klein et al 1987; Heijl and Bengtsson 1989; Montgomery and Craig 1993; Montgomery 1993). The diagnostic precision of the cup / disc ratio to predict the type and extent of W-W glaucomatous visual field loss is considered to be poor (O'Connor et al 1993; Damms and Dannheim 1993; Heijl and Molder 1993). Furthermore, the large normal between-subject variability in the cup / disc ratio, limits the use of this parameter in isolation (Lichter 1976; Montgomery and Craig 1993). The poor predictive ability of glaucomatous damage using the cup / disc ratio is further confounded by the dependence upon the total size of the optic disc (Bengtsson 1976; Jonas et al 1988b; Balaszi et al 1984; Caprioli and Miller 1987; Mikelberg et al 1986; Britton et al 1987).

An alternative technique for measurement of the optic nerve head involves photodocumentation in association with either manual (Douglas et al 1987; Mikelberg et al 1986; Varma et al 1989; Damms and Dannheim 1993) or computer assisted planimetry (Mikelberg et al 1984, 1985, 1986; Odberg and Riise 1985; Caprioli et al 1987b; Caprioli and Miller 1988; Funk et al 1988, 1993; Bishop et al 1988; Dandona et al 1989; Gramer and Siebert 1989; Jonas 1992; Tsai et al 1992; Airaksinen et al 1992; Fazio et al 1990; Hoskins et al 1993; Jonas et al 1993; Zeyen and Caprioli 1993; O' Connor et al 1993; Nanba and Iwata 1993; Tomita et al 1993). Photodocumentation may involve either conventional disc photography, stereophotography or stereovideophotography. The stereo techniques facilitate observation of the optic nerve head in three-dimensions (Cornsweet et al 1983; Donaldson et al 1980; Balazsi et al 1984; Airaksinen et al 1985a, b; Varma et al 1992; Peigne et al 1993; Katsumori et al 1993). Planimetry permits the measurement of the cup

diameter, disc diameter, neuroretinal rim width, cup / disc area ratio and neuroretinal rim area. Unfortunately, the measured parameters must also be corrected for the individual effects of magnification of the eye (Balazsi et al 1984). Indeed, Litmann (1982) described a mathematical method to correct the photographic image for the effects of ocular magnification which considered the refractive error, axial length and corneal power.

Comparisons of the measurements performed by manual planimetry with those of automated stereophotography have revealed a high degree of correlation (Mikelberg et al 1986; Douglas et al 1987; Varma et al 1989). The computerised form of image analysis is also highly reproducible (Caprioli et al 1986b; Varma et al 1988, 1989; Hoskins et al 1993) and less time-consuming than manual stereophotography (Mikelberg et al 1986). The variability in the topographical measurement of the optic nerve has been classified into a within-visit component (ie when an image is repeated within a given visit) and a between-visit component (ie the variability in images produced between different visits) (Hoskins et al 1993). Variability may arise due to variations which are operator dependent eg alignment, focussing and scanning depth, or variations which are dependent upon the patient eg fixation instability, accommodative microfluctuations, pupil size and quality of the optical media (Weinreb and Dreher 1991).

Unfortunately, both manual and automated techniques of image analysis based upon stereophotography are limited by the presence of media opacities and by a small pupil diameter (Weinreb et al 1989). In addition, the analysis for both techniques relies upon the correct delineation of the margins of both the disc and the cup to provide accurate data (Caprioli et al 1986b; Weinreb et al 1989; Damms and Dannheim 1993; Rohrschneider et al 1994). The accurate localisation of disc structures may also be limited by the presence of blood vessels across the optic nerve head (Weinreb et al 1989; Chihara and Honda 1991).

A relatively new technique for the assessment of optic nerve head topography is laser scanning tomography (Webb et al 1987; Weinreb et al 1989; Burk et al 1990, 1992, 1993; Zinser et al 1990; Kruse et al 1989; Dreher et al 1991; Cioffi et al 1993; Lusky et al 1993; Chihara et al 1993;

Manivannan et al 1994; Rohrschneider et al 1994; Tomita et al 1994). Laser scanning tomography is designed for the in-vivo three dimensional imaging and three dimensional measurement of the posterior segment of the eye.

Laser scanning tomography utilises the optical principle of confocal imaging (Figure 8.1). In a confocal imaging system, an illuminating light source, (usually a laser) is focused through a pinhole and imaged as a point source on the object of interest. The light is reflected backwards through the optical system and through a second pinhole to a detection system. Only light focused on the point of interest passes through the second pinhole. Light reflected from any other region on the image plane of focus or in a different plane of focus is attenuated. This procedure results in an enhanced contrast and an improved resolution of the required image. The laser beam is periodically deflected in two-dimensions by means of scanning mirrors or prisms so that a two dimensional view of the object can be scanned in a time sequence. The scanning process across the required object of interest results in the acquisition of an optical section. If a series of confocal optical section images is recorded sequentially and the position of the focal plane is changed along the optical axis, a volume of the object can be scanned. Alignment of the series of images using sophisticated computer software allows the topography of the object to be differentiated and permits the formation of an image of the object which is spatially resolved in three dimensions. As the detection of reflected light from only a single image point is recorded at any given time, the technique has the advantage of not being limited by the resolving power of photographic film. Furthermore, coincidence of the entrance and exit pupils within the optical system increases the proportion of reflected light from the retinal plane such that the quantity of light required to satisfactorily illuminate the retina is considerably less than for fundus cameras (Fechtner et al 1993; Masters 1994). In addition, compared to conventional imaging which illuminates an entire object, scanning laser tomography selects a small region of the object to be illuminated (ie scanned) for a short period of time. Hence reflected light from only that region is detected and the influence of intraocular light scatter on the quality of the image is reduced. The scanning strategy is repeated until the object of interest has been entirely scanned and an image of the surface outlined.

Measurements of selected features of interest using scanning laser tomography in model eyes (Dreher and Weinreb 1991; Janknecht and Funk 1994), in the normal eye (Burk et al 1993; Janknecht and Funk 1994) and in glaucomatous eyes (Burk et al 1993; Chihara et al 1993) are considered to be both accurate and reproducible. The reproducibility of the topographical measurement parameters is considered to be at least, if not better than, those obtained with previous stereoscopic techniques (Kruse et al 1989; Cioffi et al 1993; Chihara et al 1993; Mikelberg et al 1993; Rohrschneider et al 1994; Janknecht and Funk 1994). Furthermore, the confocal optical principal overcomes the limitations of earlier imaging systems such that images can be obtained through natural pupils of at least 2.5mm in diameter (Lusky et al 1993; Burk et al 1993) and in the presence of early media opacities (Burk et al 1993; Manivannan et al 1994). The repeatability of topographical parameters is reduced, however, in eyes undergoing pilocarpine therapy (Tomita et al 1994).

8.2 Relationship between optic nerve topography and the W-W visual field

Various features of the glaucomatous optic nerve head derived by planimetry, stereophotography or laser scanning tomography have been compared to the conventional W-W visual field indices. Comparisons of the neuroretinal rim area have demonstrated various types of relationship with the W-W visual field index MD. When the results of normals and OHTs are included alongside those from glaucoma patients, the relationship is either absent (Balazsi et al 1984; Caprioli et al 1987b; Lachenmayr et al 1991a; Zeyen et al 1992; Zeyen and Caprioli 1993; Chihara et al 1993), a weak linear function or a curvilinear function ($r=0.48$ - 0.84) (Airaksinen et al 1985b; Jonas et al 1988a; Drance et al 1987c, 1989; Caprioli and Miller 1987; Guthauser et al 1987; Nanba and Iwata 1993). The lack of strong correlation implies structural change prior to functional loss. The different relationships between structure and function may arise due to the considerable normal between-subject variation in total neuroretinal rim area, which is dependent on the total disc area (Britton et al 1987). Indeed, Chihara et al (1993) found that the correlation with MD increased from 0.42 to 0.84 when the neuroretinal rim area / disc area ratio was used. Alternatively, differences in the nature of the samples may account for the differences in the type of

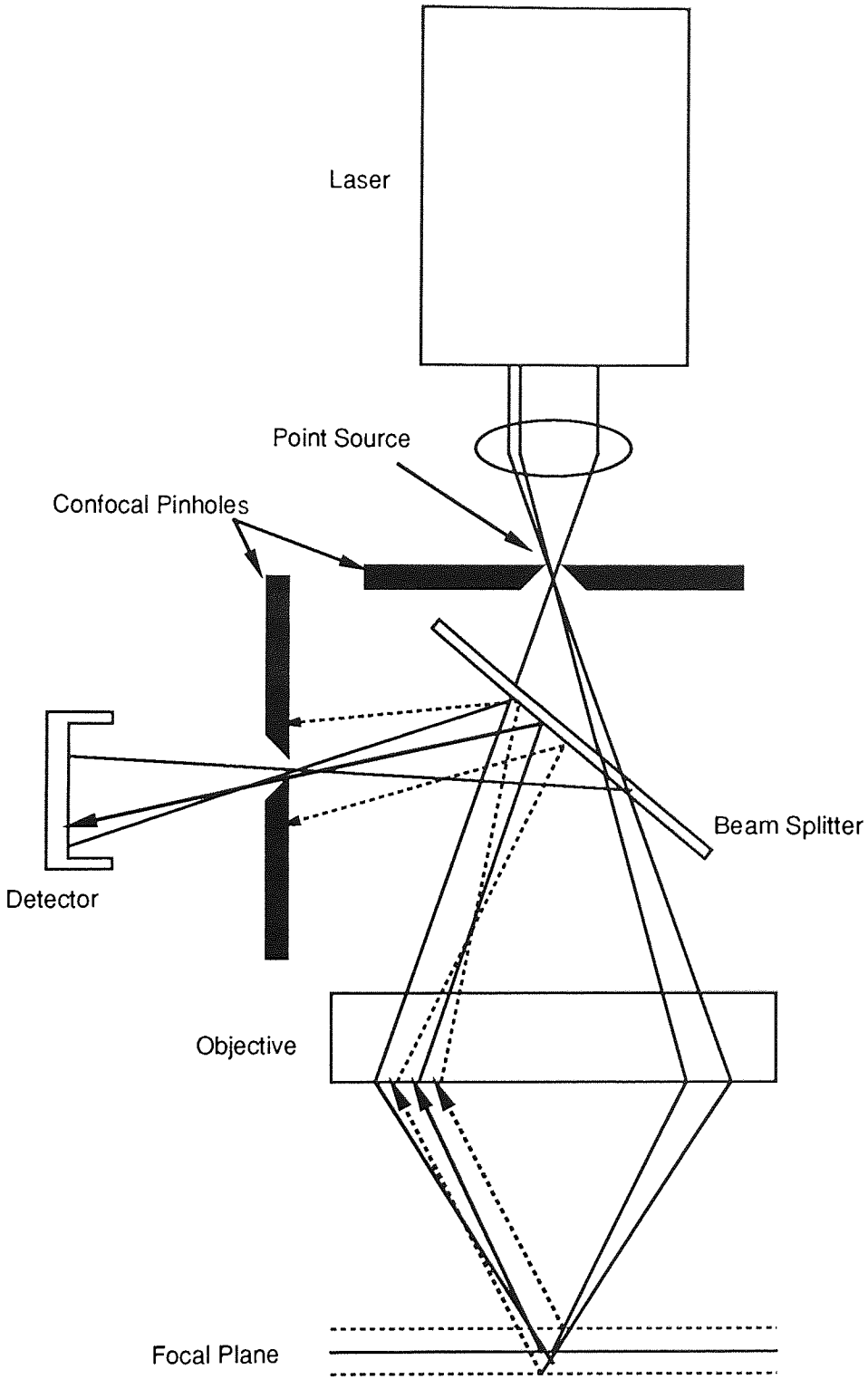

Figure 8.1. The optical principle of confocal imaging using laser scanning tomography. Two confocal pinholes are positioned conjugate to the focal plane. The solid lines represent light reflected from the actual focal plane which is subsequently focused at the plane of the detector. The dashed lines represent light reflected from outside the focal plane which is not focused at the plane of the detector.

differences in the relationship. Indeed, the ability of structural measurements and of W-W perimetry to identify progression in glaucoma is considered to be dependent upon the stage of the glaucomatous disease process (Funk et al 1988; Airaksinen et al 1992; Zeyen and Caprioli 1993). Evaluation of the disc is considered to be more sensitive in detecting the earliest signs of glaucoma prior to any recorded W-W visual field loss (Balazsi et al 1984; Caprioli et al 1987b; Funk et al 1988; Zeyen et al 1992; Zeyen and Caprioli 1993; Chihara et al 1993); however, in the later stages of the disease identification of progression is more reliable by observation of the visual field characteristics (Hitchings and Spaeth 1977; Funk et al 1988; Zeyen and Caprioli 1993). Furthermore, the application of the MD index, which is considered to be sensitive to a generalised reduction in sensitivity (Flammer 1986) has been criticised because of the inability to detect localised changes in the optic nerve head (Drance et al 1989). Indeed, the visual field index CLV, which is more sensitive to localised visual field loss, has been demonstrated to improve the differentiation between normal and glaucomatous optic nerve head appearance, particularly in conjunction with the vertical cup / disc ratio (Drance et al 1987c).

Psychophysical tests, such as contrast sensitivity, motion detection, flicker sensitivity and colour vision assessment selectively stimulate a particular visual channel and have been reported to be more sensitive in the earliest detection of glaucomatous damage. The relationship between such functional parameters and the results recorded from these psychophysical tests has been recently investigated. Using scanning laser tomography, Ruben and Fitzke (1994) demonstrated a moderate linear relationship between the neuroretinal rim area and the movement displacement threshold in a sample of 51 OHTs ($r=0.43$). However, a poor correlation is present between the neuroretinal rim area in glaucoma, measured by automated stereophotography, and both Farnsworth-Munsell 100-hue colour vision score ($r=0.19$) and flicker ($r=0.25$) (Lachenmayr et al 1991a). Conversely, Balazsi et al (1984) reported a statistically significant correlation between neuroretinal rim area and both 100-Hue score ($r=0.51$) and spatial contrast sensitivity ($r=0.69$, 3cpd) in a mixed sample of normals, OHTs and glaucoma patients. The relationship between the appearance of the optic nerve head and the functional integrity of the SWS pathways recorded by B-Y automated perimetry is unknown.

8.3. Relationship between SWS function and the optic disc parameters determined by laser scanning tomography

8.3.1. Aim of the study

The aim of this study was twofold; firstly to determine the distribution of various optic disc parameters in normal subjects and in OHT and POAG patients; and secondly, to determine any relationship in the OHT and POAG groups between the various topographical parameters and the W-W and B-Y visual field.

8.3.2 Materials and methods

Sample

The study comprised three samples: a normal age-matched control group, an OHT sample and a POAG sample.

Normal age-matched control group

The normal control group comprised 20 of the 50 age-matched normal subjects randomly recruited for the study described in Chapter 6. The inclusion criteria have been described in Section 6. 2.2. One eye, only, of each age-matched normal subject was selected for the study.

POAG group

The POAG sample comprised 24 patients (mean age 69.2 years SD 8.7) recruited from the Glaucoma Department of the Birmingham and Midland Eye Hospital for the study described in Chapter 6. The inclusion criteria, W-W visual field characteristics and treatment protocol have been outlined in Section 6.2.2.

OHT group

The OHT sample comprised 25 of the 27 patients (mean age 68.2 years (SD 6.4)) also consecutively recruited from the Glaucoma Department of the Birmingham and Midland Eye

Hospital for the study described in Chapter 6. The inclusion criteria, W-W visual field characteristics and risk classification have been outlined in Section 6.2.2.

One eye, only, of each patient was examined. The criteria for the choice of the eye used for the study has also been detailed in Section 6.2.2.

Perimetry

All subjects and patients underwent both W-W and B-Y perimetry. The perimetric procedure and subsequent data analysis has been described fully in Section 6.2.2. The B-Y data was corrected for individual ocular media absorption.

Scanning Laser Tomography

The structure of the optic nerve head was analysed using the Heidelberg Retinal Tomograph (HRT). The optical principle of this instrument has been described in Section 8.1. The system comprises a laser scanning system (Helium-Neon laser; operating wavelength 670nm; maximum laser output intensity 180μW; maximum radiance 15mWcm^{-2}sr^{-1}) mounted on an appropriate stand with a chin-rest for the subject and a computer system. At a given focal plane, the optic nerve is scanned in a short time interval (approximately 0.032 seconds, 20Hz) around an x, y, plane. The procedure forms a single confocal image. At a given location (x, y) the maximum intensity of reflected light from the optic nerve along the optical axis z, within the confocal system is recorded. The point of maximum reflectance is termed the peak of the z-profile at the location (x, y) and represents the height of the structure examined at the corresponding location (x, y). A series of height measurements generates a topographical map allowing planimetric and stereometric measurements of the structure under observation - in this case the optic nerve head. The topographical map is presented in the form of a video image and stored within the computer system. Each confocal image contains a matrix of 256 x 256 pixels. The HRT records a series of 32 confocal images at different focal planes (ranging from 0.5 to 4.0mm in depth) along the optical axis of the instrument. The total time for the completion of the entire image series is approximately 1.6 seconds. The series of 32 images are aligned and stacked by the computer to

form a single topographical image of the optic nerve head in three dimensions. Furthermore, the volume of the optic nerve can also be observed.

The size of the scanned field was set at 10 x 10 degrees. Prior to examination of each subject and patient, the individual refractive error and keratometry readings were installed into the computer to allow accurate determination of the focal image plane. Each patient and subject was positioned on the chin rest and requested to constantly view a distant fixation target. The laser was directed into the natural pupil and aligned correctly in real-time upon the optic nerve using the joystick. The exposure and focus was adjusted by the operator and the nerve head positioned in the centre of the monitor display after which the image series was acquired. Quality control software (Version 1.11) indicated the degree to which the focus, exposure and scan depth were suitable for further topographical analysis. The acquisition of the image series was repeated at least three times (Weinreb et al 1993). Any image series considered by the operator to be inadequate either due to fixation instability and / or poor image quality was discarded without further analysis. Scanning laser tomography was performed after all perimetric examinations had been completed. All topographical data was stored on the computer hard disc and analysed on a later occasion.

8.3.3 Analysis

The mean of three topographical images was derived based upon the minimum overall standard deviation in contour height. Any individuals exhibiting a standard deviation of the mean retinal height measurement greater than 50μm were excluded from the subsequent data analysis (Heidelberg software manual Version 1.11). For this reason 2 normal subjects, 1 OHT and 2 POAG patients were eliminated from the analysis at this stage.

The topographical analysis of the optic nerve head with the HRT is described by the stereometric measurement of the nerve head. Using the trackball, a contour line was drawn free-hand around the optic nerve head displayed on the computer monitor. Within this defined area the computer determined the stereometric properties of the structure for the entire nerve head and also for the

superior and inferior components. The height of structures within the contour line are based upon a standard reference plane to which all measurements are compared. Using the default setting on the HRT, this reference plane is located 50μm posteriorly of the mean contour line height between -10° and -4° (Heidelberg Software Manual 1994, Version 1.11). Stereometric parameters of the optic nerve head were generated for all 18 normal subjects and 46 patients.

The disc area, cup area, cup / disc area ratio, neuroretinal rim area, rim / disc area ratio, cup volume, mean cup depth and mean retinal nerve fibre layer (RNFL) thickness measurements were generated. The disc area was defined as the area within the defined contour line. The cup area and associated parameters were defined with reference to the region within the contour line which lay below the standard reference plane. The mean RNFL thickness was defined as the mean height of the retinal surface along the defined contour line and above the standard reference plane. To minimise the influence of total optic disc diameter upon the analysis a further 3 OHTs and 11 POAGs who had a total disc area which was beyond 2 standard deviations of the group mean mean disc area in the normal group, were also discarded from the analysis (C O'Brien (1994); personal communication). The revised sample comprised 18 normals, 22 OHT and 13 POAG patients. Each disc parameter of the normal subjects were compared with those of the OHT and glaucoma patients. In addition, the global perimetric indices: W-W MD, B-Y MD, W-W CPSD and B-Y CPSD (Chapter 6) were compared to the structural stereometric measures of the entire optic disc. In addition, the W-W and B-Y inferior and superior hemifield MDs were compared to the respective hemifield structural parameters of each disc.

8.3.4. Results

The group mean standard deviation for the overall height measurement was 32.48μm (SD 8.91), 31.70μm (SD 7.07) and 39.21μm (SD 6.37) for the normal age-matched group, OHT and POAG patients respectively. Analysis of covariance (ANCOVA) with diagnostic category (ie normal, OHT and POAG) as between-subjects factors and age as a covariate revealed that the variability of height measurements increased with age ($p=0.001$) irrespective of the diagnostic category

(p=0.307) (Table 8.1). The magnitude of the SD was significantly higher in the POAG group (p=0.005).

Variable	dF	Sums of Squares	Mean Square	F value	P value
Age	1	2.346×10^6	2.346×10^6	11.893	p=0.001
Diagnosis	2	2.359×10^6	1.180×10^6	5.981	p=0.005
Age x Diagnosis	2	4.782×10^5	2.391×10^5	1.212	p=0.307
Error	46	9.269×10^6	1.972×10^5		

Table 8.1. Summary table for the analysis of covariance for the standard deviation of the retinal height measurement.

Total Disc Analysis

The group mean mean stereometric parameters for the normals, OHT and glaucoma patients are displayed in Table 8.2 and the respective distributions in Figure 8.2 and 8.3.

	Diagnosis		
Stereometric Parameter	Normal	OHT	POAG
Optic Disc Area (mm^2)	1.69 (0.26)	1.81 (0.39)	1.92 (0.50)
Optic Cup Area (mm^2)	0.40 (0.28)	0.65 (0.46)	0.95 (0.48)
Neuroretinal Rim Area (mm^2)	1.18 (0.24)	1.11 (0.24)	0.97 (0.27)
Rim / Disc Area	0.76 (0.15)	0.66 (0.20)	0.52 (0.16)
Cup / Disc Area	0.24 (0.15)	0.34 (0.20)	0.48 (0.16)
Optic Cup Volume (mm^3)	0.08 (0.08)	0.20 (0.21)	0.30 (0.25)
Mean Cup Depth (mm)	0.21 (0.11)	0.25 (0.12)	0.30 (0.10)
Mean RNFL thickness (mm)	0.26 (0.09)	0.21 (0.06)	0.19 (0.07)

Table 8.2. Group mean mean stereometric parameters for the normal subjects, OHT and POAG patients. One standard deviation is given in parenthesis.

The distribution of each stereometric parameter for the entire disc for each individual within each diagnostic category is displayed in Figures 8.4 and 8.5. It is evident that considerable between-subject variation exists for each parameter within each group. The variability leads to overlap between all three diagnostic groups.

Analysis of covariance (ANCOVA) with diagnosis (ie normal, OHT or POAG) as a between-subjects factor and age as a covariate was separately carried out for each of the stereometric disc parameters.

The total mean disc area was independent of age (p=0.80) (Table 8.3). Furthermore, the disc area was similar across the three diagnostic categories (p=0.06), regardless of age (p=0.30).

Variable	dF	Sums of Squares	Mean Square	F value	P value
Age	1	0.009	0.009	0.062	p=0.804
Diagnosis	2	0.925	0.462	3.097	p=0.055
Age x Diagnosis	2	0.369	0.184	1.235	p=0.300
Error	46	6.870	0.149		

Table 8.3. Summary table for the analysis of covariance for the total optic disc area.

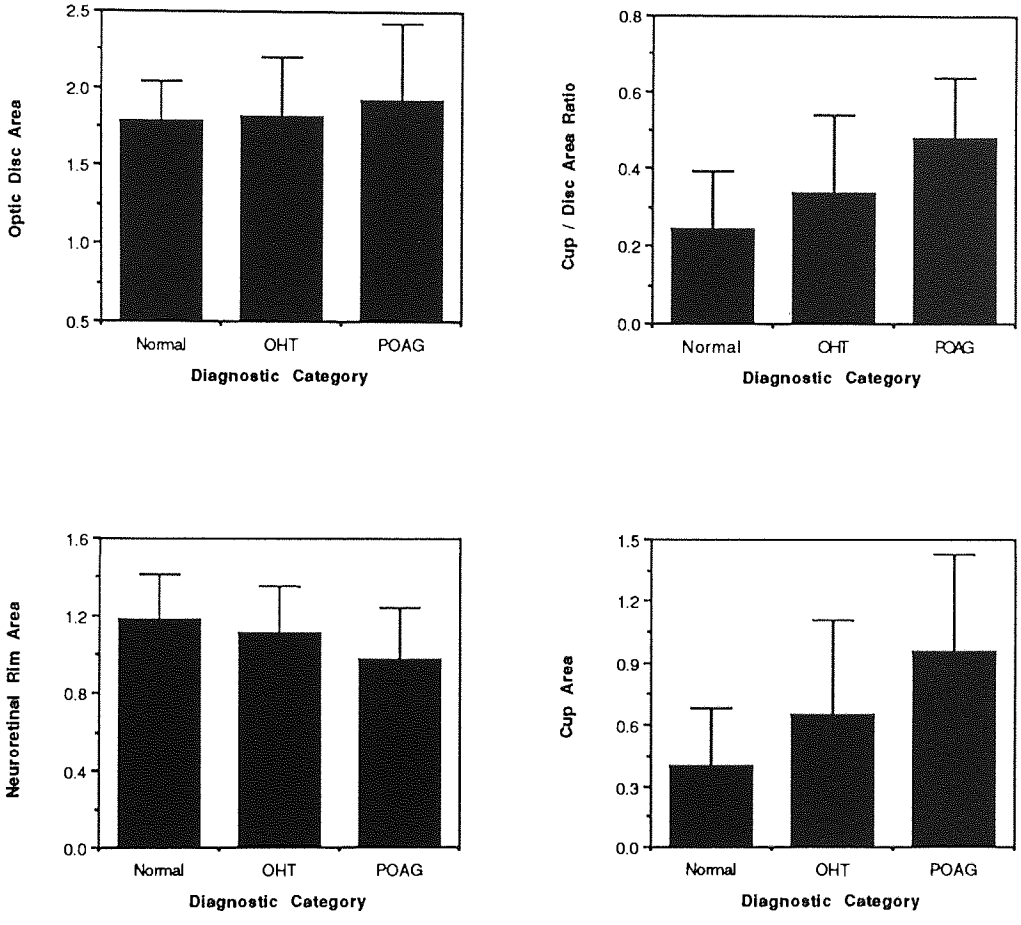

Figure 8.2. Group mean: total optic disc area (mm^2) (upper left), total neuroretinal rim area (mm^2) (lower left), total cup / disc area (upper right), total cup area (mm^2) (lower right) as a function of diagnostic category. Note the vertical scales of each graph are different. Error bars represent one standard deviation of the mean.

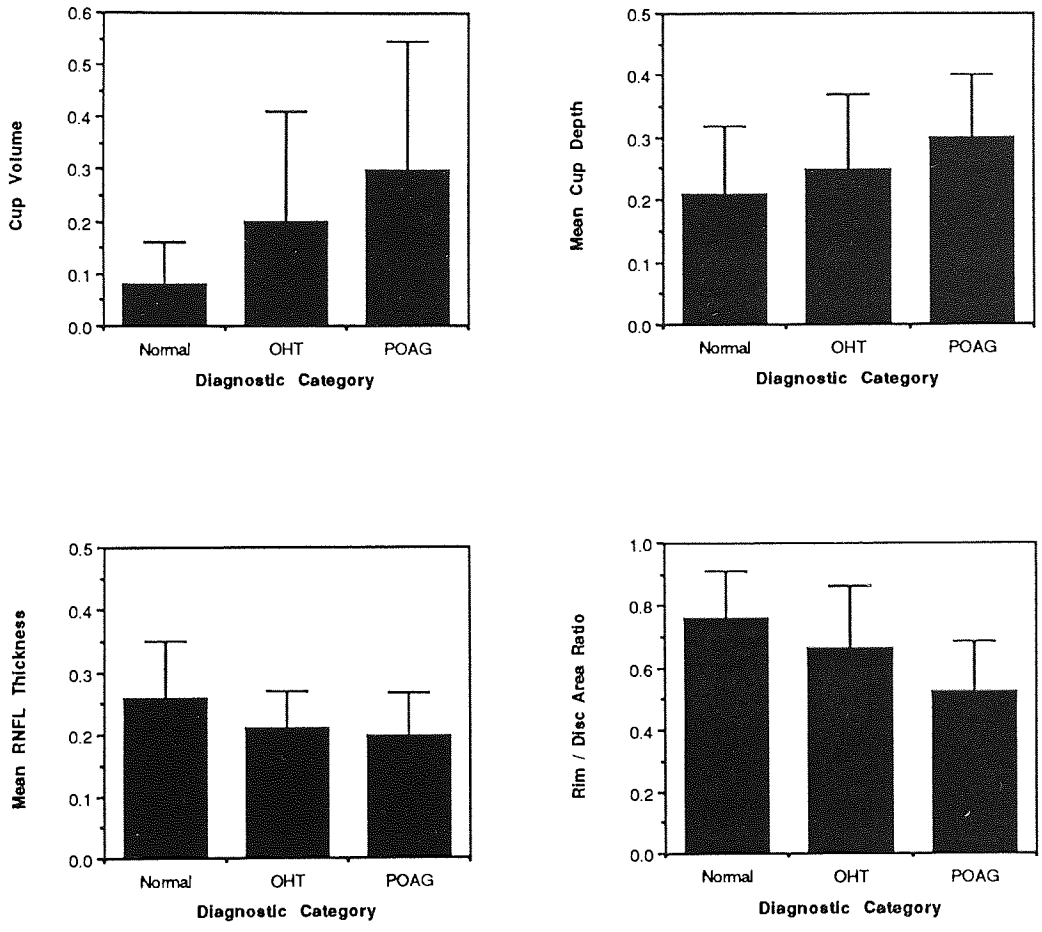

Figure 8.3. Group mean: total cup volume (mm^3) (upper left), total mean RNFL thickness (mm) (lower left), total mean cup depth (mm) (upper right), total neuroretinal rim / optic disc area ratio (lower right) as a function of diagnostic category. Note the vertical scales of each graph are different. Error bars represent one standard deviation of the mean.

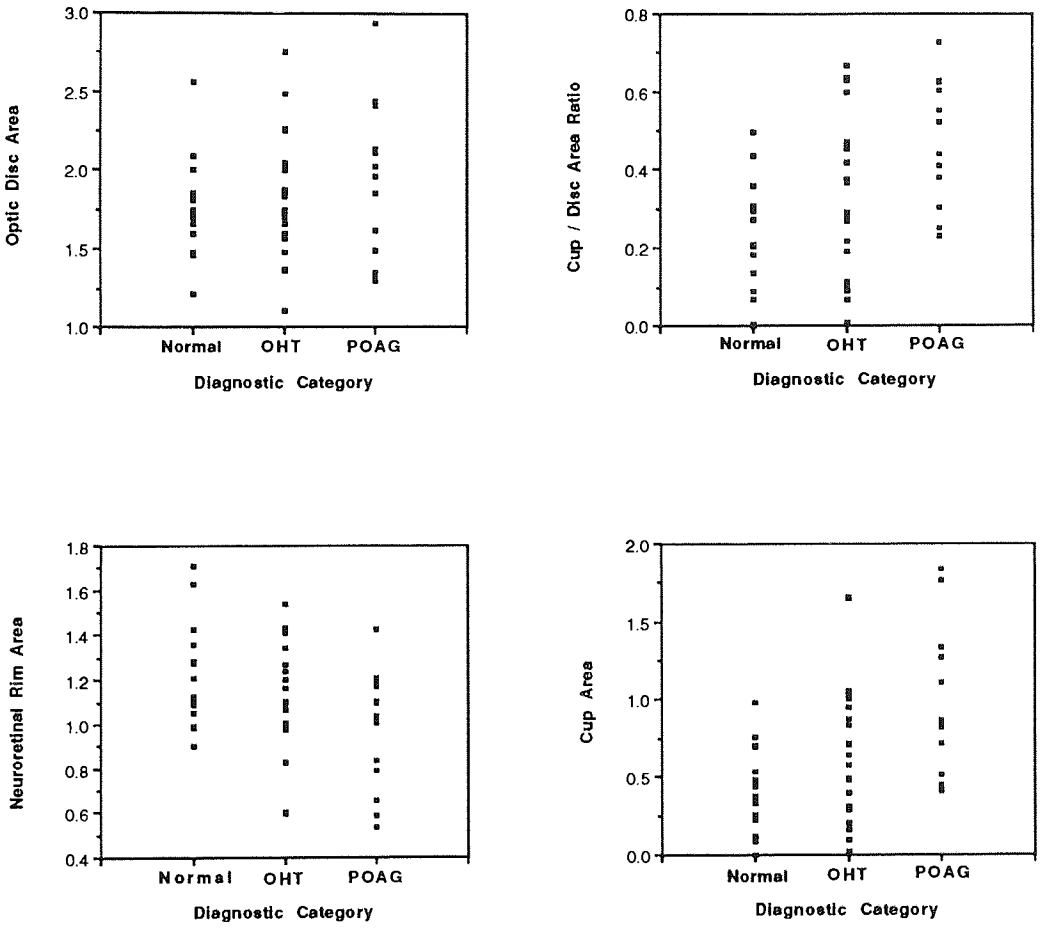

Figure 8.4. Distribution of the stereometric parameters: total optic disc area (mm^2) (upper left), total neuroretinal rim area (mm^2) (lower left), total cup / disc area ratio (upper right) and total cup area (mm^2) (lower right) as a function of diagnostic category. Each data point represents an individual subject or patient. Note the vertical scales of each graph are different.

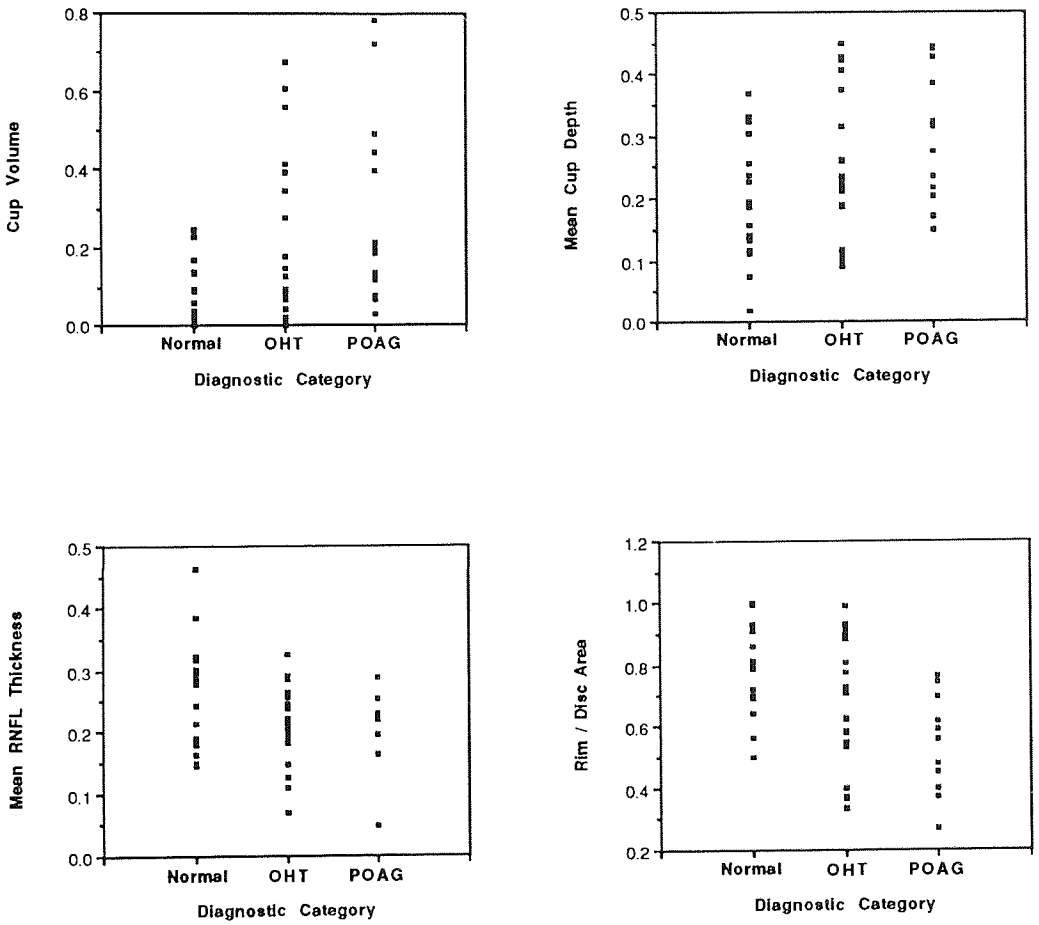

Figure 8.5. Distribution of the stereometric parameters of the total optic nerve head: total mean cup volume (mm^3) (upper left), total mean RNFL thickness (mm) (lower left), total mean cup depth (mm) (upper right) and total neuroretinal rim / optic disc area ratio (lower right) as a function of diagnostic category. Each data point represents an individual subject or patient. Note the vertical scales of each graph are different.

The area of the optic cup was independent of age (p=0.36) and the independence from age was similar across all groups (p=0.83). As would be expected the cup area differed between the groups (p=0.004) (Table 8.4). The degree of cupping was similar between the normal and OHT groups (t=1.94, p=0.06) and between the OHT and POAG groups (t=1.884, p=0.07). However, the cupping exhibited by the normal group was significantly less than that exhibited by the POAG group (t=3.449, p=0.001). The area of the cup increased as the disc area increased (r=0.67, p<0.001).

Variable	dF	Sums of Squares	Mean Square	F value	P value
Age	1	0.153	0.153	0.849	p=0.362
Diagnosis	2	2.218	1.109	6.143	p=0.004
Age x Diagnosis	2	0.068	0.034	0.189	p=0.829
Error	46	8.305	0.181		

Table 8.4. Summary table for the analysis of covariance for the total disc cupping.

The area of the total neuroretinal rim was independent of age (p=0.39) and the independence from age was similar across all groups (p=0.23) and was similar in magnitude irrespective of the diagnostic category (p=0.07) (Table 8.5). For the OHT and POAG groups combined, the neuroretinal rim area was unrelated to the disc area (r=0.161, p=0.362); however, the rim area was to some extent correlated with the cup volume (r=-0.508, p=0.002) and with the mean cup depth (r=-0.384, p=0.025). The parameter rim / disc area ratio reduces the influence of the optic disc area upon the neuroretinal rim area. Although independent of age (p=0.28) the rim / disc area ratio was significantly different between the three categories (p=0.003) (Table 8.6). The ratio in the normal subjects was similar to that of the OHTs (t=1.801, p=0.08); however, the ratio was significantly less in the POAG group compared to that exhibited for the normal subjects (t=3.539, p<0.001). Interestingly, the total rim / disc area ratio in the OHT group was significantly different from that in the glaucoma group (t=2.053, p=0.05). For the OHT and POAG groups the rim / disc

area correlated highly with the cup volume (r=-0.926, p<0.001) and moderately with cup depth (r=-0.705, p<0.001) (Figure 8.6).

Variable	dF	Sums of Squares	Mean Square	F value	P value
Age	1	0.046	0.046	0.764	p=0.387
Diagnosis	2	0.336	0.168	2.792	p=0.072
Age x Diagnosis	2	0.183	0.091	1.517	p=0.231
Error	46	2.710	0.060		

Table 8.5. Summary table for the analysis of covariance of the total neuroretinal rim area.

Variable	dF	Sums of Squares	Mean Square	F value	P value
Age	1	0.037	0.037	1.217	p=0.003
Diagnosis	2	0.409	0.205	6.659	p=0.276
Age x Diagnosis	2	0.003	0.002	0.051	p=0.950
Error	46	1.414	0.031		

Table 8.6. Summary table for the analysis of covariance of the total neuroretinal rim / disc area ratio.

Overall, the total mean cup / disc area ratio was also independent of age (p=0.27)(Table 8.7). However, it differed between the groups (p=0.003) and was significantly greater in the POAG group compared to the normal groups (t=3.541, p<0.001). The ratio was not significantly different between either the normal and the OHTs (t=1.802, p=0.078) or between the OHT and the POAG (t=2.055, p=0.046) groups.

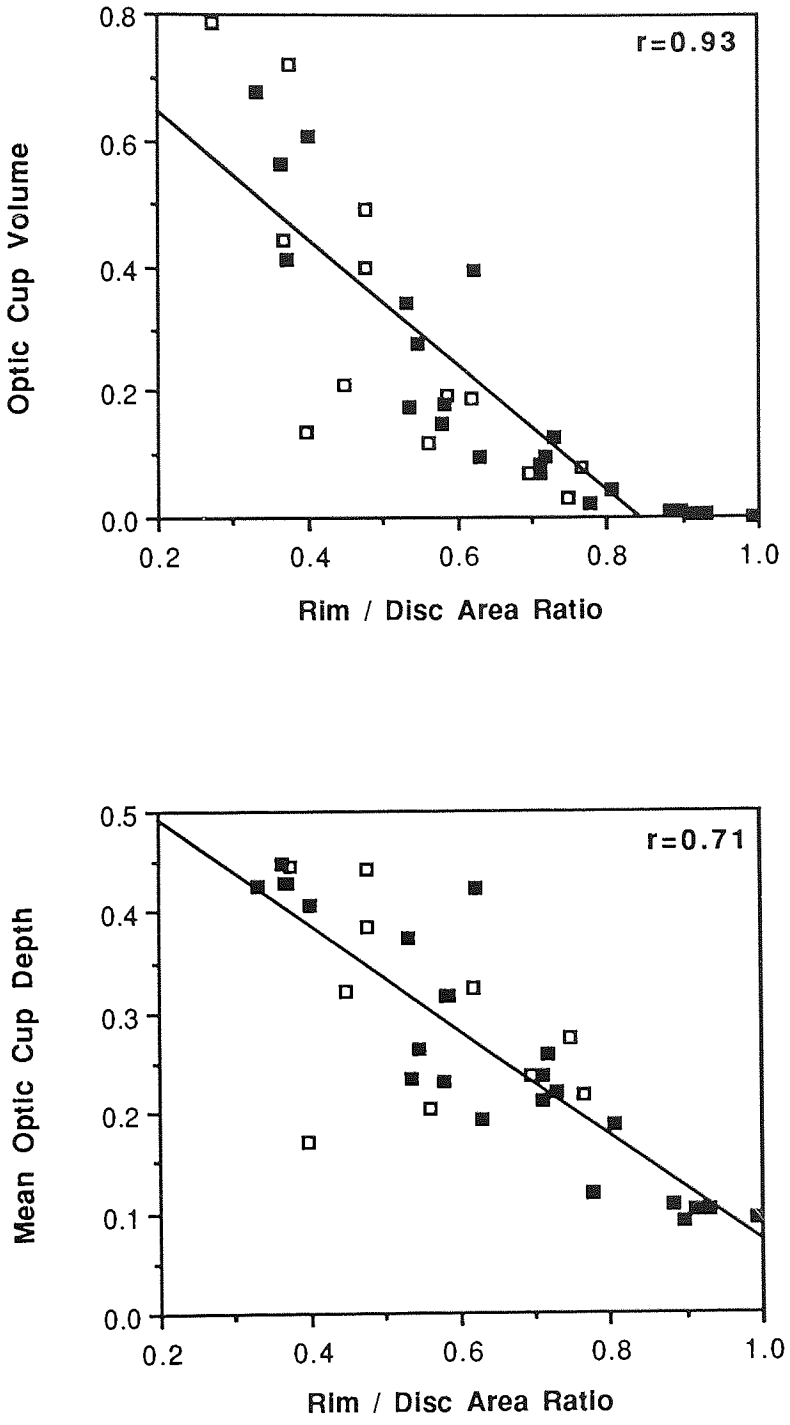

Figure 8.6. The mean cup volume (mm^3) (top) and the mean cup depth (mm) (bottom) plotted as a function of the total mean rim / disc area ratio for the OHT (filled squares) and the POAG (open squares) patients. Slopes represent the least squares regression lines. Note the vertical axes of each graph are on different scales.

Variable	dF	Sums of Squares	Mean Square	F value	P value
Age	1	0.038	0.038	1.231	p=0.273
Diagnosis	2	0.410	0.205	6.670	p=0.003
Age x Diagnosis	2	0.003	0.002	0.052	p=0.950
Error	46	1.414	0.031		

Table 8.7 Summary table for the analysis of covariance for the total cup / disc area ratio.

Consistent with the other described parameters, the volume was also independent of age (p=0.82). The total optic cup volume was significantly different between the diagnostic groups (p=0.014) (Table 8.8). The ratio was significantly greater in the POAG group compared to the normal group (t=2.984, p=0.005). The ratio in the OHT group was not significantly different from that in either the normal (t=1.919, p=0.061) or the POAG (t=1.364, p=0.179) groups. For the OHT and POAG patients there was a weak correlation between the cup volume and the mean RNFL thickness (r=-0.444, p=0.011).

Variable	dF	Sums of Squares	Mean Square	F value	P value
Age	1	0.002	0.002	0.053	p=0.820
Diagnosis	2	0.358	0.179	4.655	p=0.014
Age x Diagnosis	2	0.022	0.011	0.288	p=0.751
Error	46	1.768	0.038		

Table 8.8. Summary table for the analysis of covariance of the total optic cup volume.

There was no significant difference in the total mean mean cup depth between the diagnostic groups (p=0.10), the depth was also independent of age (p=0.70) (Table 8.9). Furthermore, there was no significant difference in the total mean RNFL thickness across the diagnostic groups (p=0.06) and this parameter was also independent of age (p=0.19). However, the rim area increased as the mean RNFL thickness increased (r=0.539, p=0.002). Furthermore, there was a

negative correlation between the cup / disc area ratio and the mean RNFL thickness and between the neuroretinal rim / disc area ratio and the mean RNFL thickness (Figure 8.7).

Variable	dF	Sums of Squares	Mean Square	F value	P value
Age	1	0.002	0.002	0.151	p=0.700
Diagnosis	2	0.062	0.031	2.398	p=0.102
Age x Diagnosis	2	0.030	0.015	1.173	p=0.319
Error	46	0.591	0.013		

Table 8.9. Summary table for the analysis of covariance of the total mean cup depth.

Variable	dF	Sums of Squares	Mean Square	F value	P value
Age	1	0.032	0.009	1.764	p=0.191
Diagnosis	2	0.062	0.016	3.046	p=0.058
Age x Diagnosis	2	0.011	0.005	1.008	p=0.373
Error	46	0.224	0.005		

Table 8.10. Summary table for the analysis of covariance of the total mean RNFL thickness.

The relationship between the visual field indices MD and CPSD for both the W-W and B-Y stimulus combinations are displayed in Figures 8.8-8.11. A weak linear relationship was evident for both the MD indices plotted as a function of the neuroretinal rim area and the rim / disc area ratio and a possible curvilinear relationship for both the CPSD indices. No relationship was evident between any of the visual field indices and any of the parameters cup / disc ratio, cup volume, mean cup depth and mean RNFL thickness.

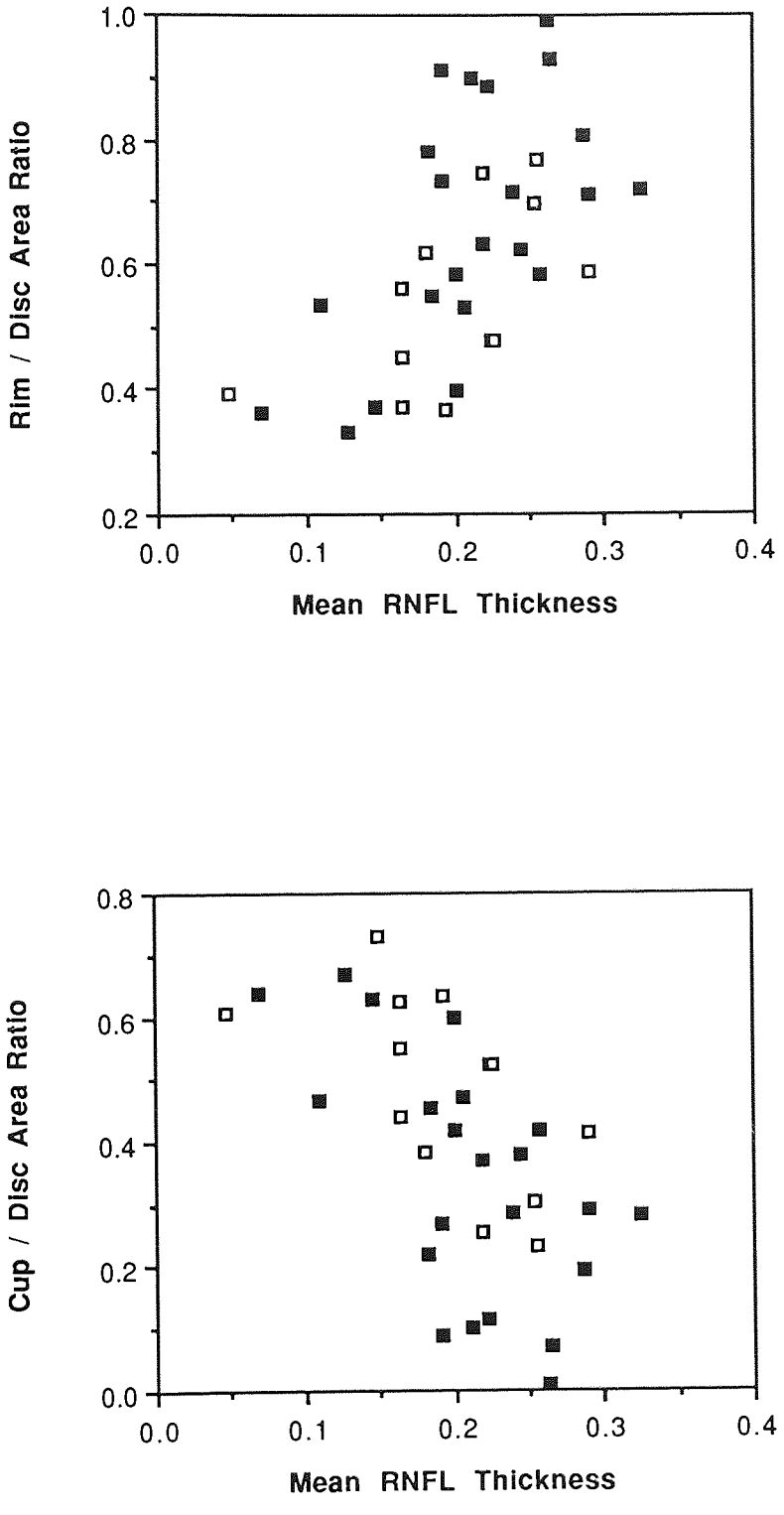

Figure 8.7. The total neuroretinal rim / disc area ratio (top) and the cup / disc area ratio (bottom) plotted as a function of the total mean RNFL thickness (mm) for the OHT (filled squares) and the POAG (open squares) patients. Slopes represent the least squares regression lines. Note the vertical axes of each graph are on different scales.

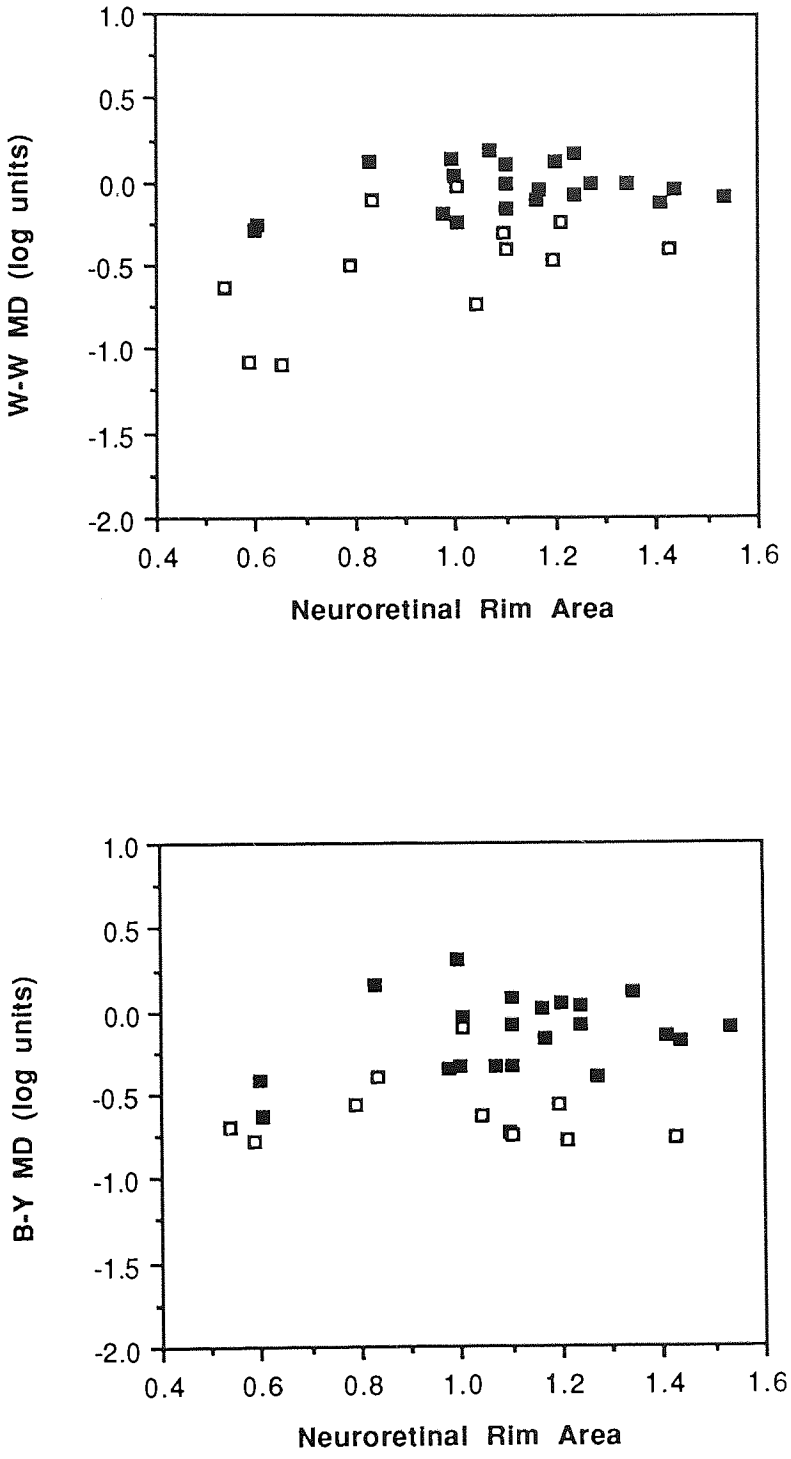

Figure 8.8. The W-W MD (top) and the B-Y MD (bottom) plotted as a function of the total mean neuroretinal rim area ratio for the OHT (filled squares) and the POAG (open squares) patients. Slopes represent the least squares regression lines.

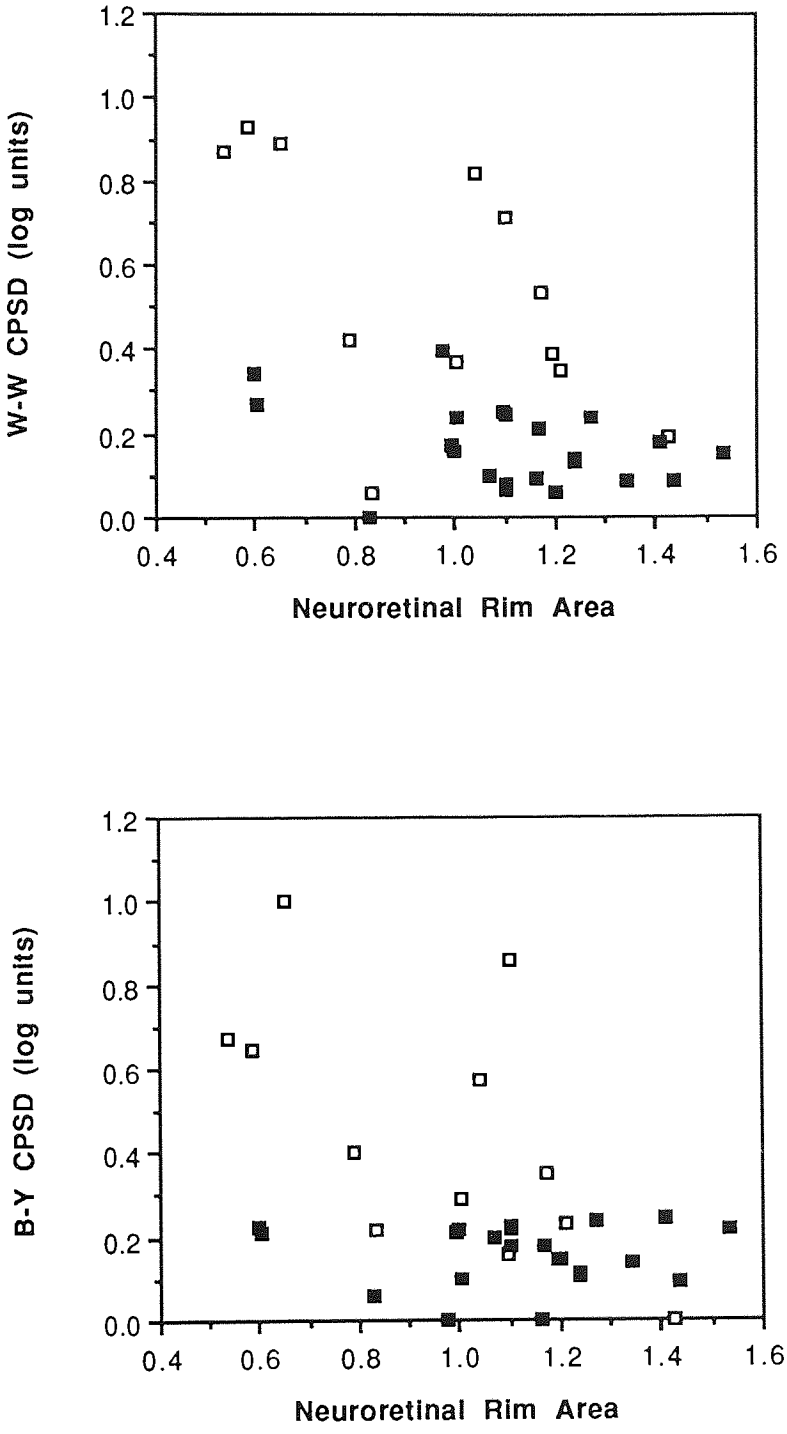

Figure 8.9. The W-W CPSD (top) and the B-Y CPSD (bottom) plotted as a function of the total mean neuroretinal rim area ratio for the OHT (filled squares) and the POAG (open squares) patients.

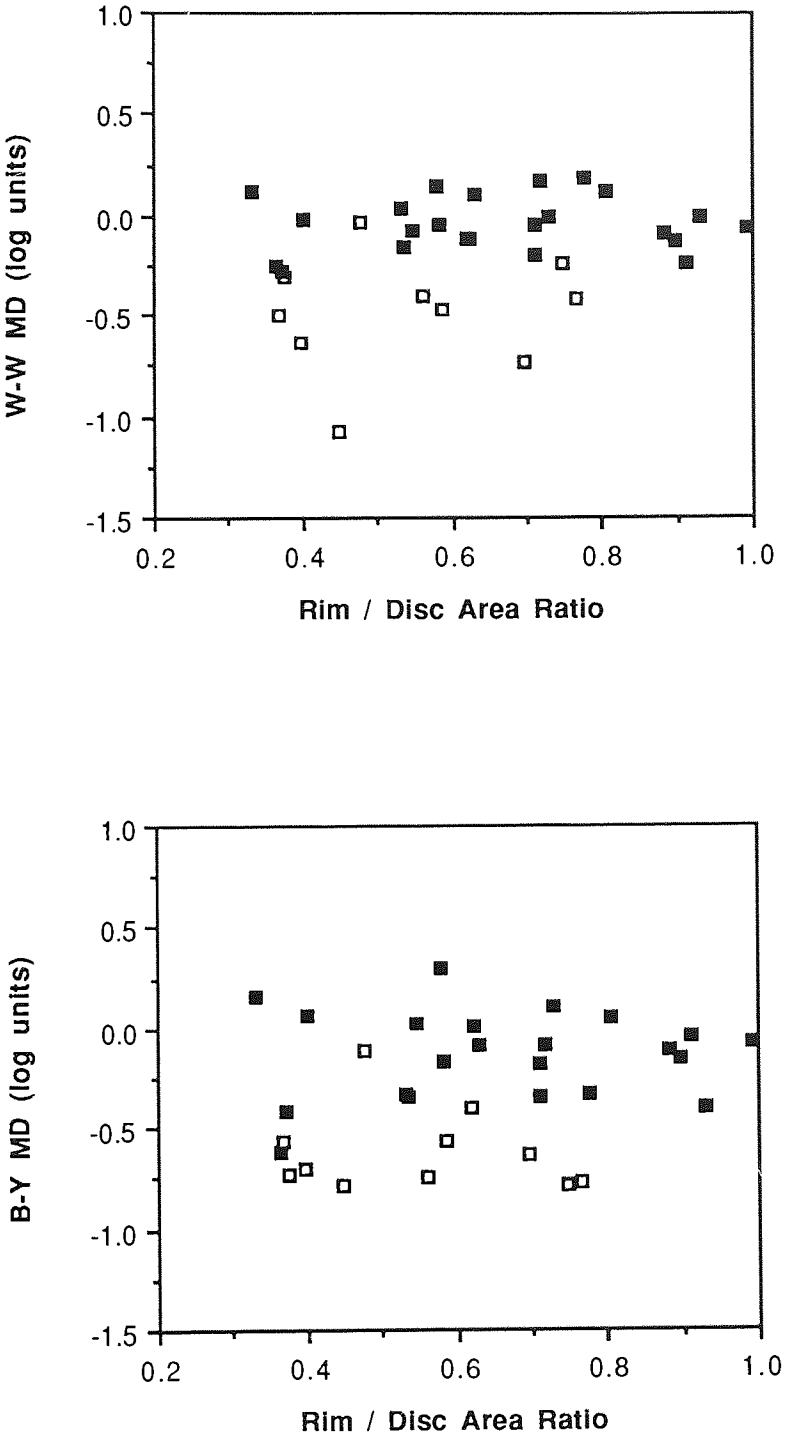

Figure 8.10. The W-W MD (top) and the B-Y MD (bottom) plotted as a function of the total mean neuroretinal rim / disc area ratio for the OHT (filled squares) and the POAG (open squares) patients.

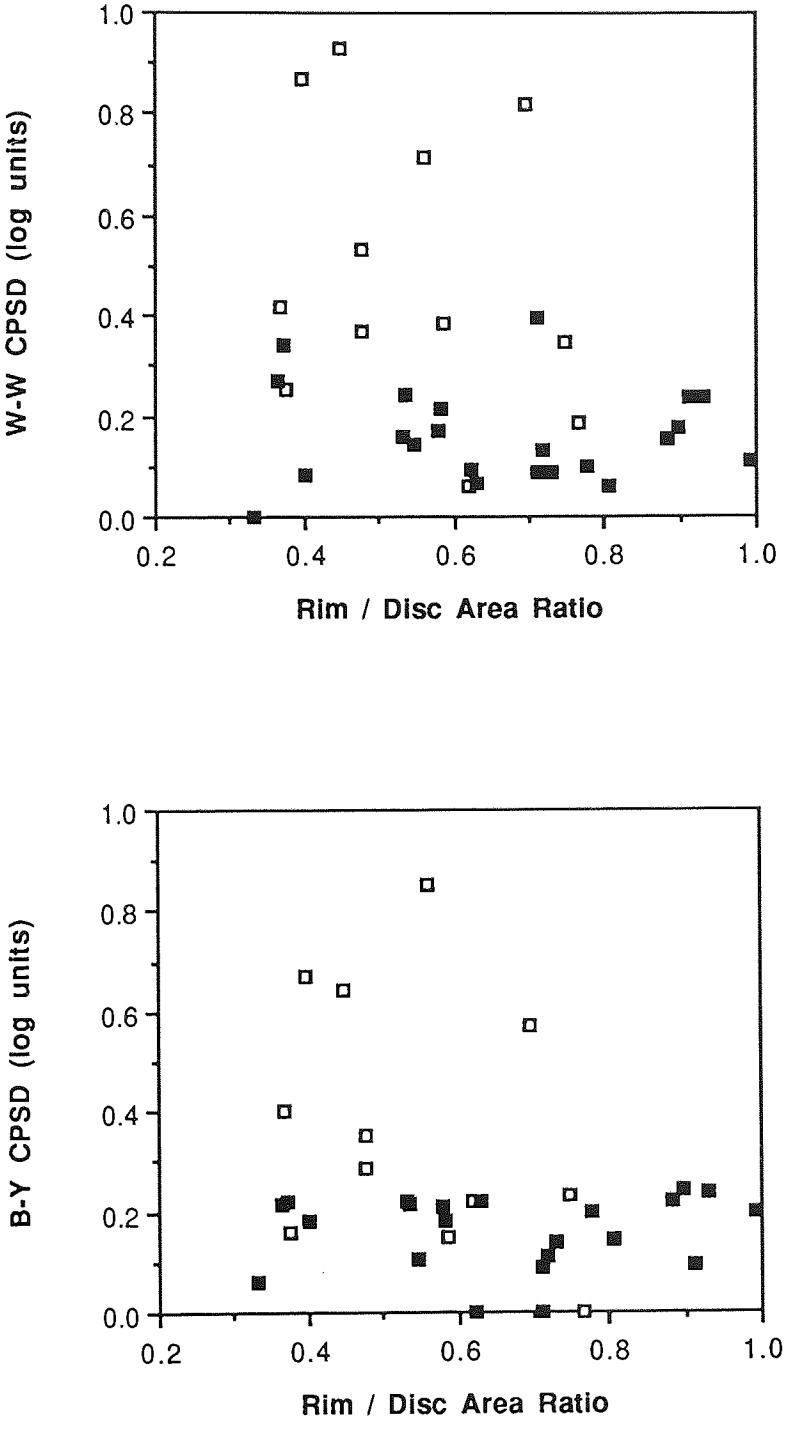

Figure 8.11. The W-W CPSD (top) and the B-Y CPSD (bottom) plotted as a function of the total mean neuroretinal rim / disc area ratio for the OHT (filled squares) and the POAG (open squares) patients.

Sector Analysis

The group mean stereometric parameters for the normals, OHT and glaucoma patients are displayed in Table 8.11.

Stereometric Parameter	Diagnosis		
	Normal	OHT	POAG
Optic Disc Area (mm^2)	0.85 (0.12)	0.97 (0.37)	1.03 (0.24)
Optic Cup Area (mm^2)	0.40 (0.28)	0.36 (0.31)	0.56 (0.24)
Neuroretinal Rim Area (mm^2)	0.62 (0.15)	0.59 (0.17)	0.47 (0.12)
Rim/ Disc Area	0.72 (0.18)	0.66 (0.20)	0.45 (0.13)
Cup / Disc Area	0.25 (0.17)	0.34 (0.20)	0.54 (0.16)
Mean RNFL thickness (mm)	0.25 (0.08)	0.21 (0.06)	0.17 (0.08)

Table 8.11. Group mean mean optic disc stereometric parameters for the combined quadrants for the normal subjects and for the OHT and POAG patients. One standard deviation is given in parenthesis.

The individual distribution of each stereometric parameter within each diagnostic category corresponding to a division of the disc into two sectors about the horizontal is displayed in Figure 8.12. The data for each sector was considered together to exclude potential bias arising from the inequality in abnormality between the two sectors. It is evident that considerable variation exists for each parameter within each group. The variability results in some degree of overlap between all three groups. The group mean results are further illustrated in Figures 8.13.

Analysis of covariance (ANCOVA) with diagnosis (ie normal, OHT or POAG) as a between-subjects factor and age as a covariate was separately carried out for each of the mean stereometric disc parameters: disc area, neuroretinal rim area, cup area, neuroretinal rim / disc area ratio, cup / disc area ratio and the mean RNFL thickness.

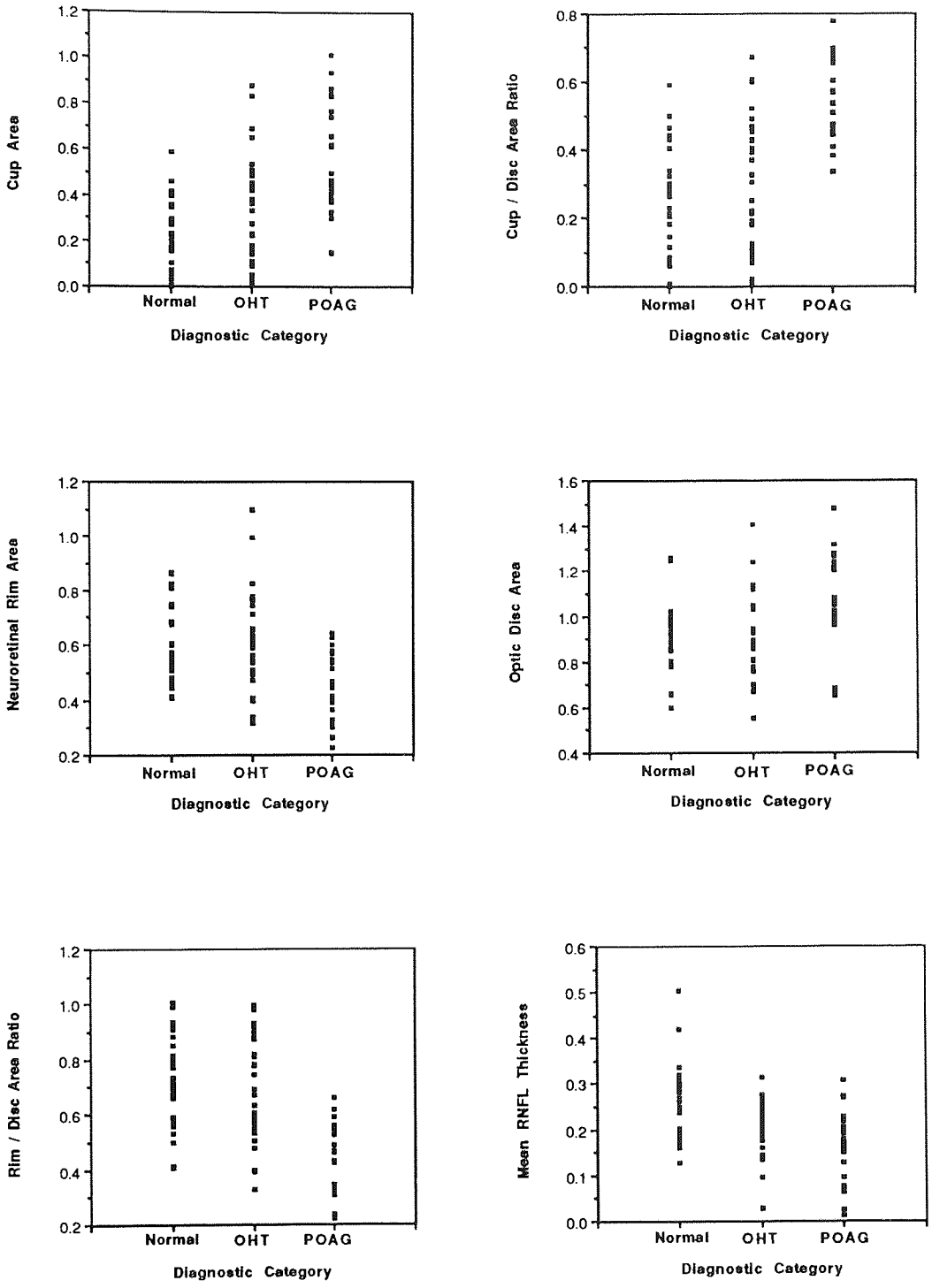

Figure 8.12. Distribution of the sector stereometric parameters: cup area (mm^2) (upper left), neuroretinal rim area (mm^2) (middle left), rim area / disc area ratio (lower left), optic cup / optic disc area ratio (upper right), optic disc area (mm^2) (middle right) and the mean RNFL thickness (mm) (lower right) for all the subjects of the normal group and for each patient in the OHT and POAG diagnostic groups. Note the vertical scales of each graph are different.

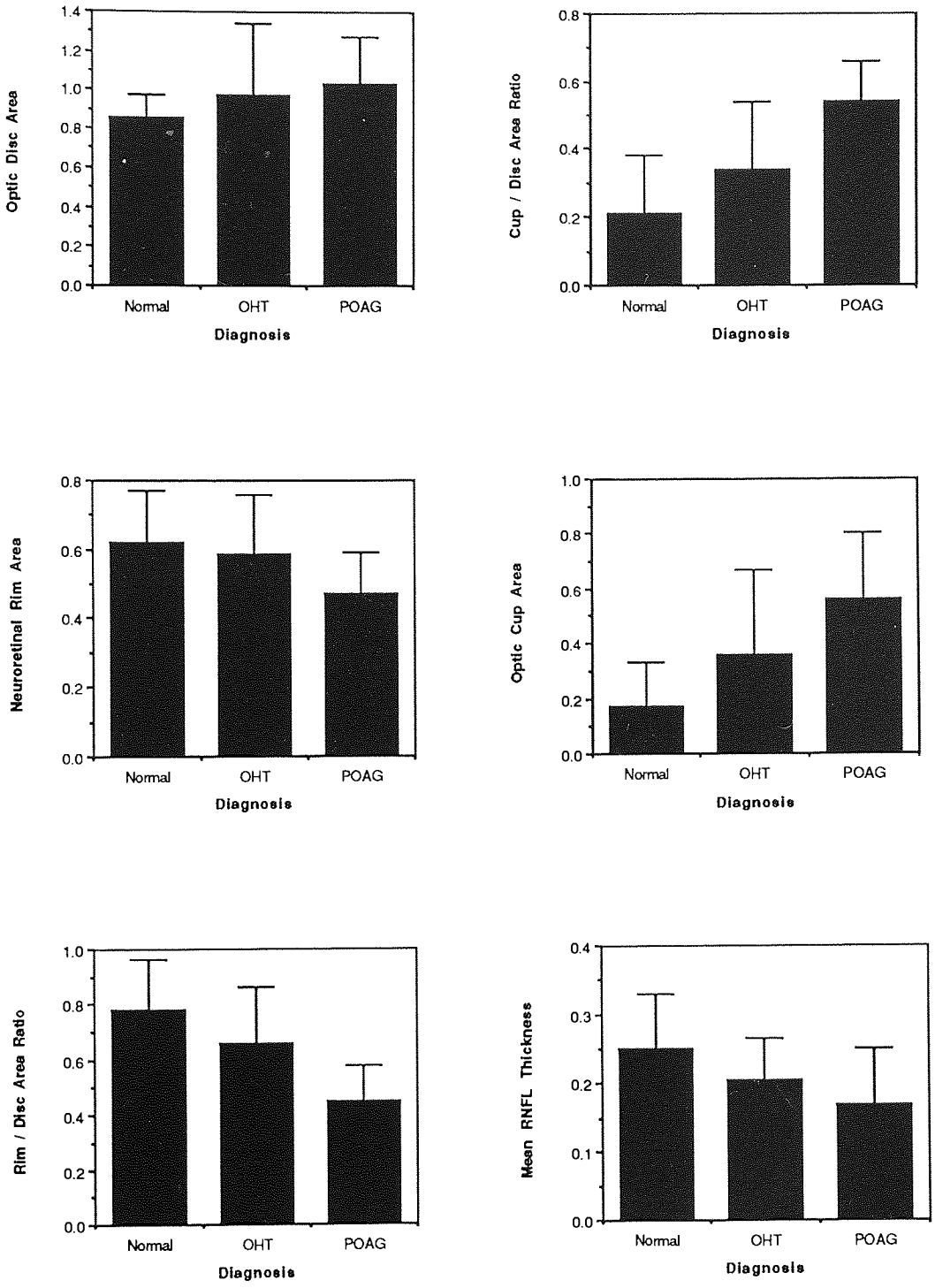

Figure 8.13. Group mean sector: optic disc area (mm^2) (top left), neuroretinal rim area (mm^2) (middle left), rim / disc area ratio (bottom left), cup / disc area ratio (top right), cup area (mm^2) (middle right), mean RNFL thickness (bottom right) for the normal group and for the OHT and POAG groups. Note the vertical scales of each graph are different. Error bars represent one standard deviation of the mean.

The disc area of each sector, combined, was independent of age (p=0.351) (Table 8.12) and similar between the three diagnostic categories (p=0.747).

Variable	dF	Sums of Squares	Mean Square	F value	P value
Age	1	0.009	0.009	0.105	p=0.747
Diagnosis	2	0.181	0.090	1.058	p=0.351
Age x Diagnosis	2	0.306	0.153	1.790	p=0.173
Error	96	8.208	0.085		

Table 8.12. Summary table for the analysis of covariance of the disc sector area.

The mean sector cup area was independent of age (p=0.553) but differed between the diagnostic categories (p<0.001) (Table 8.13). There was considerable overlap in the amount of sector cupping such that there was little difference between the normal and OHT groups (t=1.73, p=0.088). However, the sector cupping exhibited by the normal group was significantly less than that exhibited by the POAG group (t=3.888, p<0.001). The POAG group also demonstrated significantly greater cupping than the OHT group (t=2.978, p=0.004). The area of the cup increased as the disc area increased (r=0.82, p<0.001).

The mean area of the sector neuroretinal rim was independent of age (p=0.514) across all groups (p=0.700) but differed between diagnostic categories (p=0.004) (Table 8.14). For the OHT and POAG groups, the sector neuroretinal rim area increased as the disc area increased (r=0.455, p<0.001). The rim area of the OHT group was not significantly different from that of the normal group (t=0.628, p=0.532). However, the POAG group demonstrated a smaller sector rim area than both the normal (t=3.183, p=0.002) and the OHT groups (t=2.719, p=0.008).

The parameter rim / disc area reduces the influence of the disc area upon the neuroretinal rim area. Although independent, overall, of age (p=0.235) the rim / disc area ratio was significantly

different across the three categories ($p<0.001$) (Table 8.15). Compared to the normals, the ratios in the OHT ($t=2.880$, $p=0.005$) and in the POAG groups ($t=6.739$, $p<0.001$) were smaller. Furthermore, the ratio was also smaller in the POAG group than in the OHT group ($t=4.463$, $p<0.001$).

Variable	dF	Sums of Squares	Mean Square	F value	P value
Age	1	0.022	0.022	0.354	p=0.553
Diagnosis	2	2.261	1.130	46.402	p<0.001
Age x Diagnosis	2	0.240	0.120	1.960	p=0.147
Error	96	2.339	0.024		

Table 8.13. Summary table for the analysis of covariance of the sector cup area.

Variable	dF	Sums of Squares	Mean Square	F value	P value
Age	1	0.011	0.011	0.764	p=0.387
Diagnosis	2	0.304	0.152	5.915	p=0.004
Age x Diagnosis	2	0.018	0.009	0.359	p=0.700
Error	96	2.388	0.026		

Table 8.14. Summary table for the analysis of covariance of the sector neuroretinal rim area.

Variable	dF	Sums of Squares	Mean Square	F value	P value
Age	1	0.048	0.048	1.427	p=0.235
Diagnosis	2	1.490	0.745	22.202	p<0.001
Age x Diagnosis	2	0.051	0.025	0.753	p=0.474
Error	96	3.187	0.034		

Table 8.15. Summary table for the analysis of covariance of the sector neuroretinal rim / disc area ratio.

The cup / disc area ratio was independent of age (p=0.258) but was significantly different between the groups (p<0.001) (Table 8.16). The ratio was greater in the OHT (t=3.040, p=0.003) and in the POAG (t=6.790, p<0.001) groups compared to the normal group. Furthermore, the ratio in the OHTs was significantly less than that in the POAGs (t=4.376, p<0.001) groups.

Variable	dF	Sums of Squares	Mean Square	F value	P value
Age	1	0.042	0.042	1.294	p=0.258
Diagnosis	2	1.463	0.732	22.690	p<0.001
Age x Diagnosis	2	0.036	0.018	0.562	p=0.572
Error	96	3.063	0.032		

Table 8.16. Summary table for the analysis of covariance of the sector mean cup / disc area ratio.

The mean RNFL thickness was independent of age (p=0.654) (Table 8.17) but declined across the groups (p<0.001) particularly for the POAG group. The OHT (t=2.295, p=0.024) and POAG groups (t=3.809, p<0.001) both manifested a smaller RNFL compared to the normals. Interestingly, the mean RNFL thickness in the POAG group, was not significantly different from that in the OHTs (t=1.917, p=0.058). The rim area increased as the mean RNFL thickness increased (r=0.510, p<0.001). Furthermore, a negative correlation was present both between the

mean cup / disc area ratio and the mean RNFL thickness and also between the mean neuroretinal rim / disc area ratio and the mean RNFL thickness (Figure 8.14).

Variable	dF	Sums of Squares	Mean Square	F value	P value
Age	1	0.001	0.001	0.202	p=0.654
Diagnosis	2	0.088	0.044	7.988	p<0.001
Age x Diagnosis	2	0.001	0.001	0.134	p=0.875
Error	96	0.529	0.006		

Table 8.17. Summary table for the analysis of covariance of the sector mean RNFL thickness.

The relationships between the W-W and B-Y sector MD and the neuroretinal rim / disc area ratio are displayed in Figures 8.15-8.16.

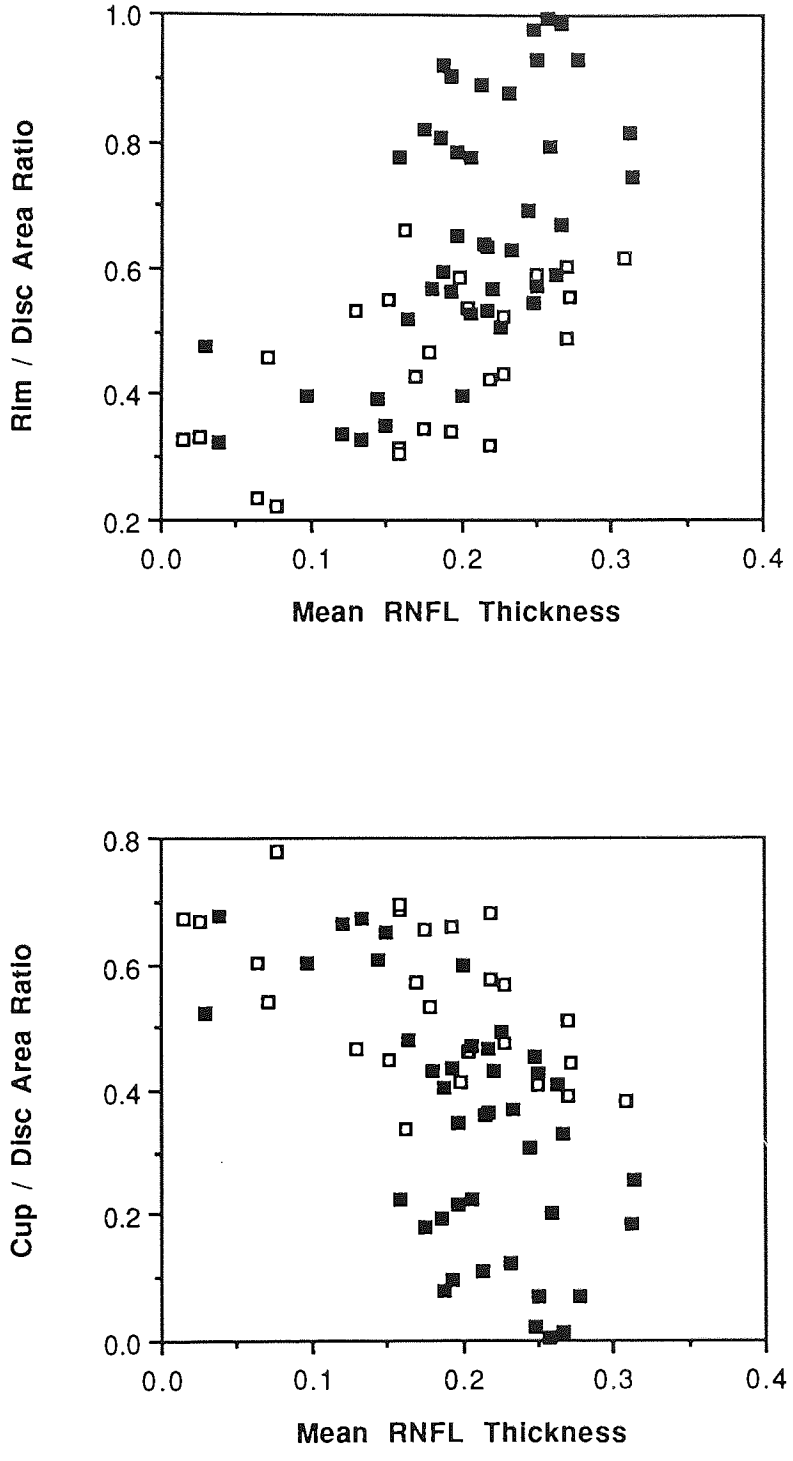

Figure 8.14. The quadrant mean RNFL thickness (mm) plotted as a function of the neuroretinal rim / disc area ratio (top) and the cup / disc area ratio (bottom) for the OHT (filled squares) and the mean POAG (open squares) patients. Note the vertical axes of each graph are on different scales.

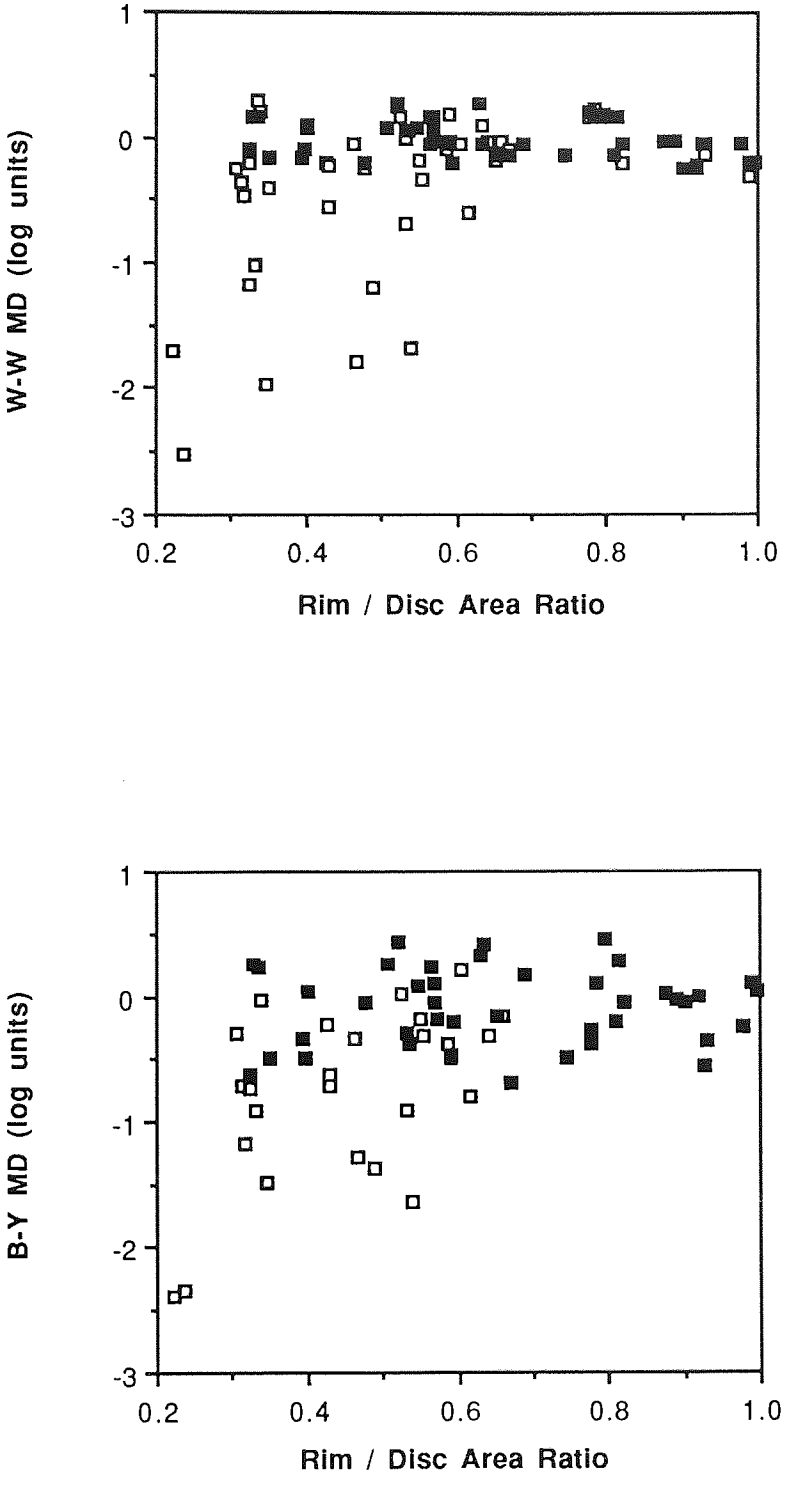

Figure 8.15. The sector mean neuroretinal rim / disc area ratio plotted as a function of the hemifield W-W MD (top) and the hemifield B-Y MD (bottom) for the OHT (filled squares) and the POAG (open squares) patients.

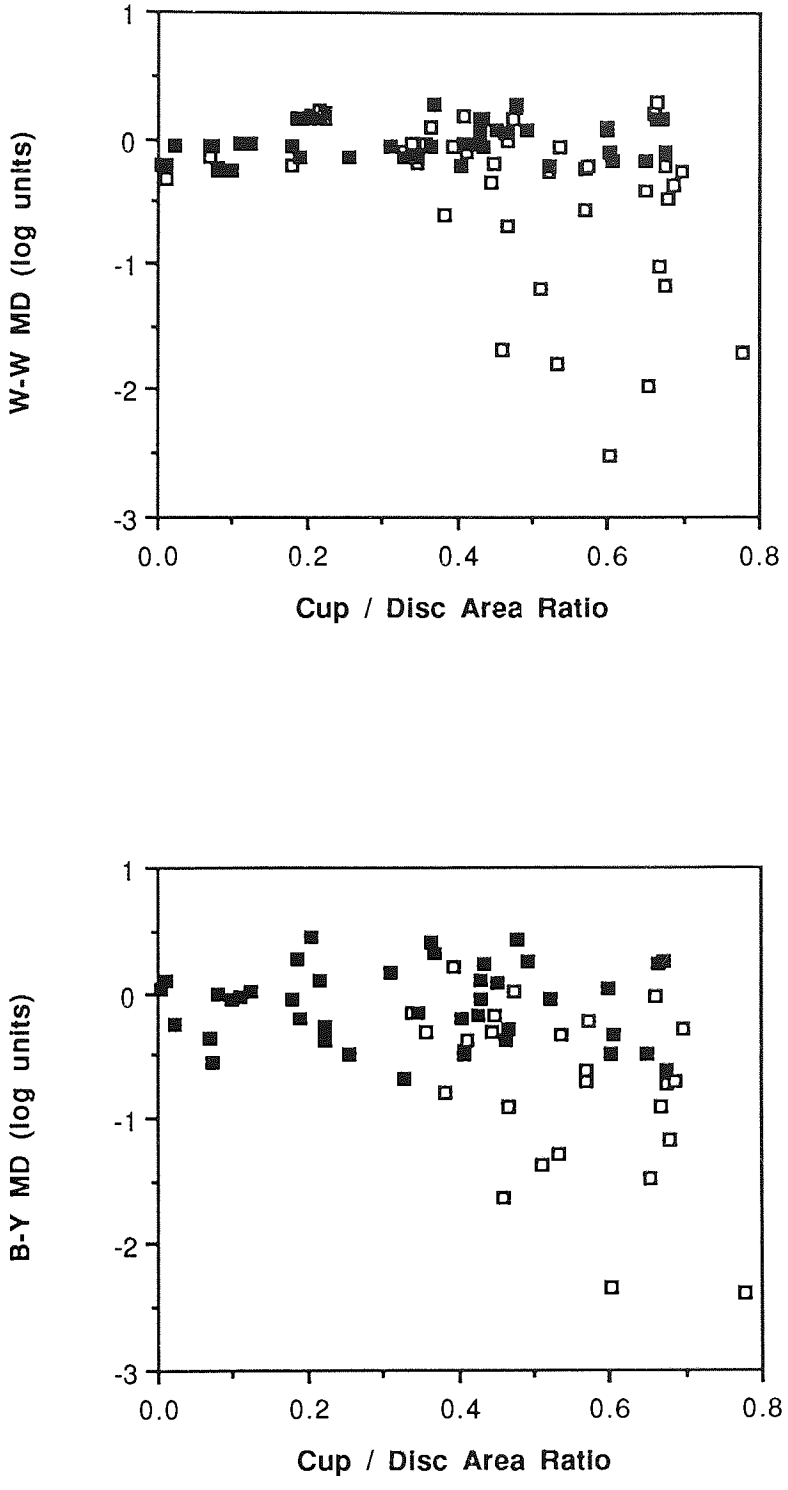

Figure 8.16. The sector mean cup / disc area ratio plotted as a function of the hemifield W-W MD (top) and the hemifield B-Y MD (bottom) for the OHT (filled squares) and the POAG (open squares) patients.

8.3.5. Discussion

This pilot study evaluated the structural parameters of the optic nerve, assessed using the new technique of scanning laser tomography, and compared the parameters to a functional assessment of the integrity of the optic nerve namely conventional W-W perimetry and the new psychophysical procedure of B-Y perimetry.

The topographical measurements of the optic nerve recorded with the HRT for the normal subjects and for the OHT and POAG patients were all within the range of values reported in other studies using laser scanning tomography (Weinreb et al 1989; Burk et al 1992; Chihara et al 1993; Rohrschneider et al 1994) and also using planimetric techniques (Caprioli et al 1987b; Gramer et al 1987; Caprioli and Miller 1988; Fazio et al 1990; Zeyen et al 1992). The results of the study also demonstrate that considerable between-subject variation exists in the optic disc parameters. The variation results in considerable overlap between the discs classified as glaucomatous and those which are considered to be normal. Such an overlap of disc parameters between-subjects has been also reported in previous studies (Caprioli et al 1987b; Caprioli and Miller 1988; Jonas 1992; Zeyen et al 1992; Nanba and Iwata 1993; Damms and Dannheim 1993). The variation in the cup area and in the neuroretinal rim area has been attributed to individual variation in the size of the optic nerve head (Bengtsson 1976; Britton et al 1987; Drance et al 1989; Jonas 1992). Indeed, the neuroretinal rim / disc area ratio has been adopted in some studies to reduce the effects of optic disc area (Chihara et al 1993). Figures 8.2 and 8.3 demonstrate that, on average, the differentiation between normal and POAG is improved when the rim / disc area ratio is considered rather than when the neuroretinal rim area is considered alone. Furthermore, the rim / disc area ratio demonstrated a strong correlation with the optic cup volume ($r=0.93$) and a moderate correlation with the mean cup depth ($r=0.71$) (Figure 8.6). Measurements of the disc rim area are considered to reflect the integrity of the optic nerve fibres (Airaksinen et al 1985a, b; Balazsi et al 1984).

Interestingly, the parameters cup volume and cup / disc area also clearly differentiated normal from POAG eyes. The respective parameters for the OHT group lie between the normal and

POAG groups. Surprisingly, the mean RNFL thickness was poor in differentiating between diagnostic groups. However, moderate correlations were present with the rim area (r=0.539), the neuroretinal rim / disc area ratio (r=0.607) and the cup / disc area ratio (r=0.607).

The diagnostic categorisation of the sample ie normal, OHT and POAG was based upon the results of visual field examination, IOP measurement, and clinical evaluation of the disc by ophthalmoscopy. However, considerable overlap was present between the groups in terms of the HRT assessment of the various disc parameters. This suggests that laser scanning tomography may be more suited to the identification of change in a given disc parameter within a follow-up period rather than as a screening instrument for abnormality. However, the ability of the HRT to identify change in glaucoma currently remains unknown.

For the age range in this study, the optic disc parameters varied independently of age both within and between diagnostic category. Indeed, age has been found to correlate poorly with rim area (Britton et al 1987; Jonas et al 1988a, b; Funk et al 1989).

Analysis of the parameters describing the entire disc may be insufficient for the detection of small changes in the neuroretinal rim particularly in view of the considerable variation in rim area encountered in the normal population. The sector analysis also exhibited overlap between the three diagnostic groups; however, the separation between the groups was improved for the rim / disc area ratio, cup area, cup / disc area ratio and the mean RNFL thickness parameters. Interestingly, the cup / disc area ratio, rim / disc area ratio and the mean RNFL thickness for the patient groups were significantly different from the normal group. Furthermore, although the cup / disc area ratio and the rim / disc area ratios were significantly greater in the POAG compared to the OHT group, the mean RNFL thickness was similar. The implications of this latter finding upon the development of glaucoma requires further study.

The correlation between the various structural parameters of the optic nerve head and psychophysical measurements is equivocal (Airaksinen et al 1985a, b, c; Balazsi et al 1984;

Drance et al 1987c; Guthauser et al 1987; Jonas et al 1988b; Lachenmayr et al 1991a; Takamoto et al 1993; Damms and Dannheim 1993) and may be absent or exhibit either a linear or curvilinear relationship. Over the range of visual field defects recorded in this study the relationship between the entire disc and the field appeared to be linear in nature. Surprisingly, only the neuroretinal rim area demonstrated a significant correlation to the W-W CPSD (r=-0.51) and to the B-Y CPSD (r=-0.47). The corresponding MDs were within the lower range reported for other studies ie W-W MD (r=0.34); B-Y MD (r=0.30) but were not statistically significant. The reason for this finding is unclear, however it may be as a result of the relatively small patient samples. The relationship between the structure and the visual field improved when the quadrant of each disc was compared to the contra-hemifield of the field for both W-W stimuli. Indeed, a significant linear relationship was demonstrated for the W-W MD (r=0.39; r=0.34) and the B-Y MD (r=0.44; r=0.40) plotted as a function of the rim / disc area ratio and the cup / disc area ratio respectively (Figures 8.15 and 8.16). Observation of the data revealed a more curvilinear distribution of points. The use of a more localised approach to the analysis in the comparison of the structural and functional parameters is in agreement with the findings of Drance et al (1989) who compared the temporal region of the disc to the visual field findings. The gradients of the slope function for the B-Y stimulus combinations are also steeper than for the corresponding W-W stimulus combinations. It is tempting to suggest that for a given rim / disc area ratio the depth of field defect may be greater for the B-Y stimulus combinations. Indeed, those POAG patients exhibiting a greater B-Y loss compared to the W-W field, described in Chapter 6, would increase the structural : functional correlation. The ability of B-Y perimetry to correlate to a greater degree with structural parameters than W-W perimetry over a wider range of field defects requires further study with a considerable larger sample of patients. Unfortunately the limited range over which pure SWS deficits may be observed ie 1.4 log units with respect to the disc changes may limit a full comparison to the range of recordable W-W defects.

This pilot study has demonstrated the ability of the Heidelberg Retinal Tomograph to record optic disc parameters in a relatively easy manner. The technique appears to produce repeatable contour measurements; however the variability of measurements increases with age and in

diseased eyes. The structural parameters of the optic disc show considerable variation between subjects which may limit the overall diagnostic power of the HRT instrument. Moderate degrees of correlation were demonstrated in more localised measures of the disc and the field using a hemifield sector approach. No significant improvement in correlation was noted using B-Y perimetry; however, the greater field loss recorded with B-Y perimetry results in a greater degree of field loss for a given structural parameter. It is clear that the variability of automated field measurements in association with the operator-based variability and patient-based variability hinder the ability to compare the relationship between structure and function. A potential solution to reduce the effects of variability would be to compare differences between the two eyes in both the field and the optic disc parameters. It would be anticipated that the variation in field and disc measurements between-eyes would be smaller than the between-subject variability. Furthermore, although the long-term variability in W-W perimetry is fully documented (Chapter 1), the long-term variability of B-Y perimetry and laser scanning tomography currently remain unknown. Until these characteristics are understood, the ability to determine progression of glaucoma, by comparisons of structure and function, using the HRT and B-Y perimetry may be compromised.

CHAPTER 9: SUMMARY, CONCLUSIONS AND FUTURE WORK

9.1 Introduction

The background to this research is based upon the knowledge that glaucoma is one of the major causes of blindness in the United Kingdom. The earliest signs of visual loss in primary open angle glaucoma generally remain unnoticed by the patient. Furthermore, conventional automated perimetry is relatively insensitive to the earliest structural damage in glaucoma, such that approximately 40% of ganglion cells are damaged prior to any detectable field loss. It is also of major importance to identify those patients with ocular hypertension (OHT) who will subsequently develop primary open angle glaucoma (POAG). Early detection of glaucomatous damage is therefore essential such that appropriate therapy may be instigated to retard the disease process.

The research has been primarily concerned with the psychophysical investigation of the visual field and the use of non-standardised perimetric stimulus parameters. These parameters may optimize the ability of automated perimetry to detect glaucomatous visual field loss. A summary of the results from the studies described in this thesis is presented in this chapter together with the potential impact / ramifications for future glaucoma research.

9.2 Evaluation of the FASTPAC strategy

The interpretation of the visual field may be hindered by potential artifacts in the recording of data which arise as a result of inexperience of the patient or due to the duration of the perimetric examination. The introduction of the FASTPAC strategy for the Humphrey Field Analyser was designed to reduce the length of the standard perimetric examination of the central field out to 30° eccentricity. Chapter 3, describes the comparison of visual field data recorded with both the standard 4-2dB strategy and the FASTPAC strategy in 98 normal subjects. Data was collected from two sites; Birmingham, UK and Waterloo, Canada. Analysis consisted of the comparison of mean sensitivity (MS), short-term fluctuation (SF), examination time and number of stimulus presentations. The efficiency of the visual field examination increased by approximately 43% with the FASTPAC strategy. However the within-test variability of the FASTPAC strategy increased by

24%, such that the overall cost: benefit ratio of the strategy remained essentially unaltered compared to the standard 4-2dB strategy. In addition, the global MS was not significantly different between the two strategies. The W-W FASTPAC strategy was advocated for the examination of low risk ocular hypertensives and for patients who have difficulty maintaining concentration over the standard 15 minute examination period with program 30-2 and the 4-2dB strategy. The increased variability demonstrated in glaucoma patients (Flanagan et al 1993b; O'Brien et al 1994), however, may render the FASTPAC strategy ineffective for the efficient identification of visual field progression.

9.3. Evaluation of Blue-Yellow perimetry

The major part of the research was concerned with the evaluation of Blue-Yellow perimetry (B-Y). The technique is designed to stimulate the blue or short-wavelength-sensitive (SWS) pathway mediated by the larger axons of the parvocellular system (deMonasterio 1979) and to suppress the activity of the green (medium-wavelength-sensitive (MWS)) and the red (long-wavelength-sensitive (LWS)) pathways.

B-Y perimetry was performed using a modified Humphrey Field Analyser. Yellow-Yellow and White-White stimulus combinations were used as a control. The influence of extraneous factors on the B-Y field were identified.

9.3.1. Effects of the ocular media on Blue-Yellow Perimetry

The study was stratified into two components: the investigation of induced light scatter on the B-Y visual field and the investigation of the effect of age-related cataract on the the B-Y visual field.

Using the modified Humphrey Field Analyser the effect of induced light scatter on the B-Y, Y-Y and W-W visual fields was evaluated in 15 normal subjects. Forward light scatter was induced using a scatter suspension placed in front of the eye during the perimetric test. Forward light scatter was quantified using the van den Berg straylight meter. Light scatter reduced perimetric sensitivity in a general manner across the field particularly for the B-Y stimulus combination. The

reduction in B-Y sensitivity was strongly related to the degree of forward light scatter. The influence of light scatter on the visual field profile was further investigated using 20 age-related cataract patients. All patients underwent B-Y, Y-Y and W-W perimetry. The field of each cataract patient was compared to that of an age-matched normal field calculated from a database of 40 normal subjects. The potential influence of ocular media absorption upon the B-Y sensitivity was addressed by measuring the individual ocular media absorption using the standard perimetric technique of Sample et al (1988b, 1989). All B-Y data was corrected for the effects of individual ocular media absorption. All cataract patients demonstrated a reduction in perimetric sensitivity (MD) compared to the normal field, the magnitude increasing as the severity of the cataract increased. The B-Y MD was greater than the corresponding Y-Y MD for all cataract patients. The chromatic content of the blue stimulus was considered to be the reason for this finding since the yellow background luminance and stimulus size were identical to the Y-Y stimulus combination. A differential effect between the B-Y and W-W stimulus combinations was demonstrated based upon the cataract type and pupil size interaction. At the high background luminances employed for B-Y perimetry the pupil constricts, compared to the pupil size for W-W perimetry ($10cdm^{-2}$). As a result of the pupil constriction in B-Y perimetry, any centrally located opacity, ie posterior subcapsular cataract, will influence B-Y field data more than the corresponding W-W field where the pupil diameter is greater. Conversely, a peripheral located opacity, ie cortical, will influence the field when the pupil is relatively large such as that when W-W perimetry is performed. Unless a suitable statistical method is adopted which separates the effects of cataract from any neural attenuation, the technique of B-Y perimetry may be limited in cases where cataract and glaucoma co-exist. The relationship between the degree of forward light scatter and the reduction in B-Y sensitivity may allow prediction of the reduction in B-Y sensitivity arising from scatter by simple measurement of the straylight function.

9.3.2 Learning effects in Blue-Yellow perimetry

Learning effects have been previously demonstrated in W-W perimetry such that an improvement in sensitivity and / or a reduction in within-test variability is demonstrated on repeated perimetry. This improvement in performance is confounded by an opposing fatiguing effect. The balance

between the learning and fatigue effects varies within a given examination of a given eye; between the two eyes under examination; and between-examinations of each eye. For the technique of B-Y perimetry to be accepted in a clinical situation it was important to assess the potential learning effects in B-Y perimetry. Sixty-one normal subjects performed perimetry on four separate occasions; one group had previous experience in W-W perimetry, whilst the other was totally naive to any perimetric technique. Learning effects were present in all groups of subjects irrespective of the degree of previous perimetric experience. An improvement in mean sensitivity of approximately 6.5% from baseline occurred together with a decline in the short-term fluctuation of approximately 16%, although considerable between-subject variation was present. Younger patients demonstrated a greater degree of improvement than the elderly groups. Evidence of a fatiguing effect was demonstrated since the magnitude of the improvement in perimetric performance was less in the second eye examined. The Troxler effect was suggested as a possible mechanism for the fatiguing effect.

Both the effects discussed in Sections 9.3.1. and 9.3.2. produce a generalised reduction in sensitivity. If B-Y perimetry is to become a clinical technique, these factors should be considered in the interpretation of B-Y visual field data. Failure to do so will limit the potential of B-Y perimetry to detect the early stages of glaucoma by mimicking the appearance of diffuse loss and / or reducing the apparent depth of any focal loss.

9.3.3. Blue-Yellow perimetry in the detection of glaucomatous visual field loss

The purpose of this study was to evaluate the ability of B-Y perimetry to detect glaucomatous visual field loss. Using a normal age-matched database, a rigid statistical procedure involving total and pattern deviation analysis was developed for B-Y perimetry similar to that found in the analytical package STATPAC. Such a procedure accounted for the normal between-subject variability as a function of age and of eccentricity, and separated generalised reductions in sensitivity from local deviations in sensitivity. The specificity of B-Y perimetry was evaluated using a separate sample of normal subjects.

B-Y and W-W visual fields were compared in 51 patients with either OHT or glaucoma. Each visual field was compared to an age-matched normal field constructed from a database of 50 normal subjects. All the B-Y visual field data were corrected for the individual effects of ocular media absorption. In the normal eye, between-subject variability increased with age and with eccentricity for both the B-Y and W-W stimulus combinations. Furthermore, overall, the B-Y field was more variable than the corresponding W-W field. The increased variability of the B-Y field was apparent even if the data had not been corrected for ocular media absorption. Confidence limits for normality were calculated from the normal group at each stimulus location for program 24-2. Each B-Y and W-W field of each patient was analysed using total and pattern probability analysis.

B-Y perimetry showed good sensitivity and specificity. All 24 glaucoma patients demonstrated abnormal B-Y fields; 25 of the 27 normal subjects were found to be normal using the pattern deviation analysis. Twelve glaucoma patients demonstrated a wider and / or deeper B-Y field defect compared to that of the W-W field. The loss was more focal in nature although 5 advanced cases demonstrated a more pronounced B-Y diffuse loss. Interestingly, one glaucoma patient demonstrated more extensive W-W field loss compared to the B-Y field. Five OHTs demonstrated a repeatable B-Y field loss which was focal in nature. No evidence of diffuse loss was present in this sample of patients. During the time period of this study, 2 of the 5 OHTs developed W-W field loss and underwent medical therapy. None of the 4 high-risk OHTs demonstrated B-Y field loss, however, all were undergoing hypotensive therapy. The relationship between the magnitude of the untreated IOP on presentation to an out-patient clinic and the presence or absence of B-Y field loss remains unknown and requires further study.

9.4. Isoluminance colour contrast sensitivity

A measure of central colour vision was assessed using isoluminance colour contrast sensitivity. Sensitivity was assessed using B-Y and R-G gratings modulated along the tritan confusion axis and 90° to this axis respectively. The isoluminance ratio was determined for R-G and B-Y gratings for each normal subject and OHT patient. Contrast sensitivity measurements were

therefore based upon chromatic differences rather than upon luminance cues. The OHTs were compared to the 95% confidence limits of the age-matched normal group. The results of the OHTs were indistinguishable from the normal group. It was hypothesized that defects in central visual function were dependent upon the presence of a diffuse type of glaucomatous loss or resulting damage in the foveal region which occurred later in the glaucomatous disease process.

9.5. Optic nerve head topography

A pilot study was carried out to investigated the relationship between the structural characteristics of the optic nerve and the B-Y visual field. Some degree of overlap for all structural parameters was evident between the normal, OHT and POAG groups. A moderate relationship was demonstrated for both the neuroretinal rim / disc area ratio and cup / disc area ratio compared to the visual field indices MD and CPSD recorded with the B-Y and W-W stimulus combinations. Although the relationship between structure and function appears rather disparate, the use of more localised analysis techniques using quadrants of the optic disc and visual field hemifields improved the relationship. Extending the study to provide a larger sample size will facilitate identification of the optimum structural and functional parameters required for the accurate detection and follow-up of glaucomatous damage.

9.6. Conclusions and Future Work

The FASTPAC strategy produced a significant reduction in the duration of the perimetric examination of the normal field encouraging the application of automated perimetry in routine visual field evaluation. Although the strategy appears limited in glaucoma patients the development of more complex algorithms such as the dynamic strategy of Weber (1991) and the probability based strategy of Olsson et al (1994b) is an exciting prospect. Both strategies allow an increase in efficiency without the associated increased threshold variability. Such algorithms, however, are not currently available in commercially available perimeters and their acceptability in the primary care situation requires further study.

The research has demonstrated that B-Y perimetry can facilitate the early detection of field loss in early glaucoma and reveal more extensive loss in some patients with confirmed glaucoma who exhibit existing W-W field loss. The potential of B-Y perimetry in the detection of glaucomatous field loss has therefore been demonstrated. However, B-Y perimetry demonstrates a number of problems which may limit its use. In particular:

1. It is not known which risk factors will render an OHT more susceptible to B-Y field loss, and the subsequent development of W-W field loss.

2. The greater normal between-subject variability for B-Y perimetry compared to W-W perimetry must be accounted for to avoid avoid high numbers of false-positive defects. This variability can be overcome using probability analysis the results of which yield good sensitivity and specificity. However, the impact of the increased B-Y within-test variability upon the long-term fluctuation and hence identification of visual field progression remains unknown.

3. The greater normal B-Y variability demonstrated with a conventional 4-2dB strategy may reduce the impact of more recently described thresholding strategies for W-W perimetry since the slope of the frequency-of-seeing curve in B-Y perimetry might be different.

4. The purpose of B-Y perimetry is to selectively test the SWS pathways. The range over which the SWS pathways are tested relies upon the selective isolation of the SWS pathways and the adaptation of the MWS and LWS channels. In B-Y perimetry, the level of isolation is approximately 1.4 log units for the given stimulus and background characteristics adopted for the perimeter. Therefore, when any stimulus location demonstrates a defect which attains a significance level of $p<0.5\%$ (a defect depth of approximately 1.4 log units) the degree of SWS response cannot be guaranteed and the response from such areas may be mediated by intrusion from the MWS pathway. The

advantage of performing B-Y perimetry in those areas of the field in which SWS isolation is lost, compared to W-W perimetry, remain currently unknown.

5. In addition to the limited range of SWS isolation for B-Y perimetry, the dynamic range over which defects can be measured and hence monitored over a period of time is reduced compared to that for W-W perimetry.

6. The results of the study have demonstrated that B-Y fields are subjected to artifacts which may arise from learning effects, ocular media absorption and forward light scatter.

a. Patients must first undergo at least one training examination irrespective of prior experience in W-W perimetry. The relatively small learning effect found in this study may have arisen due to an increased fatigue effect resulting from the Ganzfeld phenomenon; seen as a darkening of the field due to steady fixation. The rate at which darkening occurs is based upon the overall level of luminance, the chromatic content of the adapting field and the difference in the illumination between the two eyes. The relationship between these three factors and any fatigue effect requires further study but until such time, it is suggested that the patient should wear a translucent patch to occlude the non-tested eye. In this way the difference in the illumination between the eyes would be reduced.

b. The accepted psychophysical method for determining the degree of ocular media absorption is time-consuming and requires an additional visit to the clinic. There is a need to develop more rapid and objective techniques such as the prototype Lens Absorption Monitor (LAM) (Johnson et al 1993c). Alternatively, statistical methods such as hemifield analysis (Asman and Heijl 1992a, b; Sample et al 1993c) could be developed which evaluate the field in terms of a within-subject approach. However, the current study has demonstrated that the normal between-subject variability is unchanged when the B-Y data is not corrected for ocular media absorption. This would imply that the

probability analysis could be used to detect focal loss without the need to correct for absorption.

c. Forward intraocular light scatter from cataract results in a generalised reduction in sensitivity. Although the probability analysis will separate diffuse from focal defects, the differentiation between diffuse loss arising from optical factors from that due to neural factors still remains difficult. However, the results of the study suggests that measurement of the straylight parameter may predict the degree of optical attenuation with some degree of success. The prediction of optical attenuation should be further evaluated in pre- and post-operative cataract patients. In addition, the comparison between B-Y and W-W fields is further confounded by the differential effect of cataract type and pupil size upon the two stimulus combinations. The impact of forward light scatter on the degree of glaucomatous field loss for B-Y and W-W stimulus combinations is difficult to predict. Such factors together with the limited range over which SWS mechanisms can be isolated and the limited dynamic range of the perimeter suggests that B-Y perimetry may be ineffective for the detection of glaucoma in the presence of cataract.

7. One patient with glaucoma demonstrated a consistently different pattern of field loss between the B-Y and W-W field (Figure 6.11). It can be hypothesized that different mechanisms of damage may occur in glaucoma which may selectively attenuate different functional channels. Hence selective testing of a variety of channels eg achromatic sensitivity, chromatic sensitivity and motion sensitivity may reveal different patterns of visual field loss according to the mechanism of damage.

8. Commercially available colour perimeters have been developed by Humphrey Instruments and recently by Interzeag AG. The stimulus and background characteristics are different in design from those adopted by all centres involved in colour perimetry research. There is a need to establish a standard set of stimulus parameters such that

large patient populations can be tested. There is also a need to establish a large normal database of B-Y field data for the construction of an analytical software package for B-Y perimetry similar to STATPAC, program DELTA and PERIDATA for conventional automated perimetry. Until such time the interpretation of B-Y visual field data will remain relatively cumbersome in the primary care situation.

LIST OF REFERENCES

Abrahamsson M, Sjostrand J (1986) Impairment of contrast sensitivity (CSF) as a measure of disability glare. Invest Ophthalmol Vis Sci 27: 1131-1136.

Adams AJ, Rodic R (1982) Use of desaturated and saturated versions of the D-15 test in glaucoma and glaucoma-suspect patients. In: Doc Ophthal Proc Ser 33. Verriest G (ed). Junk; Amsterdam: 419-424.

Adams AJ (1982) Chromatic and luminosity processing in retinal disease. Am J Optom Physiol Opt 59: 954-960.

Adams AJ, Rodic R, Husted R, Stamper R (1982) Spectral sensitivity and color discrimination changes in glaucoma and glaucoma suspects. Invest Ophthalmol Vis Sci 23: 516-524.

Adams AJ, Heron G, Husted R (1987a) Clinical measures of central visual function in glaucoma and ocular hypertension. Arch Ophthalmol 105: 782-787.

Adams AJ, Schefrin B, Huie K (1987b) New clinical color threshold test for eye disease. Am J Optom Physiol Opt 64: 29-37.

Adams AJ, Zisman F, Ai E, Bresnick G (1987c) Macular edema reduces B cone sensitivity in diabetics. Appl Optics 26: 1455-1457.

Adams AJ, Johnson CA, Lewis RA (1991) S cone pathway sensitivity loss in ocular hypertension and early glaucoma has nerve fibre bundle pattern. In: Colour Vision Deficiencies X. Drum B, Moreland JD, Serra A (eds). Kluwer; Dordrecht: 535-542.

Aguilar M. Stiles WS (1954) Saturation of rod mechanism of the retina at high levels of stimulation. Opt Acta 1: 59-65.

Airaksinen PJ, Mustonen E, Alanko HI (1981) Optic disc haemorrhages precede retinal nerve fibre layer defects. Acta Ophthalmol 59: 627-641.

Airaksinen PJ, Heijl A (1983) Visual field and retinal nerve fibre layer in early glaucoma after optic disc haemorrhage. Acta Ophthalmol 61: 186-194.

Airaksinen PJ, Drance SM, Douglas GR (1984) Diffuse and localised nerve fibre loss in glaucoma. Am J Ophthalmol 98: 566-571.

Airaksinen PJ, Drance SM, Schulzer M (1985a) Neuroretinal rim area in early glaucoma. Am J Ophthalmol 99: 1-4.

Airaksinen PJ, Drance SM, Douglas DR, Schulzer M (1985b) Neuroretinal rim areas and visual field indices in early glaucoma. Am J Ophthalmol 99: 107-110.

Airaksinen PJ, Drance SM, Douglas GR, Schulzer M, Wijsman K (1985c) Visual field and retinal nerve fiber layer comparisons. Arch Ophthalmol 103: 205-207.

Airaksinen PJ, Lakowski R, Drance SM, Price M (1986) Color vision and retinal nerve fiber layer in early glaucoma. Am J Ophthalmol 101: 208-213.

Airaksinen PJ, Tuulonen A, Alanko HI (1992) Rate and pattern of neuroretinal rim area decrease in ocular hypertension and glaucoma. Arch Ophthalmol 110: 206-210.

Allen MJ, Vos JJ (1967) Ocular scattered light and visual performance as a function of age. Am J Optom 44: 717-727.

Alpern M (1987) A note on the action spectrum of human rod rhodopsin. Vision Res 27: 1471-1480.

Alvarez SL, Mills KB (1985) Spectral and flicker sensitivity in ocular hypertension and glaucoma. Research and Clinical Forums 7: 83-94.

Anctil JL, Anderson DR (1984) Early foveal involvement and generalised depression of the visual field in glaucoma. Arch Ophthalmol 102: 363-370.

Anderson DR (1992) In: Automated Static Perimetry. Mosby; St Louis.

Araie M, Yamagami J, Suzuki Y (1993) Visual field defects in normal-tension and high-tension glaucoma. Ophthalmology 100: 1808-1814.

Arden GB, Jacobsen JJT (1978) A simple grating test for contrast sensitivity: preliminary results indicate value in screening for glaucoma. Invest Ophthalmol Vis Sci 17: 23-32.

Arden GB, Gunduz K, Perry S (1988) Colour vision with a computer graphics system. Clin Vis Sci 2: 303-320.

Atkin A, Bodis-Wollner I, Wolkstein M, Moss A, Podos SM (1979) Abnormalities of central contrast sensitivity in glaucoma. Am J Ophthalmol 88: 205-211.

Armaly MF (1969) Ocular pressure and visual fields: a ten year follow-up study. Arch Ophthalmol 81: 25-40.

Armaly MF (1971) Visual field defects in early open angle glaucoma. Trans Am Ophthalmol Soc 69: 147-162.

Armaly MF (1972) Selective perimetry for glaucomatous defects in ocular hypertension. Arch Ophthalmol 87: 518-524.

Asman P, Britt J, Mills RP, Heijl A (1988) Evaluation of adaptive spatial enhancement in suprathreshold visual field screening. Ophthalmology 95: 1656-1662.

Asman P, Heijl A (1988) Background luminance and detection of glaucomatous field loss. Invest Ophthalmol Vis Sci 29 (suppl) : 240.

Asman A, Heijl A (1989) A clinical study of perimetric probability maps. Arch Ophthalmol 107: 199-203.

Asman P, Heijl A (1991) Cluster analysis in glaucoma. Invest Ophthalmol Vis Sci 32 (suppl): 1191.

Asman P, Heijl A (1992a) Glaucoma Hemifield Test. Automated visual field evaluation. Arch Ophthalmol 110: 812-819.

Asman P, Heijl A (1992b) Evaluation of methods for automated hemifield analysis in perimetry. Arch Ophthalmol 110: 820-826.

Asman P, Heijl (1992c) Weighting according to visual field location in computer-assisted glaucoma visual field analysis. Acta Ophthalmol 70: 671-678.

Asman P, Heijl A, Olsson J, Rootzen H (1992) Spatial analyses of glaucomatous visual fields; a comparison with traditional indices. Acta Ophthalmol 70: 679-686.

Asman P, Heijl A (1993) Arcuate cluster analysis in glaucoma perimetry. J Glaucoma 2: 13-20.

Asman P, Olsson J, Heijl A (1993) Learner's index (LI) to detect low perimetric experience. Invest Ophthalmol Vis Sci 34 (suppl): 1262.

Asman P, Heijl A (1994) Diffuse visual field loss and glaucoma. Acta Ophthalmol 72: 303-308.

Asman P (1994) Color-coded probability maps; separation of field defect types. Presented as a poster at the XIth International Perimetric Society Meeting, Washington DC, USA, July 3-7th 1994: 38.

Aspinall PA (1974) Some methodological problems in testing visual function. Mod Probl Ophthalmol 13: 2-7.

Atchison DA (1987) Effect of defocus on visual field measurement. Ophthal Physiol Opt 7: 259-265.

Atkin A, Bodis-Wollner I, Wolkstein M, Moss A, Podos SM (1979) Abnormalities of central contrast sensitivity in glaucoma. Am J Ophthalmol 88: 205-211.

Atkin A, Wolkstein M, Bodis-Wollner I et al (1980) Interocular comparison of contrast sensitivity in glaucoma patients and suspects. Br J Ophthalmol 64: 858-862.

Aulhorn E, Harms H (1967) Early visual field defects in glaucoma. In: Glaucoma Symposium: Tutzing symposium. Leydhecker W (ed). Karger; Basel: 151-186.

Aulhorn E (1969). Glaukom-Geisichtsfeld. Ophthalmologica 158: 469-487.

Aulhorn E, Harms H (1972) In: Handbook of Sensory Physiology, Vol 7/4. Hurvich LM, Jameson D (eds). Springer-Verlag; New York: 102-145.

Aulhorn E, Harms H, Karmeyer H (1979) The influence of spontaneous eye rotation on the perimetric determination of small scotomas. In: Doc Ophthalmol Proc Ser 19. Greve EL (ed). Junk; Amsterdam: 363-367.

Autzen T, Work K (1990) The effect of learning and age on short-term fluctuation and mean sensitivity of automated static perimetry. Acta Ophthalmol 68: 327-330.

Avant LL (1965) Vision in the ganzfeld. Psychological Bulletin 64: 246-258.

Balazsi AG, Rootman J, Drance SM, Shulzer M, Douglas GR (1984a) The effect of age on the nerve fiber population of the human optic nerve. Am J Ophthalmol 97: 760-766.

Balazsi AG, Drance SM, Shulzer M, Douglas GR (1984b) Neuroretinal rim area in suspected glaucoma and early chronic open-angle glaucoma. Acta Ophthalmol 102: 1011-1014.

Ballon BJ, Echelman DA, Shields B, Ollie AR (1992) Peripheral visual field testing in glaucoma by automated kinetic perimetry with the Humphrey Field Analyser. Arch Ophthalmol 110: 1730-1732.

Baraldi P, Enoch JM, Raphael S (1987) A comparison of visual field impairment caused by nuclear (NC) and posterior subcapsular (PSC) cataracts. In: Doc Ophthalmol Proc Ser 49. Greve EL, Heijl A (eds). Nijhoff / Junk; Dordrecht: 43-50.

Barlow HB (1958) Temporal and spatial summation in human vision at different background intensities. J Physiol 141: 337-350.

Bassi CJ, Lehmkuhle S (1990) Clinical implications of parallel visual pathways. J Am Optom Assoc 61: 98-110.

Bebié H, Fankhouser F, Spahr J (1976a) Static perimetry: strategies. Acta Ophthalmol 54: 325-338.

Bebié H, Fankhouser F, Spahr L (1976b) Static perimetry: Accuracy and fluctuations. Acta Ophthalmol 54: 339-348.

Bebié H, Fankhouser F (1981) Statistical program for the analysis of perimetric data. Doc Ophthalmol Proc Ser 26: 9-10.

Bebié H (1985) Computerized techniques of threshold determination. In: Computerised visual fields. Whalen W, Spaeth G (eds). Slack / Thorofare; New Jersey: 31-44.

Bebié H, Flammer J, Bebié T (1989) The cumulative defect curve: separation of local and diffuse components of visual field damage. Graefe's Arch Clin Exp Ophthalmol 227: 9-12.

Bebié H (1990) Computer-assisted evaluation of visual fields. Graefe's Arch Clin Exp Ophthalmol 228: 242-245.

Bek T, Lund-Anderson H (1989) The influence of stimulus size on perimetric detection of small scotoma. Graefe's Arch Clin Exp Ophthalmol 227: 531-534.

Bengtsson B (1976) The variation and covariation of cup and disc diameters. Acta Ophthalmol 54: 804-818.

Bennett GB, Werner EB, Seraydarian L (1991) Correlation of reliability indices and test-retest reproducibility in normal subjects undergoing automated perimetry on the Humphrey Field Analyser. Perimetry Update 1990/91. Proceedings of the IXth International Perimetric Society Meeting. Mills RP, Heijl A (eds). Kugler; Amsterdam / New York: 211-215.

van den Berg TJTP, van Spronsen R, van Veenendaal WG, Bakker D (1985) Psychophysics of intensity discrimination in relation to defect volume examination on the scoperimeter. In: Doc Ophthalmol Proc Ser 42. Greve EL, Verriest G (eds). Junk, Amsterdam: 147-151.

van den Berg TJTP (1986) Importance of pathological intraocular light scatter for visual disability. Doc Ophthalmol 61: 327-333.

van den Berg TJTP (1987) Relationship between media disturbances and the visual field. In: Doc Ophthalmol Proc Ser 49. Greve EL, Heijl A (eds). Nijhoff / Junk; Dordrecht: 33-38.

van den Berg TJTP, IJspeert JK, deWaard PWT, Meire F (1990) Functional quantification of diaphany. Doc Ophthalmol 25: 239-246.

van den Berg TJTP, IJspeert JK, deWaard PWT (1991) Dependence of intraocular straylight on pigmentation and light transmission through the ocular wall. Vision Res 31: 1361-1367.

van den Berg TJTP (1991) On the relation between glare and straylight. Doc Ophthalmol 78: 177-181.

van den Berg TJTP, IJspeert JK (1992) Clinical assessment of intraocular straylight. Appl Optics 31: 3694-3696.

Bettleheim FA. Siew EL (1982) Biological and physical basis of lens transparency. Cell biology of the eye. McDevitt D (ed). Academic Press; New York: 243-297.

Bickler-Bluth M, Trick GL, Kolker AE, Cooper DG (1989) Assessing the utility of reliability indices for automated visual fields. Ophthalmology 96: 616-619.

Bielik M, Zwas F, Shin DH, Tsai CS (1991) PERG and spectral sensitivity in ocular hypertensive and chronic open-angle glaucoma patients. Graefe's Arch Clin Exp Ophthalmol 229: 401-405.

Bigger JF, Becker B (1971) Cataracts and open-angle glaucoma. Am J Ophthalmol 71: 335-340.

Bishop KI, Werner EB, Krupin T et al (1988) Variability and reproducibility of optic disc topographic measurements with the Rodenstock Optic Nerve Head Analyser. Am J Ophthalmol 106: 696-702.

Boeglin RJ, Zulauf M, Hoffman D et al (1991) Long-term fluctuation of the visual field in clinically stable glaucoma patients. Invest Ophthalmol Vis Sci 32 (suppl): 1192.

Boettner EA, Wolter JR (1962) Transmission of the ocular media. Invest Ophthalmol Vis Sci 1: 776-783.

Bolanowski SJ, Doty RW (1987) Ganzfeld 'blankout' of monocular and binocular homogeneous fields is prevented with binocular viewing. Vision Res 27: 967-982.

Bone RA, Sparrock JMB (1971) Comparison of macular pigment densities in human eyes. Vision Res 11: 1057-1064.

Bone RA, Landrum JT, Tarsis SL (1985) Preliminary Identification of the human macular pigment. Vision Res 25: 1531-1535.

Bone RA, Landrum JT, Fernandez L, Tarsis SL (1988) Analysis of macular pigment by HPLC: retinal distribution and age study. Invest Ophthalmol Vis Sci 9: 843-849.

Bone RA, Landrum JT, Cains A (1992) Optical density of the macular pigment in vivo and in vitro. Vision Res 32: 105-110.

Bonomi L, Baravelli S, Cobbe C, Tommazzoli L (1990) Evaluation of the 701 Interzeag lens opacity meter. Graefe's Arch Clin Exp Ophthalmol 228: 447-449.

Box GEP, Cox DR (1964) An analysis of transformations. J Royal Stat Soc 25: 211-252.

Boynton RM, Enoch JM, Bush WR (1954) Physical measures of straylight in excised eyes. J Opt Soc Am 44: 879-886.

Boynton RM (1979) In: Human Color Vision. Reinhart and Winston (eds). Holt; New York: 159-206.

Bradley A, Zhang X, Thibos L (1992) Failures of isoluminance caused by ocular chromatic aberrations. Appl Optics 31: 3657-3667.

Brechner RJ, Whalen WR (1984) Creation of the transformed Q static probability distribution to aid in the detection of abnormal computerised visual fields. Ophthal Surg 15: 833-836.

Brenton RS, Phelps CD, Rojas P, Woolson RF (1986) Interocular differences of the visual field in normal subjects. Invest Ophthalmol Vis Sci 27: 799-805.

Brenton RS, Phelps CD (1986) The normal visual field on the Humphrey Field Analyser. Ophthalmologica 193: 56-74.

Brenton RS, Argus WA (1987) Fluctuations on the Humphrey and Octopus perimeters. Invest Ophthalmol Vis Sci 28: 767-771.

Breton ME, Krupin T (1987) Age covariance between 100-hue color scores and quantitative perimetry in primary open angle glaucoma. Arch Ophthalmol 105: 642-645.

Breton ME, Fletcher DE, Krupin T (1988) Influence of serial practice on Farnsworth-Munsell 100-hue scores: the learning effect. Appl Optics 27: 1038-1044.

Breton ME, Wilson TW, Wilson R, Spaeth G, Krupin T (1991) Temporal contrast sensitivity loss in primary open angle glaucoma and glaucoma suspects. Invest Ophthalmol Vis Sci 32: 2931-2941.

Britt JM, Mills RM (1987) The black hole effect in perimetry. Invest Oph Vis Sci 28 (suppl): 269.

Britton RJ, Drance SM, Schulzer M et al (1987) The area of the neuroretinal rim of the optic nerve in normal eyes. Am J Ophthalmol 103: 497-504.

Brown PK, Wald G (1963) Visual pigments in human and monkey retinas. Nature 200: 37-43.

Brusini P, Nicosia S, Weber J (1991) Automated visual field management in glaucoma with the PERIDATA program. In: Perimetry Update 1990/91. Proceedings of the IXth International Perimetric Society Meeting. Mills RP, Heijl A (eds). Kugler; Amsterdam/ New York: 273-277.

Bullimore MA, Bailey IL (1993) Considerations in the subjective assessment of cataract. Optom Vis Sci 70: 880-885.

Buncic JR, Tytla ME, Trope GE (1986) Flicker sensitivity in ocular hypertension before and during hypotensive treatment. Invest Ophthalmol Vis Sci 27 (suppl): 158.

Bundenz DL, Feuer WJ, Anderson DR (1993) The effect of simulated cataract on the glaucomatous visual field. Ophthalmology 100: 511-517.

Burk ROW, Rohrschneider K, Volcker HE, Zinser G (1990) Analysis of three-dimensional optic disc topography by laser scanning tomography: parameter definition and evaluation of parameter inter-dependence. In: Scanning laser ophthalmoscopy and topography. Naseman JE, Burk ROW (eds). Quintessenz; Munich: 161-176.

Burk ROW, Rohrschneider K, Noack H, Volcker HE (1992) Are large optic nerve heads susceptibie to glaucomatous damage at normal intraocular pressure? Graefe's Arch Clin Exp Ophthalmol 230: 552-560.

Burk ROW, Rohrschneider K, Takamoto T, Volcker HE, Schwartz B (1993) Laser scanning tomography and stereophotogrammetry in three-dimensional optic disc analysis. Graefe's Arch Clin Exp Ophthalmol 231: 193-198.

Campbell FW, Green DG (1965) Optical and retinal factors affecting visual resolution. J Physiol 187: 576-593.

Campbell FW, Gubisch RW (1966) Optical quality of the human eye. J Physiol 186: 558-578.

Campbell FW, Andrews PR (1992) Motion reveals spatial visual defects. Ophthal Physiol Opt 12: 131-132.

Caprioli J, Spaeth GL (1984) Comparison of visual field defects in the low-tension glaucomas with those in the high tension glaucomas. Am J Ophthalmol 97: 730-737.

Caprioli J, Sears M, Spaeth GL (1986a) Comparison of visual field defects in low-tension glaucoma and high tension glaucoma [letter]. Am J Ophthalmol 102: 402-404.

Caprioli J, Klingbeil U, Sears M, Pope B (1986b) Reproducibility of optic disc measurements with computerized analysis of stereoscopic video images. Arch Ophthalmol 104: 1035-1039.

Caprioli J, Sears M, Miller JM (1987a) Patterns of early visual field loss in glaucoma. Am J Ophthalmol 103: 512-517.

Caprioli J, Miller J, Sears M (1987b) Quantitative evaluation of the optic nerve head in patients with unilateral visual field loss from primary open angle glaucoma. Ophthalmology 94: 1484-1487.

Caprioli J, Miller J (1987) Optic disc rim area is related to disc size in normal subjects. Arch Ophthalmol 105: 1683-1685.

Caprioli J, Miller JM (1988) Videographic measurements of optic nerve topography in glaucoma. Invest Ophthalmol Vis Sci 29: 1294-1298.

Caprioli J (1989) The contour of the juxtapapillary nerve fiber layer in glaucoma. Ophthalmology 97: 358-366.

Caprioli J, Miller JM (1989) Measurement of relative nerve fiber layer surface height in glaucoma. Ophthalmology 96: 633-641.

Caprioli J (1990) Automated perimetry in glaucoma. Am J Ophthalmol 111: 235-239.

Capris P, Gandolfo E, Camoriano GP, Zingirian M (1989). Kinetic visual field indices. In: Perimetry Update 1988/89. Proceedings of the VIIIth International Perimetric Society Meeting. Heijl A (ed). Kugler / Ghedini; Amsterdam / Berkeley / Milano: 223-227.

Casson EJ, Shapiro LR, Johnson CA (1990) Short-term fluctuation as an estimate of variability in visual field data. Invest Ophthalmol Vis Sci 31: 2459-2463.

Casson EJ, Johnson CA, Nelson-Quigg JM (1993a) Temporal modulation perimetry: the effects of ageing and eccentricity on sensitivity in normals. Invest Ophthalmol Vis Sci 34: 3096-3102.

Casson EJ, Johnson CA, Shapiro LR (1993b) Longitudinal comparison of temporal-modulation perimetry with white-on-white and blue-on-yellow perimetry in ocular hypertension and early glaucoma. J Opt Soc Am 10: 1792-1806.

Celesia GG, Daly RF (1977) Effects of ageing on visual evoked responses. Arch Neurol 34: 403-407.

Chauhan BC, Drance SM, Douglas GR, Johnson CA (1989a) Visual field damage in normal-tension and high-tension glaucoma. Am J Ophthalmol 108: 636-642.

Chauhan BC, Henson DB, Hobley AJ (1989b) Cluster analysis in suprathreshold perimetry. In: Perimetry Update 1988/89. Proceedings of the VIIIth International Perimetric Society Meeting. Kugler / Ghedini; Amsterdam / Berkeley / Milano: 217-221.

Chauhan BC, Drance SM, Lai C (1989c) A cluster analysis for threshold perimetry. Graefe's Arch Clin Exp Ophthalmol 227: 216-220.

Chauhan BC, Drance SM, Douglas GR (1990a) The use of visual field indices in detecting changes in the visual field in glaucoma. Invest Ophthalmol Vis Sci 31: 512-520.

Chauhan BC, House PH, Drance SM (1990b) A study of intra-test variability in conventional and high-pass resolution perimetry. Invest Ophthalmol Vis Sci 30 (suppl): 15.

Chauhan BC, Tompkins JD, LeBlanc RP, McCormick TA (1993) Characteristics of frequency-of-seeing curves in normal subjects, patients with suspected glaucoma, and patients with glaucoma. Invest Ophthalmol Vis Sci 34: 3534-3540.

Chihara E, Honda Y (1992) Multiple defects in the retinal nerve fiber layer in glaucoma. Graefe's Arch Clin Exp Ophthalmol 230: 201-205.

Chihara E, Takahashi F, Chihara K (1993) Assessment of optic disc topography with scanning laser ophthalmoscope. Graefe's Arch Clin Exp Ophthalmol 231: 1-6.

Choplin NT, Sherwood MB, Spaeth GL (1990) The effect of stimulus size on the measured threshold values in automated perimetry. Ophthalmology 97: 371-374.

Chylack LT, Leske MC, Sperduto R, Khu P, McCarthy D (1988) Lens opacities classification system. Arch Ophthalmol 106: 330-334.

Chylack LT, Leske MC, McCarthy D, Khu P, Kashiwagi T, Sperduto R (1989) Lens opacities classification system II (LOCS II) Arch Ophthalmol 107: 991-997.

Chylack LT, Padhye N, Khu PM et al (1993a) Loss of contrast sensitivity in diabetic patients with LOCS II classified cataracts. Br J Ophthalmol 77: 7-11.

Chylack LT, Wolfe JK, Singer DM et al (1993b) The Lens Opacities Classification System III. Arch Ophthalmol 111: 831-836.

Chylack LT, Wolfe JK, Friend J et al (1993c) Quantifying cataract and nuclear brunescence, the Harvard and LOCS systems. Optom Vis Sci 70: 886-895.

Cioffi GA, Robin AL, Eastman RD (1993) Reproducibility of optic nerve head topographic measurmenets with the confocal laser scanning ophthalmoscope. Ophthalmology 100: 57-62.

Clarke FJJ, Belcher SJ (1962) On the localization of Troxler's effect in the visual pathway. Vision Res 2: 53-68.

Clarke MP, Pearson JCG, Vernon SA, Matthews JC (1990) Influence of pupil size on measurements made with the Lens Opacity Meter 701. Br J Ophthalmol 74: 526-527.

Cleland BG, Levick WR, Sanderson KJ (1973) Properties of sustained and transient ganglion cells in the cat retina. J Physiol 228: 473-496.

Cohen W (1958) Color perception in the chromatic ganzfeld. Am J Psychol 71: 390-394.

Coman L, Flanagan JG, Wild JM (1994) Perimetric fatigue and its reduction using strategies to improve vigilance. Presented as a poster at the XIth International Perimetric Society Meeting, Washington DC, USA; July 3-7th 1994: 53.

Coren S, Girgus JS (1972) Density of human lens pigmentation: in vivo measures over an extended age range. Vision Res 12: 343-346.

Coren S, Ward LM (1989) In: Sensation and Perception (3rd edition). Harcourt-Brace / Jovanovich; San Diego/ New York / Chicago / Austin / Washington DC / London / Sydney / Tokyo: 446-447.

Cornsweet TN (1962) The staircase method in psychophysics. Am J Psychol 75: 485-491.

Cornsweet TN (1970) In: Visual Perception. Academic; New York: 68-89.

Cornsweet TN, Hersh S, Humphries JC, Beesman RJ, Cornsweet DW (1983) Quantification of the shape and colour of the optic nerve head. In: Advances in Diagnostic Visual Optics. Breinin GM, Siegel IM (eds). Springer-Verlag; Berlin: 141.

Costagliola C, Iuliano G, Rinaldi E et al (1989) In vivo measurement of human lens ageing using the lens opacity meter. Ophthalmologica 199: 158-161.

Crosswell HH, Stewart WC, Cascairo MA, Hunt HH (1991) The effect of background intensity on the components of fluctuation as determined by threshold-related automated perimetry. Graefe's Arch Clin Exp Ophthalmol 229: 119-122.

Cyrlin M, Rosenshein J, Cunningham S et al (1991) New methods of analysis of serial visual fields. In: Perimetry Update 1990/91. Proceedings of the IXth International Perimetric Society Meeting. Mills RP (ed). Kugler; Amsterdam / New York: 257-271.

Damms T, Dannheim F (1993) Sensitivity and specificity of optic disc parameters in chronic glaucoma. Invest Ophthalmol Vis Sci 34: 2246-2250.

Dandona L, Quigley HA, Jampel HD (1989) Reliability of optic nerve head topographic measurements with computerised image analysis. Am J Ophthalmol 108: 414-421.

Dandona L, Hendrickson A, Quigley HA (1991) Selective effects of experimental glaucoma on axonal transport by retinal ganglion cells to the dorsal lateral geniculate nucleus. Invest Ophthalmol Vis Sci 32: 1593-1599.

Dannheim F (1987) First experiences with the new Octopus G1 program in chronic simple glaucoma. In: Doc Ophthalmol Proc Ser 49. Greve EL, Heijl A (eds). Nijhoff / Junk; Dordrecht: 321-328.

Day RM, Scheie HG (1953) Simulated progression of visual field defects of glaucoma. Arch Ophthalmol 50: 418-433.

Delaye M, Clark JI, Benedek GB (1982) Identification of the scattering elements responsible for lens opacification in cold cataracts. Biophys J 37: 647-656.

DeMott DW, Boynton RM (1958) Sources of entoptic straylight. J Opt Soc Am 48: 120-125.

DeNatale R, Flammer J, Zulauf M, Bebié H (1988) Influence of age on the transparency of the lens in normals: a population study with the help of the Lens Opacity Meter 701. Ophthalmologica 196: 14-18.

Dengler-Harles M, Wild JM, Cole MD, O'Neill EC, Crews SJ (1990) The influence of forward light scatter on the visual field indices in glaucoma. Graefe's Arch Clin Exp Ophthalmol 228: 326-331.

Dengler-Harles M, Wild JM, Searle AET, Crews SJ (1991) The relationship between backward and forward intraocular light scatter. In: Perimetry Update 1990/91. Proceedings of the IXth

International Perimetric Society Meeting. Mills RP, Heijl A (eds). Kugler; Amsterdam / New York: 577-582.

Dengler-Harles M, Wild JM, Cole MD, O'Neill EC (1993) The influence of stimulus parameters on the visual field indices by automated projection perimetry. Graefe's Arch Clin Exp Ophthalmol 231: 337-343.

DeValois RL, Abramov I, Jacobs GH (1966) Analysis of response patterns of LGN cells. J Opt Soc Am 56: 966-977.

DeValois RL, DeValois KK (1993) A multi-stage color model. Vision Res 8: 1053-1065.

Devaney KO, Johnson HA (1980) Neuron loss in the ageing visual cortex of man. J Gerontol 35: 836-841.

DeYeo EA, van Essen DC (1988) Concurrent processing streams in monkey visual cortex. Trends Neurosci 11: 219-226.

Derrington AM, Lennie P (1984) Spatial and temporal contrast sensitivities of neurons in lateral geniculate nucleus of macaque. J Physiol 357: 219-240.

Dolman CL, McCormick AQ, Drance SM (1980) Ageing of the optic nerve. Arch Ophthalmol 98: 2053-2058.

Donaldson D, Prescott R, Kennedy S (1980) Simultaneous stereoscopic fundus camera utilising a single optical axis. Invest Ophthalmol Vis Sci 19: 289-297.

Donovan HC, Weale RA, Wheeler C (1978) The perimeter as a monitor of glaucomatous changes. Br J Ophthalmol 62: 705-708.

Douglas GR, Drance SM, Mikelberg FS, Schwartz B, Takamoto T (1987) Optic nerve head analysis using the Rodenstock Analyser. In: Glaucoma Update III. Kriegelstein GK (ed). Springer-Verlag; Berlin / Heidelberg / New York: 106-111.

Drance SM, Berry V, Hughes A (1967) Studies on the effects of age on the central and peripheral isopters of the visual field in normal subjects. Am J Ophthalmol 63: 1667-1672.

Drance SM, Wheeler C, Patullo M (1967) The use of static perimetry in the early detection of glaucoma. Can J Ophthalmol 2: 249-258.

Drance SM (1981) Richardson-Cross Lecture. Early disturbances of colour vision in chronic open angle glaucoma. In: Doc Ophthal Proc Ser 26. Greve EL, Verriest G (eds). Junk; Amsterdam: 155-159.

Drance SM, Lakowski R (1983) Colour vision in glaucoma. In: Glaucoma Update II. Kriegelstein GK, Leydhecker W (eds). Springer-Verlag; Berlin: 117-121.

Drance SM (1985a) Epidemiological considerations of visual field screening for glaucoma. In: Automated perimetry: a practical guide. Drance SM, Anderson D (eds). Grune / Stratton; New York: 55-59.

Drance (1985b) The Shaffer Lecture: The early structural and functional disturbances of chronic open angle glaucoma. Ophthalmology 92: 853-857.

Drance SM, Lakowski R, Schulzer M, Douglas GR (1987a) Acquired color vision changes in glaucoma. Use of 100 hue test and Pickford anomaloscope as predictors of glaucomatous change. Arch Ophthalmol 99: 829-831.

Drance SM, Douglas GR, Airaksinen PJ, Schulzer M, Hitchings RA (1987b) Diffuse visual field loss in chronic open-angle glaucoma and low-tension glaucoma. Am J Ophthalmol 104: 577-580.

Drance SM, Airaksinen PJ, Price M et al (1987c) The use of psychophysical, structural, and electrodiagnostic parameters to identify glaucomatous damage. Graefe's Arch Clin Exp Ophthalmol 225: 365-368.

Drance SM, Wijsman K, Schulzer M, Douglas GR (1989) The correlation between neuroretinal rim and visual field indices. In: Perimetry Update 1988/89. Proceedings of the VIIIth International Perimetric Society Meeting. Heijl A (ed). Kugler / Ghedini; Amsterdam / Berkeley / Milano: 285-287.

Drance SM (1991) Diffuse visual field loss in open-angle glaucoma. Ophthalmology 98: 1533-1538.

Drance SM (1992): Bowman Lecture. Glaucoma - changing concepts. Eye 6: 337-342.

Dreher AW, Tso PC, Weinreb RN (1991) Reproducibility of topographic measurements of normal and glaucomatous optic nerve head with the laser tomographic scanner. Am J Ophthalmol 111: 221-229.

Dreher AW, Weinreb RN (1991) Accuracy of topographic measurement in a model eye with the laser tomographic scanner. Invest Ophthalmol Vis Sci 32: 2992-2996.

Drum B, Armaly MF, Huppert W (1986) Scotopic sensitivity loss in glaucoma. Arch Ophthalmol 104: 712-717.

Drum B, Armaly MF, Huppert WE (1989) Chromatic and achromatic sensitivity in glaucoma. In: Colour Vision Deficiencies IX. Drum B, Verriest G (eds). Kluwer; Dordrecht: 261-272.

Duggan C, Sommer A, Auer C, Burkhardt K (1985) Automated differential threshold perimetry for detecting glaucomatous visual field loss. Am J Ophthalmol 100: 420-468.

Dunn PM, Lakowski R (1981) Fully photopic and scotopic summation in chromatic perimetry. In: Doc Ophthalmol Proc Ser 26. Greve EL, Verriest G (eds). Junk; Amsterdam: 199-206.

Eichenberger D, Hendrickson P, Robert Y, Gloor B (1987) Influence of ocular media on perimetric results, 2. Effect of simulated cataract. In: Doc Ophthalmol Proc Ser 49. Greve EL, Heijl A (eds). Nijhoff / Junk; Dordrecht: 9-13.

Eisner A, MacLeod DI (1980) Blue-sensitive cones do not contribute to luminance. J Opt Soc Am 70: 121-123.

Eisner A, Fleming SA, Klein ML, Mauldin WM (1987) Sensitivites in older eyes with good acuity: cross-sectional norms. Invest Ophthalmol Vis Sci 28: 1824-1831.

Eizenman M, Frecker RC, Hallet PE (1984) Precise non-contact measurement of eye movements using corneal reflex. Vision Res 24: 167-174.

Eizenman M, Buys YM, Nadler M, Trope GE (1993) Increase of the short-term fluctuation at the slope of a scotoma. Invest Ophthalmol Vis Sci 34 (suppl): 1263.

Elder MJ (1992) Diazepam and its effects on visual fields. Austr NZ J Ophthalmol 20: 267-270.

Elliott DB (1987) Contrast sensitivity decline with ageing: a neural or optical phenomenon? Ophthal Physiol Opt 7: 415-419.

Elliott DB, Hurst MA (1989) Assessing the effect of cataract: A clinical evaluation of the opacity lensmeter 701. Optom Vis Sci 66: 257-263.

Elliott DB, Gilchrist J, Whitaker D (1989) Contrast sensitivity and glare sensitivity changes with three types of cataract morphology. Are these techniques necessary in a clinical evaluation of cataract? Ophth Physiol Opt 9: 25-30.

Elliott DB, Hurst MA, Weatherill J (1991a) Comparing clinical tests of visual loss in cataract patients using quantification of forward light scatter. Eye 5: 601-606.

Elliott DB, Mitchell S, Whitaker D (1991b) Factors affecting light scatter in contact lens wearers. Optom Vis Sci 68: 629-633.

Engel S. (1942) Influence of a constricted pupil on the field in glaucoma. Arch Ophthalmol 27: 1184-1187.

Enger C, Sommer A (1987) Recognising glaucomatous field loss with the Humphrey Statpac. Arch Ophthalmol 105: 1355-1357.

Enoch JM, Campos EC, Bedell HE (1979) Visual resolution in a patient exhibiting a visual fatigue or saturation-like effect. Arch Ophthalmol 97: 76-78.

Enoch JM, Campos EC (1979) Analysis of patients with open-angle glaucoma using perimetric techniques reflecting receptive field-like properties. In: Doc Ophthalmol Proc Ser 19. Greve EL (ed). Junk; Amsterdam: 137-149.

Falcao-Reis FM, O'Donoghue E, Buceti R, Hitchings R, Arden GB (1990) Peripheral contrast sensitivity in glaucoma and ocular hypertension. Br J Ophthalmol 74: 712-716.

Falcao-Reis FM, O'Sullivan F, Spileers W, Hogg C, Arden GB (1991) Macular colour contrast sensitivity in ocular hypertension and glaucoma: evidence for two types of defect. Br J Ophthalmol 75: 598-602.

Fankhouser F, Schmidt T (1960) Die optimalen bedingungen fur die untersuchung der raumlichen summation mit stehender reizmarch nach der methode der quantitativen licht-sinnperimetrie. Ophthalmologica 139: 409-423.

Fankhouser F, Enoch JM (1962) The effect of blur on perimetric thresholds. Arch Ophthalmol 68: 240-251.

Fankhouser F (1969). Kinetische Perimetrie. Ophthalmologica 158: 406-418.

Fankhouser F, Koch P, Roulier A (1972) On automation of perimetry. Albrecht von Graefes Arch Klin Ophthalmol 184: 126-150.

Fankhouser F, Spahr J, Bebié H (1977) Some aspects on the automation of perimetry. Surv Ophthalmol 22: 131-141.

Fankhouser F (1979). Problems relating to the design of automatic perimeters. Doc Ophthalmol 47: 89-138.

Fankhouser F, Bebié H (1979) Threshold fluctuations, interpolations and spatial resolution in perimetry. In: Doc Ophthalmol Proc Ser 19. Greve EL (ed). Junk; Amsterdam: 295-309.

Fankhouser F, Haeberlin H (1980) Dynamic range and straylight: an estimate of the falsifying effects of straylight in perimetry. Doc Ophthalmol 50: 143-167.

Fankhouser F, Jenni A (1981) Programs Sargon and Delta: Two new principles for the automated analysis of the visual field. Albrecht von Graefe's Arch Klin Ophthalmol 216: 41-48.

Fankhouser F, Bebié H, Flammer J (1988) Threshold fluctuations in the Humphrey Field Analyser and in the Octopus automated perimeter (letter). Invest Ophthalmol Vis Sci 29: 1466.

Fankhouser F (1993) Influence of missed catch trials on the visual field in normal subjects. Graefe's Arch Clin Exp Ophthalmol 231: 58-59.

Fankhouser F, Fankhouser F, Geiger H (1993) A cluster and scotoma analysis based on empiric criteria. Graefe's Arch Clin Exp Ophthalmol 231: 697-703.

Farber DB, Flannery JG, Lolley RN, Bok D (1985) Distribution patterns of photoreceptors, protein, and cyclic nucleotides in the human retina. Invest Ophthalmol Vis Sci 26: 1558-1568.

Fazio P, Krupin T, Feitl ME, Werner EB, Carre DA (1990) Optic disc topography in patients with low-tension glaucoma and primary open angle glaucoma. Arch Ophthalmol 108: 705-708.

Fechtner RD, Weinreb RN (1994) Mechanisms of optic nerve damage in primary open angle glaucoma. Surv Ophthalmol 39: 23-42.

Feeny S, Kaiser PK, Thomas JP (1966) An analysis of data gathered by the staircase method. Am J Psychol 79: 652-654.

Felius J, de Jong LAMS, van den Berg TJTP, Greve EL (1993) Automated scotopic in glaucoma. In: Perimetry Update 1992/93. Proceedings of the Xth International Perimetric Society Meeting. Mills RP (ed). Kugler; Amsterdam / New York: 339-343.

Fellman RL, Lynn JR, Starita RJ, Swanson WH (1989) Clinical importance of spatial summation in glaucoma. In: Perimetry Update 1988/89. Proceedings of the VIIIth International Perimetric Society Meeting. Heijl A (ed). Kugler / Ghedini; Amsterdam: 313-324.

Feree CE, Rand G, Monroe MM (1929) Errors of refraction: age and sex in relation to the size of the form field. Am J Ophthalmol 12: 659-654.

Feree C, Rand G, Hardy C (1931) Refraction for the peripheral field of vision. Arch Ophthalmol 5: 717-731.

Feuer WJ, Anderson DR (1989) Static threshold asymmetry in early glaucomatous field loss. Ophthalmology 96: 1285-1297.

Fishman GA, Krill AE, Fishman M (1974) Acquired colour vision defects in patients with open-angle glaucoma and ocular hypertension. Mod Probl Ophthalmol 13: 335-338.

Fitzke FW, McNaught AI (1994) The diagnosis of visual field progression in glaucoma. Curr Opin Ophthalmol 5: 110-115.

Flammer J, Drance SM, Zulauf M et al (1984a) Differential light threshold: short- and long-term fluctuation in patients with glaucoma, normal controls and patients with suspected glaucoma. Arch Ophthalmol 102: 704-706.

Flammer J, Drance SM, Fankhouser et al (1984b) Differential light threshold in automated static perimetry: factors influencing short-term fluctuation. Arch Ophthalmol 102: 876-879.

Flammer J, Drance SM, Schulzer M (1984c) Covariates of the long-term fluctuation of the differential light threshold. Arch Ophthalmol 102: 880-882.

Flammer J, Drance SM (1984) Correlation between color vision scores and quantitative perimetry in suspected glaucoma. Arch Ophthalmol 102: 38-39.

Flammer J (1984) Diffuse visual field damage in glaucoma. In: Recent advances in glaucoma. Ticho U, David R (eds). Elsevier; New York: 9-12.

Flammer J, Drance SM, Augustiny L, Funkhouser AT (1985) Quantification of glaucomatous visual field defects with automated perimetry. Invest Ophthalmol Vis Sci 26: 76-81.

Flammer J (1985) Psychophysics in glaucoma: a modified concept of the disease. In: Proceedings of the 2nd European Glaucoma Symposium. Greve EL, Leydhecker W, Raitta C (eds). Junk; Dordrecht:11-17.

Flammer J (1986) The concept of visual field indices. Graefe's Arch Clin Exp Ophthalmol 224: 389-392.

Flammer J, Jenni F, Bebié H, Keller B (1987) The Octopus glaucoma G1 program. Glaucoma 9: 67-72.

Flammer J, Bebié H (1987) Lens Opacity Meter: A new method to quantify lens opacity. Ophthalmologica 195: 69-72.

Flanagan JG, Wild JM, Wood JM (1988) Stimulus configuration and the format of the normal sensitivity gradient. Doc Ophthalmol 69: 371-383.

Flanagan JG, Trope GE, Popick W, Grover A (1991a) Perimetric isolation of the SWS cones in OHT and early POAG. In: Perimetry Update 1990/91. Proceedings of the IXth International Perimetric Society Meeting. Mills RP, Heijl A (eds). Kugler / Ghedini; Amsterdam / New York: 331-337.

Flanagan JG, Wild JM, Hovis JK (1991b) The differential light threshold as a function of retinal adaptation- the Weber-Fechner / Rose-de-Vries controversy revisited. In: Perimetry Update 1990/91. Proceedings of the IXth International Perimetric Society Meeting. Mills RP, Heijl A (eds). Kugler; Amsterdam / New York: 551-554.

Flanagan JG, Wild JM, Trope GE (1993a) The visual field indices in primary open-angle glaucoma. Invest Ophthalmol Vis Sci 34: 2266-2274.

Flanagan JG, Wild JM, Trope GE (1993b) Evaluation of FASTPAC, a new strategy for threshold estimation with the Humphrey Field Analyser, in a glaucomatous population. Ophthalmology 100: 949-954.

Forbes M (1966) Influence of miotics on visual fields in glaucoma. Invest Ophthalmol Vis Sci 5: 139-145.

Friedmann AI (1991) Blue stimuli versus white stimuli in glaucoma. In: Perimetry Update 1990/91. Proceedings of the IXth International Perimetric Society Meeting. Mills RP, Heijl A (eds). Kugler; Amsterdam / New York: 321-324.

Fry GA (1954) A re-evaluation of the scatter theory of glare. Illum Eng 49: 98-102.

Fuhr PS, Hershner TA, Daum KM (1990) Ganzfeld blankout occurs in bowl perimetry and is eliminated by translucent occlusion. Arch Ophthalmol 108: 983-988.

Fujimoto N, Adachi-Usami E (1992a) Effect of number of test points in automated perimetry. Am J Ophthalmol 113: 317-320.

Fujimoto N, Adachi-Usami E (1992b) Increased sensitivity with decreased numbers of test points and decreased test field size in automated perimetry of normal subjects. Ophthalmologica 204: 88-92.

Funk J, Bornscheuer C, Grehn F (1988) Neuroretinal rim area and visual field in glaucoma. Graefe's Arch Clin Exp Ophthalmol 226: 431-434.

Funk J, Soriano JM, Ebner D (1993) Correlation between optic disc changes and visual field loss in patients with unilateral glaucoma. In: Perimetry Update 1992/93. Proceedings of the Xth International Perimetric Society Meeting. Mills RP (ed). Kugler; Amsterdam / New York: 159-163.

Funkhouser AT, Fankhouser F (1985) Spatially adaptive programs. In: Computerised Visual Fields: What are they and how to use them? Whalen WR, Spaeth G (eds). Slack; New Jersey: 110-116.

Funkhouser A, Fankhouser F (1991) The effects of weighting the "mean defect" visual field index according to threshold variability in the central and midperipheral visual field. Graefe's Arch Clin Exp Ophthalmol 229: 228-331.

Funkhouser AT (1991) A new diffuse loss index for estimating general glaucomatous visual field depression. Doc Ophthalmol 77: 57-72.

Funkhouser A, Flammer J, Fankhouser F, Hirsbrunner HP (1992a) A comparison of five methods for estimating general glaucomatous visual field depression. Graefe's Arch Clin Exp Ophthalmol 230: 101-106.

Funkhouser AT, Fankhouser F, Weale RA (1992b) Problems related to diffuse versus localised loss in the perimetry of glaucomatous visual fields. Graefe's Arch Clin Exp Ophthalmol 230: 243-247.

Gartner S, Henkind P (1981) Ageing and degeneration of the human macula. Outer nuclear layer and photoreceptors. Br J Ophthalmol 65: 23-28.

Gaspar AZ, Flammer J, Hendrickson P (1994) Factors influencing the duration of a perimetric test. Glaucoma 16: 40-43.

Geier SA, Kronawitter U, Bogner JB et al (1993) Impairment of colour contrast sensitivity and neuroretinal dysfunction in patients with symptomatic HIV infection or AIDS. Br J Ophthalmol 77: 716-720.

Genio C, Friedmann AI (1981) A comparison between the white light and blue light in 70 eyes in patients with early glaucoma using the mark II Visual Field Analyser. In: Doc Ophthalmol Proc Ser 26. Greve EL, Verriest G (eds), Junk; Amsterdam: 207-214.

Gilbert C, Wiesel TN (1991) Soc Neurosci Abstr 17: 1090. (Cited in: Campbell FW, Andrews PR (1992) Motion reveals spatial visual defects. Ophthal Physiol Opt 12: 131-132).

Gilpin LB, Stewart WC, Hunt HH, Broom CD (1990) Threshold variability using different Goldmann stimulus sizes. Acta Ophthalmol 68: 674-676.

Glass E, Schaumberger M, Lachenmayr BJ (1993) Computer simulations for FASTPAC and the standard 4-2dB threshold strategy of the Humphrey Field Analyser. Invest Ophthalmol Vis Sci 34 (suppl): 1264.

Gloor B, Schmied U, Fassler A (1980) Changes of glaucomatous field defects: degree of accuracy and measurements with the automated perimeter Octopus. Int Ophthal 3: 5-10.

Gloor BP, Schmied U, Fassler A (1981) Changes of glaucomatous field defects. Analysis of Octopus fields with programme Delta. In: Doc Ophthalmol Proc Ser 26. Greve EL, Verriest G (eds). Junk; Amsterdam: 11-15.

Gloor B, Gloor E (1986) Die Erfassbarkeit glaukomatoser Gesichtsfeldausfalle mit dem automatischen Perimeter Oktopus. Ein Vergleich zwischen Program G1 und den Programmen 31 und 32 und deren Kombination. Klin Monatsbl Augenheilkd 188: 33-38.

Glovinsky Y, Quigley HA, Dunkelberger GR (1991) Retinal ganglion cell loss is size dependent in experimental glaucoma. Invest Ophthalmol Vis Sci 32: 484-491.

Glovinsky Y, Quigley HA, Drum B, Bissett RA, Jampel HD (1992) A whole-field scotopic retinal sensitivity test for the detection of early glaucoma. Arch Ophthalmol 110: 486-490.

Glovinsky Y, Gershovitz A (1994) Evaluation of the Humphrey fast strategy for follow-up of glaucoma suspects and glaucoma patients. Invest Ophthalmol Vis Sci 35 (suppl): 2183.

Glowazki A, Flammer J (1987) Is there a difference between glaucoma patients with rather localised visual field damage and patients with more diffuse visual field damage? In: Doc Ophthalmol Proc Ser 49. Greve EL, Heijl A (eds). Nijhoff / Junk; Dordrecht: 317-320.

Goldbaum MH, Sample PA, White H, Weinreb RH (1990) Discrimination of normal and glaucomatous visual fields by neural networks. Invest Ophthalmol Vis Sci 31 (suppl): 503.

Goldbaum MH, Sample PA, White H (1994) Interpretation of automated perimetry for glaucoma by neural network. Invest Ophthalmol Vis Sci 35: 3362-3373.

Goldmann H (1945a) Grundlagen exakter Perimetrie. Ophthalmologica 109: 57-70.

Goldmann H (1945b) Ein selbstregistrierendes Projektion-skugelperimeter. Ophthalmologica 109: 71-79.

Gollamundi SR, Liao P, Hirsch J (1988) Evaluation of corrected loss variance as a visual field index. II Corrected loss variance in conjunction with mean defect may identify stages of glaucoma. Ophthalmologica 197: 144-150.

Gougnard L (1961) Etude des sommations spatiales chez le Sujet normal par la perimetrie statique. Ophthalmologica 142: 469-486.

Gouras P (1968) Identification of cone mechanisms in monkey ganglion cells. J Physiol 199: 533-547.

Gouras P (1969) Antidromic responses of orthodromically identified ganglion cells in monkey retina. J Physiol 204: 407-419.

Gramer E, Kontic D, Kriegelstein GK (1981) Die computerperimetrische Darstellung glaukomatoser Geisichtsfelddefekte in Abhangigkeit von der Stimulusgrosse. Ophthalomologica 183: 162-167.

Gramer E, Steinhouser B, Kriegelstein GK (1982a) The specificity of the automated suprathreshold perimeter Fieldmaster 200. Albrecht von Graefe's Arch Klin Ophthalmol 218: 253-255.

Gramer E, Gerlach R, Kriegelstein GK, Leydhecher W (1982b) Topography of early visual field defects in computerised perimetry. Klin Monatsbl Augenheilkd 180: 515-523.

Gramer E, DeNatale R, Leydhecker W (1986) Training effects and fluctuations in long-term follow up of glaucomatous visual field defects calculated with program Delta of the Octopus perimeter 201. New Trends Ophthalmol 1: 219-228.

Gramer E, Siebert M (1989) Optic nerve head measurements: the optic nerve head analyser - its advantages and limitations. Int Ophthalmol 13: 3-13.

Gramer E, Althaus G, Korner U (1993) Are visual field defects in the lower hemifield a risk factor in POAG. Perimetry Update 1992/93, Proceedings of the Xth International Perimetric Society Meeting. Mills RP (ed). Kugler; Amsterdam / New York: 81-87.

Green DG (1968) The contrast sensitivity of colour mechanisms of the human eye. J Phsiol 196: 415-429.

Greenstein VC, Hood DC, Ritch R, Steinberger D, Carr RE (1989) S (blue) cone pathway vulnerability in retinitis pigmentosa, diabetes and glaucoma. Invest Ophthalmol Vis Sci 30: 1732-1737.

Greve EL, Wijnans M (1973) The statistical evaluation of measurements in static campimetry and its consequences for multiple stimulus campimetry. Ophthal Res 4: 355-366.

Greve EL (1973) Single and multiple stimulus static perimetry in glaucoma, the two phases of perimetry. Doc Ophthalmol 36: 144-146.

Greve EL, Verduin WM, Ledeboer M (1974) Two-color threshold in static perimetry. Mod Probl Ophthalmol 13: 113-118.

Greve EL (1975) Static perimetry. Ophthalmologica 171: 26-38.

Greve EL, Verduin WM (1977) Detection of early glaucomatous damage. Part I. Visual field examination. In: Doc Ophthalmol Proc Ser 14. Greve EL (ed). Junk; Amsterdam: 103-114.

Greve EL (1979) Visual fields, glaucoma and cataract. In: Doc Ophthalmol Proc Ser 22. Greve EL (ed). Junk; Amsterdam: 79-88.

Greve EL (1980) Some aspects of visual field examination related to strategies for detection and assessment. Doc Ophthalmol Proc Ser 22. Greve EL (ed). Junk; Amsterdam: 15-28.

Greve EL (1982) Performance of computer assisted perimeters. Doc Ophthalmol 53: 343-380.

Guilford JP (1954) In: Psychometric Methods. McGraw-Hill, New York: 101-117.

Gunderson KG, Heijl A, Asman P (1993) Stimulus size and normal inter-individual variability in static perimetry. Invest Ophthalmol Vis Sci 34 (suppl): 1262.

Gunduz K, Arden GB, Perry S, Weinstein GW, Hitchings RA (1988) Color vision defects in ocular hypertension and glaucoma: A quantification with a computer-driven color vision system. Arch Ophthalmol 106: 929-935.

Gundunz K, Arden GB (1989) Changes in colour contrast sensitivity associated with operating argon lasers. Br J Ophthalmol 73: 241-246.

Gur M (1989) Color and brightness fade-out in the Ganzfeld is wavelength dependent. Vision Res 29: 1335-1341.

Gur M (1991) Perceptual fade-out occurs in the binocularly viewed Ganzfeld. Perception 20: 645-654.

Guthauser U, Flammer J, Niesel P (1987) The relationship between the visual field and the optic nerve head in glaucomas. Graefe's Arch Clin Exp Ophthalmol 225: 129-132.

Guthauser U, Flammer J (1988) Quantifying visual field damage caused by cataract. Am J Ophthalmol 106: 480-484.

Gutteridge IF (1984) A review of strategies for screening of the visual fields. Aust J Optom 67: 9-18.

Guttridge NM, Allen PM, Rudnicka AR, Edgar DF, Renshaw AE (1991) Influence of learning on the peripheral field as assessed by automated perimetry. In: Perimetry Update 1990/91. Proceedings of the IXth International Perimetric Society Meeting. Mills RP, Heijl A (eds). Kugler; Amsterdam / New York: 567-575.

Guttridge NM, Edgar DF, Crabb D (1992) The effect of the menstrual cycle on automated perimetry. Invest Ophthalmol Vis Sci 33 (suppl): 969.

Haas A, Flammer J (1985) Influence of diazepam on differential light sensitivity. Doc Ophthalmol Proc Ser 42. Greve EL (ed). Junk; Amsterdam: 527-532.

Haas A, Flammer J, Schnieder U (1986) Influence of age on the visual fields of normal subjects. Am J Ophthalmol 101: 199-203.

Haeberlin H, Funkhouser A, Fankhouser F (1983) Angioscotoma: preliminary results using the new spatially adaptive program SAPRO. In: Doc Ophthalmol Proc Ser 35. Greve EL (ed). Junk; Amsterdam: 331-334.

Haegestrom-Portnoy G (1988) Short-wavelength sensitive cone sensitivity losses with ageing: A protective role for macular pigment. J Opt Soc Am 5: 2140-2144

Haegestrom-Portnoy G, Hewlett SE, Barr SAN (1989) S cone loss with ageing. In: Colour Vision Deficiencies IX. Drum B, Verriest G (eds). Kluwer; Dordrecht: 345-352.

Haider M, Dixon F (1961) Influences of training and fatigue on the continuous recording of a visual differential threshold. Br J Psychol 52: 227-229.

Haley MJ (1987) The Field Analyser Primer. Allergan Humphrey, San Leandro, CA.

Ham WT, Mueller HA, Sliney DH (1976) Retinal sensitivity to radiation damage from short wavelength light. Nature 260: 153-158.

Hamill TR, Post RB, Johnson CA, Keltner JL (1984) Correlation of colour vision deficits and observable changes in the optic disc in a population of ocular hypertensives. Arch Ophthalmol 102: 1637-1639.

Hammond BR, Fuld K (1992) Interocular differences in macular pigment density. Invest Ophthalmol Vis Sci 33: 350-355.

Hard AL, Beckman C, Sjostrand J (1993) Glare measurements before and after cataract surgery. Acta Ophthalmol 71: 471-476.

Harding JJ, Egerton M, van Heyningen R, Harding RS (1993) Diabetes, glaucoma, sex, and cataract: analysis of combined data from two case control studies. Br J Ophthalmol 77: 2-6.

Hardy KJ, Craven B, Foster DH, Scarpello JH (1994) Extent and duration of practice effects on performance with the Farnsworth-Munsell 100-Hue test. Ophthal Physiol Opt 14: 306-309.

Harms H (1952) Die praktische Bedeuting quantitatativer Perimetric. Klin Mbl Augenheilk 121: 683-692.

Harrington DO (1981) In: The visual fields; a textbook and atlas of clinical perimetry. Mosby; St Louis: 215.

Hart WM, Hartz RK (1982) Computer-generated display for three-dimensional static perimetry. Arch Ophthalmol 100: 312-318.

Hart WM, Becker B (1982) The onset and evolution of glaucomatous visual field defects. Ophthalmology 89: 268-279.

Hart WM, Hartz RK, Hagen RW, Clark KW (1984) Color contrast perimetry. Invest Ophthalmol Vis Sci 25: 400-413.

Hart WM, Gordon MO (1984) Color perimetry of glaucomatous visual field defects. Ophthalmology 91: 338-346.

Hart WM (1987) Acquired dyschromatopsias. Surv Ophthalmol 32: 10-31.

Hart WM (1987) In: Adler's Physiology of the eye (8th edition). Moses RA, Hart WM (eds). Mosby; St Louis, Washington DC, Toronto: 430-431.

Hart WM (1989) Blue/Yellow color contrast perimetry compared to conventional kinetic perimetry in patients with established visual field defects. In: Perimetry Update 1988/89. Proceedings of the VIIIth International Perimetric Society Meeting. Heijl A (ed). Kugler / Ghedini; Amsterdam / Berkeley / Milano: 23-30.

Hart WM, Silverman SE, Trick GJ et al (1990) Glaucomatous visual field damage. Luminance and color contrast sensitivities. Invest Ophthalmol Vis Sci 31: 359-367.

Hart WM, Gordon MO, Silverman, Kass (1991) Equiluminant blue/yellow color contrast perimetry (CCP) in high risk ocular hypertension (OHT) and glaucoma (POAG). In: Perimetry Update 1990/91. Proceedings of the IXth International Perimetric Society Meeting. Mills RP, Heijl A (eds). Kugler; Amsterdam / New York: 325-329.

Harwerth RS, Sperling HG (1975) Effects of intense visible radiation on the increment-threshold spectral sensitivity of the rhesus monkey eye. Vision Res 15: 1193-1204.

Harwerth RS, Smith EL, DeSantis L (1993) Mechanisms mediating visual detection in static perimetry. Invest Ophthalmol Vis Sci 34: 3011-3023.

Hatch W, Flanagan JG, Trope GE (1994) Evaluation of the repeatability of FASTPAC in glaucoma. Presented as a poster at the XIth International Perimetric Society Meeting, Washington DC, USA; July 4-7th 1994: 69.

Heijl A, Krakau CET (1975a) An automatic static perimeter, design and pilot study. Acta Ophthalmol 53: 293-310.

Heijl A, Krakau CET (1975b) An automatic perimeter for glaucoma visual field screening and control: Construction and clinical cases. Graefe's Arch Clin Exp Ophthalmol 197: 13-23.

Heijl A (1977a) Computer test logics for automated perimetry. Acta Ophthalmol 55: 837-853.

Heijl A (1977b) Time changes of contrast thresholds during automated perimetry. Acta Ophthalmol 55: 696-708.

Heijl A, Krakau CET (1977) A note on fixation during perimetry. Acta Ophthalmol 55: 854-861.

Heijl A, Drance SM (1983) Changes in differential threshold in patients with glaucoma during prolonged perimetry. Br J Ophthalmol 67: 512-516.

Heijl A (1984) Computerised perimetry. Trans Ophthalmol Soc UK 104: 76-87.

Heijl A (1985a) The Humphrey Field Analyser. Construction and concepts. In: Doc Ophthalmol Proc Ser 49. Greve EL (ed). Junk; Amsterdam: 77-84.

Heijl A (1985b) Strategies for detection of glaucoma defects. In: Automated Perimetry in Glaucoma, a practical guide. Drance SM, Anderson D (eds). Grune / Stratton; Orlando / London: 43-54.

Heijl A, Lindgren G, Olsson J (1987a) Reliability parameters in computerised perimetry. In: Doc Ophthalmol Proc Ser 49. Proceedings of the VIIth International Perimetric Society Meeting. Greve EL, Heijl A (eds). Junk; Amsterdam: 593-600.

Heijl A, Lindgren G, Olsson J (1987b) Normal variability of static perimetric threshold values across the central visual field. Arch Ophthalmol 105: 1544-1549.

Heijl A, Lindgren G, Olsson J (1987c) A package for the statistical analysis of computerised fields. Doc Ophthalmol Proc Ser 49. Proceedings of the VIIth International Perimetric Society Meeting. Greve EL, Heijl A (eds). Junk; Amsterdam: 153-168.

Heijl A, Lindgren G, Olsson J (1988) Perimetric threshold variability and age. Arch Ophthalmol 106: 450-452.

Heijl A (1989) Lack of diffuse loss of differential light sensitivity in early glaucoma. Acta Ophthalmol 67: 353-360.

Heijl A, Lindgren G, Olsson J (1989a) The effect of perimetric experience in normal subjects. Arch Ophthalmol 107: 81-86.

Heijl A, Lindgren A, Lindgren G (1989b) Test-retest variability in glaucomatous visual fields. Am J Ophthalmol 108: 130-135.

Heijl A, Lindgren F, Olsson J, Asman P (1989c) Visual field interpretation with empiric probability maps. Arch Ophthalmol 107: 204-208.

Heijl A, Lindgren A, Lindgren G (1989d) Inter-point correlations of deviations of threshold values in normal and glaucomatous visual fields. In: Perimetry Update 1988/89. Proceedings of the IXth International Perimetric Society Meeting. Heijl A (ed). Kugler / Ghedini; Amsterdam / Berkeley / Milano: 177-183.

Heijl A, Asman P (1989) A clinical study of perimetric probability maps. Arch Ophthalmol 107: 199-203.

Heijl A, Bengtsson B (1989) Diagnosis of early glaucoma with flicker comparison of serial disc photographs. Invest Ophthalmol Vis Sci 30: 2376-2384.

Heijl A, Lindgren G, Lindgren A et al (1991) Extended empirical statistical package for evaluation of single and multiple fields in glaucoma: statpac 2. Perimetry Update 1990/91. Proceedings of the IXth International Perimetric Society Meeting. Mills RP, Heijl A (eds). Kugler / Ghedini; Amsterdam / New York: 305-315.

Heijl A (1991) Some characteristics of glaucomatous visual field loss. In: Glaucoma Update IV. Kriegelstein GK (ed), Springer-Verlag, Berlin / Heidelberg: 133-139.

Heijl A (1993) Perimetric point density and detection of glaucomatous visual field loss. Acta Ophthalmol 71: 445-450.

Heijl A, Molder H (1993) Optic disc diameter influences the ability to detect glaucomatous disc damage. Acta Ophthalmol 71: 122-129.

Heijl A, Bengtsson B (1994) Perimetric learning in glaucoma. Presented as a paper at the XIth International Perimetric Society Meeting, Washington DC, USA; July 3-7th 1994: 62.

Heidin A, Verriest G (1981) Is clinical colour perimetry useful? In: Doc Ophthalmol Proc Ser 26. Greve EL, Verriest G (eds). Junk; Amsterdam: 161-181.

Hendrickson P, Eichenberger D, Gloor B, Robert Y (1987) Influence of ocular media on perimetric results: Effect of IOL implantation. In: Doc Ophthalmol Proc Ser 49. Greve EL, Heijl A (eds). Nijhoff / Junk; Dordrecht: 3-8.

Henson DB, Bryson H (1991) Is variability in glaucomatous field loss due to poor fixation control? In: Perimetry Update 1990/ 91. Proceedings of the IXth International Perimetric Society Meeting. Mills RP, Heijl A (eds). New York; Kugler / Ghedini: 217-220.

Henson DB, Morris EJ (1993) Effect of uncorrected refractive errors upon central visual field testing. Ophthal Physiol Opt 13: 339-343.

Henson D, Spenceley S, Bull D (1994) Application of artificial neural networks to progressive field loss in glaucoma. Presented as a paper at the XIth International Perimetric Society Meeting, July 2-7th 1994, Washington DC, USA: 20.

Heron G, Adams AJ, Husted R (1988) Central visual fields for short wavelength sensitive pathways in glaucoma and ocular hypertension. Invest Ophthalmol Vis Sci 29: 64-72.

Hess RF, Garner LF (1977) The effect of corneal oedema on visual function. Invest Ophthalmol Vis Sci 16: 5-13.

Hess RF, Woo G (1978) Vision through cataracts. Invest Ophthalmol Vis Sci 17: 428-435.

Heur DK, Anderson DR, Knighton RW, Feuer WJ, Gressel MG (1988) The influence of simulated light scatter on automated perimetric threshold measurements. Arch Ophthalmol 106: 1247-1251.

Heur DK, Anderson DR, Feuer WJ, Gressel MG (1989) The influence of decreased retinal illumination on automated perimetric threshold measurements. Am J Ophthalmol 108: 643-650.

Higgins KE, Jaffe MJ (1988) Spatial contrast sensitivity: effects of age, test-retest, and psychophysical method. J Opt Soc Am 5: 2173-2180.

Hills JF, Johnson CA (1988) Evaluation of the t-test as a method of detecting visual field changes. Ophthalmology 95: 261-266.

Hirsbrunner HP, Fankhouser F, Jenni A, Funkhouser A (1990) Evaluating a perimetric expert system: experience with Octosmart. Graefe's Arch Clin Exp Ophthalmol 228: 237-241.

Hitchings RA, Spaeth GL (1977) The optic disc in glaucoma: Correlation of the appearance of the optic disc with the visual field. Br J Ophthalmol 61: 107-113.

Hitchings RA, Powell DJ, Arden GB, Carter RM (1981) Contrast sensitivity gratings in glaucoma family screening. Br J Ophthalmol 65: 515-517.

Hitchings RA, Anderton SA (1983) A comparative study of visual field defects seen in patients with low-tension glaucoma and chronic simple glaucoma. Br J Ophthalmol 67: 818-821.

Hitchings RA, Poinoosawmy D, Poplar N, Sheth GP (1987) Retinal nerve fiber layer photography in glaucomatous patients. Eye 1: 621-625.

Hitchings RA, Midgal CM, Fitzke FW (1991) Intraocular pressure control: does it protect the visual field. In: Glaucoma Update IV. Kriegelstein GK (ed). Springer-Verlag; Berlin / Heidelberg: 179-182.

Hochberg JE, Triebel W, Seaman G (1951) Color adaptation under conditions of homogeneous visual stimulation (ganzfeld). J Exp Psychol 41: 153-159.

Holladay LL (1926) The fundamentals of glare and visibility. J Opt Soc Am 12: 271-319.

Holmin C, Krakau CET (1979) Variability of glaucomatous visual field defects in computerised perimetry. Albrecht von Graefes Arch Klin Ophthalmol 210: 235-250.

Holmin C, Krakau CET (1980) Visual field decay in normal subjects and in cases of chronic glaucoma. Graefe's Arch Clin Exp Ophthalmol 213: 291-298.

Holmin C, Krakau CET (1982) Regression analysis of the central visual field in chronic glaucoma cases: a follow-up study using automated perimetry. Acta Ophthalmol 60: 264-267.

Hood DC, Benimoff NI, Greenstein VC (1984) The response range of the blue-cone pathways: a source of vulnerability to disease. Invest Ophthalmol Vis Sci 25: 864-867.

Hoskins HD, Magee SD, Drake MV, Kidd MN (1988) Confidence intervals for change in automated visual fields. Br J Ophthalmol 72: 591-597.

Hoskins HD, Hetherington J, Glenday M, Samuels SJ, Verdooner SR (1993) Repeatability of the Glaucoma-Scope measurements of optic nerve head topography. In: Perimetry Update 1992/93. Proceedings of the Xth International Perimetric Society Meeting. Mills RP (ed). Kugler; Amsterdam / New York: 177-185.

House PH, Chauhan BC (1991) Thresholding strategies in conventional and high-pass resolution perimetry. Invest Ophthalmol Vis Sci 32 (suppl) : 1191.

Hoyt WF, Schlicke B, Eckelhoff RJ (1972) Fundoscopic appearance of a nerve fibre bundle defect. Br J Ophthalmol 56: 577-583.

Hoyt WF, Frisen L, Newman NM (1973) Fundoscopy of nerve fiber layer defects in glaucoma. Invest Ophthalmol Vis Sci 12: 814-829.

Hudson C, Wild JM (1993) Influences of pre-receptoral absorption in blue-yellow perimetry. In: Perimetry Update 1992/93. Proceedings of the Xth International Perimetric Society Meeting. Mills RP (ed). Kugler; Amsterdam / New York: 451-457.

Hudson C, Wild JM, O'Neill EC (1994) Fatigue effects during a single session in normals and ocular hypertensives. Invest Ophthalmol Vis Sci 35: 268-280.

Hugkulstone CE, Vernon SA (1992) Blue versus white stimuli in ocular hypertension with the Friedmann Mark I visual field analyser. Eye 6: 356-360.

Humanski RA, Wilson HR (1992) Spatial frequency mechanisms with short-wavelength-sensitive cone inputs. Vision Res 32: 549-560.

Hurvich LM, Jameson D (1957) An opponent-process theory of color vision. Psychol Rev 64: 384-404.

Hutchings N, Wild JM, Hussey MK, Flanagan JG, Trope GE (1993) The homogeneous and heterogeneous components of the long term fluctuation in glaucomatous field loss. Invest Ophthalmol Vis Sci 34 (suppl): 1263.

IJspeert JK, deWaard PWT, van den Berg TJTP, de Jong PTVM (1990) The intraocular straylight function in 129 healthy volunteers: dependence on angle, age and pigmentation. Vision Res 30: 699-707.

Ingling C, Martinez E (1980) The spatio-temporal signal of the r-g channel. In: Colour Vision. Mollon JD, Sharpe LT (eds). Academic; London: 433-444.

Jacobsen SG, Voigt WJ, Parel JM et al (1986) Automated light- and dark- adapted perimetry for evaluating retinitis pigmentosa. Ophthalmology 93: 1604-1611.

Jaffe GF, Alvarado JA, Juster RP (1986) Age-related changes of the normal visual field. Arch Ophthalmol 104: 1021-1025.

Janknecht P, Funk J (1994) Optic nerve head analyser and Heidelberg retina tomograph: accuracy and reproducibility of topographic measurements in a model eye and in volunteers. Br J Ophthalmol 78: 760-768.

Jay BS (1962) The effective pupillary area at varying perimetric angles. Vision Res 1: 418-424.

Jayle GE, Aubert L (1958) Le champ visuel mesopique en pathologie oculaire. In: Actualites Latines d'Ophtalmologie. Masson; Paris: 50-115.

Johnson CA, Keltner JL, Balestrery F (1978) Effects of target size and eccentricity on visual detection and resolution. Vision Res 18: 1217-1222.

Johnson CA, Choy D (1987) On the definition of age-related norms for visual function testing. Appl Optics 26: 1449-1454.

Johnson CA, Adams CW, Lewis RA (1988a) Fatigue effects in automated perimetry. Appl Optics 27: 1030-1037.

Johnson CA, Adams AJ, Twelker JD, Quigg JM (1988b) Age-related changes in the central visual field for short-wavelength sensitive pathways. J Opt Soc Am 5: 2131-2319.

Johnson CA, Adams AJ, Lewis RA (1988c) Automated perimetry of blue-sensitive mechanisms in ocular hypertension and early glaucoma. Invest Ophthalmol Vis Sci 29 (suppl): 42.

Johnson CA, Adams AJ, Lewis RA (1989a) Automated perimetry of short-wavelength mechanisms in glaucoma and ocular hypertension. In: Perimetry Update 1988/89. Proceedings of the VIIIth International Perimetric Society Meeting. Heijl A (ed). Kugler / Ghedini; Amsterdam / New York: 31-37.

Johnson CA, Adams AJ, Lewis RA (1989b) Evidence for a neural basis of age-related visual field loss in normal observers. Invest Ophthalmol Vis Sci 30: 2056-2064.

Johnson CA, Shapiro LR (1989) A comparison of MOBS (modified binary search) and staircase test procedures in automated perimetry. In: Technical digest series: Noninvasive assessment of the visual system 7: 84-87.

Johnson CA, Shapiro LR (1991) A rapid heuristic test procedure for automated perimetry In: Perimetry Update 1990/91. Proceedings of the IXth International Perimetric Society Meeting. Mills RP, Heijl A, (eds). Kugler; Amsterdam / New York: 533-537.

Johnson CA., Chauhan BC, Shapiro LR (1992) Properties of staircase procedures for estimating thresholds in automated perimetry. Invest Ophthalmol Vis Sci 33: 2966-2974.

Johnson CA, Adams AJ, Casson EJ, Brandt JD (1993a) Blue-on-Yellow perimetry can predict the development of glaucomatous visual field loss. Arch Ophthalmol 111: 645-650.

Johnson CA, Adams AJ, Casson EJ, Brandt JD (1993b) Progression of early glaucomatous visual field loss as detected by blue-on-yellow and standard white-on-white automated perimetry. Arch Ophthalmol 111: 651-656.

Johnson CA, Howard DL, Murphy CJ, Shu H (1993c) A rapid, noninvasive video-based method of measuring wavelength-dependent lens transmission properties in the human eye. Optom Vis Sci 70: 944-955.

Johnson CA, Adams AJ, Casson EJ (1993d) Blue-on-Yellow perimetry: a five-year overview. In: Perimetry Update 1992/93. Proceedings of the Xth International Perimetric Society Meeting. Mills RP (ed). Kugler; Amsterdam / New York: 459-465.

Johnson CA, Nelson-Quigg JM (1993) A prospective three-year study of response properties of normal subjects and patients during automated perimetry. Ophthalmology 100: 269-274.

deJong LAMS, Snepvangers CEJ, van den Berg TJTP, Langerhorst CT (1990) Blue-yellow perimetry in the detection of early glaucomatous damage. Doc Ophthalmol 75: 303-314.

deJong LAMS, Felius J, van den Berg TJTP, Greve EL (1993) Comparison of color vision scores with visual field indices in white-on-white and blue-on-yellow automated perimetry in glaucomatous damage. Invest Ophthalmol Vis Sci 34 (suppl): 1267.

Jonas JB, Gusek GC, Naumann GOH (1988a) Optic disc morphometry in chronic primary open-angle glaucoma. I. Morpholometric intrapapillary characteristics. Graefe's Arch Clin Exp Ophthalmol 226: 522-530.

Jonas JB, Gusek GC, Naumann GOH (1988b) Optic disc, cup, and neuroretinal rim size, configuration, and correlations in normal eyes. Invest Ophthalmol Vis Sci 29: 1151-1158.

Jonas JB (1992) Size of glaucomatous optic discs. German J Ophthalmol 1: 41-44,

Jonas JB, Fernandez MC, Sturmer J (1993) Patterns of glaucomatous neuroretinal rim loss. Ophthalmology 100: 63-68.

Jonas JB, Schiro D (1994) Localised wedge-shaped defects of the retinal nerve fibre layer in glaucoma. Br J Ophthalmol 78: 285-290.

Kalloniatis M, Harwerth RS, Smith EL, DeSantis L (1993) Colour vision anomalies following experimental glaucoma in monkeys. Ophthal Physiol Opt 13: 56-67.

Kalloniatis M, Harwerth RS (1993) Modelling sensitivity losses in ocular disorders: colour vision anomalies following intense blue-light exposure. Ophthal Physiol Opt 13: 155-166.

Kaplan E, Shapley RM (1986) The primate retina contains two types of ganglion cells, with high and low contrast sensitivity. Proc Natl Acad Sci 83: 2755-2757.

Karbassi M, Singer DM, Chylack LT (1993) Evaluation of lens opacities classification system III applied at the slit lamp. Optom Vis Sci 70: 923-928.

Katsumori N, Fujii M, Mizokami K (1993) Comparison of visual field defects and optic disc cupping in low tension glaucoma and primary open angle glaucoma. In: Perimetry Update 1992/ 93. Proceedings of the Xth International Perimetric Society Meeting. Mills RP (ed). Kugler; Amsterdam / New York: 225-229.

Katz J, Sommer A (1986) Asymmetry and variation in the normal hill of vision. Arch Ophthalmol 104: 65-68.

Katz J, Sommer A (1987) A longitudinal study of the age-adjusted variability of automated visual fields. Arch Ophthalmol 105: 1083-1086.

Katz J, Sommer A (1988) Reliability indexes of automated perimetric tests. Arch Ophthalmol 106: 1252-1254.

Katz J, Sommer A (1990) Screening for glaucomatous visual field loss. The effect of patient reliability. Ophthalmology 97: 1032-1037.

Katz J, Sommer A, Gaasterland DE, Anderson DR (1991) Comparison of analytic algorithms for detecting glaucomatous visual field loss. Graefe's Arch Clin Exp Ophthalmol 109: 1684-1689.

Kaufman H, Flammer J (1989) Clinical experience with the Bebié-curve. In: Perimetry Update 1988/89. Proceedings of the VIIIth International Perimetric Society meeting. Heijl A (ed). Kugler / Ghedini; Amsterdam / Berkeley / Milano: 235-238.

Kaufmann H, Flammer J, Rutishauser C (1990) Evaluation of fields by ophthalmologists and by Octosmart program. Ophthalmologica 201: 104-109.

Keating D, Mutlukan E, Damato E, Damato BE, Evans A (1992) A back propagation neural network for the classification of visual field data. Invest Ophthalmol Vis Sci 33 (suppl): 970.

Kelly DH (1974) Spatio-temporal frequency characteristics of color-vision mechanisms. J Opt Soc Am 64: 983-990.

Kelman SE, Perell HF, D'Autrechy L, Scott RJ (1991) A neural network can differentiate glaucoma and optic neuropathy visual fields through pattern recognition. In: Perimetry Update 1990/91. Proceedings of the IXth International Perimetric Society meeting. Mills RP, Heijl A (eds). Kugler; Amsterdam / New York: 287-290.

Keltner JL (1979) Comments on automated perimetry papers. Ophthalmology 86: 1317-1319.

Keltner JL, Johnson CA (1981) Capabilities and limitations of automated suprathreshold static perimetry. Doc Ophthalmol Proc Ser 26. Greve EL (ed). Junk; Amsterdam: 49-55.

Khu PM, Chylack LT, Leske MC, McCarthy D, Wu SY (1989) Measuring the rate of age-related cataract formation in vivo using LOCS II standard photographs. Invest Ophthalmol Vis Sci 30 (suppl): 164.

Kilbride PE, Hutman LP, Fishman M, Read KS (1986) Foveal cone pigment density difference in the ageing human eye. Vision Res 26: 321-325.

Kilbride PE, Alexandra KR, Fishman M, Fishman GA (1989) Human macular pigment assessed by imaging fundus reflectometry. Vision Res 29: 663-674.

King D, Drance SM, Douglas GR et al (1986a) Comparison of visual field defects in normal tension glaucoma and high-tension glaucoma. Am J Ophthalmol 101: 204-207.

King D, Drance SM, Douglas GR, Wijsman K (1986b) The detection of paracentral scotomas with varying grids in computed perimetry. Arch Ophthalmol 104: 524-525.

King-Smith PE, Carden D (1976) Luminance and opponent-color contributions to visual detection and adaptation and to temporal and spatial integration. J Opt Soc Am 66: 709-717.

King-Smith PE, Chioran GM, Sellars KL, Alvarez SL (1983) Normal and deficient colour discrimination analysed by colour television. In: Colour Vision: Physiology and Psychophysics. Mollon JD, Sharpe LT (eds). Academic; London: 167-172.

King-Smith PE, Lubow M, Benes BC (1984) Selective damage to chromatic mechanisms in neuro-ophthalmic diseases I. Review of published evidence. Doc Ophthalmol 58: 241-250.

Kirshfeld K (1982) Carotenoid pigments: their possible role in protecting against photo-oxidation in eyes and photo-receptor cells. Proc R Soc B 216: 71-85.

Klein BEK, Moss SE, Magli YL et al (1987) Optic disc cupping as clinically estimated from photographs. Ophthalmology 94: 1481-1483.

Klein BEK, Klein R, Ritter LL (1993) Relationship of drinking alcohol and smoking to prevalence of open-angle glaucoma. Ophthalmology 100: 1609-1613.

Klewin KM, Radius RL (1986) Background illumination and automated perimetry. Arch Ophthalmol 104: 395-397.

Klimaschka T, Weber J (1994) Test time and efficiency of the dynamic strategy in glaucoma perimetry. Presented as a poster at the XIth International Perimetric Society Meeting, Washington DC, USA; July 4-7th 1994.

Knoblauch K, Saunders F, Kusuda M et al (1987) Age and illuminance effects in the Farnsworth-Munsell 100-hue test. Appl Opt 26: 1441-1448.

Koch P, Rolier A, Fankhouser F (1972) Perimetry: The information and theoretical basis for perimetry. Vision Res 12: 1619-1630.

Korth M, Horn F, Storck B, Jonas JB (1989) Spatial and spatiotemporal contrast sensitivity of normal and glaucoma eyes. Graefe's Arch Clin Exp Ophthalmol 227: 428-435.

Korth M, Nguyen NX, Junemann A, Martus P, Jonas JB (1992) VEP test of the blue-sensitive pathway in glaucoma. Invest Ophthalmol Vis Sci 35: 2599-2610.

Korth M, Horn F, Jonas J (1993) Utility of the color pattern electroretinogram (PERG) in glaucoma. Graefe's Arch Clin Exp Ophthalmol 231: 84-89.

Korth M, Nguyen NX, Junemann A, Martus P, Jonas JB (1994) VEP test of the blue-sensitive pathway in glaucoma. Invest Ophthalmol Vis Sci 35: 2599-2610.

Krakau CET (1978) Aspects on the design of an automatic perimeter. Acta Ophthalmol 56: 389-405.

Krauskopf J, Williams DR, Heeley DW (1982) Cardinal directions of color space. Vision Res 22: 1123-1131.

Kruse FE, Burk ROW, Volcker HE, Zinser G, Harbarth U (1989) Reproducibility of topographic measurements of the optic nerve head with laser topographic scanning. Ophthalmology 96: 1320-1324.

Kulze JC, Stewart WC, Sutherland SE (1990) Factors associated with a learning effect in glaucoma patients using automated perimetry. Acta Ophthalmol 68: 681-686.

Kurzel RB, Wolbarsht ML (1973) Spectral studies on normal and cataractous intact human lenses. Exp Eye Res 17: 65-71.

Lachenmayr B, Rothbacher H, Gleissner M (1989) Automated flicker perimetry versus quantitative static perimetry in early glaucoma. In: Perimetry Update 1988/89. Proceedings of the VIIIth International Perimetric Society Meeting. Heijl A (ed). Kugler / Ghedini; Amsterdam / Berkeley / Milano: 359-368.

Lachenmayr BJ, Airaksinen PJ, Drance SM, Wijsman K (1991a) Correlation of retinal nerve fiber-layer loss, changes at the optic nerve head and various psychophysical criteria in glaucoma. Graefe's Arch Clin Exp Ophthalmol 229: 133-138.

Lachenmayr BJ, Drance SM, Douglas GR, Mikelberg FS (1991b) Light-sense, flicker and resolution perimetry in glaucoma: a comparative study. Graefe's Arch Clin Exp Ophthalmol 229: 246-251.

Lachenmayr BJ, Drance SM, Chauhan BC, House PH, Lalani S (1991c) Diffuse and localised glaucomatous field loss in light-sense, flicker and resolution perimetry. Graefe's Arch Clin Exp Ophthalmol 229: 267-273.

Lachenmayr BJ, Drance SM, Airaksinen JP (1992a) Diffuse field loss and diffuse retinal nerve-fiber loss in glaucoma. German J Ophthalmol 1: 22-25.

Lachenmayr BJ, Angstwurm K, Kojetinsky S, Schaumberger M (1992b) The normal visual field in flicker perimetry. Invest Ophthalmol Vis Sci 33 (suppl): 3010.

Lachenmayr BJ, Drance SM (1992a) The selective effects of elevated intraocular pressure on temporal resolution. German J Ophthalmol 1: 26-31.

Lachenmayr BJ, Drance SM (1992b) Diffuse field loss and central visual function. German J Ophthalmol 1: 67-73.

Lachenmayr BJ, Gleissner M (1992) Flicker perimetry resists retinal image degradation. Invest Ophthalmol Vis Sci 13: 3539-3542.

Lachenmayr BJ, Kojetinsky S, Ostermaier N et al (1994) The different effects of ageing on normal sensitivity in flicker and light-sense perimetry. Invest Ophthalmol Vis Sci 35: 2741-2748.

Lakowski R (1958) Age and colour vision. Adv Sci 59: 231-236.

Lakowski R, Bryett J, Drance SM (1972) A study of color vision in ocular hypertensives. Can J Ophthalmol 7: 86-95.

Lakowski R, Goldthwaite D, Drance SM (1976) Chromatic extrafoveal dark adaptation function in normal and glaucomatous eyes. Mod Probl Ophthalmol 17: 304-310.

Lakowski R, Wright WD, Oliver K (1977) A Goldmann perimeter with high luminance chromatic targets. Can J Ophthalmol 12: 203-210.

Lakowski R, Drance SM (1978) Acquired dyschromatopsias. The earliest functional losses in glaucoma. Doc Ophthal Proc Ser 19. Greve EL (ed). Junk; Amsterdam: 159-173.

Lam BL, Alward WLM, Kolder HE (1991) Effect of cataract on automated perimetry. Ophthalmology 98: 1066-1070.

Lam BL, Fishman GA, Anderson RJ et al (1992) Effect of mydriasis on visual field area in retinitis pigmentosa. Ophthalmology 99: 1724-1727.

Langerhorst CT, van den Berg TJTP, van Spronsen R, Greve EL (1985) Results of a fluctuation analysis and defect volume program for automated static threshold perimeter with the scoperimeter. Doc Ophthalmol Proc Ser 42. Greve EL, Heijl A (eds). Nijhoff / Junk; Dordrecht: 1-6.

Langerhorst CT, van den Berg TJTP, Nooteboom R, Greve EL (1987a) Short term and long term fluctuation of thresholds in automated perimetry and the influence of the defect volume. Doc Ophthalmol Proc Ser 49. Greve EL, Heijl A (eds). Nijhoff / Junk; Dordrecht: 71-76.

Langerhorst CT, van den Berg TJTP, Veldman E, Greve EL (1987b) Population study of global and local fatigue with prolonged threshold testing in automated perimetry. Doc Ophthalmol Proc Ser 49. Greve EL, Heijl A (eds). Nijhoff / Junk; Dordrecht: 657-662.

Langerhorst CT (1988) In: Automated perimetry in Glaucoma. Fluctuation behaviour and general and local reduction of sensitivity. Kugler / Ghedini; Amsterdam / Berkeley / Milano.

Langerhorst CT, van den Berg TJTP, Greve EL (1989a). Fluctuation and general health in automated perimetry in glaucoma. In: Perimetry Update 1988/89. Heijl A (ed). Kugler / Ghedini; Amsterdam / Berkeley / Milano: 159-164.

Langerhorst CT, Thomas JTP, van den Berg TJTP, Greve E (1989b) Is there a general reduction of sensitivity in glaucoma? Int Ophthalmol 3: 31-35.

Lasa MSM, Datiles MB, Podgor M, Magno B (1992) Contrast and glare sensitivity: association with the type and severity of cataract. Ophthalmology 99: 1045-1049.

LeBlanc RP (1985) Abnormal values in computerised perimetry. Computerised Visual Fields. Whalen WR, Spaeth GL (eds). Thorofare; New Jersey: 165-193.

Lee J, Stromeyer CF (1989) Contribution of human short-wave cones to luminance and motion detection. J Physiol 413: 563-593.

Lee M, Zulauf M, Hoffman D, Caprioli J (1991) A new reliability index for threshold automated perimetry. Invest Ophthalmol Vis Sci 21 (suppl): 1105.

Lennie P (1980) Parallel visual pathways: A review. Vision Res 20: 561-594.

Leske MC, Chylack LT, Wu SY (1988) The lens opacities case-control study: risk factors for cataract. Arch Ophthalmol 109: 244-251.

Levene RZ (1980) Low-tension glaucoma: a critical review and new material. Surv Ophthalmol 24: 621-664.

Leventhal AG, Rodieck RW, Dreher B (1981) Retinal ganglion cell classes in the Old World monkey: morphology and central projections. Science 213: 1139-1142.

Levi DM, Klein SA (1987) Spatial summation and separation discrimination in central and peripheral vision: effects of contrast and polarity. Invest Ophthalmol Vis Sci 28: 138.

Levitt H (1971) Transformed up-down methods in psycho-acoustics. J Acoustical Soc Am 49: 467-477.

Lewis RA, Hayreh SS, Phelps CD (1983) Optic disc and visual field correlations in primary open-angle glaucoma and low-tension glaucoma. Am J Ophthalmol 96: 148-152.

Lewis RA, Johnson CA, Adams AJ (1993) Automated perimetry and short wavelength sensitivity in patients with asymmetric intraocular pressures. Graefe's Arch Clin Exp Ophthalmol 231: 274-278.

Li SG, Spaeth GL, Scimecca HA et al (1979) Clinical experiences with the use of an automated perimeter (Octopus) in the diagnosis and management of patients with glaucoma and neurologic disease. Ophthalmology 86: 1302-1311.

Lichter PR (1976) Variability of expert observers in evaluating the disc. Trans Am Ophthalmol Soc 74: 532-572.

Lindenmuth KA, Skuta GL, Rabbani R, Musch DC (1989) Effects of pupillary constriction on automated perimetry in normal eyes. Ophthalmology 96: 1298-1301.

Lindenmuth KA, Skuta GL, Rabbani et al (1990) Effects of pupillary dilation on automated perimetry in normal patients. Ophthalmology 97: 367-370.

Littman H (1982) Zur Bestimmung der wahren Grosse eines Objektes auf dem Hintergrund des lebendes Auges. Klin Mbl Augenheilk 180: 286-289.

Livingstone MS, Hubel DH (1987) Psychophysical evidence for separate channels for the perception of form, color, movement and depth. J Neurosci 7: 3416-3468.

Livingstone MS, Hubel DH (1988) Do the relative mapping densities of the magno- and parvocellular systems vary with eccentricity. J Neurosci 8: 4334-4339.

Logan N, Anderson DR (1983) Detecting early glaucomatous visual field changes with a blue stimulus. Am J Ophthalmol 95: 432-434.

Luske M, Bosem ME, Weinreb RN (1993) Reproducibility of optic nerve head topography measurements in eyes with undilated pupils. J Glaucoma 2: 104-109.

Lustgarten JS, Marx MS, Podos SM et al (1990) Contrast sensitivity and computerised perimetry in early detection of glaucomatous damage. Clin Vis Sci 5: 407-413.

Lynn AJ, Phillips CI (1969) Visual field defects due to opacities in the optical media. Br J Ophthalmol 53: 119-122.

Lynn JR, Batson EP, Fellman RL (1985) Internal consistencies vs root mean square as means of threshold variability. Doc Ophthalmol Proc Ser 36. Greve EL, Heijl A (eds). Junk; Amsterdam: 7-15.

Magno BV, Datilles MB, Lasa SM (1993) Senile cataract progression studies using the lens opacities classification system II. Invest Ophthalmol Vis Sci 34: 2138-2141.

Maione M, Carta F, Barberini E, Scoccianti L (1976) Achromatic isopters on coloured backgrounds in some acquired color vision deficiencies. Mod Probl Ophthalmol 17: 86-93.

Mandava S, Caprioli J, Zulauf M (1992) Glaucoma pattern index to quantify glaucomatous visual field loss. J Glaucoma 1: 178-183.

Mandava S, Zulauf M, Zeyen T, Caprioli J (1993) An evaluation of clusters in the glaucomatous visual field. Am J Ophthalmol 116: 684-691.

Manivannan A, Kirkpatrick JNP, Sharp PF, Forrester JV (1994) Clinical investigation of an infrared digital scanning laser ophthalmoscope. Br J Ophthalmol 78: 84-90.

Mann CG, Orr AC, Rubillowicz M, LeBlanc R (1989) Automated static perimetry in chloroquine and hydroxychloroquine therapy. In: Perimetry Update 1988/89. Proceedings of the VIIIth International Perimetric Society Meeting. Heijl A (ed). Kugler / Ghedini. Amsterdam / Berkeley / Milano: 417-421.

Mantyjarvi M, Terasvirta M (1993) Contrast sensitivity in ocular hypertension and glaucoma. Ophthalmologica 206: 182-186.

Maraini G, Pasquini P, Tomba MC (1989) An independent evaluation of the Lens Opacities Classification System II (LOCS II). Ophthalmology 96: 611-615.

Maraini G, Pasquini P, Sperduto RD (1991) The effect of cataract severity and morphology on the reliability of the lens opacities classification system II (LOCS II). Invest Ophthalmol Vis Sci 32: 2400-2403.

Marchini G, Pisano F, Bertagnin F et al (1991) Perimetric learning effect in glaucoma patients. Glaucoma 13: 102-106.

Mamor MF, Aquirre G, Arden G et al (1983) Retinitis pigmentosa: a symposium on terminology and methods of examination. Ophthalmology 90: 126-131.

Marmor MF, Gawande A (1988) Effect of visual blur on contrast sensitivity. Ophthalmology 95: 139-143.

Marra G, Flammer J (1991) The learning and fatigue effect in automated perimetry. Graefe's Arch Clin Exp Ophthalmol 229: 501-504.

Marré M, Marré E (1978) Different types of acquired color vision deficiencies. Mod Probl Ophthalmol 19: 248-252.

Marshall J, Laties A (1985) Special pathology of the ageing macula. In: Retinal Degeneration, Experimental and Clinical Studies. Hollyfield LG, Anderson RE (eds). Liss; New York: 389-400.

Marshall J (1987) The ageing retina: physiology or pathology. Eye 1: 282-295.

Marshall J (1979) Ageing changes in human cones. In: Proceedings of 23rd Int Congress Ophthalmol. Shimizu K, Oosterhuis JA (eds). Excerpta Medica; Amsterdam / Oxford: 375-378.

Martin-Bogland LM, Wanger P (1991) Computer-assisted evaluation of the results from high-pass resolution perimetry: a knowledge-based system. In: Perimetry Update 1990/91. Proceedings of the IXth International Perimetric Society Meeting. Mills RP, Heijl A (eds). Kugler; Amsterdam / New York: 297-301.

Masters BR (1994) The scanning laser ophthalmoscope: a new view on the retina. Br J Ophthalmol 78: 81.

Matsumoto C, Uyama K, Okuyama S et al (1991) Study of the influence of target size on the pericentral visual field. In: Perimetry Update 1990/91. Proceedings of the IXth International Perimetric Society Meeting. Mills RP, Heijl A (eds). Kugler; Amsterdam / New York: 153-159.

Maudgal PC, Stout RWO, Van Balen A (1988) VCTS chart evaluation as a screening test. Doc Ophthalmol 69: 399-405.

McCluskey DJ, Douglas JP, O'Connor PS et al (1986) The effect of pilocarpine on the visual field in normals. Ophthalmology 93: 843-846.

Mellerio J (1971) Light absorption and scatter in the human lens. Vision Res 11: 129-141.

Mellerio J (1987) Yellowing of the human lens: nuclear and cortical contributions. Vision Res 27: 1581-1587.

Merigan WH (1989) Chromatic and achromatic vision of macaques: role of the P pathway. J Neurosci 9: 776-783.

Metha AB, Vingrys AJ, Badcock DR (1993) Calibration of a color monitor for visual psychophysics. Behaviour Res Methods, Instruments and Computers 25: 371-383.

Mikelberg FS, Drance SM (1984) The mode of progression of visual field defects in glaucoma. Am J Ophthalmol 98: 443-445.

Mikelberg FS, Douglas GR, Schulzer M et al (1984) Reliability of optic disc topographic measurements recorded with a video-ophthalmograph. Am J Ophthalmol 98: 98-102.

Mikelberg FS, Airaksinen PJ, Douglas GR, Schulzer M, Wijsman K (1985) The correlation between optic disc topography measured by the video-ophthalmograph (Rodenstock analyser) and clinical measurement. Am J Ophthalmol 100: 417-419.

Mikelberg FS, Douglas GR, Schulzer M et al (1986) The correlation between cup-disc ratio, neuroretinal rim area, and optic disc area measured by the video-ophthalmograph (Rodenstock Analyser) and clinical measurement. Am J Ophthalmol 101: 7-12.

Mikelberg FS, Wijsman K, Schulzer M (1993) Reproducibility of topographic parameters obtained with the Heidelberg Retina Tomograph. J Glaucoma 2: 101-103.

Miller D, Benedek G (1973) In: Intraocular light scattering. Thomas CC (ed). Springfield; New York.

Miller KN, Quigley HA (1988) The clinical appearance of the lamina cribrosa as a function of the extent of glaucomatous optic nerve damage. Ophthalmology 95: 135-138.

Miller KN, Shields B, Ollie AR (1989) Automated kinetic perimetry with two peripheral isopters in glaucoma. Arch Ophthalmol 107: 1316-1320.

Mills RP (1984) A comparison of Goldmann, Fieldmaster 200 and Dicon AP2000 perimeters used in a screening mode. Ophthalmology 91: 347-353.

Mills RP (1985) Quantitative perimetry: Dicon. In: Automatic perimetry in glaucoma. Drance SM, Anderson DR (eds). Grune / Stratton; Florida: 99-112.

Mills RP, Lau W, Schulzer M (1990) Estimating short-term fluctuation without double threshold determinations. Validation of a method. Perimetry Update 1990/91. Mills RP, Heijl A (eds). Kugler; Amsterdam / New York: 203-208.

Mills RP, Yang T, Li Y (1994) The effect of audio and visual cueing on visual field testing. Presented as a poster at the XIth International Perimetric Society Meeting, Washington DC, USA; July 3-7th 1994: 70.

Mitchell ES, Hurst MA (1993) The relationship between forward light scatter and cataract. Invest Ophthalmol Vis Sci 34 (suppl): 1414.

Mizokami K, Asai T (1989) Contrast sensitivity, visual field defect and retinal nerve fiber layer defect in glaucoma. In: Perimetry Update 1988/89. Proceedings of the VIIIth International Perimetric Society Meeting. Heijl A (ed). Kugler / Ghedini; Amsterdam / Berkeley / Milano: 297-302.

deMonasterio FM, Gouras P (1975) Functional properties of ganglion cells of the rhesus monkey retina. J Physiol 251: 167-195.

deMonasterio FM (1978) Properties of concentrically organised X and Y ganglion cells of macaque retina. J Neurophysiol 41: 1394-1417.

deMonasterio FM (1979) Asymmetry of on- and off-pathways of blue-sensitive cones of the retina of macaques. Brain Res 166: 39-48.

Montgomery DM (1993) Clinical disc biometry in early glaucoma. Ophthalmology 100: 52-56.

Montgomery DM, Craig JP (1993) Optic disc interpretation in glaucoma: is confidence misplaced? Ophthal Physiol Opt 13: 383-386.

Moreland JD (1972) The effect of inert ocular pigments on anomaloscope matches and its reduction. Mod Probl Ophthalmol 11: 12-18.

Moreland JD, Bhatt P (1984) Retinal distribution of macular pigment. In: Colour Vision Deficiencies VII. Verriest G (ed). Junk; Amsterdam: 127-132.

Motolko M, Drance SM, Douglas GR (1982a) Visual field defects in low-tension glaucoma. Arch Ophthalmol 100: 1074-1077.

Motolko M, Drance SM, Douglas GR (1982b) The early psychophysical disturbances in chronic open-angle glaucoma. A study of visual functions with asymmetric disc cupping. Arch Ophthalmol 100: 1632-1634.

Mullen KT (1985) The contrast sensitivity of human colour vision to red-green and biue-yellow chromatic gratings. J Physiol 359: 381-409.

Mullen KT (1991) Colour vision as a post-receptoral specialization of the central visual field. Vision Res 31: 119-130.

Mutlukan E, Keating D (1994) Visual field interpretation with a personal computer based neural network. Eye 8: 321-323.

Nagata S, Kani K, Sugiyama A (1991) A computer-assisted visual field diagnosis system using a neural network. In: Perimetry Update 1990/91. Proceedings of the IXth International Perimetric Society Meeting. Mills RP, Heijl A (eds). Kugler; Amsterdam / New York: 291-295.

Nameda N, Kawara T, Ohzu H (1989) Human visual spatio-temporal frequency performance as a function of age. Optom Vis Sci 66: 760-765.

Nanba K, Iwata K (1993) Correlation of optic disc changes and visual field defects in glaucoma. In: Perimetry Update 1992/93. Proceedings of the Xth International Perimetric Society Meeting. Mills RP (ed). Kugler; Amsterdam / New York: 165-169.

Nara T (1979) Visual field changes in mesopic and scotopic conditions using Friedmann Visual Field Analyser. Doc Ophthalmol Proc Ser 19. Greve EL (ed). Junk, Amsterdam: 403-407.

Nelson-Quigg JM, Johnson CA, Casson EJ, Adams AJ (1990) Long and short term variability for perimetry of short wavelength sensitive (SWS) mechanisms. Invest Ophthalmol Vis Sci 31 (suppl): 190.

Nelson-Quigg JM, Johnson CA, Morse LS, Chu TG (1994) Comparison of lens transmission in diabetics and non-diabetics using the lens absorption monitor (LAM). Invest Ophthalmol Vis Sci 35 (suppl): 1823.

Niesel P, Chamel Ch, Chamel BOS, Weidmann BOS (1978) Das verhalten von perimetrischen untersuchungsbefunden bei entwichlung einer katarakt. Klin monatsbl augenheilk 172: 477-480.

Niesel P, Wiher CI (1982) Modellexperimente zum verhalten glaukomatoser gesichtsfeldausfalle bei kataraktentwicklung. Klin monatsbl augenheilk 180: 461-463.

Niles CR, Trope GE (1988) The influence of experience on mean defect and reliability factors in automated perimetry. Invest Ophthalmol Vis Sci 29 (suppl): 356.

Nordmann J, Topouzis P, Laroche L, Saraux H (1992) Three year follow-up of glaucoma patients using contrast sensitivity. Invest Ophthalmol Vis Sci 33 (suppl): 3469.

von Norren D, Vos JJ (1974) Spectral transmission of the human ocular media. Vision Res 14: 1237-1243.

von Norren D, Tiemeijer LF (1986) Spectral reflectance of the human eye. Vision Res 26: 313-320.

von Norren D, van Meel GJ (1985) Density of human cone photopigments as a function of age. Invest Ophthalmol Vis Sci 26: 1014-1016.

Noureddin BN, Poinoosawmy D, Fitzke FW, Hitchings RA (1991) Regression analysis of visual field progression in low tension glaucoma. Br J Ophthalmol 75: 493-495.

O'Brien C, Schwartz B (1990) The visual field in chronic open angle glaucoma: the rate of change in different regions of the field. Eye 4: 557-562.

O'Brien C, Schwartz B, Takamoto T, Wu DC (1990) Intraocular pressure and the rate of visual field loss in chronic open angle glaucoma. Am J Ophthalmol 111: 491-500.

O'Brien C, Schwartz B (1993) Point by point linear regression analysis of automated visual fields in primary open angle glaucoma. Perimetry Update 1992/93. Proceedings of the Xth International Perimetric Society meeting. Mills RP (ed). Kugler; Amsterdam / New York: 149-152.

O'Brien C, Poinoosawmy D, Wu J, Hitchings R (1994) Evaluation of the Humphrey FASTPAC threshold program in glaucoma. Br J Ophthalmol 78: 516-519.

O'Connor DJ, Zeyen T, Caprioli J (1993) Comparisons of methods to detect glaucomatous optic nerve damage. Ophthalmology 100: 1498-1503.

Odberg T, Riise D (1985) Early diagnosis of glaucoma: the value of successive stereophotography of the optic disc. Acta Ophthalmol 63: 257-263.

O' Donnell NP, Birch MK, Trope GE (1994) FASTPAC error is within long-term fluctuation of Humphrey STATPAC field analyses. Presented as a poster at the XIth International Perimetric Society Meeting, Washington DC, USA; July 4-7th 1994: 69.

Ogawa T, Suzumara H, Yabuki K et al (1993) Analysis of the progression of visual field changes in low tension glaucoma. Perimetry Update 1992/93. Proceedings of the Xth International Perimetric Society Meeting. Mills RP (ed). Kugler; Amsterdam / New York: 115-119.

Olbert D, Hockwin O, Baumgartner A, Wahl P, Hasslacher C (1985) Follow-up of lenses of diabetics by linear densitometry of Schiempflug photos. Ophthalmology 82: 374-376.

Olsson J, Rootzen H, Heijl A (1989) Maximum likelihood estimation of the frequency of false-positive and false-negative answers from the up-and-down staircases of computerised threshold perimetry. In: Perimetry Update 1988/89, Proceedings of the VIIIth International Perimetric Society Meeting. Heijl A (ed). Kugler / Ghedini; Amsterdam / Berkeley / Milano: 245-251.

Olsson J, Asman P, Rootzen H, Heijl A (1991) Improved threshold estimates using full staircase data. In: Perimetry Update 1990/91. Proceedings of the IXth International Perimetric Society Meeting. Mills RP, Heijl A (eds). Kugler; Amsterdam / New York: 245-249.

Olsson J, Heijl A, Bengtsson B, Rootzen H (1993) Frequency-of-seeing in computerised perimetry. In Perimetry Update 1992/93. Proceedings of the Xth International Perimetric Society Meeting. Mills RP (ed). Kugler; Amsterdam / New York: 551-556.

Olsson J, Bengtsson B, Heijl A, Rootzen H (1994a) Improving estimates of false positive and false negative responses in computerized perimetry. Presented as a paper at the XIth International Perimetric Society Meeting, Washington DC, USA; July 3-7th 1994: 26.

Olsson J, Bengtsson B, Heijl A, Rootsen H (1994b) New thresholding algorithms for automated static perimetry. Presented as a poster at the XIth International Perimetric Society Meeting, Washington DC, USA; July 4-7th 1994: 38.

Owsley C, Sekuler R, Siemsen D (1983) Contrast sensitivity throughout adulthood. Vision Res 23: 689-699.

Paige GD (1985) Effect of increased background luminance on static threshold perimetry. Invest Ophthalmol Vis Sci 26 (suppl): 226.

Paulsson LE, Sjostrand J (1980) Contrast sensitivity in the presence of a glare light. Invest Ophthalmol Vis Sci 19: 401-406.

Pearson PA, Baldwin LB, Smith TJ (1989) The Q-statistic in glaucoma and ocular hypertension. In: Perimetry Update 1988/89. Proceedings of the VIIIth International Perimetric Society Meeting. Heijl A (ed). Kugler / Ghedini; Amsterdam / Berkeley / Milano: 229-233.

Pearson PA, Baldwin LB, Smith TJ (1990) The relationship of mean defect to corrected loss variance in glaucoma and ocular hypertension. Ophthalmologica 200: 16-21.

Pease PL, Adams AJ (1983) Macular pigment difference spectrum from sensitivity measures of a single cone mechanism. Am J Optom Physiol Opt 60: 667-672.

Pease PA, Adams AJ, Nuccio E (1987) Optical density of the human macular pigment.Vision Res 27: 705-710.

Pederson JE, Anderson DR (1980) The mode of progressive disc cupping in ocular hypertension and glaucoma. Arch Ophthalmol 98: 490-495.

Peigne G, Schwartz B, Takamoto T (1993) Differences of retinal nerve fiber layer thickness between normal and glaucoma-like optic discs (physiological cups). Matched by optic disc area. Acta Ophthalmol 71: 451-457.

Pennebaker GE, Stewart WC, Stewart JA, Hunt HH (1992) The effect of stimulus duration upon the components of fluctuation in static automated perimetry. Eye 6: 353-355.

Perry VH, Cowey AH (1981) The morphological correlates of X- and Y-like retinal ganglion cells in the retina of monkeys. Exp Brain Res 43: 226-228.

Perry VH, Oehler R, Cowey A (1984) Retinal ganglions which project to the dorsal lateral geniculate nucleus in the macaque monkey. Neuroscience 12: 1101-1123.

Phelps CD, Motolko MA (1982) Contrast sensitivity and glaucoma. In: Glaucoma Update II. Kriegelstein GK, Leydheckjer W (eds). Springer-Verlag, Heidelberg: 103-105.

Phelps CD, Hayreh SS, Montague PR (1983) Visual fields in low-tension glaucoma, primary open-angle glaucoma and anterior ischaemic optic neuropathy. Doc Ophthalmol Proc Ser 35. Greve EL, Heijl A (eds). Junk; Amsterdam: 113-124.

Phelps CD, Hayreh SS, Montague PR (1984) Comparison of visual field defects in the low-tension glaucomas with those in the high-tension glaucomas [letter]. Am J Ophthalmol 98: 823-825.

Phelps CD (1985) Choosing an automatic perimeter. In: Automatic perimetry in glaucoma. A practical guide. Drance SM, Anderson DR (eds). Grune / Stratton: Orlando:175-181.

Phelps-Brown NA (1993) The morphology of cataract and visual performance. Eye 7: 63-67.

Pinkers A (1980) Colour vision and age. Ophthalmologica 181: 23-30.

Piltz JR, Starita RJ (1990) Test-retest variability in glaucomatous visual fields. Am J Ophthalmol 109: 109-110.

Piltz JR, Bose S, Grunwald JE, Petrig BL, Riva CE (1993) Effect of nimodopine on automated threshold perimetry, spatial contrast sensitivity and macular blood flow in normal tension glaucoma and controls. Invest Ophthalmol Vis Sci 34 (suppl):1287.

Pirenne MH, Marriott FHC (1962) Visual functions in man. In: The eye, vol 2. Davson H (ed). Academic; New York.

Poinoosawmy D, Nagasubramanian S, Gloster J (1980) Colour vision in patients with chronic simple glaucoma and ocular hypertension. Br J Ophthalmol 64: 852-857.

Poinoosawmy D, Wu JX, Fitzke FW, Hitchings RA (1993) Discrimination between progression and non-progression visual field loss in low tension glaucoma using MDT. Perimetry Update 1992/93. Proceedings of the Xth International Perimetric Society Meeting. Mills RP (ed). Kugler; Amsterdam / New York: 109-114.

Pokorny J, Smith VC, Lutze M (1987) Ageing of the human lens. Appl Optics 26: 1437-1440.

Pomerance GN, Evans DW (1994) Test-retest reliability of the CSV-1000 contrast test and its relationship to glaucoma therapy. Invest Ophthalmol Vis Sci 35: 3357-3361.

Pinckers A (1980) Color vision and age. Ophthalmologica 181: 23-30.

Piltz J, Bose S, Grunwald J, Petrig L, Riva C (1993) Effect of nimodipine on automated threshold perimetry, spatial contrast sensitivity and macular blood flow in normal tension glaucoma and controls. Invest Ophthalmol Vis Sci 34 (suppl): 2881.

Phelps CD, Motolko MA (1983) Contrast sensitivity and glaucoma. In: Glaucoma Update II. Kriegelstein GK, Leydhecker W (eds). Springer-Verlag; Heidelberg: 103-106.

Quigley HA, Green WR (1979) The histology of human glaucoma cupping and optic nerve damage. Clinicopathological evidence in 21 eyes. Trans Am Acad Ophthalmol 86: 1803-1830.

Quigley HA, Miller NR, George T (1980) Clinical evaluation of nerve fiber layer atrophy as an indicator of glaucomatous optic nerve damage. Arch Ophthalmol 98: 1564-1571.

Quigley HA (1982) Optic nerve damage in human glaucoma. III. Quantitative correlation of nerve fiber loss and visual field defect in glaucoma, ischaemic neuropathy, disc oedema and toxic neuropathy. Arch Ophthalmol 100: 135-146.

Quigley HA, Sanchez RM, Dunkelberger GR et al (1987) Chronic glaucoma selectively damages large optic nerve fibres. Invest Ophthalmol Vis Sci 28: 913-920.

Quigley HA (1987a) Are some ganglion cells killed by glaucoma before others? In: Glaucoma Update III. Kriegelstein GK (ed). Springer-Verlag; Berlin / Heidelberg: 23-26.

Quigley HA (1987b) Reappraisal of the mechanisms of glaucomatous optic nerve damage. Eye 1: 318-322.

Quigley HA, Dunkelberger GR, Green WR (1988) Chronic human glaucoma causes selectively greater loss of large optic nerve fibres. Ophthalmology 95: 357-363.

Quigley HA, Dunkelberger GR, Green WR (1989) Studies of retinal ganglion cell atrophy correlated with automated perimetry in human eyes with glaucoma. Am J Ophthalmol 107: 453-464.

Quigley HA, Glovinsky Y, Drum B et al (1991) Scotopic ganzfeld sensitivity test for the detection of early glaucoma damage to large (M) retinal ganglion cells. Invest Ophthalmol Vis Sci 32 (suppl): 2566.

Quigley HA (1993) Medical progress: Open-angle glaucoma. New Eng J Med 328: 1097-1106.

Quigley HA, Reacher M, Katz J et al (1993) Quantitative grading of nerve fiber layer photographs. Ophthalmology 100: 1800-1807.

Rabineau PA, Gloor BP, Tobler HJ (1985) Fluctuations in threshold and effects of fatigue in automated static perimetry (with the Octopus 201). Doc Ophthalmol Proc Ser 42. Greve E (ed). Junk; Dordrecht: 25-33.

Radius RL (1978) Perimetry in cataract patients. Arch Ophthalmol 96: 1574-1579.

Radius RL (1987) Anatomy of the optic nerve head and glaucomatous optic neuropathy. Surv Ophthalmol 32: 35-44.

Rau S, Weber J (1991) The frequency of seeing curve under perimetric conditions. In: Perimetry Update 1990/91. Proceedings of the IXth International Perimetric Society Meeting. Mills RP, Heijl A (eds). Kugler; Amsterdam / New York: 555.

Reading VM, Weale RA (1974) Macular pigment and chromatic aberration. J Opt Soc Am 64: 231-234.

Rebolleda G, Munoz FJ, Fernandez VJM et al (1992) Effects of pupillary dilation on automated perimetry in glaucoma patients receiving pilocarpine. Ophthalmology 99: 418-423.

Reidel KG, Gilg T, Leibhardt E (1985) Wahrnehmungsstorungen im peripheren Gesichtsfeld unter Alkoholeinflu. Klin Monatsbl Augenheilkd 186: 279-283.

Reynolds M, Stewart WC, Sutherland S (1990) Factors that influence the prevalence of positive catch trials in glaucoma patients. Graefe's Arch Clin Exp Ophthalmol 228: 338-341.

Robinson DA (1964) The mechanics of human saccadic eye movement. J Physiol 174: 245-264.

Rock WJ, Drance SM, Morgan RW (1973) Visual field screening in glaucoma. An evaluation of the Armaly technique for screening glaucomatous visual fields. Arch Ophthalmol 89: 287-290.

Rohrschneider K, Burk ROW, Kruse FE, Volcker HE (1994) Reproducibility of the optic nerve head topography with a new laser tomographic device. Ophthalmology 101: 1044-1049.

Ronchi L, Salvi G (1973) Performance decrement, under prolonged testing, across the visual field. Ophthalmol Res 5: 113-120.

Rose RM, Teller DY, Rendleman P (1970) Statistical properties of staircase estimates. Perception and Psychophysics 8: 199-204.

Ross JE, Bron AJ, Clarke DD (1984) Contrast sensitivity and visual disability in chronic simple glaucoma. Br J Ophthalmol 68: 821-827.

Ross JE, Clarke DD, Bron AJ (1985a) Effect of age on contrast sensitivity function: uniocular and binocular findings. Br J Ophthalmol 69: 51-56.

Ross JE, Bron AJ, Reeves BC, Emmerson PG (1985b) Detection of optic nerve damage in ocular hypertension. Br J Ophthalmol 69: 897-903.

Rouhiainen P, Rouhiainen H, Notkola IL, Salonen J (1993) Comparison of the lens opacities classification system II and lensmeter 701. Am J Ophthalmol 116: 617-621.

Ruben S, Fitzke F (1994) Correlation of peripheral displacement thresholds and optic disc parameters in ocular hypertension. Br J Ophthalmol 78: 291-294.

Ruddock KH (1963) Evidence for macular pigmentation from colour matching data. Vision Res 3: 417-429.

Ruddock KH (1965) The effect of age upon colour vision: II. Changes with age in light transmission of the ocular media. Vision Res 5: 47-58.

Rutishauser C, Flammer J (1988) Retests in static perimetry. Graefe's Arch Clin Exp Ophthalmol 226: 75-77.

Rutihauser C, Flammer J, Hass A (1989) The distribution of normal values in automated perimetry. Graefe's Arch Clin Exp Ophthalmol 227: 513-517.

Sadun AA, Libondi T (1990) Transmission of light through cataracts. Am J Ophthalmol 110: 710-712.

Safran AB, Bader C, Brazitikos PD et al (1992) Increasing short-term fluctuation by increasing the intensity of the fixation aid during perimetry. Am J Ophthalmol 113: 193-197.

Said FS, Weale RA (1959) The variation with age of the spectral transmissivity of the living human crystalline lens. Gerontologica 3: 213-231.

Sample PA, Weinreb RN, Boynton RM (1986a) Acquired dyschromatopsia in glaucoma. Surv Ophthalmol 31: 54-64.

Sample PA, Weinreb RN, Boynton RM (1986b) Blue-on-yellow color perimetry. Invest Ophthalmol Vis Sci 27 (suppl): 159.

Sample PA, Boynton R, Weinreb RN (1988a) Isolating the color vision loss in glaucoma. Am J Ophthalmol 106: 686-691.

Sample PA, Esterson FD, Weinreb RN, Boynton RM (1988b) The ageing lens: in vivo assessment of light absorption in 84 human eyes. Invest Ophthalmol Vis Sci 29: 1306-1311.

Sample PA, Esterson FD, Weinreb RN (1989) A practical method for obtaining an index of lens density with an automated perimeter. Invest Ophthalmol Vis Sci 30: 786-787.

Sample PA, Weinreb RN (1989) Color perimetry in glaucoma: Isolation of short-wavelength mechanisms. Invest Ophthalmol Vis Sci 30 (suppl): 56.

Sample PA, Weinreb RN (1990) Color perimetry for assessment of primary open-angle glaucoma. Invest Ophthalmol Vis Sci 31: 1869-1875.

Sample PA, Quirante JS, Weinreb RN (1991a) Age-related changes in the human lens. Acta Ophthalmol 69: 310-314.

Sample PA, Juang PSC, Weinreb RN (1991b) Isolating the effects of primary open-angle glaucoma on the contrast sensitivity function. Am J Ophthalmol 112: 308-316.

Sample PA, Weinreb RN (1992) Progressive visual field loss in glaucoma. Invest Ophthalmol Vis Sci 33: 2068-2071.

Sample PA, Cook JN, Weinreb RN (1993a) Variability and sensitivity of short-wavelength color visual fields in normal and glaucoma eyes. In: Noninvassive Assessment of the Visual System Tech Digest Ser: 292-295.

Sample PA, Taylor JDN, Martinez GA, Lusky M, Weinreb RN (1993b) Short-wavelength color visual fields in glaucoma suspects at risk. Am J Ophthalmol 115: 225-233.

Sample PA, Martinez GA, Weinreb RN (1993c) Color perimetry in glaucoma eyes without correction for lens density. Invest Ophthalmol Vis Sci 34 (suppl): 1268.

Sample PA, Martinez GA, Weinreb RN (1993d) Color visual fields: a five-year prospective study in suspect eyes and eyes with primary open angle glaucoma. In: Perimetry Update 1992/93. Proceedings of the Xth International Perimetric Society Meeting. Mills RP (ed), Kugler; Amsterdam / New York: 473-476.

Sample PA, Juang PSC, Weinreb RN (1994) Short-wavelength automated perimetry for analysis of secondary and normal tension glaucoma. Invest Ophthalmol Vis Sci 35 (suppl): 2189.

Samuelson TW, Spaeth GL (1993) Focal and diffuse visual field defects: Their relationship to intraocular pressure. Ophth Surgery 24: 519-525.

Sanabria O, Feuer WJ, Anderson DR (1991) Pseudo-loss of fixation in automated perimetry. Ophthalmology 98: 76-78.

Savage GL, Haegestrom-Portnoy G, Adams AJ, Hewlett SE (1993) Age changes in the optical density of human ocular media. Clin Vis Sci 8: 97-108.

Schiller PH, Malpeli JG (1977) Properties and tectal projections of monkey ganglion cells. J Neurophysiol 40: 428-445.

Schmied U (1980) Automated (Octopus) and manual (Goldmann) perimetry in glaucoma. Graefe's Arch Clin Exp Ophthalmol 213: 239-244.

Schneck M, Adams AJ (1988) Changes in S-cone system sensitivity and ocular media absorption with age. Invest Ophthalmol Vis Sci 29 (suppl): 301.

Schulzer M, Mills RP, Hopp RH, Lau W, Drance SM (1990) Estimation of the short-term fluctuation from a single determination of the visual field. Invest Ophthalmol Vis Sci 31: 730-735.

Schwartz B, Nagin P (1985) Probability maps for evaluating automated visual fields. Doc Ophthalmol Proc Ser 42. Greve EL, Heijl A (eds), Nijhoff / Junk; Dordrecht: 39-48.

Searle AET, Shaw DE, Wild JM, O'Neill EC (1991a) Within and between test learning and fatigue effects in normal perimetric sensitivity. In: Perimetry Update 1990/01. Proceedings of the IXth International Perimetric Society Meeting. Mills RP, Heijl A (eds); Kugler; Amsterdam / New York: 533-537.

Searle AET, Wild JM, Shaw DE, O'Neill EC (1991b) Time-related variation in normal automated static perimetry. Ophthalmology 98: 701-707.

Sekuler R, Hutman LP, Owsley C (1980) Human ageing and spatial vision. Science 209: 1255-1256.

Shapley R, Perry VH (1986) Cat and monkey retinal ganglion cells and their visual functional roles. Trends Neurosci 9: 229-235.

Shields SM, Trick GL (1990) Applying neural networks in glaucoma: prediction of the risk of visual field loss. Invest Ophthalmol Vis Sci 31 (suppl): 503.

Shiga S (1968) Visual field changes with loaded illumination. Am J Optom Physiol Opt 66: 245-263.

Shin YS, Suzumura H, Furono F et al (1991) Classification of glaucomatous visual field defects using the Humphrey Field Analyser box plots. In: Perimetry Update 1990/91. Proceedings of the IXth International Perimetric Society Meeting. Mills RP, Heijl A (eds). Kugler; Amsterdam / New York: 235-243.

Shokoohi K, Zwas F, Shin DH, Paslawski DA (1994) Contrast sensitivity measurements in patients with chronic open-angle glaucoma. Invest Ophthalmol Vis Sci 35 (suppl): 2187.

Siegelman J, Trokel SL, Spector A (1974) Quantitative biomicroscopy of lens light back scatter. Arch Ophthalmol 92: 437-442.

Singer W, Zihl J, Poppel X (1977) Subcorneal centres of visual thresholds in humans. Evidence of modality of specific and retinotopically organised mechanisms of selective attention. Exp Brain Res 29: 173-190.

Singh H, Cooper RL, Alder VA et al (1981) The Arden grating acuity: Effect of age and optical factors in the normal patient, with prediction of the false-negative screening in glaucoma. Br J Ophthalmol 65: 518-524.

Sloan LL (1939) Instruments and techniques for the clinical testing of light sense. III. An apparatus studying regional differences in light sense. Arch Ophthalmol 22: 233-251.

Sloan LL (1961) Area and luminance of test object as variables in examination of the visual field by projection perimetry. Vision Res 1: 121-138.

Snodderly DM, Brown PK, Delon FC, Auran JD (1984) The macular pigment II. Spatial distribution in primate retinas. Invest Ophthalmol Vis Sci 25: 674-685.

Sokol S, Domar A, Moskowitz A (1980) Utility of the Arden grating test in glaucoma screening: high false-positive rate in normals over 50 years of age. Invest Ophthalmol Vis Sci 19: 1529-1533.

Sommer A, Miller NR, Pollack I et al (1977) The nerve fibre layer in the diagnosis of glaucoma. Arch Ophthalmol 95: 2149-2156.

Sommer A, Enger C, Witt K (1987) Screening for glaucomatous visual field loss with automated threshold perimetry. Am J Ophthalmol 103: 681-684.

Sommer A, Katz J, Quigley HA (1991) Clinically detectable nerve fiber atrophy precedes the onset of glaucomatous field loss. Arch Ophthalmol 109: 77-83.

Spaeth GL (1994) A new classification of glaucoma including focal glaucoma. Surv Ophthalmol 38: 9-17.

Spahr J, Fankhouser F (1974) Octopus - an automated perimeter. Rev Sensory Disability 7: 5-8.

Spahr J (1975) Optimization of the presentation pattern in automated static perimetry. Vision Res 15: 1275-1281.

Sperling HG, Johnson CA, Harwerth RS (1980) Differential photic damage to primate cones. Vision Res 20: 1117-1125.

Sponsel WE, DePaul KL, Martone JF et al (1991) Association of Vistech contrast sensitivity and visual nfield findings in glaucoma. Br J Ophthalmol 75: 558-560.

Spring KH, Stiles WS (1948) Apparent shape and size of the pupil viewed obliquely. Br J Ophthalmol 32: 347-354.

Stamper RL, Hsu-Winges C, Sopher M (1982) Arden contrast sensitivity testing in glaucoma. Arch Ophthalmol 100: 947-950.

Steen R, Whitaker D, Elliott DB, Wild JM (1994) Age-related effects of glare on luminance and colour contrast sensitivity. Optom Vis Sci (In Press).

Steinschneider T, Ticho U, Adler D (1984) Correlation between color vision deficiency and results of clinical examination in glaucomatous patients. In: Colour vision deficiencies VII. Verriest G (ed). Junk; Amsterdam: 407-411.

Stewart WC, Shields MB, Ollie AR (1989) Full threshold versus quantification of defects for visual field testing in glaucoma. Graefe's Arch Clin Exp Ophthalmol 227: 51-54.

Stewart WC (1992) Static versus kinetic testing in the nasal peripheral field in patients with glaucoma. Acta Ophthalmol 70: 79-84.

Stiles WS (1929) The effect of glare on the brightness difference threshold. Proc R Soc 104B: 322-355.

Stiles WS (1930) The scattering theory of the effect of glare on the brightness difference threshold. Proc R Soc 105B: 131-141.

Stiles WS, Crawford BH (1934) The effect of a glaring light source on extrafoveal vision. Proc R Soc 122B: 255-280

Stockman A, MacLeod DI, DePriest DD (1991) The temporal properties of the human short-wave photoreceptors and their associated pathways. Vision Res 31: 189-208.

Sturmer J, Gloor B, Tobler HJ (1985) The glaucomatous visual field in detail as revealed by the Octopus F-programs. Doc Ophthalmol Proc Ser 42. Greve EL, Heijl A (eds). Nijhoff / Junk; Dordrecht: 391-401.

Sucs FE, Verriest G (1988) Increment thresholds and spatial summation for colour targets in ocular hypertension and glaucoma. In: Colour Vision Deficiencies IX. Drum B, Verriest G (eds). Kluwer; Dordrecht: 273-279.

Sunga RN, Enoch JM (1970) Further perimetric analysis of patients with lesions of the visual pathways. Am J Ophthalmol 70: 403-422.

Suzuki Y, Araie M, Ohashi Y (1993) Sectorisation of the central 30° visual field in glaucoma. Ophthalmology 100: 69-75.

Swanson WH (1991) Clinical assessment of short-wavelength sensitive cone acuity. In: Proceedings of the Noninvasive Assessment of the Visual System Tech Digest Series 1: 66-69.

Tan KEWP (1971) Vision in the ultraviolet. PhD thesis, Utrecht, Netherlands. (Cited in: Pokorny et al (1987) Ageing of the human lens).

Tate GW, Lynn JR (1977) Principles of quantitative perimetry: testing and interpreting the visual field. Grune/ Stratton; New York: 69.

Taylor K, McManus P, Miller D (1984) Ophthalmic Technology: Computerised perimeters. Ann Ophthalmol 16: 915-917.

Thibos LN, Bradley A, Still DL, Zhang X, Howarth PA (1990) Theory and measurement of ocular chromatic aberration. Vision Res 30: 33-49.

Tholen A, Tremmel L, Maurer W et al (1992) Lateral differences indicate future glaucoma. Graefe's Arch Clin Exp Ophthalmol 230: 29-35.

Tomita G, Maeda M, Sogano S, Kitazawa Y (1993) An analysis of the relationship between high-pass resolution perimetry and neuro-retinal rim area in normal-tension glaucoma. Acta Ophthalmol 71: 196-200.

Tomita G, Honbe K, Kitazawa Y (1994) Reproducibility of measurements by laser scanning tomography in eyes before and after pilocarpine treatment. Graefe's Arch Clin Exp Ophthalmol 232: 406-408.

Traquair HM (1927) Cited In: Traquair's Clinical Perimetry. Scott GI (ed) 1957. Kimpton; London.

Trick GL, Cooper D, Kolker AE, Bickler-Bluth M (1988) Dissociation of visual deficits in ocular hypertension. Invest Ophthalmol Vis Sci 29: 1486-1491.

Trope GE, Britton R (1987) A comparison of Goldmann and Humphrey automated perimetry in patients with glaucoma. Br J Ophthalmol 71: 489-493.

Trope GE, Eizenman M, Coyle E (1989) Eye movement perimetry in glaucoma. Can J Ophthalmol 24: 197-199.

Tsai CS, Ritch R, Shin DH, Wan JY, Chi T (1992) Age-related decline of disc rim area in visually normal subjects. Ophthalmology 99: 29-35.

Tulunary-Keesey U, Ver Hoeve JN, Terkla-McGrane C (1988) Threshold and suprathreshold spatio-temporal response throughout adult hood. J Opt Soc Am 5: 2191-2200.

Tuulonen A, Airaksinen PJ (1991a) Statpac 2 compared to clinical evaluation of visual fields. Perimetry Update 1990/91. Mills RP, Heijl A (eds). Kugler; Amsterdam / New York: 231-233.

Tuulonen A, Airaksinen PJ (1991b) Initial glaucomatous optic disc and retinal nerve fibre layer abnormalities and their progression. Am J Ophthalmol 111: 485-490.

Tuulonen A, Lehtola J, Airaksinen PJ (1993) Nerve fibre layer defects with normal visual fields. Ophthalmology 100: 587-598.

Tyler CW (1981) Specific deficits of flicker sensitivity in glaucoma and ocular hypertension. Invest Ophthalmol Vis Sci 20: 204-213.

Tyler CW, Ryu S, Stamper RW (1984) The relation between visual sensitivity and intraocular pressure in normal eyes. Invest Ophthalmol Vis Sci 25: 103-105.

Tytla M, Trope G, Buncic J (1990) Flicker sensitivity in treated ocular hypertension. Ophthalmology 97: 36-43.

Urner-Bloch U (1987) Simulation of the influence of lens opacities on the perimetric results, investigated with orthoptic occluders. Doc Ophthalmol Proc Ser 49. Greve E (ed). Nijhoff / Junk; Dordrecht: 3-8.

Uyama K, Matsumoto C, Okuyama S, Otori T (1993) Influence of the target size on the sensitivity of the central visual field with early glaucoma. Perimetry Update 1992/93, Proceedings of the Xth International Perimetric Society. Mills RP (ed). Kugler; Amsterdam / New York: 381-385.

Vaegan Halliday BL (1982) A forced-choice test improves clinical contrast sensitivity testing. Br J Ophthalmol 66: 477-491.

Varma R, Steinmann WC, Spaeth GL, Wilson RP (1988) Variability in digital analysis of optic disc topography. Graefe's Arch Clin Exp Ophthalmol 226: 435-442.

Varma R, Spaeth GL, Steinmann WC, Katz LJ (1989) Agreement between clinicians and an image analyser in estimating cup-to-disc ratios. Arch Ophthalmol 107: 526-530.

Varma R, Quigley HA, Pease ME (1992) Changes in optic disc characteristics and the number of nerve fibres in experimental glaucoma. Am J Ophthalmol 114: 554-559.

Verriest G (1963) Further studies on acquired deficiency of color discrimination. J Opt Soc Am 53: 185-195.

Verriest P, Israel A (1965) Application du perimetrie statique de Goldmann au releve topographique des seuils differentiels de luminance pour de petits objects colores projetes sur un fond blanc. Vision Res 5: 151-174.

Verriest G, Uvijls A (1977) Spectral increment thresholds on a white background in different age groups of normal subjects and in acquired diseases. Doc Ophthalmol Proc Ser 43. Greve EL (ed). Junk; Amsterdam: 217-248.

Verriest G, Laethem J, Uvijls A (1982) A new assessment of the normal ranges of the Farnsworth-Munsell 100-Hue test scores. Am J Ophthalmol 93: 635-642.

Vingrys AJ, King-Smith PE (1988) The value of color perimetry for detecting glaucomatous field losses. In: Non-Invasive Assessment of the Visual System Tech Digest Series 31: 180-183.

Vingrys AJ, King-Smith PE, Benes SC (1989) Color perimetry can be more sensitive than achromatic perimetry. Clin Vision Sci 4: 197-209.

Vingrys AJ, Demirel S (1993) The effect of fixational loss on perimetric thresholds and reliability. In: Perimetry Update 1992/93, Proceedings of the Xth International Perimetric Society Meeting. Mills RP (ed). Kugler; Amsterdam / New York: 521-526.

Vivell PMO, Lachenmayr BJ, Zimmerman P (1991) Vergleichsstudie vershiedener perimetrischer strategien. Fortschr Ophthalmol 88: 819-823.

Vivino MA, Chintalagiri S, Trus B, Datiles MB (1993) Development of a Schiempflug slit lamp camera system for quantitative densitometric analysis. Eye 7: 791-798.

Vos JJ (1984) Disability Glare: A state of the art report. CIE Journal 3: 39-53.

deWaard PWT, IJspeert JK, van den Berg TJTP, de Jong PTVM (1992) Intraocular light scattering in age-related cataracts. Invest Ophthalmol Vis Sci 33: 618-625.

Wald G (1964) The receptors of human colour vision. Science 145: 1007-1016.

Wall M, Kardon R, Moore P (1993) Effect of stimulus size on test-retest variability. Perimetry Update 1992/93. Proceedings of the Xth International Perimetric Society Meeting. Mills RP (ed). Kugler; Amsterdam / New York: 371-376.

Weale RA (1954) Light absorption by the lens of the human eye. Opt Acta 1: 107-110.

Weale RA (1959) Photochemical reactions in normal and cone-monochromatic retinae. Opt Acta 6: 158-174.

Weale RA (1963) In: The Ageing Eye. HK Lewis (ed). London.

Weale RA, Wheeler C (1977) A note on stray light in the Tubingen perimeter. Br J Ophthalmol 61: 133-134.

Weale RA (1988) Age and the transmittance of the human crystalline lens. J Physiol 395: 577-587.

Weale RA (1992) In: The senescence of human vision. Oxford; Oxford / New York / Tokyo.

Webb RH, Hughes GW, Delori FC (1987) Confocal scanning laser ophthalmoscope. Appl Opt 26: 1492-1499.

Weber J, Dobek K (1986) What is the most suitable grid for computer perimetry in glaucoma patients? Ophthalmologica 192: 88-96.

Weber J, Geiger R (1989) Gray scale display of perimetric results. The influence of different interpolation procedures. In: Perimetry Update 1988/89. Proceedings of the VIIIth International Perimetric Society Meeting. Heijl A (ed). Kugler / Ghedini; Amsterdam / Berkeley / Milano: 447-454.

Weber J, Kriegelstein GK (1989) Graphical analysis of topographical trends (GATT) in automated perimetry. Int Ophthalmol 13: 351-356.

Weber J, Cohn H (1989) Stratégie dynamique dans la périmétre automatisée du glaucome. Presented at the 95th Congress of the Société Française d'Ophtalmologie, Paris, 7-11 May.

Weber J (1990) Eine neue strategie fur die automatiserte statische perimetrie. Fortschr Ophthalmol 87: 37-40.

Weber J, Ulrich H (1991) A perimetric nerve fibre bundle map. Int Ophthalmol 15: 193-200.

Weber J (1991) The concept of the new perimeter Peristat 433. In Perimetry Update 1990/91. Proceedings of the IXth International Perimetric Society Meeting. Mills RP, Heijl A (eds). Kugler; Amsterdam/ New York: 395-401.

Weber J, Rau S (1992) The properties of perimetric thresholds in normal and glaucomatous eyes. German J Ophthalmol 1: 79-85.

Weber J, Diestelhorst M (1992) Perimetric follow-up in glaucoma with a reduced set of test points. Germ J Ophthalmol 1: 409-414.

Weber J, Papoulis C (1993) A graphic bar to visualize the quantitative development of visual fields. Perimetry Update 1992/93. Proceedings of the Xth International Perimetric Society meeting. Mills RP (ed), Kugler, Amsterdam / New York: 49-52.

Weber J (1993) Quantification of congruence between the right and left visual fields. Graefe's Arch Clin Exp Ophthalmol 231: 704-710.

Webster AR, Luff AJ, Canning CR, Elkington AR (1993) The effect of pilocarpine on the glaucomatous visual field. Br J Ophthalmol 77: 721-725.

Wegener A, Hockwin O (1988) First experiences with the lens opacity meter in measuring normal and cataractous lens. Lens Res 5: 183-190.

Weinreb RN, Perlman JP (1986) The effect of refractive correction on automated perimetric thresholds. Am J Ophthalmol 101: 706-709.

Weinreb RN, Dreher AW, Bille JF (1989) Quantitative assessment of the optic nerve head with the laser tomographic scanner. Int Ophthalmol 13: 25-29.

Weinreb RN, Sample PA (1991) Short-wavelength visual field testing in eyes with primary open-angle glaucoma. In: Glaucoma Update IV. Kriegelstein GK (ed). Springer-Verlag; Berlin / Heidelberg: 146-155.

Weinreb RN, Dreher AW (1991) Reproducibility and accuracy of topographic measurements of the optic nerve with the laser tomographic scanner. In: Scanning laser ophthalmoscopy and topography. Naseman JE, Burk ROW (eds). Quintessenz; Munich: 177-192.

Weinreb RN, Lusky M, Bartsch D, Morsman D (1993) Effect of repetitive imaging on topographic measurements of the optic nerve head. Arch Ophthalmol 111: 636-638.

Weleber RG (1981) The effect of age on human cone and rod electroretinograms. Invest Ophthalmol Vis Sci 20: 384-392.

Werner EB, Drance SM (1977) Early visual field disturbances in glaucoma. Arch Ophthalmol 95: 1173-1175.

Werner EB, Saheb N, Patel S (1982) Lack of generalised constriction of affected visual field in glaucoma patients with visual field defects in one eye. Can J Ophthalmol 17: 53-55.

Werner EB, Adelson A, Krupin T (1988) Effect of patient experience on the results of automated perimetry in clinically stable glaucoma patients. Ophthalmology 95: 764-767.

Werner EB, Petrig B, Krupin T, Bishop K (1989) Variability of automated visual fields in clinically stable glaucoma patients. Invest Ophthalmol Vis Sci 30: 1083-1089.

Werner EB, Krupin T, Adelson A, Feitl ME (1990) Effect of patient experience on the results of automated perimetry in glaucoma suspect patients. Ophthalmology 97: 44-48.

Werner EB, Ganigan G, Balazsi AG (1991) Effect of test point location on the magnitude of threshold fluctuation in glaucoma patients undergoing automated perimetry. In: Perimetry Update 1990/91. Mills RP, Heijl A (eds). Kugler; Amsterdam / New York: 175-181.

Werner JS (1982) Development of scotopic sensitivity and the absorption spectrum of the human ocular media. J Opt Soc Am 72: 247-258.

Werner JS, Hardenberg FE (1983) Spectral sensitivity of the pseudophakic eye. Arch Ophthalmol 101: 758-760.

Werner JS, Donnelly SK, Kliegl R (1987) Ageing and human macular pigment density. Appended with translations from the work of Max Schultze and Ewald Hering. Vision Res 27: 257-268.

Werner JS, Steele VG (1988) Sensitivity of human foveal color mechanisms throughout the life span. J Opt Soc Am 5: 2122-2130.

Werner JS, Peterzell DH, Scheetz AJ (1990) Light, vision, and ageing. Optom Vis Sci 67: 214-229.

Whitaker D, Steen R, Elliott DB (1993) Light scatter in the normal young, elderly and cataractous eye demonstrates little wavelength dependency. Optom Vis Sci 70: 963-968.

Whitaker D, Elliott DB, Steen R (1994) Confirmation of the validity of the psychophysical light scattering factor. Invest Ophthalmol Vis Sci 35: 317-321.

Wiesel TB, Hubel DH (1966) Spatial and chromatic interactions in the lateral geniculate body of the rhesus monkey. J Neurophysiol 29: 1115-1156.

Wild JM, Wood JM, Flanagan JG (1986) Spatial summation and the cortical magnification of perimetric profiles. Ophthalmologica 195: 88-96.

Wild JM, Wood JM, Worthington FM, Crews SJ (1987) Some concepts on the use of three-dimensional isometric plots for the representation of differential sensitivity. Doc Ophthalmol Proc Ser 49. Greve EL, Heijl A (eds). Nijhoff / Junk; Dordrecht: 423-432.

Wild JM, Wood JM, Crews SJ (1988) Peripheral refractive correction and automated perimetric profiles. Acta Ophthalmol 66: 249-254.

Wild JM, Dengler-Harles M, Hussey MK et al (1989a) Regression techniques in the analysis of visual field loss. Perimetry Update 1988/89. Proceedings of the IXth International Perimetric Society Meeting. Heijl A (ed). Kugler / Ghedini; Amsterdam / Berkeley / Milan: 207-216.

Wild JM, Betts TA, Ross K, Kenwood C (1989b) Influence of antihistamines on central visual field assessment. In: Perimetry Update 1988/89. Proceedings of the VIIIth International Perimetric Society Meeting. Heijl A (ed). Kugler / Ghedini; Amsterdam / Berkeley / Milano: 439-445.

Wild JM, Dengler-Harles M, Searle AET et al (1989c) The influence of the learning effect on automated perimetry in patients with suspected glaucoma. Acta Ophthalmol 67: 537-545.

Wild JM, Betts TA, Shaw DE (1990) The influence of a social dose of alcohol on the central visual field. Jpn J Ophthalmol 34: 291-297.

Wild JM, Hussey MK, Flanagan JG, Trope GE (1991a) Pointwise analysis of serial fields in glaucoma. In: Perimetry Update 1990/91. Proceedings of the IXth International Perimetric Society Meeting. Mills RP, Heijl A (eds). Kugler; Amsterdam / New York: 193-199.

Wild JM, Searle AET, Dengler-Harles M, O'Neill EC (1991b) Long-term follow-up of baseline learning and fatigue effects in automated perimetry of glaucoma and ocular hypertensive patients. Acta Ophthalmol 69: 210-216.

Wild JM, Hussey MK, Flanagan JG, Trope GE (1993) Pointwise topographical and longitudinal modelling of the visual field in glaucoma. Invest Ophthalmol Vis Sci 34: 1907-1916.

Wild JM, Hudson C (1995) The influence of macular pigment on the Blue-Yellow visual field. Ophthalmology: (In Press).

Wildberger H, Robert Y (1988) Visual fatigue during prolonged visual field testing in optic neuropathies. Neuro-ophthalmology 8: 167-174.

Wilensky JT, Joondeph BC (1984) Variation in visual field measurements with an automated perimeter. Am J Ophthalmol 97: 328-331.

Wilensky JT, Mermelstein JR, Siegel HG (1986) The use of different sized stimuli on automated perimetry. Am J Ophthalmol 101: 710-713.

Williams TD (1983) Ageing and central visual field area. Am J Optom Physiol Opt 60: 888-891.

Wilson ME (1967) Spatial and temporal summation in impaired regions of the visual field. J Physiol 189: 189-208.

Witmer FK, van den Brom HJB, Kooijman AC, Blanksma LJ (1989) Intraocular light scatter in pseudophakia. In: Doc Ophthalmol 72: Greve EL, Heijl A (eds). Nijhoff / Junk; Dordrecht: 335-340.

Wolf E (1960) Glare and age. Arch Ophthalmol 64: 502-514.

Wolf E, Gardiner JS (1965) Studies on the scatter of light in dioptric media of eyes as a basis of visual glare. Arch Ophthalmol 74: 338-345.

Wolfe J, Chylack LT, Leske MC et al (1991) Nuclear lens changes with image analysis and LOCS II photograding. Invest Ophthalmol Vis Sci 32 (suppl): 1244.

Wood JM, Wild JM, Drasdo N, Crews SJ (1986) Perimetric profiles and cortical representation. Ophthalmic Res 18: 301-308.

Wood JM, Wild JM, Hussey MK, Crews SJ (1987a) Serial examination of the normal visual field using Octopus automated projection perimetry: Evidence for a learning effect. Acta Ophthalmol 65: 326-333.

Wood JM, Wild JM, Crews SJ (1987b) Induced intraocular light scatter and the sensitivity gradient of the normal visual field. Graefe's Arch Clin Exp Ophthalmol 225: 369-373.

Wood JM, Wild JM, Bullimore MA, Gilmartin B (1988) Factors affecting the normal perimetric profile derived by automated static threshold LED perimetry. I. Pupil size. Ophthal Physiol Opt 8: 26-31.

Wood JM, Wild JM, Smerdon DL, Crews SJ (1989) Alterations in the shape of the automated perimetric profile arising from cataract. Graefe's Arch Clin Exp Ophthalmol 227: 157-161.

Wood JM, Lovie-Kitchen JE (1992) Diagnostic efficacy of contrast sensitivity techniques for the detection of early primary open-angle glaucoma. Optom Vis Sci 69: 175-181.

Wood JM, Lovie-Kitchen JE (1993) Contrast sensitivity measurement in subjects with ocular hypertension. Glaucoma 15: 110-116.

Wood JM, Bruce AS (1993) The value of visual field indexes in screening and threshold testing of glaucoma. Glaucoma 15: 140-146.

Wooten BR, Geri GA (1987) Psychophysical determination of intraocular light scatter as a function of wavelength. Vision Res 27: 1291-1298.

Wright WD (1951) The visual sensitivity of normal and aphakic observers in the ultra-violet. Ann Psychol 50: 169-177.

Wu DC, Schwartz B, Nagin P (1987) Trend analysis of automated visual fields. Doc Ophthalmol Proc Ser 49: 175-189.

Wu J, Cheng G, Poinooswamy D, Liu X, Hitchings R (1994) Improved reliability estimates in the Humphrey visual field test in glaucoma using a knowledged based system. Presented as a paper at the XIth International Perimetric Society Meeting, Washington DC, USA. July 3-7th 1994: 25.

Wyszecki G. Stiles WS (1967) In: Color Science. Wiley; New York.

Yager D, Yuan R, Matthews S (1992) What is the utility of the psychophysical light scattering factor? Invest Ophthalmol Vis Sci 33: 688-690.

Yamazaki Y, Lakowski R, Drance SM (1989) A comparison of the blue color mechanism in high and low-tension glaucoma. Ophthalmology 96: 12-15.

Yeh T, Smith V, Pokorny T (1989) The effect of background luminance on cone sensitivity functions. Invest Ophthalmol Vis Sci 30: 2077-2089.

Yu TC, Falcao-Reis F, Spileers W, Arden GB (1991) Peripheral color contrast. A new screening test for preglaucomatous visual loss. Invest Ophthalmol Vis Sci 32: 2779-2789.

Yuodelis C, Hendrickson A (1986) A qualitative and quantitative analysis of the human fovea during development. Vision Res 26: 847-855.

Zalta AH (1989) Lens rim artifact in automated threshold perimetry. Ophthalmology 96: 1302-1311.

Zalta AH. Burchfield JC (1990) Detecting early glaucomatous field defects with the size I stimulus and Statpac. Br J Ophthalmol 74; 289-293.

Zalta AH (1991) Use of a central 10° field and size V stimulus to evaluate and monitor small central islands of vision in end stage glaucoma. Br J Ophthalmol 75: 151-154.

Zeimer RC, Noth JM (1984) A new method of measuring in vivo the lens transmittance, a study of lens scatter, fluorescence and transmittance. Ophthalmic Res 16: 246-255.

Zeiter JH, Shin DH, Juzych MS et al (1992) Visual field defects in patients with normal-tension glaucoma and patients with high-tension glaucoma. Am J Ophthalmol 114: 758-763.

Zeki S, Shipp S (1988) The functional logic of cortical connections. Nature 335: 311-317.

Zeyen TG, Caprioli J (1993) Progression of disc and field damage in early glaucoma. Arch Ophthalmol 111: 62-65.

Zeyen TG, Raymond M, Caprioli J (1993) Disc and field damage in patients with unilateral visual field loss from primary open-angle glaucoma. Doc Ophthalmol 85: 279-286.

Zeyen TG, Zulauf M, Caprioli J (1993) Priority of test locations for automated perimetry in glaucoma. Ophthalmology 100: 518-523.

Zinser G, Harbarth U, Schroder H (1990) Formation and analysis of three-dimensional data with the laser tomographic scanner LTS. In: Scanning laser ophthalmoscopy and topography. Naseman JE, Burk ROW (eds). Quintessenz; Munich: 243-252.

Zuckerman JL, Miller D, Dyes W, Keller M (1973) Degradation of vision through a simulated cataract. Invest Ophthalmol Vis Sci 12: 213-224.

Zulauf M, Flammer J, Signer C (1986) The influence of alcohol on the outcome of automated perimetry. Graefe's Arch Clin Exp Ophthalmol 224: 525-528.

Zulauf M, Caprioli J, Hoffman, Tressler CS (1991) Fluctuation of the differential light sensitivity in clinically stable glaucoma patients. In: Perimetry Update 1990/91. Mills RP, Heijl A (eds). Kugler; Amsterdam / New York: 183-188.

Zulauf M, Caprioli J, Boeglin RJ, Lee M (1992) Number of stimuli as a reliability parameter in perimetry. German J Ophthalmol 1: 86-90.

Zulauf M, Caprioli J (1993) Stimulus sizes 3 and 5 in perimetry for glaucoma. Invest Ophthalmol Vis Sci 34 (suppl): 1262.

Zulauf M, Fehlman P, Flammer J (1994) Efficiency of the standard Octopus bracketing procedure compared to that of the "dynamic" strategy of Weber. Presented as a poster at the XIth International Perimetric Society Meeting, Washington DC, USA; July 4-7th 1994: 52.

Zwas F, Shin DH, MacKinnon PF (1982) Loss of blue-cone sensitivity in glaucoma. Invest Ophthalmol Vis Sci 22 (suppl): 95.

Zwas F, Shin DH (1987) Blue cone sensitivity in ocular hypertension. Invest Ophthalmol Vis Sci 28 (suppl): 129.

APPENDIX: A1

Publications to support the research

Flanagan JG, **Moss ID**, Wild JM et al (1993) Evaluation of FASTPAC: a new strategy for threshold estimation with the Humphrey Field Analyser. Graefe's Arch Clin Exp Ophthalmol 231: 465-469.

Moss ID, Wild JM (1994) Influence of induced forward light scatter on the Blue-Yellow perimetric profile. Graefe's Arch Clin Exp Ophthalmol 232: 409-414.

Moss ID, Wild JM, Whitaker D (1995) Effect of age-related cataract in Blue-on-Yellow perimetry. Invest Ophthalmol Vis Sci (In Press).

Wild JM, **Moss ID**, Whitaker D, O'Neill EC (1995) The statistical interpretation of Blue-on-Yellow field loss. Invest Ophthalmol Vis Sci (In Press).

Refereed conference publications

Moss ID, Wild JM, Whitaker D (1992) Learning effects in Blue-Yellow perimetry. In: Perimetry Update 1992/93. Proceedings of the Xth International Perimetric Society Meeting. Mills RP (ed). Kugler; Amsterdam / New York: 467-471.

Moss ID, Wild JM, Whitaker D (1992) The effect of light scatter on chromatic sensitivity thresholds. In: Perimetry Update 1992/93. Proceedings of the Xth International Perimetric Society Meeting. Mills RP (ed). Kugler; Amsterdam / New York: 477-483.

Moss ID, Wild JM, O'Neill EC (1995) Blue-Yellow perimetry in OHT and POAG. In: Perimetry Update 1994/95. Proceedings of the XIth International Perimetric Society Meeting. Mills RP, Wall M (eds). Kugler; Amsterdam / New York: (In Press).

Moss ID, Wild JM, Whitaker D (1995) Influence of age-related cataract in Blue-Yellow perimetry. In: Perimetry Update 1994/95. Proceedings of the XIth International Perimetric Society Meeting. Mills RP, Wall M (eds). Kugler; Amsterdam / New York: (In Press).

Abstracts

Moss ID, Hudson C, Dengler-Harles M et al (1992) A 3dB step single crossing algorithm for threshold automated perimetry. Investigative Ophthalmol Vis Sci 33 (Suppl): 969.

Moss ID, Wild JM, Whitaker D (1993) Induced forward light scatter in Blue-Yellow perimetry. Invest Ophthalmol Vis Sci 34 (suppl): 1268.